MOVEMENT AND MIGRATION ECOLOGY OF ALASKAN GOLDEN EAGLES

By

Joseph Michael Eisaguirre, B.A., M.S.

A Dissertation Submitted in Partial Fulfillment of the Requirements

for the Degree of

Doctor of Philosophy

in

Biological Sciences

University of Alaska Fairbanks

May 2020

APPROVED:

Dr. Greg Breed, Committee Chair
Dr. Travis Booms, Committee Member
Dr. Pat Doak, Committee Member
Dr. Knut Kielland, Committee Member
Dr. Carol McIntyre, Committee Member
Dr. Knut Kielland, Program Chair
Wildlife Biology & Conservation Program
Dr. Kinchel Doerner, Dean
College of Natural Sciences & Mathematics
Dr. Michael Castellini, *Dean of the Graduate School*

Abstract

Golden eagles *Aquila chrysaetos* are distributed across the Holarctic; however, in Alaska and other northern areas, many are long-distance migrants. Being soaring birds, golden eagles can use weather and features of the energy landscape to offset the energetic costs of movement and migration. In this dissertation, I investigate how dynamic energy landscapes, in addition to other habitat and anthropogenic features, affect the movement and migration ecology of Alaskan golden eagles; in most cases I did such by developing and applying new, biologically-appropriate statistical methods. First, I identified a single, discrete navigation decision that each eagle made during migration and determined which weather variables are primary factors in driving that decision. I found that wind was the primary correlate to the decision, consistent with eagles likely avoiding poor migration conditions and choosing routes based on favorable wind conditions. Second, I investigated how different forms of flight subsidies, which were orographic uplift, thermal uplift, and wind support, drove behavioral budgets and migratory pacing of eagles. I found a consistent daily rhythm in eagle behavior and migratory pace, seemingly driven by daily development of thermal uplift, with extended periods of slower-paced movements, consistent with periods of opportunistic foraging. Third, I investigated the effects of anthropogenic linear features, such as roads and railroads, on eagle movement during migration. I found that eagles selected for roads during spring migration and were more likely to be near roads when making slower-paced movements, which would be most frequent during times when limited thermal uplift is available. Lastly, I compared how floaters (breeding-age, non-territorial individuals) and territorial eagles used space and selected for resources, specifically interested in how their movements and space use might overlap. I found that floater space use was much more expansive, yet they only selected for habitats and resources slightly differently than territorial eagles. I also found their home ranges overlap substantially, suggesting that floaters play a key role in the population ecology of migratory golden eagles in Alaska.

Table of Contents

Page

Title Page i

Abstract iii

Table of Contents v

List of Figures viii

List of Tables xvi

Acknowledgments xix

Chapter 1: Introduction 1
1.1 References 4

Chapter 2: Local meteorological conditions reroute a migration 9
2.1 Abstract 9
2.2 Introduction 9
2.3 Methods 12
2.3.1 Model system 12
2.3.2 Data collection 13
2.3.3 Analyses 15
2.3.4 Candidate models 16
2.4 Results 17
2.5 Discussion 18
2.6 Ethics 20
2.7 Data, code, and materials 20
2.8 Competing interests 21
2.9 Authors' contributions 21
2.10 Funding 21
2.11 Acknowledgements 21
2.12 References 21
2.13 Figures & Tables 27

Chapter 3: Dynamic-parameter movement models reveal drivers of migratory pace in a soaring bird 31
3.1 Abstract 31
3.2 Introduction 32
3.3 Methods 35
3.3.1 Model system 35
3.3.2 Data collection 36
3.3.3 Movement model 37
3.3.4 Model fitting 39

3.4 Results ... 42
3.4.1 Model performance & diagnostics ... 42
3.4.2 Behavior during migration ... 43
3.4.3 Environmental covariates ... 44
3.5 Discussion ... 45
3.5.1 Model performance ... 45
3.5.2 Flight subsidies as drivers migration of behavior ... 46
3.5.3 Daily rhythm & migratory pace ... 49
3.5.4 Implications & conclusions ... 52
3.6 Data accessibility ... 54
3.7 Conflicts of interest ... 54
3.8 Ethical approval ... 54
3.9 Author contributions ... 54
3.10 Acknowledgements ... 55
3.11 References ... 55
3.12 Figures ... 66
3.13 Tables ... 70

Chapter 4: Novel step selection analyses on energy landscapes reveal how linear features alter migrations of soaring birds ... 72
4.1 Abstract ... 72
4.2 Introduction ... 73
4.3 Methods ... 77
4.3.1 Model system ... 77
4.3.2 Telemetry data collection ... 77
4.3.3 Energy landscape step selection function ... 78
4.3.4 Inference ... 80
4.3.5 Candidate models of movement & selection ... 82
4.3.6 Covariate data ... 84
4.4 Results ... 86
4.4.1 Atmospheric flight subsidies ... 86
4.4.2 Model selection ... 87
4.4.3 Natural landscape features ... 87
4.4.4 Anthropogenic linear features ... 87
4.4.5 Effects of behavior on habitat use ... 88
4.5 Discussion ... 88
4.5.1 Extending SSFs ... 90
4.5.2 Eagle migration & anthropogenic linear features ... 91
4.5.3 Effects of habitat on eagle space use ... 93
4.5.4 Individual heterogeneity in movement and space use ... 95
4.5.5 Conclusions & Implications ... 96
4.6 Acknowledgements ... 97
4.7 Data accessibility ... 97
4.8 References ... 98
4.9 Figures ... 111
4.10 Tables ... 120

Chapter 5: Differential resource selection between territorial and floater golden eagles revealed with an Ornstein-Ulhenbeck space use model 121
5.1 Abstract 121
5.2 Introduction 122
5.3 Methods 126
5.3.1 Study area & system 126
5.3.2 Telemetry data 127
5.3.3 Mechanistic space use model 127
5.3.4 Weather and habitat variables 129
5.3.5 Inference 130
5.4 Results 131
5.4.1 Movement parameters 132
5.4.2 Habitat selection 132
5.4.3 Realized home range size 133
5.5 Discussion 133
5.5.1 Energy home range 134
5.5.2 Terrain & habitat use 135
5.5.3 Home range structure 136
5.5.4 Implications & conclusions 137
5.6 Acknowledgements 138
5.7 References 139
5.8 Figures 147
5.9 Tables 154

Chapter 6: Conclusion 155
6.1 References 158

Appendix 161

List of Figures

Page

Figure 2.1 Relief map of the study area with relevant mountain ranges labeled and golden eagle route choice around the Wrangell Mountains illustrated. Labeled arrows correspond to the approximate direction of migration for the indicated season. Beige points correspond to the discrete GPS locations recorded by the transmitters for 28 example eagle tracks with transmitters on intervals of one to several hours with dashed lines showing linear interpolations between. Green filled circle is the spatial location weather data were interpolated to. Yellow filled square is the location of Gunsight Mountain. Location of Chitistone Pass shown by red lines. 27

Figure 2.2 Model predictions of effects of meteorological variables on the proportion of 135 eagle decisions resulting in a route north of the Wrangell Mountains. Violins are composed of 1000 posterior predictive draws from top fitting models with vertical bars showing means. Zero indicates posterior predictive draws with observed data—done as a posterior predictive check to confirm the models predict reasonably well—and plus and minus indicate the empirical values + and − one standard deviation, respectively. Vertical lines represent the observed proportions of eagles that chose the north route. N-S wind corresponds to the velocity of the wind from south to north. Distributions right of the observed proportion indicate that variable, if changed, would increase the proportion of eagles choosing the north route. 28

Figure 3.1 Time series of behavior parameter γ from correlated random walk model with full behavioral process (orographic uplift, thermal uplift, and wind support as predictors) for two golden eagles during spring migration with PTTs reporting on different duty cycles. Upper panel is 13 hourly centered on solar noon plus one at midnight, and the lower panel is 8 hourly centered on solar noon. γ close to one reflect movements associated with migratory behavior, and γ close to zero stopover behavior. Points are times of observations, and lines are linear interpolations between points. Hue indicates intensity of thermal uplift, with yellow indicating greater and blue lower. Note the daily rhythm in behavior associated with intense thermal uplift, stopover periods of one or more days, and the intermediate periods suggesting fly-and-forage. 66

Figure 3.2 Time series of behavior parameter γ from correlated random walk model with full behavioral process (orographic uplift, thermal uplift, and wind support as predictors) for three golden eagles during fall migration with PTTs reporting on different duty cycles. Upper panel is 13 hourly centered on solar noon plus one at midnight, middle panel is 8 hourly centered on solar noon, and lower panel is fixed 3-hr interval. γ close to one reflect movements associated with migratory behavior, and γ close to zero stopover behavior. Points are times of observations, and lines are linear interpolations between points. Hue indicates intensity of thermal uplift, with yellow indicating greater thermal uplift and blue lower. Note the daily rhythm in behavior and extended stopovers as well as periods intermediate values suggesting fly-and-forage. 67

Figure 3.3 Golden eagle migration trajectories ($N = 15$ spring and $N = 16$ fall). Hue indicates value of behavioral parameter γ estimated with the correlated random walk model with full behavioral process, including orographic uplift, thermal uplift, and wind support as predictors. Insets show the relative frequencies of estimates of γ assigned to the displacements between observed daytime GPS locations. γ close to one reflect movements associated with migratory behavior, and γ close to zero stopover behavior. Daily rhythms, revealed in figures 3.1 and 3.2, are not apparent here because the birds moved so little at night. 68

Figure 3.4 Point estimates of environmental covariate effect parameters (β_{ou}, β_{tu}, β_{tw}) on golden eagle behavior and movements during migration ($N = 15$ spring and $N = 16$ fall). Estimates are from the correlated random walk model with full behavioral process, including orographic uplift, thermal uplift, and wind support as predictors. 69

Figure 4.1 Map of 45 spring and 39 fall individual golden eagle migrations recorded with GPS transmitters in western North America 2014-2017. Insets show frequency distributions of γ_i, a time-varying latent variable driven by flight subsidies in a CRW movement model. γ_i close to one (red) indicates more directed, larger-scale migratory movements, and γ_i close to zero (blue) more tortuous, smaller-scale stopover movements 111

Figure 4.2 Example movement kernels from an SSF fitted to golden eagle migrations 2014-2017 conditioned on the displacement vector from $\mathbf{x}_{i-2}$ to $\mathbf{x}_{i-1}$. (a) $p(\mathbf{x}_i^j|\mathbf{X} = \mathbf{x}_{i-1}, \mathbf{x}_{i-2})$ is the conditional posterior predictive distribution of the fitted selection independent kernel $\phi(\mathbf{x}_i|\mathbf{x}_{i-1}, \mathbf{x}_{i-2})$, (b) is an elevation map showing roads and waterways, representing aspects of the landscape Z, and (c) $\hat{f}(\mathbf{x}_i|\mathbf{x}_{i-1}, \mathbf{x}_{i-2}; Z)$ is the product of the fitted selection independent kernel and fitted habitat weighting function. Grey points show example available points $\mathbf{x}_i^j$ drawn from $p(\mathbf{x}_i^j|\mathbf{X} = \mathbf{x}_{i-1}, \mathbf{x}_{i-2})$ for use in estimation of $\omega(\cdot)$ with the use-availability design. Note that both (a) and (c) show spatiotemporally explicit probability densities for $\mathbf{x}_i$, a golden eagle's location during migration at time t_i given that the eagle traveled from $\mathbf{x}_{i-2}$ to $\mathbf{x}_{i-1}$ with (estimated) correlation $\gamma_i \approx 1$ driven by uplift. 112

Figure 4.3 Effects of flight subsidies (orographic uplift, thermal uplift, and wind support) on golden eagle movement during migration 2014-2017 estimated with a CRW movement model. $\hat{\alpha} > 0$ indicates the flight subsidy is associated with more directed, larger-scale migratory movements, and $\hat{\alpha} < 0$ more tortuous, smaller-scale stopover movements. 113

Figure 4.4 Empirical use distributions smoothed with a generalized additive model ($df = 4$; shaded areas are 95% confidence intervals) over all golden eagle spring and fall migrations 2014-2017 as a function of the movement parameter γ_i. γ_i is a time-varying latent variable driven by flight subsidies in a CRW movement model. γ_i close to one indicates more directed, larger-scale migratory movements, and γ_i close to zero more tortuous, smaller-scale stopover movements. 114

Figure 4.5 Effects of habitat variables on golden eagle habitat selection during spring and fall migration 2014-2017 estimated with SSFs. Points are posterior means and horizontal lines 95% highest posterior density (HPD) intervals for the population-level effects. Crosses correspond to the individual-level posterior means. Predictors included were elevation ('elev'), slope southing ('slope'), percent snow cover ('snow'), percent vegetation cover ('veg'), and distance to nearest railroad ('rail'), road ('road'), waterway ('water'), some as an interaction with latitude ('lat'). Negative estimates on distance to nearest linear feature correspond to selection for areas close to the linear feature. Estimates are on a standardized scale. Note that we have shortened the x axis here for clarity, but the full version is provided in the Appendix. 115

Figure 4.6 Empirical use distributions for linear features smoothed with a generalized additive model ($df = 4$; shaded areas are 95% confidence intervals) over all golden eagle spring and fall migrations 2014-2017 as a function of the estimated movement parameter γ_i. γ_i is a time-varying latent variable driven by flight subsidies in a CRW movement model. γ_i close to one indicates more directed, larger-scale migratory movements, and γ_i close to zero more tortuous, smaller-scale stopover movements. 116

Figure 4.7 Average effect of distance to nearest linear feature on space use of golden eagles during spring and fall migrations 2014-2017 estimated with SSFs. This is conditioned on how habitat was distributed within the availability distribution for the population sampled (Avgar et al., 2017). Curves depict the smoothed (generalized additive model, $df = 6$) nonparametric function between the distance to linear feature and relative probability of use, and shaded areas correspond to 95% confidence intervals. 117

Figure 4.8 Smoothed empirical distributions of distance from 17,386 daytime golden eagle GPS transmitter locations to the nearest road, railroad, and waterway during spring and fall migrations 2014-2017 in western North America. 118

Figure 4.9 Population-level (solid) and two individual-level (dashed and dotted) preference curves for anthropogenic linear features predicted by an SSF fitted to golden eagle migrations 2014-2017. These describe the relative probability of selection by golden eagles during spring and fall migration, assuming road distances are uniformly distributed and equally available to eagles (Avgar et al., 2017). Individual-level curves shown to highlight the variation among individuals. 'low', 'mid', and 'high' latitude correspond to approximately 41°, 51°, and 61°N latitude, respectively. 119

Figure 5.1 Summaries of the number of home range cores K, posterior means of the movement variance parameter σ, and posterior means of the centralizing tendency parameter ω in an Ornstein-Uhlenbeck space use model for golden eagles summering in southcentral Alaska.. Summaries of the OU parameters are for the most used home range core, and the model was fit separately for early and late breeding. K was estimated with a k-means clustering algorithm. 147

Figure 5.2 Estimated marginal posteriors for the population-level selection coefficients from an Ornstein-Uhlenbeck space use model fit to summer golden eagle GPS data in southcentral Alaska. The model was fit separately for early and late breeding season and floater and territorial eagles. 'bare' (bare ground) is the reference category. 148

Figure 5.3 Proportion of habitat types used by golden eagles summering in southcentral Alaska. 149

Figure 5.4 (a.) Estimated marginal posteriors for the population-level selection coefficients for golden eagles in southcentral Alaska estimated with an Ornstein-Uhlenbeck (OU) space use model, and (b.) probability of a golden eagle using a spatial location within its breeding season home range in southcentral Alaska as a function of habitat variables. The model was fit separately for early and late breeding season and floater and territorial eagles. In b. predictions were smoothed over the availability points with a generalized additive model ($df = 6$) and ribbons are 95% confidence intervals. Units are radians for orographic uplift (angle of incidence). Higher hill shade corresponds to more direct sun and greater thermal uplift potential. Years were pooled for presentation, but the year-specific figures are provided in the Appendix. 150

Figure 5.5 Estimated among-home range core variance and among-individual variance for the selection coefficients from an Ornstein-Uhlenbeck space use model fit to summer golden eagle GPS data in southcentral Alaska. The model was fit separately for early and late breeding season and floater and territorial eagles. Points are posterior means, and horizontal lines are 95% credible intervals. Note the horizontal axis has been truncated for presentation. 151

Figure 5.6 Posterior predictive densities of a hierarchical Gamma regression on golden eagle home range size predicted with an Ornstein-Uhlenbeck home range model for golden eagles summering in southcentral Alaska 2014-2017. Period of breeding season (early or late) and status (floater or territorial) were included as fixed effects, and individual and year were included as random effects. 152

Figure 5.7 Estimated home range boundaries for nine territorial (blue hues) and four floater (red hues) golden eagles in southcentral Alaska during late breeding season in 2016. Home range estimates are the 95% contour of the utilization distribution constructed from the posterior predictive distribution of an Ornstein-Uhlenbeck space use model. 153

List of Tables

Page

2.1 Proportion of golden eagles tracked that chose a northern migration route around the Wrangell Mountains and the summary statistics of meteorological variables interpolated to the approximate location and time each eagle chose a route. Pooled summaries and summaries specific to route choice presented. N-S wind is velocity of south to north wind. Negative thermal uplift (surface sensible heat flux) is flux towards the surface. 29

2.2 Candidate models of route choice around the Wrangell Mountains ranked by leave-one-out cross-validation approximated by Pareto-smoothed importance sampling. Lower information criterion (looic) indicates better model fit. Top 10 candidate models and null intercept-only model shown. All models include random intercept for individual. Interaction models include all main effects. Meteorological predictors were interpolated to the approximate location and time each eagle chose a route. 'Wind' is the velocity of south to north wind. Negative thermal uplift (surface sensible heat flux) is flux towards the surface. 30

3.1 Summary statistics of flight subsidies encountered by migrating golden eagles that summer in Alaska. Variables were interpolated in space and time from weather reanalyses to eagle locations recorded by GPS telemetry. Units for all variables are m/s. 70

3.2 Number of golden eagle migration tracks recorded by GPS transmitters that each candidate formulation of the behavioral process in the correlated random walk model fit the best, according to approximate leave-one-out cross-validation (Table S7.1). 'therm' corresponds to thermal uplift, 'oro' to orographic uplift, and 'twind' to wind suppport. 71

4.1 Ranking of candidate models of habitat selection by golden eagles during migration 2014-2017 by the widely-applicable information criterion (WAIC). 'terrain' includes elevation and slope southing; 'cover' includes percent vegetation and snow cover; and linear features (roads, railroads, and waterways) were included as distance to nearest. * corresponds to the model with only natural variables chosen to include with anthropogenic linear features. 120

5.1 Median (interquartile range) dates of arrival on and departure from the summer range of golden eagles tagged with GPS telemetry in southcentral Alaska. 154

Acknowledgments

I would like to thank my committee: to Pat Doak and Knut Kielland who continuously challenged me to think more broadly; to Carol McIntyre who kept my work grounded in eagle ecology and never failed to have questions; to Travis Booms for facilitating my graduate project and for his unbelievable support and mentorship over the years; and to Greg Breed for introducing me to the world of quantitative ecology and for being a superb advisor and mentor.

I would also like to thank Chris Barger, who this project would not have been possible without. Additionally, I thank Steve Lewis for offering some transmitters to use and for thoughtful contributions to my work. There are many others to thank who aided with field work and various aspects of the project; these specific acknowledgements are provided in the respective chapters herein.

I am grateful for the support of the Alaska Department of Fish and Game and the federal State Wildlife Grant Program, the Calvin J. Lensink Fund, the Institute of Arctic Biology, and the UAF Graduate School.

I owe many thanks to my family for their incredible support. Finally, members of the lab, including Janelle, Roxanne, Mike, Stefan, Abigail, Kathryn, and Matt, other fellow students, and UAF community members all contributed to my development as an ecologist and production of this work. To all these friends, I most grateful.

Chapter 1: Introduction

Understanding an organism's movement, including where, when, and why it occurs on a landscape, is fundamental to understanding its ecology. Movement is driven by suites of intrinsic and extrinsic mechanisms, which can vary across multiple temporal and spatial scales, giving rise to diverse animal movement and space use patterns (Nathan et al., 2008). Movements at the the largest spatial scales include population-level intra-annual shifts in distribution resulting from seasonal migration. Annual migrations allow individuals to take advantage of seasonally varying resources to maximize lifetime reproductive success (Newton, 2008; Avgar et al., 2014). The processes by which such large scale movements occur, however, are emergent from numerous large and small scale processes and decisions (Nathan et al., 2008). Emergent population-level migration patterns, therefore, result from the time series of small and large scale decisions an individual makes as it moves through landscapes informed by internal physiology and external environmental cues.

The landscapes through which animals move are themselves dynamic. Snow depth, for example, can vary markedly on the temporal scale of hours and spatial scales of tens of meters and can impact the movements of large terrestrial mammals. Further, water currents can subsidize or impede movement of marine and aquatic species (Avgar et al., 2013; Brillinger and Stewart, 2010). Similarly, air currents strongly influence the movement and decisions of many birds (Gill, 2007). Soaring birds can use air currents to offset energy expenditures of flight (Duerr et al., 2012; Gill, 2007). Such subsidies can be collected from a wide variety of air and fluid flow, including ocean waves modifying airflow, wind striking topography to generate orographic uplift, and thermal uplift which forms from the differential pressure in the atmospheric boundary layer created by the sun heating the earth's surface. Horizontal air flow can both subsidize or impede movement rate to increase or decrease migration efficiency (Shamoun-Baranes et al., 2010).

While, dynamic conditions are important drivers of animal movement, static landscape features also affect animal movement. Topography is one example, as are water

features, plant communities, and anthropogenic features relative to both the lifetime of the an individual and the temporal-spatial scale of the movement process. Humans have extensively modified the landscape, adding a wide variety of such static features. Linear features, such as roads, railroads, and transmission line corridors, are major anthropogenic modifications known to disrupt the natural spatial heterogeneity of habitats. Linear features have changed how animals move (James and Stuart-Smith, 2000; Dyer et al., 2002; Whittington et al., 2004, 2005, 2011; Dickson et al., 2005; Latham et al., 2011; Dickie et al., 2017; Scrafford et al., 2018), altering many aspects of animal ecology and behavior (McKenzie et al., 2012; Wasser et al., 2011; Haddad et al., 2003). Despite roadway mortality and mortality associated with transmission line strikes (i.e. collision and electrocution) being substantial sources of mortality in birds (Loss et al., 2015), work to understand the effects of linear features on individual animal movement has been almost entirely restricted to movement of large mammals. Consequently, the effects of linear features on on individual- and population-level avian movement are largely unknown.

The effects of static and dynamic landscape features are not limited to migration. After arriving on seasonal home ranges following migration, soaring birds likely modify their movements within breeding or wintering territories to minimize energy expenditure and maximize energy intake (Shepard et al., 2011, 2013; Murgatroyd et al., 2018). Such effects should impact decisions and behaviors to give rise to extremely dynamic space use patterns driven by changes in air flow and weather. For example, some hillsides within home ranges used by a soaring species may only be used when the wind direction generates orographic uplift or the sun is at an appropriate angle to generate thermal uplift. Such patterns have been formalized under the idea of an 'energy landscape', where movement is driven, in part, by the energetic costs or subsidies associated with moving over certain landscapes and associated features (Shepard et al., 2013).

Like most animals, the movement and space use of soaring birds is not only driven exclusively by extrinsic favors such as habitat and the energy landscape, but also internal state variables such as age, reproductive status, and condition. 'Floating' is a strategy employed by sexually mature individuals attempting to enter a breeding population.

Floaters are common across many taxa, but the term is most often used to describe a feature of avian mating systems, and they are a common demographic class in territorial bird species with prolonged pre-breeding periods, including raptors (Newton, 1998; Hunt, 1998). Floaters can be pre-breeders but also individuals that have bred but were later usurped from breeding habitat or a territory. As breeding habitat is often very limited, many raptors have large floater portions of populations (Hunt, 1998). We know concerningly little about the behavior of these floaters and their strategies for entering the breeding population. This is especially problematic given the growing theoretical and empirical evidence that these population segments play critical roles in buffering population dynamics, population regulation, and evolution (Kokko and Sutherland, 1998; Hunt, 1998; Penteriani et al., 2005, 2011; Lee et al., 2017).

Golden eagles Aquila chrysaetos are a large, long-lived, soaring raptor distributed across the Holarctic (Watson, 2010). Their flight and behavior is driven by the environment, and are highly sensitive to atmospheric conditions and airflow, which allow eagles, like other soaring birds, to subsidize the energetic costs of flight and migration (Duerr et al., 2012, 2015; Katzner et al., 2015; Miller et al., 2016; Rus et al., 2017). Golden eagles are opportunistic predators, capable of using many taxa for food resources, ranging from small mammals and birds to ungulates, and often scavenging carrion (Kochert et al., 2002; Watson, 2010). Most golden eagles that summer and breed at high latitudes are long-distance migrants (Watson, 2010; Kochert et al., 2002). They exhibit high territory fidelity and most commonly nest on cliffs, which are likely limiting resources. Golden eagles are central place foragers (Kochert et al., 2002; Watson, 2010), so suitable nesting habitat must lie within or adjacent to suitable foraging habitat. In most areas across their range the number of viable territories is usually limited, which can give rise to large numbers of floaters, about which we know very little (Watson, 2010). Migratory golden eagles are, therefore, an excellent model system for investigating some of the environmental drivers and mechanisms that give rise to emergent animal movement and space use patterns and differences in strategies and movement decisions behind each demographic class.

In this dissertation, I investigate four primary questions regarding the external and internal factors that give rise to individual- and population-level movement and behavioral patterns in animals, using migratory golden eagles as a model system. These are: (1) How can discrete decisions give rise to large changes in animal movement corridors? (2) How do the behavioral budgets and the energetic subsidies that drive those budgets vary between spring and fall migration? (3) How do anthropogenic linear features affect the movement and space use of soaring birds? and (4) How do space use and resource selection patterns vary between floater and territorial breeding individuals? I investigate these questions by pairing GPS telemetry data for migratory golden eagles with statistical models designed specifically for each question. In collaboration with Alaska Department of Fish & Game, the GPS transmitters were deployed on 53 primarily adult eagles during spring migrations 2014-2017. In addition to this introduction, there are four chapters, in which each of the aforementioned questions is addressed, followed by concluding remarks summarizing key findings in chapter 6.

1.1 References

Avgar T, Mosser A, Brown GS, Fryxell JM. 2013. Environmental and individual drivers of animal movement patterns across a wide geographical gradient. *Journal of Animal Ecology* **82**: 96–106. doi: 10.1111/j.1365-2656.2012.02035.x.

Avgar T, Street G, Fryxell JM. 2014. On the adaptive benefits of mammal migration. *Canadian Journal of Zoology* **92**: 481–490. doi: 10.1139/cjz-2013-0076.

Brillinger DR, Stewart BS. 2010. Stochastic modeling of particle movement with application to marine biology and oceanography. *Journal of Statistical Planning and Inference* **140**: 3597–3607. doi: 10.1016/j.jspi.2010.04.026.

Dickie M, Serrouya R, McNay RS, Boutin S. 2017. Faster and farther: wolf movement on linear features and implications for hunting behaviour. *Journal of Applied Ecology* **54**: 253–263. doi: 10.1111/1365-2664.12732.

Dickson BG, Jenness JS, Beier P. 2005. Influence of Vegetation, Topography, and Roads on Cougar Movement in Southern California. *Journal of Wildlife Management* **69**: 264–276. doi: 10.2193/0022-541X(2005)069<0264:IOVTAR>2.0.CO;2.

Duerr AE, Miller Ta, Lanzone M, Brandes D, Cooper J, O'Malley K, Maisonneuve C, Tremblay J, Katzner T. 2012. Testing an emerging paradigm in migration ecology shows surprising differences in efficiency between flight modes. *PLoS ONE* **7**: e35548. doi: 10.1371/journal.pone.0035548.

Duerr AE, Miller TA, Lanzone M, Brandes D, Cooper J, O'Malley K, Maisonneuve C, Tremblay JA, Katzner T. 2015. Flight response of slope-soaring birds to seasonal variation in thermal generation. *Functional Ecology* **29**: 779–790. doi: 10.1111/1365-2435.12381.

Dyer SJ, O'Neill JP, Wasel SM, Boutin S. 2002. Quantifying barrier effects of roads and seismic lines on movements of female woodland caribou in northeastern Alberta. *Canadian Journal of Zoology* **80**: 839–845. doi: 10.1139/z02-060.

Gill FB. 2007. *Ornithology.* New York: W. H. Freeman and Company, third edition.

Haddad NM, Bowne DR, Cunningham A, Danielson BJ, Levey DJ, Sargent S, Spira T. 2003. Corridor use by diverse taxa. *Ecology* **84**: 609–615.

Hunt W. 1998. Raptor floaters at Moffat's equilibrium. *Oikos* **82**: 191–197.

James A, Stuart-Smith A. 2000. Distribution of caribou and wolves in relation to linear corridors. *The Journal of Wildlife Management* **64**: 154–159.

Katzner TE, Turk PJ, Duerr AE, Miller TA, Lanzone MJ, Cooper JL, Brandes D, Tremblay JA, Lemaître J. 2015. Use of multiple modes of flight subsidy by a soaring terrestrial bird, the golden eagle Aquila chrysaetos, when on migration. *Journal of Royal Society Interface* **12**: 20150530. doi: 10.1098/rsif.2015.0530.

Kochert MN, Steenhof K, McIntyre CL, Craig EH. 2002. Golden Eagle (Aquila chrysaetos). In Poole A (ed.) *The Birds of North America.* Ithaca: Cornell Lab of Ornithology.

Kokko H, Sutherland WJ. 1998. Optimal floating and queuing strategies: consequences for density dependence and habitat loss. *The American Naturalist* **152**: 354–366. doi: 10.1086/286174.

Latham ADM, Latham MC, Boyce MS, Boutin S. 2011. Movement responses by wolves to industrial linear features and their effect on woodland caribou in northeastern alberta. *Ecological Applications* **21**: 2854–2865. doi: 10.1890/11-0666.1.

Lee AM, Reid JM, Beissinger SR. 2017. Modelling effects of nonbreeders on population growth estimates. *Journal of Animal Ecology* **86**: 75–87. doi: 10.1111/1365-2656.12592.

Loss SR, Will T, Marra PP. 2015. Direct mortality of birds from anthropogenic causes. *Annual Review of Ecology, Evolution, and Systematics* **46**: annurev–ecolsys–112414–054133. doi: 10.1146/annurev-ecolsys-112414-054133.

McKenzie HW, Merrill EH, Spiteri RJ, Lewis MA. 2012. How linear features alter predator movement and the functional response. *Interface Focus* **2**: 205–216. doi: 10.1098/rsfs.2011.0086.

Miller TA, Brooks RP, Lanzone MJ, Brandes D, Cooper J, Tremblay JA, Wilhelm JAY, Duerr A, Katzner TE. 2016. Limitations and mechanisms influencing the migratory performance of soaring birds. *Ibis* **158**: 116–134. doi: 10.1111/ibi.12331.

Murgatroyd M, Photopoulou T, Underhill LG, Bouten W, Amar A. 2018. Where eagles soar: Fine-resolution tracking reveals the spatiotemporal use of differential soaring modes in a large raptor. *Ecology and Evolution* **8**: 6788–6799. doi: 10.1002/ece3.4189.

Nathan R, Getz WM, Revilla E, Holyoak M, Kadmon R, Saltz D, Smouse PE. 2008. A movement ecology paradigm for unifying organismal movement research. *Proceedings of the National Academy of Sciences* **105**: 19052–9. doi: 10.1073/pnas.0800375105.

Newton I. 1998. *Population limitation in birds.* San Diego: Academic Press.

Newton I. 2008. *The migration ecology of birds.* London: Academic Press.

Penteriani V, Ferrer M, Delgado MM. 2011. Floater strategies and dynamics in birds, and their importance in conservation biology: Towards an understanding of nonbreeders in avian populations. *Animal Conservation* **14**: 233–241. doi: 10.1111/j.1469-1795.2010.00433.x.

Penteriani V, Otalora F, Ferrer M. 2005. Floater survival affects population persistence. The role of prey availability and environmental stochasticity. *Oikos* **108**: 523–534. doi: 10.1111/j.0030-1299.2005.13514.x.

Rus AI, Duerr AE, Miller TA, Belthoff JR, Katzner TE. 2017. Counterintuitive roles of experience and weather on migratory performance. *The Auk* **134**: 485–497. doi: 10.1642/AUK-16-147.1.

Scrafford M, Avgar T, Heeres R, Boyce MS. 2018. Roads elicit negative movement and habitat-selection responses by wolverines (Gulo gulo luscus). *Behavioral Ecology* **29**: 534–542. doi: 10.1093/beheco/arx182.

Shamoun-Baranes J, Bouten W, Van Loon EE. 2010. Integrating meteorology into research on migration. *Integrative and Comparative Biology* **50**: 280–292. doi: 10.1093/icb/icq011.

Shepard EL, Lambertucci SA, Vallmitjana D, Wilson RP. 2011. Energy beyond food: Foraging theory informs time spent in thermals by a large soaring bird. *PLoS ONE* **6**: 1–6. doi: 10.1371/journal.pone.0027375.

Shepard ELC, Wilson RP, Rees WG, Grundy E, Lambertucci SA, Vosper SB. 2013. Energy landscapes shape animal movement ecology. *The American Naturalist* **182**: 298–312. doi: 10.1086/671257.

Wasser SK, Keim JL, Taper ML, Lele SR. 2011. The influences of wolf predation, habitat loss, and human activity on caribou and moose in the Alberta oil sands. *Frontiers in Ecology and the Environment* **9**: 546–551. doi: 10.1890/100071.

Watson J. 2010. *The Golden Eagle*. New Haven: Yale University Press, second edition.

Whittington J, Hebblewhite M, Decesare NJ, Neufeld L, Bradley M, Wilmshurst J, Musiani M. 2011. Caribou encounters with wolves increase near roads and trails: A time-to-event approach. *Journal of Applied Ecology* **48**: 1535–1542. doi: 10.1111/j.1365-2664.2011.02043.x.

Whittington J, St Clair CC, Mercer G. 2004. Path tortuosity and the permeability of roads and trails to wolf movement. *Ecology and Society* **9**. doi: 10.5751/ES-00617-090104.

Whittington J, St Clair CC, Mercer G. 2005. Spatial responses of wolves to roads and trails in mountain valleys. *Ecological Applications* **15**: 543–553. doi: 10.1890/03-5317.

Chapter 2: Local meteorological conditions reroute a migration

2.1 Abstract

For migrating animals, realized migration routes and timing emerge from hundreds or thousands of movement decisions made along migration routes. Local weather conditions along migration routes continually influence these decisions, and even relatively small changes in *en route* weather may cumulatively result in major shifts in migration patterns. Here, we analyzed satellite tracking data to score a discrete navigation decision by a large migratory bird as it navigated a high-latitude, 5000-m elevation mountain range to understand how those navigational decisions changed under different weather conditions. We showed that wind conditions in particular areas along the migration pathway drove a navigational decision to reroute a migration; conditions encountered predictably resulted in migrants routing either north or south of the mountain range. With abiotic conditions continuing to change globally, simple decisions, such as the one described here, might additively emerge into new, very different migration routes.

2.2 Introduction

Migration routes and strategies strongly affect fitness, and migration corridors provide important connectivity between geographically distant systems (Webster et al., 2002). Routes and timing are closely tied to environmental conditions, and timing in particular has been clearly demonstrated to have substantial impacts to fitness (Winkler et al., 2014). However, migratory behavior of birds is changing with climate variation (Cotton, 2003; Both et al., 2004; Winkler et al., 2014; La Sorte and Fink, 2017). Phenological miscuing and disjunction occur when initiation of migration is mistimed due to some cue (e.g., weather) and reproductive stages are poorly aligned with resource availability in breeding areas (Crick, 2004). Severe miscuing or disjunctions often result in failed

Eisaguirre, JM, TL Booms, CP Barger, CL McIntyre, SB Lewis, GA Breed. 2018. Local meteorological conditions reroute a migration. Proceedings of the Royal Society B 285: 20181779.

breeding attempts and heighten the probability of adult mortality, with commensurate harmful effects to populations (Both et al., 2006).

As climate change can alter migratory behavior (Cotton, 2003; Both et al., 2004; Winkler et al., 2014; La Sorte and Fink, 2017), efforts to understand climate's effects on migration have generally focused on large-scale, cross-sectional or population-level behavioral phenomena, such as phenological miscuing, disjunction, and short-stopping (Crick, 2004; Teitelbaum et al., 2016). These large-scale patterns, however, emerge from many hundreds or thousands of smaller scale decisions made by individuals along migration routes, each affected by a suite of intrinsic and extrinsic factors that animals experience before and during migration (Nathan et al., 2008). For example, some individual decisions can be as simple as going one way or another around a particular landscape feature. The effect of local *en route* conditions on these individual decisions can emerge as altered migration behavior that may or may not respond adaptively to ongoing environmental change (Both, 2010). Limited study of fine-scale movement of free-living animals has left us with a poor understanding of movement decisions during migration, how climate-related changes might affect them, and how they sum to overall migration patterns at both individual and population levels (Nathan et al., 2008).

A major area of work in the growing field of movement ecology involves investigating how fine-scale movement decisions interact with intrinsic and extrinsic factors to emerge as an animal's observed movement pattern (Nathan et al., 2008). Technologies to track animals are advancing rapidly, as are new analytical methods to parse the often rich data streams they create. It is now possible to probe the environmental and physiological processes affecting individual movement decisions that occur during migrations (Breed et al., 2017; Hooten et al., 2017).

A key aspect of these movement decisions is energy expenditure and efficiency. The movement efficiency of animals migrating through moving fluids, such as birds in the air, can be drastically improved or reduced by changes in ambient conditions and fluid flow (Mandel et al., 2008; Lanzone et al., 2012; Vansteelant et al., 2017). Soaring species, including many raptors, are dependent upon upward air motion, such as thermal uplift,

for efficient locomotion (Mandel et al., 2008; Duerr et al., 2012). Constant adjustments in response to conditions in the air column allow an individual to move efficiently by taking advantage of energetic flight subsidies provided by local meteorological phenomena along migration routes (Katzner et al., 2015). Such reliance on atmospheric conditions directly links movement capacity and the energy landscape to climate-affected environmental variables (Nathan et al., 2008; Shepard et al., 2013). Changes in climate and weather along migration corridors will affect the efficiency and risk associated with certain migration routes and timing (Vansteelant et al., 2017). These effects will also interact with climate-driven landcover change to influence both *en route* weather conditions and food resources. Identifying how weather, such as wind and cloud prevalence, drives individual decisions is, therefore, key to predicting potential shifts in migration routes. Weather is well known to influence aerial migrant decision making (Shamoun-Baranes et al., 2010; Katzner et al., 2015; Vansteelant et al., 2017); however, despite being a source of changes in migration routes, discrete navigation decisions are infrequently addressed in the migration literature (Shamoun-Baranes et al., 2017). Predicting such shifts in route requires an understanding of how individual navigation decisions are made and could prove important to placing energy infrastructure, such as wind turbines, that are known to impose increased mortality on wildlife (Drewitt and Langston, 2006).

Here, we examine the movement behavior of a holarctic, large soaring bird and apex predator, the golden eagle *Aquila chrysaetos*, at a point along a migration corridor to understand how local weather affects a movement decision resulting in a major shift in the realized migration route. Some golden eagles that summer and breed in southcentral Alaska and overwinter at temperate latitudes of western North America make a nearly 4000-km migration biannually, negotiating the highest mountain ranges in North America. Near the Alaska-Canada border in southeastern Alaska these eagles migrate around the Wrangell and Saint Elias Mountains with peaks over 5000 m and the largest glaciers and ice fields on the continent. Eagles must fly either north of the Wrangell Mountains, or make a meridional shift to a more southern route via 1800-m elevation mountain passes (Fig. 2.1).

Understanding that migratory movements of soaring birds are affected by weather, we hypothesized that meteorological conditions proximate to the Wrangell Mountains encountered *en route* would, at least in part, determine the choice of route around the mountain range. We first predicted that cloudier and rainier conditions would affect the navigability of mountain passes by limiting visibility and because the moisture in the air would negatively affect performance of flight feathers, which would make the southern route less favorable. Given the general meridional orientation of the transition between routes, we also expected that velocity of the north-south wind would influence route choice, with headwinds in passes making the south route more energetically demanding and thus less favorable. Also, eagles are known to use orographic uplift as a flight subsidy (Katzner et al., 2015), so uplift generated by wind along each route could make a route energetically favorable. Lastly, thermal uplift is also known to influence flight performance of soaring birds (Mandel et al., 2008; Katzner et al., 2015), so we predicted it could affect this navigation decision such that thermals radiating from south-facing slopes might favor choice of the southern route, where south-facing slopes would be more abundant and receive greater solar radiation. We also considered that any combination of these hypothesized effects of weather could be additively driving route choice.

2.3 Methods

2.3.1 Model system

Golden eagles are a large soaring raptor distributed across the Holarctic (Watson, 2010). While some populations are classified as partially migratory, most individuals that summer and breed above approximately 55°N in North America are true long-distance migrants (Watson, 2010; Kochert et al., 2002). Golden eagles are predatory and opportunistic, utilizing for food resources many taxa, ranging from small mammals and birds to ungulates, often scavenging carrion (Kochert et al., 2002; Watson, 2010). Recent observations indicate that golden eagles likely occupy Alaska at high summer densities (McIntyre and Lewis, 2016).

Tracking efforts by the Alaska Department of Fish & Game (ADF&G), National

Park Service (NPS), and US Fish & Wildlife Service (USFWS) indicate that many of the golden eagles that summer and breed in southwestern and southcentral Alaska use a narrow migration corridor near Gunsight Mountain, Alaska (61.67°N 147.35°W; Fig. 2.1). Prior to reaching the corridor in the spring and just after moving through it in the fall, each individual eagle appears to select a migratory route—north or south—around the Wrangell Mountains. If the southern route is chosen, individuals must fly through 1800-m elevation mountain passes or occasionally at a high altitude over the southern aspect of the Saint Elias Mountains. The northern route requires no movement through such high-elevation terrain and is characterized by foothills and mountains with ∼700–1000-m valleys and passes. Additionally, neither route is shorter than the other (Fig. 2.1), and there is little evidence that either route has obvious advantages independent of weather conditions. Chitistone and Skolai passes, through which eagles fly to take the southern migration route, mark the eastern edge of the Wrangell Mountains and the western edge of the Saint Elias Mountains. The passes descend into the low elevation (∼200–300-m) Chitina River valley between the Wrangell and Chugach Mountains. It is important to note that while this population of eagles migrates between northern breeding grounds and southern overwintering areas, individuals migrate through southeastern/-central Alaska *east to west* during spring migration and *west to east* during fall migration (Fig 2.1). Hence, winds along the north-south axis, possibly modified by topography, can offer head-/tailwinds and/or orographic uplift for an eagle while transitioning to the chosen route. We explore the effects of wind and its effect on movement through mountain passes further in the Discussion.

2.3.2 Data collection

Golden eagles were captured with a remote-fired net launcher placed over carrion bait near Gunsight Mountain. Captures occurred during spring migration from mid March to mid April 2014-2016. Eagles were equipped with back pack solar-powered Argos/Global Positioning System (GPS) platform transmitter terminals (PTTs; Microwave Telemetry, Inc., Columbia, MD, USA). All eagles were sexually mature, with age estimated as en-

tering their 4th year at capture—though most were >5th year—so we did not consider effects of age (Bloom and Clark, 2001). PTTs were programmed to record GPS locations on duty cycles, ranging from 8-14 fixes per day during migration (8 hourly, 13 hourly plus midnight, or 3 hr fixed interval). Short days often resulted in insufficient battery voltage for PTTs to take fixes, so the resulting GPS tracks had missing observations.

During migration, route choice was scored (north or south) based on the individual's latitudinal location between 144.3°W and 142.3°W longitude, which approximately correspond to the east- and western edges of the Wrangell Mountains. Timestamps were recorded for the GPS location just prior to reaching those points. In none of the cases was route assignment ambiguous; eagles were either north of the mountain range or south, making it a clear binary decision for migrating individuals. If a tag did not record a complete enough track through the area to determine route, that decision was not scored nor included in the analyses.

Meteorological data were gathered from the National Centers for Environmental Prediction (NCEP)/National Center for Atmospheric Research (NCAR) Reanalysis I. Variables were interpolated in latitude, longitude, and time trilinearly with R and the package 'RNCEP' (Kemp et al., 2012) from the nearest four spatial points and two temporal times of prediction (2.5° spatial and 6-h temporal resolution). Each decision was assigned the values of environmental variables interpolated from the reanalysis to the surface at 61.744469°N 141.461205°W and 62.108325°N 145.554793°W for spring and fall migration, respectively, and the timestamp recorded by the transmitter just prior to reaching those areas of route divergence (Fig. 2.1). These environmental data are predicted on a much larger scale than how an animal interacts with them at precise points, so our results must be interpreted carefully. The overarching driver of the route choice process is likely the prevailing regional weather conditions, which are larger than the NCEP/NCAR model grid and also influence finer-scale weather, so although a finer model grid might capture more complexity, the weather variables interpolated to the chosen points should be representative of the process. Higher resolution data—both in terms of the movement data and meteorological data—would allow for more precise inferences on details of behaviors

and decisions; however, more complex analytical frameworks would be required.

2.3.3 Analyses

We modeled this binary decision of route choice as a Bernoulli random variable. We used the Bayesian equivalent of a Generalized Linear Model (GLM) with a *logit* link and hierarchical structure to account for effects of individual. The model was fit with Hamiltonian Monte Carlo (HMC) in R and Stan using the package 'rstanarm' (Stan Development Team, 2016). This was done with the function 'stan_glmer', using 20,000 HMC iterations, including 10,000 warm-up, and default weakly informative priors ($\mathcal{N}(0, 2.5^2)$ on coefficients and $\mathcal{N}(0, 10^2)$ intercepts). We confirmed model convergence to the posterior distribution with traceplots, Gelman diagnostics, effective sample sizes, and posterior plots of parameters (Stan Development Team, 2016).

We compared candidate models with leave-one-out cross-validation approximated by Pareto-smoothed importance sampling (PSIS-LOO) in R with the package 'loo' (Vehtari et al., 2016, 2017). We ranked the models by the expected *log* pointwise predictive density (i.e. out-of-sample predictive accuracy) transformed onto the deviance scale (i.e. looic; Vehtari et al., 2017), which allowed applying the rules of more traditional information-theoretic model selection (e.g., Δlooic > 2 to accept model as better fit; Burnham and Anderson, 2004). Lastly, to assess model fit and illustrate the effects of varying environmental conditions, we sampled from the posterior predictive distribution of the top model with the function 'posterior_predict' in 'rstanarm.' For models with multiple covariates, posterior predictive draws were done with the other covariate(s) (i.e. those not being visualized) held constant at the empirical values. The empirical data were shifted up or down one standard deviation to observe effects. Posterior predictive draws using the empirical data provided evidence of good model fit and predictive ability (Fig. 2.2 & S1). R code and the decision data are provided as supplementary material (see Appendix).

2.3.4 Candidate models

To understand the potential effect of meteorological conditions on how eagles choose a route around the Wrangell Mountains, we used four environmental predictor variables. We included barometric pressure as a predictor to capture approaching large scale weather systems. Weather fronts can approach the area from the Gulf of Alaska, deteriorating conditions along the south route. Blocking high pressure is predominant in Interior Alaska in spring, however, so low pressure could indicate a transition to a progressive pattern, which would make weather along the north route less predictable. Clouds and precipitation could also be caused by local, more stochastic conditions. To capture such a potential effect, we used relative humidity. At 100% humidity, clouds form and precipitation falls. Note that high humidity at the surface can indicate 100% humidity aloft, resulting in precipitation falling to the surface without air at the surface reaching 100% humidity. Winds can generate flight subsidies (orographic uplift) for eagles as well as turbulence. NCEP provides the zonal and meridional components of wind. We chose to include the meridional component (i.e. velocity of wind from south to north) in models, which would generally correspond to head- or tailwind support during a meridional shift in route. Positive meridional wind corresponds to winds from the south and negative winds from the north. We only used one wind component to avoid collinearity, and initial exploratory data summaries and modeling showed the zonal component to be much more consistent in magnitude and have little to no predictive power. The relatively low resolution of the movement data through the study area due to the programmed duty cycles and missing data did not permit using tailwind as a predictor. Lastly, surface sensible heat flux was used to approximate available thermal uplift, as it is often used to model uplift (Bohrer et al., 2012). We gave day of year careful thought as a predictor, as it could serve as a proxy for physiological changes and/or changes in urgency during migration, and constructed a candidate model set that included it (Table S2). Weather makes predictable seasonal progressions, however, so the addition of day of year into candidate models imparted collinearity. Additionally, an effect of day of year implies that one route is inherently shorter than the other, independent of weather, for which we do

not have evidence. We thus decided not to include it in the final set of candidate models; however, we would like to note that the modeling we did that included day of year did not find it to be a strong predictor of route choice (Table S2), despite evidence of its importance to other behavioral aspects of migration (Duerr et al., 2015; Miller et al., 2016).

Considering our hypothesized meteorological effects, we constructed a set of 30 candidate models, in addition to a null intercept-only model (Table S1). These included interactions with season, as we expected weather might have season-specific effects on route choice. As we did not have specific predictions about how certain combinations of variables might drive route choice, our model set was constructed with all possible additive combinations of variables and interactions with season. A north-south wind by season interaction would be expected due to opposing directions of migration between seasons, so we included wind only with a season interaction. All candidate models included a random intercept of individual to account for variability in route preference among individuals. Random slopes were not considered due to small individual-level sample sizes. Empirical meteorological predictor distributions were centered and standardized. Relative humidity is proportional, so we first applied the logistic transform to map it to an unconstrained space. Models with interactions included the main effects of the interacting variables as well. The predictor variables showed some correlation: Barometric pressure and sensible heat flux showed very little correlation ($r = 0.02$), wind and humidity showed the greatest amount of correlation ($r = 0.65$), and the remaining pairwise combinations showed low correlation ($-0.18 < r < 0.32$).

2.4 Results

We identified route choice for 44 individuals during spring and fall migrations 2014-17 (total of 73 fall and 62 spring individual migrations) and detected the ability to use either the north or south route for half of the 34 eagles tracked through the study area over multiple migrations. Northern routes were used 26% less often in the fall than spring (Table 2.1), but variability among intercept estimates indicates there was individual-level

variability in the probability of choosing the north route (Fig. S2-4), indicating that individuals exhibit an inherent preference for one route. Migrants generally encountered stronger winds, higher humidity, and greater thermal uplift in the spring than in the fall (Table 2.1).

The top two performing models provide evidence for effects of wind, season, and barometric pressure on the choice of route around the Wrangell Mountains (Table 2.2); the ranking indicates that the wind $\times$ season model was a negligibly better fit than the model including pressure. The effects of wind were season specific: Stronger winds from south to north in the fall caused more migrants to use the north route, whereas stronger south to north winds in the spring tended to shift use to the south route (Fig. 2.2). The model results indicate an increase in south to north wind of $\sim$2 m/s corresponds to $\sim$14% more eagles choosing the north route in fall and $\sim$7% fewer in spring, with similar opposite effect sizes for a reduction in south to north wind (Table 2.1, Figs. 2.2 & S2). Lastly, a reduction in barometric pressure by $\sim$0.01 bar increased use of the southern route in spring by $\sim$15% (Table 2.1, Figs. 2.2 & S3).

2.5 Discussion

Our results show how local to regional scale meteorological conditions can drive a discrete navigation decision, rerouting a migration. As weather patterns are changing on large scales with climate, it is reasonable to expect choice of migration routes to change. Reduction of the equatorial-polar thermal gradient via climate warming at the poles and anthropogenic increases in surface roughness have reduced wind speeds in North America and globally over the last few decades, with decay expected to continue (Pryor et al., 2009; Vautard et al., 2010; McVicar et al., 2012). Even small changes in wind have already been shown to alter ecology and trophic dynamics (Barton, 2014), highlighting the importance of understanding the effects of wind patterns on ecological and animal decision-making processes, such as annual migration.

The magnitude of the north wind clearly affects an eagle's choice to migrate north or south of the Wrangell Mountains, but uplift dynamics and how wind drives those

dynamics are also important. Winds would generate orographic uplift in the form of upslope winds in the foothills along each route. Migrants heading north in the spring migrate along the Wrangell Mountains in a general westbound direction (Fig. 2.1), and north winds would generate orographic uplift along the north-facing slopes of the north route. South winds could also generate orographic uplift along south-facing slopes of the south route and key passes in transitioning to the route. Orographic uplift has been shown to be an important energetic subsidy for migrating eagles (Katzner et al., 2015). In fall, north winds might offer tailwind support for eagles moving southwest to the south route, and south winds, a tailwind in moving northwest to the north route. Also, strong winds can cause clouds and precipitation along the windward route due to the orographic effect, which could favor use of the leeward route (Fig. 2.1). Furthermore, due to the solar trajectory, the more abundant south-facing slopes along the southern slope of the Wrangell Mountains would likely become free of snow earlier, offering additional flight subsidy in the form of thermal uplift and possibly incentive for shifting to the south route in spring (Lanzone et al., 2012; Vansteelant et al., 2017; Katzner et al., 2015; Duerr et al., 2012). Although the top two models were slightly better fits (Table 2.2), the third ranked model indicates individuals shift to the south route at a higher rate when thermal uplift is more limited in spring (Fig. 2.2).

Evidence for weather systems influencing migration timing exists (Shamoun-Baranes et al., 2006); however, we found evidence that changes in large scale weather patterns influence migration on scales as fine as discrete route choice (Table 2.2). Blocking high pressure is predominant in springtime interior Alaska, so a transition to a progressive or active weather pattern, signaled by a downward pressure trend, would correspond to much less predictable weather along the north route, likely making it less favorable to migrants. Our top model with barometric pressure predicted a strong effect of changes in pressure on spring route choice (Fig. 2.2), consistent with a meteorological progression away from the predominant, favorable conditions along the north route. Weather systems modifying pressure gradients can also shift migration routes due to inherent effects on wind conditions (Dokter et al., 2013).

Changes in migration routes due to individual decisions could additively have large-scale effects. Variable migratory behavior can affect energy expenditure (Flack et al., 2016; Teitelbaum et al., 2016), which can carry over to influence individual survival and reproductive success (Newton, 2006); these, in turn, can precondition population-level declines (Both et al., 2006). As we have shown, how fine-scale movement decisions emerge into a population-level movement corridors of migrants can be associated with individual preference and variables that will be altered by climate change. Monitoring fine-scale movement decisions of long-distance migrants, in particular, will be crucial as climate change advances, as dynamic conditions will alter decision-making processes and thus likely the basal energy expenditure associated with each possible decision (Shamoun-Baranes et al., 2017). Animals may be limited to fewer possible routes, or change might make additional routes available. For example, receding glaciers could open avenues of favorable uplift dynamics for soaring migrants in newly ice-free areas. In either case, an animal's decision will be driven, in part, by the environment, and better decisions will increase the chance of safe arrival to breeding areas, improve survival, and increase reproductive success (Shamoun-Baranes et al., 2017).

2.6 Ethics

Field procedures were conducted following the Alaska Department of Fish & Game Animal Care & Use Committee protocol #2013-036 and University of Alaska Fairbanks Institutional Animal Care & Use Committee protocol #859448.

2.7 Data, code, and materials

R code is provided as supplementary material (see Appendix). Raw movement data are archived in Movebank (`www.movebank.org`; IDs 17680093 and 19389828). The movement data contain information about the nest locations of a federally protected species and currently cannot be made publicly available per state mandate. However, the data can be made available for research at the discretion of the Alaska Department of Fish & Game and US Fish & Wildlife Service.

2.8 Competing interests

We have no competing interests.

2.9 Authors' contributions

JME, TLB, CPB, CLM, and SBL conceived and designed the study and collected the data. JME and GAB analyzed the data. All authors interpreted the results. JME wrote the initial draft of the paper, and GAB contributed to subsequent drafts. All authors edited and provided approval of the final draft.

2.10 Funding

Funding was provided by the Alaska Department of Fish & Game through the federal State Wildlife Grant Program, and the U.S. Fish & Wildlife Service (USFWS) provided transmitters and data. JME was supported by the Calvin J. Lensink Fund while conducting some of this research. The findings and conclusions of this article are those of the authors and do not necessarily represent the views of the USFWS.

2.11 Acknowledgements

We thank M. Kohan, B. Robinson, T. & D. Hawkins and many others for support in the field, and P. Doak and K. Kielland for helpful comments on drafts of the manuscript. We also thank the associate editor, J. M. Morales, T. Katzner, P. A. E. Alarcón, and three anonymous reviewers who provided additional constructive feedback during the review process.

2.12 References

Barton BT. 2014. Reduced wind strengthens top-down control of an insect herbivore. *Ecology* **95**: 2375–2381. doi: 10.1890/13-2171.1.

Bloom PH, Clark WS. 2001. Molt and sequence of plumages of golden eagles and a technique for in-hand ageing. *North American Bird Bander* **26**: 97–116.

Bohrer G, Brandes D, Mandel JT, Bildstein KL, Miller TA, Lanzone M, Katzner T, Maisonneuve C, Tremblay JA. 2012. Estimating updraft velocity components over large spatial scales: contrasting migration strategies of golden eagles and turkey vultures. *Ecology Letters* **15**: 96–103. doi: 10.1111/j.1461-0248.2011.01713.x.

Both C. 2010. Flexibility of timing of avian migration to climate change masked by environmental constraints en route. *Current Biology* **20**: 243–248. doi: 10.1016/j.cub.2009.11.074.

Both C, Artemyev AV, Blaauw B, Cowie RJ, Dekhuijzen AJ, Eeva T, Enemar A, Gustafsson L, Ivankina EV, Jarvinen A, Metcalfe NB, Nyholm NEI, Potti J, Ravussin PA, Sanz JJ, Silverin B, Slater FM, Sokolov LV, Torok J, Winkel W, Wright J, Zang H, Visser ME. 2004. Large-scale geographical variation confirms that climate change causes birds to lay earlier. *Proceedings of the Royal Society B: Biological Sciences* **271**: 1657–1662. doi: 10.1098/rspb.2004.2770.

Both C, Bouwhuis S, Lessells CM, Visser ME. 2006. Climate change and population declines in a long-distance migratory bird. *Nature* **441**: 81–83. doi: 10.1038/nature04539.

Breed GA, Golson EA, Tinker MT. 2017. Predicting animal home-range structure and transitions using a multistate Ornstein-Uhlenbeck biased random walk. *Ecology* **98**: 32–47. doi: 10.1002/ecy.1615.

Burnham KP, Anderson R. 2004. Multimodel inference: understanding AIC and BIC in model selection. *Sociological Methods & Research* **33**: 261–304. doi: 10.1177/0049124104268644.

Cotton PA. 2003. Avian migration phenology and global climate change. *Proceedings of the National Academy of Sciences* **100**: 12219–12222. doi: 10.1073/pnas.1930548100.

Crick HQP. 2004. The impact of climate change on birds. *Ibis* **146**: 48–56.

Dokter AM, Shamoun-Baranes J, Kemp MU, Tijm S, Holleman I. 2013. High Altitude Bird Migration at Temperate Latitudes: A Synoptic Perspective on Wind Assistance. *PLoS ONE* **8**: 1–8. doi: 10.1371/journal.pone.0052300.

Drewitt AL, Langston RHW. 2006. Assessing the impacts of wind farms on birds. *Ibis* **148**: 29–42. doi: 10.1111/j.1474-919X.2006.00516.x.

Duerr AE, Miller Ta, Lanzone M, Brandes D, Cooper J, O'Malley K, Maisonneuve C, Tremblay J, Katzner T. 2012. Testing an emerging paradigm in migration ecology shows surprising differences in efficiency between flight modes. *PLoS ONE* **7**: e35548. doi: 10.1371/journal.pone.0035548.

Duerr AE, Miller TA, Lanzone M, Brandes D, Cooper J, O'Malley K, Maisonneuve C, Tremblay Ja, Katzner T. 2015. Flight response of slope-soaring birds to seasonal variation in thermal generation. *Functional Ecology* **29**: 779–790. doi: 10.1111/1365-2435.12381.

Flack A, Fiedler W, Blas J, Pokrovsky I, Kaatz M, Mitropolsky M, Aghababyan K, Fakriadis I, Makrigianni E, Jerzak L, Azafzaf H, Feltrup-Azafzaf C, Rotics S, Mokotjomela TM, Nathan R, Wikelski M. 2016. Costs of migratory decisions: A comparison across eight white stork populations. *Science Advances* **2**: e1500931. doi: 10.1126/sciadv.1500931.

Hooten MB, Johnson DS, McClintock BT, Morales JM. 2017. *Animal movement: statistical models for telemetry data.* New York: CRC Press.

Katzner TE, Turk PJ, Duerr AE, Miller TA, Lanzone MJ, Cooper JL, Brandes D, Tremblay JA, Lemaître J. 2015. Use of multiple modes of flight subsidy by a soaring terrestrial bird, the golden eagle Aquila chrysaetos, when on migration. *Journal of Royal Society Interface* **12**: 20150530. doi: 10.1098/rsif.2015.0530.

Kemp MU, Emiel van Loon E, Shamoun-Baranes J, Bouten W. 2012. RNCEP: global weather and climate data at your fingertips. *Methods in Ecology and Evolution* **3**: 65–70. doi: 10.1111/j.2041-210X.2011.00138.x.

Kochert MN, Steenhof K, McIntyre CL, Craig EH. 2002. Golden Eagle (Aquila chrysaetos). In Poole A (ed.) *The Birds of North America.* Ithaca: Cornell Lab of Ornithology.

La Sorte FA, Fink D. 2017. Projected changes in prevailing winds for transatlantic migratory birds under global warming. *Journal of Animal Ecology* **86**: 273–284. doi: 10.1111/1365-2656.12624.

Lanzone MJ, Miller Ta, Turk P, Brandes D, Halverson C, Maisonneuve C, Tremblay J, Cooper J, O'Malley K, Brooks RP, Katzner T. 2012. Flight responses by a migratory soaring raptor to changing meteorological conditions. *Biology Letters* **8**: 710–713. doi: 10.1098/rsbl.2012.0359.

Mandel JT, Bildstein KL, Bohrer G, Winkler DW. 2008. Movement ecology of migration in turkey vultures. *Proceedings of the National Academy of Sciences of the United States of America* **105**: 19102–19107. doi: 10.1073/pnas.0801789105.

McIntyre CL, Lewis SB. 2016. Observations of migrating Golden Eagles (Aquila chrysaetos) in Eastern Interior Alaska offer insights on population size and migration monitoring. *Journal of Raptor Research* **50**: 254–264.

McVicar TR, Roderick ML, Donohue RJ, Li LT, Van Niel TG, Thomas A, Grieser J, Jhajharia D, Himri Y, Mahowald NM, Mescherskaya AV, Kruger AC, Rehman S, Dinpashoh Y. 2012. Global review and synthesis of trends in observed terrestrial near-surface wind speeds: Implications for evaporation. *Journal of Hydrology* **416-417**: 182–205. doi: 10.1016/j.jhydrol.2011.10.024.

Miller TA, Brooks RP, Lanzone MJ, Brandes D, Cooper J, Tremblay JA, Wilhelm JAY, Duerr A, Katzner TE. 2016. Limitations and mechanisms influencing the migratory performance of soaring birds. *Ibis* **158**: 116–134. doi: 10.1111/ibi.12331.

Nathan R, Getz WM, Revilla E, Holyoak M, Kadmon R, Saltz D, Smouse PE. 2008. A movement ecology paradigm for unifying organismal movement research. *Proceedings of the National Academy of Sciences* **105**: 19052–9. doi: 10.1073/pnas.0800375105.

Newton I. 2006. Can conditions experienced during migration limit the population levels of birds? *Journal of Ornithology* **147**: 146–166. doi: 10.1007/s10336-006-0058-4.

Pryor SC, Barthelmie RJ, Young DT, Takle ES, Arritt RW, Flory D, Gutowski WJ, Nunes A, Roads J. 2009. Wind speed trends over the contiguous United States. *Journal of Geophysical Research Atmospheres* **114**: D14105. doi: 10.1029/2008JD011416.

Shamoun-Baranes J, Bouten W, Van Loon EE. 2010. Integrating meteorology into research on migration. *Integrative and Comparative Biology* **50**: 280–292. doi: 10.1093/icb/icq011.

Shamoun-Baranes J, Liechti F, Vansteelant WM. 2017. Atmospheric conditions create freeways, detours and tailbacks for migrating birds. *Journal of Comparative Physiology A: Neuroethology, Sensory, Neural, and Behavioral Physiology* **203**: 509–529. doi: 10.1007/s00359-017-1181-9.

Shamoun-Baranes J, van Loon E, Alon D, Alpert P, Yom-Tov Y, Leshem Y. 2006. Is there a connection between weather at departure sites, onset of migration and timing of soaring-bird autumn migration in Israel? *Global Ecology and Biogeography* **15**: 541–552. doi: 10.1111/j.1466-822X.2006.00261.x.

Shepard ELC, Wilson RP, Rees WG, Grundy E, Lambertucci SA, Vosper SB. 2013. Energy landscapes shape animal movement ecology. *The American Naturalist* **182**: 298–312. doi: 10.1086/671257.

Stan Development Team. 2016. rstanarm: Bayesian applied regression modeling via Stan. R package version 2.13.1.

Teitelbaum CS, Converse SJ, Fagan WF, Böhning-Gaese K, O'Hara RB, Lacy AE, Mueller T. 2016. Experience drives innovation of new migration patterns of whooping cranes in response to global change. *Nature Communications* **7**: 12793. doi: 10.1038/ncomms12793.

Vansteelant WMG, Shamoun-Baranes J, Mclaren J, van Diermen J, Bouten W. 2017. Soaring across continents: decision-making of a soaring migrant under changing atmospheric conditions along an entire flyway. *Journal of Avian Biology* **48**: 887–896. doi: 10.1111/jav.01298.

Vautard R, Cattiaux J, Yiou P, Thépaut JN, Ciais P. 2010. Northern Hemisphere atmospheric stilling partly attributed to an increase in surface roughness. *Nature Geoscience* **3**: 756–761. doi: 10.1038/ngeo979.

Vehtari A, Gelman A, Gabry J. 2016. loo: efficient leave-one-out cross-validation and WAIC for Bayesian models. R package version 1.0.0.

Vehtari A, Gelman A, Gabry J. 2017. Practical Bayesian model evaluation using leave-one-out cross-validation and WAIC. *Statistics and Computing* **27**: 1413–1432. doi: 10.1007/s11222-016-9696-4.

Watson J. 2010. *The Golden Eagle*. New Haven: Yale University Press, second edition.

Webster MS, Marra PP, Haig SM, Bensch S, Holmes RT. 2002. Links between worlds: unraveling migratory connectivity. *Trends in Ecology and Evolution* **17**: 76–83. doi: 10.1016/S0169-5347(01)02380-1.

Winkler DW, Jørgensen C, Both C, Houston AI, McNamara JM, Levey DJ, Partecke J, Fudickar A, Kacelnik A, Roshier D, Piersma T. 2014. Cues, strategies, and outcomes: how migrating vertebrates track environmental change. *Movement Ecology* **2**: 10. doi: 10.1186/2051-3933-2-10.

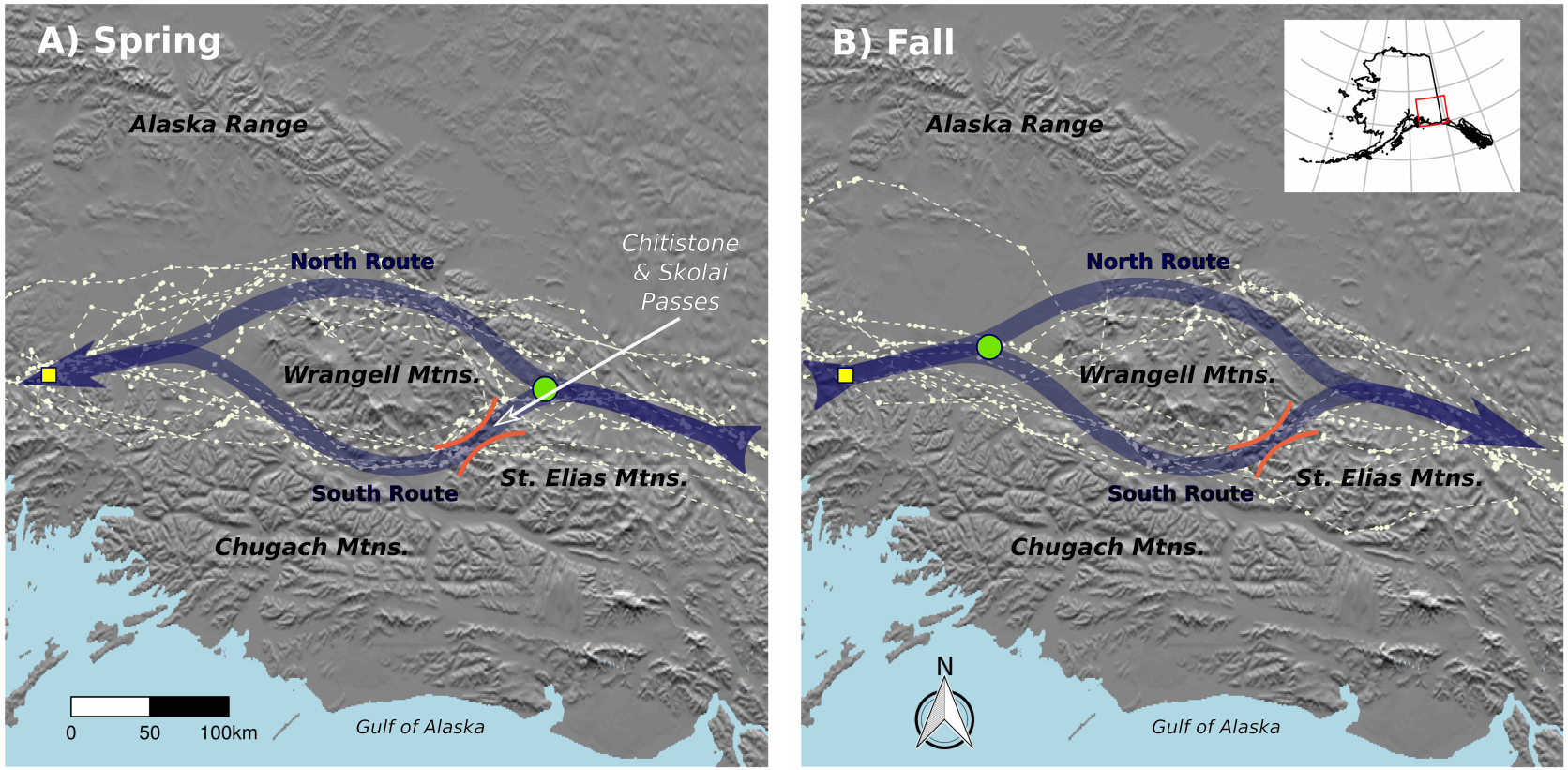

Figure 2.1: Relief map of the study area with relevant mountain ranges labeled and golden eagle route choice around the Wrangell Mountains illustrated. Labeled arrows correspond to the approximate direction of migration for the indicated season. Beige points correspond to the discrete GPS locations recorded by the transmitters for 28 example eagle tracks with transmitters on intervals of one to several hours with dashed lines showing linear interpolations between. Green filled circle is the spatial location weather data were interpolated to. Yellow filled square is the location of Gunsight Mountain. Location of Chitistone Pass shown by red lines.

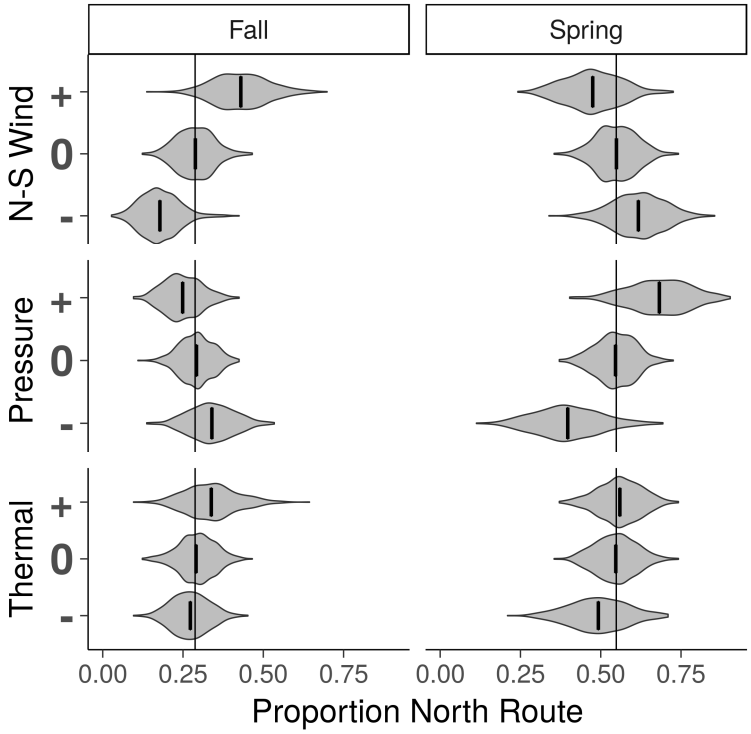

Figure 2.2: Model predictions of effects of meteorological variables on the proportion of 135 eagle decisions resulting in a route north of the Wrangell Mountains. Violins are composed of 1000 posterior predictive draws from top fitting models with vertical bars showing means. Zero indicates posterior predictive draws with observed data—done as a posterior predictive check to confirm the models predict reasonably well—and plus and minus indicate the empirical values + and − one standard deviation, respectively. Vertical lines represent the observed proportions of eagles that chose the north route. N-S wind corresponds to the velocity of the wind from south to north. Distributions right of the observed proportion indicate that variable, if changed, would increase the proportion of eagles choosing the north route.

Table 2.1: Proportion of golden eagles tracked that chose a northern migration route around the Wrangell Mountains and the summary statistics of meteorological variables interpolated to the approximate location and time each eagle chose a route. Pooled summaries and summaries specific to route choice presented. N-S wind is velocity of south to north wind. Negative thermal uplift (surface sensible heat flux) is flux towards the surface.

Season	Route	Proportion North Route	N-S Wind m/s $(s.d.)$	Relative Humidity % $(s.d.)$	Barometric Pressure Bar $(s.d.)$	Thermal Uplift Wm^{-2} $(s.d.)$
Fall		0.29	−0.66 (1.88)	76.61 (17.18)	1.011 (0.012)	−29.48 (26.85)
	North		−0.20 (1.68)	81.59 (14.98)	1.007 (0.009)	−24.82 (28.49)
	South		−0.84 (1.94)	74.60 (17.73)	1.012 (0.013)	−31.37 (26.21)
Spring		0.55	1.92 (2.23)	90.50 (7.69)	1.008 (0.006)	−3.21 (25.09)
	North		1.61 (1.91)	90.24 (7.97)	1.009 (0.006)	−0.38 (24.61)
	South		2.30 (2.56)	90.81 (7.46)	1.007 (0.006)	−6.65 (25.69)

Table 2.2: Candidate models of route choice around the Wrangell Mountains ranked by leave-one-out cross-validation approximated by Pareto-smoothed importance sampling. Lower information criterion (looic) indicates better model fit. Top 10 candidate models and null intercept-only model shown. All models include random intercept for individual. Interaction models include all main effects. Meteorological predictors were interpolated to the approximate location and time each eagle chose a route. 'Wind' is the velocity of south to north wind. Negative thermal uplift (surface sensible heat flux) is flux towards the surface.

Model	looic	Δlooic
wind $\times$ season	146.5	0
wind $\times$ season + pressure $\times$ season	148.1	1.6
wind $\times$ season + thermal	148.8	2.3
wind $\times$ season + pressure $\times$ season + thermal	149.2	2.7
wind $\times$ season + pressure	149.4	2.9
pressure $\times$ season	149.5	3.0
wind $\times$ season + humidity	149.9	3.4
wind $\times$ season + thermal $\times$ season	151.0	4.5
pressure $\times$ season + thermal	151.3	4.8
season	151.4	4.9
null	159.7	13.2

Chapter 3: Dynamic-parameter movement models reveal drivers of migratory pace in a soaring bird

3.1 Abstract

Long distance migration can increase lifetime fitness, but can be costly, incurring increased energetic expenses and higher mortality risks. Stopover and other en route behaviors allow animals to rest and replenish energy stores and avoid or mitigate other hazards during migration. Some animals, such as soaring birds, can subsidize the energetic costs of migration by extracting energy from flowing air. However, it is unclear how these energy sources affect or interact with behavioral processes and stopover in long-distance soaring migrants. To understand these behaviors and the effects of processes that might enhance use of flight subsidies, we developed a flexible mechanistic model to predict how flight subsidies drive migrant behavior and movement processes. The novel modelling framework incorporated time-varying parameters informed by environmental covariates to characterize a continuous range of behaviors during migration. This model framework was fit to GPS satellite telemetry data collected from a large soaring and opportunist foraging bird, the golden eagle (*Aquila chrysaetos*), during migration in western North America. Fitted dynamic model parameters revealed a clear circadian rhythm in eagle movement and behavior, which was directly related to thermal uplift. Behavioral budgets were complex, however, with evidence for a joint migrating/foraging behavior, resembling a slower paced fly-and-forage migration, which could facilitate efficient refueling while still ensuring migration progress. In previous work, ecological and foraging conditions are usually considered to be the key aspects of stopover location quality, but taxa, such as the golden eagle, that can tap energy sources from moving fluids to drive migratory locomotion may pace migration based on both foraging opportunities and available flight subsidies.

Eisaguirre, JM, M Auger-Méthé, CP Barger, SB Lewis, TL Booms, GA Breed. 2019. Dynamic-parameter movement models reveal drivers of migratory pace in a soaring bird. Frontiers in Ecology and Evolution 7: 317.

3.2 Introduction

Long-distance migration can relax competition and permit use of seasonally available resources, helping many animals maximize lifetime fitness (Newton, 2008; Avgar et al., 2014). Those benefits, however, come at substantial costs, including greater vulnerability to predators, uncertain conditions, mechanical wear, elevated energy expenditure, and time (Alerstam and Hedenström, 1998; Clark and Butler, 1999; Hedenström, 2008; Newton, 2008; Avgar et al., 2014). As many migrant species cannot store sufficient energy for nonstop, long-distance migration, stopover evolved as a behavior for strategically resting and refueling en route (Gill, 2007).

Migrant species are adapted for utilizing either soaring or flapping flight, and the different flight modes translate into stopover strategy (Hedenström, 1993; Gill, 2007). Generally, soaring flight is favorable for larger birds and flapping flight for smaller birds, though the partitioning of time for each flight mode during migration is dependent on the tradeoff between time and energy (Hedenström, 1993; Duerr et al., 2015; Katzner et al., 2015; Miller et al., 2016). In theory, a time-minimizing migrator would be expected to fly with greater directional persistence and stronger directional bias than would an energy-expenditure minimizer. Such net energy maximizers would be expected to take advantage of en route foraging opportunities and may divert or delay to replenish energy reserves. (Note that “energy minimization" has been used to describe this strategy (e.g., Alerstam, 2011; Miller et al., 2016), but we use “net energy maximization" for clarity.) If time is less important, a net energy maximizer is less restricted and can spend additional time seeking an energetically superior path; the emergent path would then be more tortuous with less directional bias toward the final destination at any given point along the route. Time minimization and net energy maximization strategies are not mutually exclusive, however, and the emergent strategy and behaviors in any given migrating individual lies along a continuum (Alerstam, 2011; Miller et al., 2016).

Obligate soaring migrants must also consider routes based on their energy landscape (Shamoun-Baranes et al., 2010), the energetic constraints of movement over space (Shepard et al., 2013), which also contributes to a migrant’s location along the behavioral

continuum. While soaring migrants can stopover, their energy landscape is more complex. Meteorological conditions are at least as important as foraging resources for soaring migrants, which can be extremely dynamic and subsidize the energetic cost of flight directly via uplift (Pennycuick, 1971; Alerstam, 1979; Spaar and Bruderer, 1997; Gill, 2007; Duerr et al., 2012; Murgatroyd et al., 2018).

The flight performance of soaring migrants relative to subsidies provided by meteorological conditions has been well documented (Pennycuick, 1971; Alerstam, 1979; Spaar and Bruderer, 1997), establishing a clear link between diurnal migrant behavior and development of the atmospheric boundary layer. Two primary forms of uplift arise by (1) wind interacting with topography to form upslope wind or mountain waves (air currents forming standing waves established on the lee side of mountains; hereafter orographic uplift) and (2) solar heating of the earth's surface to generate thermal uplift. Other forms arise from turbulent eddies over small landscape features and ocean waves modifying the air. The dynamic nature of atmospherically-driven flight subsidies requires detailed movement data as well as carefully designed analytical techniques to investigate certain mechanisms hidden in those data.

Our understanding of migratory processes has advanced enormously in the past 30 years, as animal tracking technology developed from a novelty of coarse observation to a core method for observing animal behavior and movement in incredible detail (Luschi et al., 1998; Sawyer et al., 2005; Bridge et al., 2011; Katzner et al., 2015; Hooten et al., 2017). Global Positioning System (GPS) telemetry, in particular, allows remote observation of animal relocations across a broad spatiotemporal scale. GPS transmitters are now light and reliable enough to study the complete migrations of many large soaring migrants, including golden eagles *Aquila chrysaetos*, which often rely on flight subsidies during migration (Katzner et al., 2015). Golden eagles and other large soaring birds have been used as model systems for phenomenologically evaluating questions about migratory flight performance and migration strategies (*sensu* Duerr et al., 2012; Lanzone et al., 2012; Katzner et al., 2015; Vansteelant et al., 2015; Miller et al., 2016; Shamoun-Baranes et al., 2016; Rus et al., 2017). For example, Lanzone et al. (2012) and Katzner et al. (2015) found

that golden eagles use both thermal and orographic uplift to subsidize migratory flight, although thermal soaring was often more efficient in long distance, directed flight (Duerr et al., 2012). While these studies have contributed to our understanding of soaring migration and have laid a foundation for more detailed approaches, they relate meteorology to derived movement metrics, rather than incorporate them into process-based models that mechanistically predict movement, and ignore the temporal dependence between serially observed locations (i.e. autocorrelation). Not accounting for such autocorrelation imparts bias on certain estimated parameters (e.g., variances) thereby affecting inference through, for example, underestimating uncertainty. Consequently, the links between resources distributed over the landscape, such as flight subsidies, and behavioral budgets, including stopover behavior, during migrations of soaring birds remain unclear.

Unlike previous approaches, process-based, mechanistic movement models allow explicit inference of the underlying mechanisms driving movement (e.g., changes in behavior) that may not be available from conventional phenomenological analytical approaches (Turchin, 1998; Nathan et al., 2008; Hooten et al., 2017). While it is impossible to understand fully the intricacies in animal movement, we can pose mathematical models (e.g., correlated random walks) to approximate the movement process (Kareiva and Shigesada, 1983; Turchin, 1998). We can then fit these models statistically to observed data to estimate parameters describing behavior and its relationship with dynamic environmental features that moving animals experience (Blackwell, 1997, 2003; Morales et al., 2004; Breed et al., 2017; Hooten et al., 2017). Many of the recently developed mechanistic movement models are built in a discrete state-switching framework, where animals switch between discrete behavioral states (see (Hooten et al., 2017) and references cited therein). Choosing both the biologically relevant and quantitatively supported number of states, as well as interpreting the identified states in a biological context, remains challenging (Patterson et al., 2017; Pohle et al., 2017). Often, this challenge leads researchers to artificially limit the number of states and/or collapse two or more states into one biologically interpretable state. For example (Pirotta et al., 2018), presented a model with five discrete kinds of avian flight, but the complexity of the model made interpreting those

states difficult and poorly matched classifications manually identified by an expert.

In many cases, a more natural approach to modeling an animal's movement process is along a dynamic continuum, rather than as switching between discrete behavioral states (Breed et al., 2012; Auger-Méthé et al., 2017; Jonsen et al., 2019). Modelling along a continuum may be an especially useful approach for understanding movement behavior in soaring birds, considering the dynamic nature of atmospheric processes that influence movements. Here, we developed and applied a flexible mechanistic movement model based on a correlated random walk with time-varying parameters. This novel model was fit to movement data collected via GPS telemetry to understand how individuals in a population of long-distance soaring migrants use flight subsidies and budget stopover and migration behavior. Specifically, we were interested in identifying which flight subsidies influence stopover and migratory behavior and how the effect of key subsides and behaviors varied between spring and fall migrations. Our approach resembled continuous-time correlated random walks (Johnson et al., 2008; Blackwell et al., 2015; Gurarie et al., 2017; Michelot and Blackwell, 2019), but was easily implemented and yielded a relatively small number of dynamic parameters that could be directly interpreted biologically. A set of candidate models could be ranked, with model selection approaches, providing inference on how behavioral budgets and meteorological variables interacted to give rise to the observed migration paths. Modeling the effects of dynamic wind and uplift variables as time-varying movement behaviors of migratory golden eagles further allowed new details to emerge without imposing artificially discrete states.

3.3 Methods

3.3.1 Model system

The golden eagle is a large, soaring raptor, distributed across the Holarctic (Watson, 2010). Golden eagles are predatory and opportunistic, utilizing many taxa for food resources, ranging from small mammals and birds to ungulates, often scavenging carrion (Kochert et al., 2002; Watson, 2010). While many populations are classified as partial migrants, most individuals that summer and breed above approximately 55°N in North

America are considered true long-distance migrants (Watson, 2010; Kochert et al., 2002). The population we observed in this study migrates over the mountainous regions of western North America between a breeding range primarily in southcentral Alaska, USA and a broad overwintering range in western North America that ranges from the southwestern US to central British Columbia and Alberta, Canada (Bedrosian et al., 2018).

3.3.2 Data collection

We captured golden eagles with a remote-fired net launcher, placed over carrion bait near Gunsight Mountain, Alaska (61.67°N 147.35°W). Captures occurred between mid-March and mid-April 2014-2016. Fifty-three adult and sub-adult eagles were equipped with 45-g back pack solar-powered Argos/GPS platform transmitter terminals (PTTs; Microwave Telemetry, Inc., Columbia, MD, USA). Eagles were sexed molecularly and aged by plumage.

PTTs were programmed to record GPS locations on duty cycles, ranging from 8-14 fixes per day during migration, depending on year of deployment. PTTs deployed in 2014 were set to record 13 locations at one-hour intervals centered around solar noon plus a location at midnight local time. PTTs deployed in 2015 were programmed to record 8 locations with one-hour intervals centered around solar noon, and PTTs deployed in 2016 took eight fixes daily at regular 3-hr time intervals. Note that the PTTs deployed in 2015 did not record locations overnight. Poor battery voltage from September to March often resulted in PTTs failing to take all programmed fixes, so the resulting GPS tracks had missing observations during these periods. Tags lasted multiple seasons, and in fact many are still deployed and transmitting at this writing. We chose to limit this analysis to the migrations that occurred in 2016. The spring and fall migratory pathways of the 2016 migration from 26 tags were available and suitable for analysis in that year: 11 deployed in 2014, 7 deployed 2015, and 8 deployed 2016. Tracks were suitable for analysis based on having few missing data, with no more than a few days of consecutive missing locations.

Movement data were managed in the online repository Movebank (www.movebank.org/), and we used the Track Annotation Service (Dodge et al., 2013) to extract flight subsidy

(wind and uplift) data, specific to each PTT location and time of recording that location, along eagle tracks. The Track Annotation Service derives uplift variables from elevation models and weather and atmospheric reanalyses (Bohrer et al., 2012). We followed the Movebank recommendations for interpolation methods; details are below.

3.3.3 Movement model

We developed a correlated random walk (CRW) movement model to reveal how changes in behavior give rise to the movement paths of migrating eagles. We chose to use a dynamic, time-varying correlation parameter, which represents behavior as a continuum rather than discrete categories, to capture complex behavioral patterns that could occur on multiple temporal and spatial scales (Breed et al., 2012; Auger-Méthé et al., 2017; Jonsen et al., 2019). We believe this approach can offer substantial flexibility, as a continuous range of behaviors is more realistic and, as we show, more naturally allows modeling behavior as a function of covariates.

The basic form of the model was a first-difference CRW presented by Auger-Méthé et al. (2017), which can take the form:

$$\mathbf{x}_i|\mathbf{x}_{i-1},\mathbf{x}_{i-2} \sim \mathcal{N}_2\left(\mathbf{x}_{i-1} + \gamma_i \frac{\Delta t_i}{\Delta t_{i-1}}(\mathbf{x}_{i-1} - \mathbf{x}_{i-2}),\ \mathbf{\Sigma}_i\right), \tag{3.1}$$

where

$$\mathbf{\Sigma}_i = \begin{bmatrix} \Delta t_i^2\sigma_x^2 & 0 \\ 0 & \Delta t_i^2\sigma_y^2 \end{bmatrix}, \quad \sigma_x, \sigma_y > 0. \tag{3.2}$$

Here, $\Delta t_i = t_i - t_{i-1}$ represents the time interval between Cartesian coordinate vectors $\mathbf{x}_i$ and $\mathbf{x}_{i-1}$ for the observed locations of the animal at times t_i and t_{i-1}. Incorporating autocorrelation in behavior, γ_i constitutes a random walk, such that

$$\gamma_i|\gamma_{i-1} \sim \mathcal{N}\left(\gamma_{i-1},\ \Delta t_i^2\sigma_\nu^2\right), \quad \sigma_\nu > 0. \tag{3.3}$$

γ_i correlates displacements (or 'steps') and can be interpreted to understand the type of movement, and thus behavior, of migrating individuals: estimates of γ_i closer to one

indicate directionally-persistent, larger-scale migratory movement, while estimates of γ_i closer to zero indicate more-tortuous, smaller-scale stopover movement (Breed et al., 2012; Auger-Méthé et al., 2017). Scaling γ_i by $\frac{\Delta t_i}{\Delta t_{i-1}}$ and the variance components by Δt_i^2 allows us to accommodate unequal time intervals (Auger-Méthé et al., 2017), which can arise from a PTT's pre-programmed duty cycles and/or missed location attempts. This assumes that over longer time intervals an animal is likely to move greater distances and that the previous step will have less influence on the current step. Notably, in introducing Δt_i, this CRW essentially becomes a correlated velocity model presented in terms of displacement vectors $(\mathbf{x}_{i-1} - \mathbf{x}_{i-2})$ (Johnson et al., 2008; Blackwell et al., 2015; Gurarie et al., 2017), most closely resembling the autocorrelated velocity model presented by Gurarie et al. (2017). Because location error of GPS data is negligible compared to the movement of most large vertebrates (Hooten et al. 2017), we did not incorporate an observation equation to handle location error. While a covariance parameter could be added to the model, we chose to fix covariance to zero (equation 2), which assumes that movement in the x and y dimensions are independent. This assumption has been suggested to be potentially problematic (Dunn and Gipson, 1977; Blackwell, 1997); however, it is common and has been shown to draw reasonable inference from real data, as well as recover known parameters from simulated data (Breed et al., 2012; Auger-Méthé et al., 2017; Breed et al., 2017; Jonsen et al., 2019). To support this, we compared results from the model assuming zero covariance to one fit assuming equal variance in x and y—like estimating covariance, this ensures invariance under linear transformation of the coordinate system—to illustrate that inference remains unaffected by this assumption (see Appendix).

Extending this CRW to introduce environmental covariates, we first made the assumption that an individual's behavior can be adequately explained by the previous behavior plus some effects of environmental conditions and random noise. This modeling approach and philosophy aligns with the movement ecology paradigm presented by Nathan et al. (2008): An animal's movement path is influenced by its internal state and the environmental conditions it experiences. We modified the behavioral (or internal state)

process—previously described above as a pure random walk in one dimension (equation 3)—similar to a linear model with a *logit* link function. The *logit* link constrains $\gamma_i \in [0, 1]$ and allowed us to model it as a linear combination of continuously-distributed random variables (Jonsen et al., 2019). These variables were different meteorological conditions affecting flight subsidies. Now,

$$\gamma_i' = \log\left(\frac{\gamma_i}{1-\gamma_i}\right), \tag{3.4}$$

where

$$\gamma_i' = \gamma_{i-1}' + \mathbf{Z}_i^{\mathrm{T}}\boldsymbol{\beta} + \epsilon_i, \tag{3.5}$$

$$\epsilon_i \sim \mathcal{N}\left(0,\ \Delta t_i^2 \sigma_\nu^2\right), \tag{3.6}$$

and $\mathbf{Z}_i^{\mathrm{T}}$ is the row vector of environmental covariates associated with $\mathbf{x}_i$. Each element of the vector $\boldsymbol{\beta}$ is an estimated parameter representing the magnitude and direction of the effect of its respective covariate on the correlation parameter γ_i in addition to the effect of γ_{i-1}. Note that including γ_{i-1} here preserves explicit serial correlation in the behavioral process so that any additional environmental effect is not overestimated. γ_i' is only used to estimate γ_i; any behavioral interpretations are made in terms of γ_i.

3.3.4 Model fitting

Subsetting tracks.. Of the 26 eagles producing suitable data in 2016, we fit the model to 15 spring and 16 fall adult golden eagle migration tracks recorded by 18 adult males and 8 adult females in 2016. This included both spring and fall migrations for five individuals. In reporting the results, we assumed any individual random effects of including both migrations for these few individuals to be negligible, which seems reasonable given fitted parameters presented in Table S7.1. The model was fit only to the migratory periods, plus two fixes prior to departure to ensure valid parameter estimates at the onset of migration. Data were constrained to migratory periods under the following rules: The first migration step was identified as the first directed movement away from what was

judged to be an individual's summer (or winter) range with no subsequent return to that range, and the final migration step was defined as the step terminating in the apparent winter (or summer) range. This assignment was usually straightforward; however, in some cases there were apparent pre-migration staging areas. These were not considered part of migration and excluded from the analysis here; movement data from these individuals collected during the breeding and overwintering periods are neither presented nor analyzed here.

Environmental covariates.. Golden eagles can switch between using thermal and orographic uplift as flight subsidies (Lanzone et al., 2012; Katzner et al., 2015), so we included both variables as covariates affecting the correlation parameter in the behavioral process of the CRW (equation 5). Thermal uplift $\mathbf{z}_{tu}$ and orographic uplift $\mathbf{z}_{ou}$ are measured in m/s with $\mathbf{z}_{tu}, \mathbf{z}_{ou} \in [0, \infty)$. Thermal uplift was bilinearly interpolated from European Centre for Medium-Range Weather Forecasts (ECMWF) reanalyses, and orographic uplift from the nearest neighbor (grid cell) by pairing National Center for Environmental Predictions (NCEP) North American Regional Reanalysis (NARR) data with the Advanced Spaceborne Thermal Emission Reflection Radiometer (ASTER) Global Digital Elevation Model (GDEM; Brandes and Ombalski, 2004; Bohrer et al., 2012). We also introduced wind as a covariate in the behavioral process, as it can influence eagle flight as well as the flight and energy landscape of many birds during migration (Shamoun-Baranes et al., 2017). Wind data were bilinearly interpolated from the NCEP NARR u (easterly/zonal) and v (northerly/meridional) components of wind predicted 30 m above ground in m/s, from which we calculated the wind support $\mathbf{z}_{tw}$, such that $\mathbf{z}_{tw} \in (-\infty, \infty)$ (Safi et al., 2013), where positive values correspond to tailwind and negative values headwind. The bearings used to calculate each $z_{tw,i}$ were the compass bearings required to arrive at $\mathbf{x}_{i+1}$ from $\mathbf{x}_i$.

We included a time of day interaction in the model because of clear diurnal effects. This also helped reduce zero inflation, particularly for thermal uplift, which often decays to zero after sunset due to heat flux and atmospheric boundary layer dynamics. To introduce the interaction, we used a dummy variable $\mathbf{z}_0$, such that $z_{0,i} = 0$ when t_i fell

after sunset but before sunrise and $z_{0,i} = 1$ when t_i fell after sunrise but before sunset. This assumed behavior was not dependent on the covariates at night—the combination of covariates becomes zero when $z_{0,i} = 0$—which is sensible given observed diurnal behavioral cycles. Sunrise and sunset times local to each GPS point were calculated in R with the 'sunriset' function in the package 'maptools' (R Core Team, 2016; Bivand and Lewin-Koh, 2016). Writing out the matrix operation in equation 5, the final overall formulation of the behavioral process for the full model was:

$$\gamma_i' = \gamma_{i-1}' + [\beta_0 + \beta_{ou}(z_{ou,i} \times z_{0,i}) + \beta_{tu}(z_{tu,i} \times z_{0,i}) + \beta_{tw}(z_{tw,i} \times z_{0,i})] + \epsilon_i, \tag{3.7}$$

Prior to fitting the model, we followed Gelman et al. (2008) and *log*-transformed the uplift covariates and standardized variance to 0.25. We used a shifted *log*-transformation (Fox and Weisberg, 2019); adding one to the covariates prior to the *log*-transformation preserved zeros (i.e. zeros mapped to zero under the transformation). The distribution of raw wind support data appeared Gaussian, so it was only centered and standardized.

Parameter estimation & model selection.. We fit our correalted random walk (CRW) in a Bayesian framework. Because the model has explicit serially correlated parameters, we used Hamiltonian Monte Carlo (HMC) over more conventional Markov-chain Monte Carlo (MCMC; e.g., Metropolis steps) to sample efficiently from a posterior with such correlation.

Gelman et al. (2008) suggested Cauchy priors for logistic regression parameters; however, Ghosh et al. (2015) found that sampling from the posterior can be inefficient due to the fat tails of the Cauchy distribution. We thus chose Student-t priors centered on zero ($\mu = 0$ and $\sigma = 2.5$) with five degrees of freedom as weakly informative priors for the covariate parameters. Weakly informative normal priors were placed on the variance parameters of the model.

We implemented HMC with R and Stan through the package 'rstan' (R Core Team, 2016; Stan Development Team, 2016). Working R and Stan code, including details on prior choice, are provided as supplementary material, as well as supplementary tables and figures (see Appendix). The model was fit to each track independently with five chains

of 300,000 HMC iterations, including a 200,000 iteration warm-up phase, and retaining every tenth sample. Convergence to the posterior distribution was checked with trace plots, effective sample sizes, posterior plots of parameters, and Gelman diagnostics ($\hat{R}$) for each model fit.

We compared candidate models with leave-one-out cross-validation approximated by Pareto-smoothed importance sampling (PSIS-LOO) in R with the package 'loo' (Vehtari et al., 2016, 2017). The candidate models included possible combinations of environmental covariates plus a null CRW model without covariates. To limit model complexity and because we were interested in competing hypotheses about key predictors of behavior, we chose not to include interactions beyond time-of-day. We ranked the models by the expected *log* pointwise predictive density (elpd; i.e. out-of-sample predictive accuracy) transformed onto the deviance scale (looic; Vehtari et al., 2017), which created a measure on the same scale as common information criterion (e.g., AIC) and allowed applying the rules of more traditional information-theoretic model selection (e.g., Burnham and Anderson, 2004). The model with the lowest looic was considered the best fit to the data, but if other models were within two looic of the top model, each, including the top model, were considered equally supported by the data.

To understand how the predictive ability of the full model varied among tracks, we also computed a pointwise average of the elpd for each track (Vehtari et al., 2017). Normalizing by the sample size allowed comparing the out of sample predictive ability of the full model across individual migration tracks (Table S7.1). The elpd (and looic), being sums, are otherwise dependent on the sample size for each model fit.

3.4 Results

3.4.1 Model performance & diagnostics

We fit eight candidate formulations of our CRW model to 31 migration tracks, equating to 248 total model fits. Chain mixing, Gelman diagnostics ($\hat{R}$) close to one, and large effective sample sizes for all parameters indicated convergence to the posterior for most model fits. Posteriors of parameters appeared symmetric, also indicating the model

was well behaved (Fig. S7.1). Across all migration tracks, the full model showed strong evidence of convergence, but for five tracks, we did not consider the null model converged to the posterior (e.g., $\hat{R} > 1.01$). The five migrations for which the null model did not converge were not included from formal model selection.

3.4.2 Behavior during migration

Median (interquartile range) departure and arrival dates were 5 March (4.5 *d*) and 27 March (6.4 *d*) in the spring and 29 September (11.7 *d*) and 16 November (15.5 *d*) in the fall. On average, eagles encountered similar orographic uplift in spring and fall but more intense thermal uplift and tailwind in the spring (Table 3.1).

The model revealed that eagles changed their behavior on multiple scales. First, there were very strong daily rhythms in behavior during migration, with birds migrating or moving more slowly and tortuously during the day and stopping at night (Figs. 3.1 & 3.2). Explicitly including a time-of-day interaction could cause a daily rhythm to emerge as an artifact of model specification. However, accounting for serial correlation in behavior (equation 5) limited that possibility. Additionally, prolonged periods of movement without an apparent daily rhythm suggest that, where daily rhythms are observed they are not a product of model specification (Fig. 3.2). Second, there was some evidence of stopover-like behavior, but with individuals continually moving along the migration route while exhibiting less directional persistence in movement (Fig. 4.1). The continuation along the migration route while in a stopover-like state is highlighted by track segments extended over space associated with low and intermediate estimates of γ_i (blue/purple in figure 4.1).

There was also a clear effect of season on movement patterns and behavior. Spring was characterized by straighter, more direct trajectories and punctuated by slower, more tortuous, stopover-like movement; whereas, fall movements were much more tortuous overall and regular patterns in changes in movement rate and/or tortuosity less clear (Figs. 3.1–4.1). The distributions of estimated γ values also clearly indicate that daytime movements were most frequently directed migratory moves in the spring; whereas,

in the fall, the bimodal distribution indicates more equivalent partitioning between directed migratory moves and slower stopover type movement, with significant time spent exhibiting behaviors associated with intermediate tortuosity and movement rate (Fig. 4.1).

3.4.3 Environmental covariates

While there were differences in some environmental covariates between spring and fall (Table 3.1), parameter estimates from the full model (all covariates) indicate that there was little to no difference in effect of flight subsidies (i.e. wind and uplift) on behavior between spring and fall (Fig. 3.4, Table S7.1). Including environmental covariates in the behavioral process, though, improved model fit for almost all fitted migrations (Table 3.2). Positive coefficients on the thermal uplift covariate indicate that increasing thermal uplift resulted in more highly-correlated displacements, or migratory movements. Despite that, there were some migration bouts not associated with great thermal uplift (Figs. 3.1 & 3.2). Coefficients close to zero for orographic uplift and wind support indicate that, in general, they were not strong drivers of directionally-persistent movements.

Based on the model selection, the best-fitting formulation of the environmental drivers of the behavioral process was variable across individuals. However, in almost all cases, some form of flight subsidy was used and there was little difference between the spring and fall seasons in the pattern of subsidy use (Table 3.2). The high variability across individuals (Table S7.1) was likely due to differing weather patterns and thus subsidy sources encountered and/or used by each eagle as migrations were not synchronous (in time or space) across individuals. In addition, inter-individual variation was much larger than any difference attributable to demographic variables; we found no evidence that difference in sex or age explained patterns of flight subsidy use during migration. Note, though, that all eagles included in this analysis were in adult plumage, so strong age effects would not necessarily be expected.

Comparing the pointwise elpd across tracks revealed that the out of sample predictive ability of the full model varied among individuals (Table S7.1). It also showed that

predictive ability was greater for fall migrations than spring.

3.5 Discussion

Here, we develop and demonstrate how dynamic parameter CRW models fit to GPS data reveal the effects of variable flight subsides available along migration routes. Use of these subsidies gives rise to diverse patterns in the movement of a long-distance soaring migrant. Behavioral changes occur continuously as available subsidies shift over time and space. These key driving mechanisms underlie emergent movement paths, yet such processes are often hidden in the discrete satellite observations available. Our mechanistic modeling approach allowed linking of dynamic meteorology to changes in behavior, and those changes in behavior to the observed movement paths, revealing time series of behaviors more complex than individuals simply apportioning time between migration and stopover.

3.5.1 Model performance

Incorporating time-varying parameters into movement models has been a relatively infrequently utilized approach (Breed et al., 2012; Auger-Méthé et al., 2017; Jonsen et al., 2019). Here we provide a case study for its utility and developed the approach for achieving practical biological inference about movement processes. Modeling the serial correlation in movement as a function of environmental covariates (equation 4), allowed simultaneous inference of behavior and the effect of environmental covariates on behavior from animal trajectories with regular and irregular duty cycles and containing missing observations. While other methods exist to handle missing data, the behavioral patterns we found would be more difficult to reveal with a state-switching movement model (e.g., hidden Markov models (HMMs); Michelot et al., 2016) because each step would be forced into a discrete behavioral state from a set of usually 2-3 discrete states. Moreover, although hidden-state models have been introduced that have more than five discrete states (e.g., McClintock et al., 2012), these states can require ancillary data streams (e.g., accelerometry) to discriminate and remain extremely difficult to employ and interpret in

practice (Patterson et al., 2017; Pohle et al., 2017). Finally, as HMMs include greater numbers of potential states, they tend to fit better than models with fewer states as judged by classical model selection approaches, such as AIC, even when additional states are neither biologically meaningful nor sensible (Pohle et al., 2017). Implementing models with dynamic parameters that can be interpreted along a behavioral continuum seems a more natural approach for many animal movement questions.

Effects of tag programming. While our CRW model revealed the same trends across duty cycles and was generally robust to the different duty cycles (Figs. 3.1 & 3.2), the most detail in daily behavioral rhythms was revealed in tracks with a fixed 3-hr time interval (lower panel in figure 3.2), as it provided data throughout the 24-hr day at regular intervals. The other duty cycles were initially chosen to minimize the risk of battery depletion overnight. Although generally robust, duty cycles did affect model fitting. HMC permitted Bayesian inference rather efficiently for our model, considering elevated correlation in the posterior of parameters due to the model formulation. Model fits typically took no more than a few hours, though tracks with much more than several hundred locations sometimes took longer. Preliminary fitting of our model with Stan and Template Model Builder (TMB; following Auger-Méthé et al., 2017) suggested that Maximum Likelihood estimation (when fit with TMB) tends to fail frequently when tag programming results in uneven temporal coverage of each day (e.g., our 2015 duty cycle), while Bayesian inference still provided sensible parameter estimates in most cases. Although the model presented herein and the model presented by Auger-Méthé et al. (2017) can make up for irregular time intervals between observations, they do have limitations. Breed et al. (2011) offer an in-depth discussion of tag programming and its effects on model fitting and inference.

3.5.2 Flight subsidies as drivers migration of behavior

Thermal uplift is a flight subsidy dependent on daily atmospheric boundary layer dynamics, and it was clearly an important driver of the daily rhythm in eagle movement (Fig. 3.4, Table S7.1). Intense thermal uplift was often associated with the peaks in

daily migration bouts (Fig. 3.1). The larger magnitude of the thermal uplift effect, relative to orographic uplift, was somewhat surprising, as many individuals in our sample followed the Rocky Mountains, a large potential source of orographic uplift. Golden eagles are known to use orographic uplift as a flight subsidy while migrating through the Appalachian Mountains in eastern North America (Katzner et al., 2015). Much of the Appalachians, however, is characterized by long, unbroken, linearly-oriented ridges. Wind blowing over these ridges produces long stretches of predictable orographic uplift (Rus et al., 2017). The Rocky Mountains, by contrast, are far more rugged and nonuniform, and conditions that might produce suitable upslope winds and mountain waves, as well as strong tailwinds, likely also generate violent turbulence and could impede efficient migratory flight. Soaring raptors have been shown to use small-scale turbulence to achieve subsidized flight (Allen et al., 1996; Mallon et al., 2016); however, unpredictable, non-stationary violent turbulence, which can occur in large, high-elevation mountain ranges (Ralph et al., 1997), could produce unfavorable migratory conditions. The large effect of thermal uplift, thus, could indicate that the Rocky Mountains, a spine that spans almost the entire migration corridor for this population, as well as some areas further west (Bedrosian et al., 2018), serves as a network of thermal streets for migrating eagles (Pennycuick, 1998). More explicitly, intense sun on south facing slopes would be expected to generate linear series of thermals that birds could glide between during both spring and fall migration. It is important to keep in mind that the migrants could capitalize on fine-scale, localized features of certain flight subsidies, like orographic uplift and tailwind, that may not have been captured by the interpolated meteorological data used in our analyses. However, model selection for models including those variables did indicate they explained some variance in eagle movement, which we discuss further below.

Despite meteorological conditions along migration paths that differed between spring and fall and a stark difference between behavioral budgets, our results showed no clear difference in the use of flight subsidies between the spring and fall seasons (Fig. 3.4). This finding contrasts with season-specific effects of flight subsidies on golden eagle migration shown phenomenologically in eastern North America, where thermal uplift was shown

to be the key subsidy in migratory performance during spring, while wind with some additional support from thermal uplift is most important in the fall (Duerr et al., 2015; Rus et al., 2017). Although our results indicate that eagles use similar flight subsidizing strategies in both seasons, consistent with the differences from the eastern population, the actual behaviors performed during spring and fall migrations differed considerably. In spring, eagles used subsidies to drive a migration that allows timely arrival on the breeding grounds, consistent with a time minimization strategy. In the fall, flight was subsidized to minimize net energy use, which emerged as a much more diverse behavioral repertoire during a slower fall migration (Fig. 4.1; Miller et al., 2016). The more rapid and direct flight punctuated by bouts of tortuous, stopover-like movement in the spring (Fig. 4.1), suggest eagles pause, refuel, and/or perhaps wait for better migration conditions. This suggests eagles may employ, at least in part, a net energy maximization strategy (Hedenström, 1993; Miller et al., 2016), despite the need for timely arrival on the breeding grounds to avoid fitness costs (Both and Visser, 2001).

The behavioral time series of spring migrations showed some evidence of individuals responding less to thermal uplift as latitude increased (Fig. 3.1). This likely corresponded to a general decay in thermal uplift as individuals migrated northward (Supplementary Material, Fig. S7.2). Reduced thermal uplift availability would be expected at higher latitudes due to the larger amounts of remaining spring snowpack and lower solar angles. Thus, golden eagles, and likely other soaring birds, migrating to high latitudes may need to budget behaviors carefully between time minimization and net energy maximization during spring migration to best take advantage of the reduced flight subsidy from thermal uplift and mitigate the greater energy demands of flight at higher latitudes.

While our results show that thermal uplift is the most important flight subsidy for the majority of migrating eagles sampled, the model selection indicated orographic uplift and wind support improved out of sample predictive accuracy and explained some variance in eagle movement. Additionally, variability in top models across individuals (Tables 3.2 & S7.1) suggests among-individual variance in flight-subsidizing strategy. Although some of this variability can be attributed to real individual differences in behavioral strategy,

it is at least as likely that individuals encountered different subsidies en route and used the subsidies they had available, as migrations across our sample were not synchronous. Given that orographic uplift and wind support parameter estimates were negative or close to zero for many individuals (Fig. 3.4, Table S7.1), those covariates likely predicted the periods of slower, more tortuous movements (i.e. γ_i closer to zero). Wind support occurred in top models for more individuals in the fall (Tables 3.2 & S7.1), which is consistent with findings from others (McIntyre et al., 2008; Rus et al., 2017) and suggests it may be important during southbound migrations. Additionally, although there was variance among the types and combinations of subsidies used, the null model (without flight subsidies) was the best fitting model for very few tracks (Tables 3.2 & S7.1), evidence that weather and flight subsidies are of importance to migrating golden eagles, and likely also to the migrations of similar soaring species. Lastly, we found that the full model had, on average, better predictive ability in fall than spring (Table S7.1), suggesting that the weather variables explained more of the variance within movement paths in fall compared to spring; during spring migration, other internal state variables associated with greater time limitation that were not explicitly accounted for in the models were likely responsible for this seasonal difference.

3.5.3 Daily rhythm & migratory pace

The full movement model revealed two clear, nested behavioral patterns in the long-distance migrations of golden eagles. First, there was a daily rhythm where inferred directed migratory movements (i.e. γ_i close to one) occurred most frequently around midday or early afternoon (Figs. 3.1 & 3.2). Mechanistic models of animal movement have revealed diel behavioral rhythms in other taxa (Jonsen et al., 2006). The basic aspects of daily rhythms in vertebrate behavior have hormone controls (Cassone, 1990), but the benefits can include balancing migration progress and foraging bouts (Newton, 2008). Soaring migrants also benefit by synchronizing diel movement patterns with diel atmospheric cycles. That is, consistent with our results, diurnal soaring migrants express a general circadian behavioral rhythm, where flight performance and behavior is strongly

tied to thermal development of the planetary boundary layer to take best advantage of atmospherically generated flight subsides (Kerlinger et al., 1985; Leshem and Yom-Tov, 1989; Spaar and Bruderer, 1996, 1997; Mateos-Rodríguez and Liechti, 2012).

The second behavioral pattern revealed was a general stopover pattern, whereby eagles changed behavior for one to several days while en route (Figs. 3.1–4.1). These changes were consistent with searching movements (i.e. γ intermediate or close to zero), possibly representing foraging behavior. In terms of soaring raptors, however, very few reports of movement patterns and behavior during stopovers have been published. Stopover segments have been previously identified by speed or some other metric calculated from tracks, then excluded from subsequent analyses (e.g., Vansteelant et al., 2015; Katzner et al., 2015); occasionally, authors noted apparent enhanced tortuosity but explored it no further (e.g., Vansteelant et al., 2017). On occasions where stopover behavior was considered, classifications based on stay duration and travel distance or speed with hard, often arbitrarily chosen cutoffs between migrating and stopover segments were used (Duerr et al., 2015; Chevallier et al., 2011; Katzner et al., 2012; Miller et al., 2016). In contrast, our modeling framework aligned with the movement ecology paradigm (Nathan et al., 2008); it used the observed data—GPS locations, rather than a derived metric—and a theoretical movement process to infer behavior from movement patterns along tracks on a spectrum ranging from stopped to rapid, directionally-persistent movement.

Our analyses, however, showed that eagles still tended to continue along their migration route during periods of movement most resembling stopover, but with reduced movement rate and directional persistence (Figs. 3.1–4.1). This pattern suggests a joint migration/opportunistic foraging behavior that resembles fly-and-forage migration (Strandberg and Alerstam, 2007; Åkesson et al., 2012; Klaassen et al., 2017), which is consistent with observations of en route hunting behavior of golden eagles by Dekker (1985). Such behavior could be used to maintain balance between time expenses and energy intake, as it allows simultaneous migration progress and foraging.

This pattern does not fall very well within the "stopover" paradigm (Gill, 2007; Newton, 2008), however, as true stops during the migrations we observed were rare, except

for expected nightly stops. Rather, migrants seemed to change their *pace*—either by slowing down, moving more tortuously, or both—but still generally moved toward their migratory destination (Figs. 3.1–4.1). Thus, instead of a discrete behavioral framework, whereby migrants switch between two migratory phases (migration and stopover) with very different movement and behavioral properties, we propose that, for certain taxa, a continuous alternative framework "migratory pacing" may be more appropriate and a natural way to interpret en route migratory behavior and movement dynamics. Such taxa would include some and perhaps many soaring migrants, as well some migrating species in other fluid environments such as fishes and marine mammals. Soaring birds, even when energy reserves are relatively depleted, likely can still make steady progress toward a migratory goal when flight subsidies are available. Flapping migrants, on the other hand, would not be able to achieve this as readily, due in part to the greater energy demands for sustained flight, and would require more regular refueling stopovers where migration progress is temporarily completely arrested. Both opportunism in foraging and use of energetic subsidies are likely key characters of fly-and-forage behavior and the ability to change pace of migration without actually stopping, as they relax the need for individuals to stopover in specific, food-rich habitats, which are required by most migrants with less flexibility in food and that lack the morphological specialization to maximally exploit the energetic subsidies available in moving fluids (Piersma, 2007; Gill, 2007).

Our model results revealed seasonal variability in migratory pacing by golden eagles. The tendency for eagles to exhibit movements matching fly-and-forage behavior, and pace their migrations more slowly was most apparent during fall migration. In contrast, spring migration was usually composed of much more punctuated events of slower-paced movements but these were still extended over space (Fig. 4.1), indicating the eagles pace their migration and employ a mixed behavioral strategy to some extent in spring as well. During spring, hibernating mammalian prey would be minimally available, leaving carrion, along with a few non-migratory and -hibernating species (e.g., ptarmigan *Lagopus* spp. and hare *Lepus* spp.), as major food sources, which could help explain the more punctuated bouts of slower-pacing. Alternatively, individuals could have been slowed by

poor weather conditions (Rus et al., 2017). Scavenging large ungulate carcasses would be extremely rewarding in terms of energy accumulation. Much of the carrion we used successfully to capture eagles was large ungulate (e.g., moose *Alces alces*), strongly suggesting that the population we sampled uses carcasses during migration. The bimodal distribution for the behavioral parameter γ in fall shows that eagles tended to budget daytime behaviors approximately equally between rapid, directed and slower-paced movements (Fig. 4.1); the high frequency and range of intermediate values are, again, evidence for the more complex fly-and-forage and pacing dynamic, rather than eagles simply switching between stopover and migration. This behavioral complexity might be biologically important, allowing eagles to arrive on winter home ranges in better condition compared to migration strategies that do not incorporate en route foraging opportunity. In contrast to fall, daytime movements in the spring were typically faster-paced (i.e. larger-scale and directionally-persistent; Fig. 4.1), consistent with a time minimization strategy, where eagles need to partition time more in favor of migration progress to ensure timely arrival on breeding grounds (Hedenström, 1993; Alerstam, 2011; Miller et al., 2016). We thus see in eagles, and propose more generally, that such pacing varies between and within seasons along the continuum between time minimization and net energy maximization strategies (Alerstam, 2011; Miller et al., 2016). A migrant's pace would be expected to depend upon their energetic demands, energetic subsidies available from the environment, and the importance of arriving at the migration terminus in a timely fashion (Nathan et al., 2008).

3.5.4 Implications & conclusions

We developed and applied a movement model with time-varying parameters to help reveal the mechanisms underlying the migration of a long-distance soaring migrant that relies on incredibly dynamic flight subsidies. We found that variation in flight subsidies gives rise to changes in migrant behavior with thermal uplift seemingly most important. While these findings might be expected given previous phenomenological analyses (e.g., Duerr et al., 2012; Lanzone et al., 2012; Katzner et al., 2015; Vansteelant et al., 2015;

Miller et al., 2016; Shamoun-Baranes et al., 2016; Rus et al., 2017), we were able to show how meteorology is a mechanism influencing changes in movement patterns and thus behavior.

In the behavioral budgets of migrating golden eagles, we identified an expected daily rhythm, as well as evidence for behavioral dynamics that would allow nearly simultaneous foraging and migration, which is greater complexity than the traditional stopover paradigm allows. Migratory pacing, facilitated by fly-and-forage behavior, expands the traditional notion of stopover, whereby a bird migrates until resting and refueling is required, at which point it stops for a brief period in specific habitat suitable for efficient foraging (Gill, 2007; Newton, 2008). This advance was enabled by incorporating time-varying parameters into the movement model, which revealed new behavioral patterns during migration of long-distance soaring migrants. While time-varying, dynamic parameters have been infrequently employed in movement modeling (Breed et al., 2012; Jonsen et al., 2013; Auger-Méthé et al., 2017), we have shown it is a promising approach that can overcome certain limitations in discrete state-switching models and help provide novel insight into animal behavior.

This approach also has potential for further development and for revealing additional new patterns in soaring bird movement; it has already been shown to help provide new insight for other taxa as well (Jonsen et al., 2019). Although we demonstrated the approach for several individual eagles, applying our methods across a larger sample and across more years will increase the inferential strength of our results. For example, previous work found effects of wind support and orographic uplift (e.g., Katzner et al., 2015; Vansteelant et al., 2015), where we, in accounting for an eagles' underlying movement process and the inherent autocorrelation in that process, found that those meteorological variables may be of less importance, at least compared to thermal uplift. It remains unclear though, whether these are system-specific findings or a more general result. Additionally, the model we present has potential to help assess effects of habitat on the movement decisions of soaring birds and other species. One potential avenue for such would be incorporating the model into a resource selection framework (e.g., step selec-

tion function). Furthermore, given the movement process is parameterized in terms of coordinate vectors, the position likelihood could be straightforwardly extended to include the z axis to investigate questions regarding flight height of soaring birds or dive depth of marine species, assuming data of acceptable temporal resolution and location error are, or become, available.

3.6 Data accessibility

All movement data used for this manuscript are managed in the online repository Movebank (https://www.movebank.org/; IDs 17680093 and 19389828). The data contain information considered sensitive by the State of Alaska, but they could be made available at the discretion of the Alaska Department of Fish & Game and U.S. Fish & Wildlife Service. Code to fit the movement model to data is provided as supplementary material.

3.7 Conflicts of interest

The authors declare that they have no conflict of interest.

3.8 Ethical approval

Field procedures were conducted following the ADF&G Animal Care & Use Committee protocol #2013-036 and University of Alaska Fairbanks Institutional Animal Care & Use Committee protocol #859448.

3.9 Author contributions

JME and GAB conceived the ideas of the research presented herein. JME, MA-M, and GAB designed analytical methods, and TLB, CPB, and SBL designed the field methodology. TLB, CPB, SBL, and JME collected the data. JME analyzed the data, and led the manuscript. All authors contributed to drafts and editing of the manuscript and provided final approval for publication.

3.10 Acknowledgements

We thank M. Kohan, B. Robinson, T. & D. Hawkins and many others for support in the field and J. Liguori and N. Paprocki for help aging eagles. We also thank T. Avgar, P. Doak, T. Katzner, K. Kielland, and C. McIntyre for helpful comments on drafts of the manuscript. Funding was provided by the Alaska Department of Fish & Game (ADF&G) through the federal State Wildlife Grant Program, and the U.S. Fish & Wildlife Service (USFWS) provided PTTs and data. JME was supported by the Calvin J. Lensink Fund during part of the project. MA-M acknowledges the support of the Natural Sciences and Engineering Research Council of Canada. The findings and conclusions of this paper are those of the authors and do not necessarily represent the views of the USFWS.

3.11 References

Åkesson S, Klaassen R, Holmgren J, Fox JW, Hedenström A. 2012. Migration routes and strategies in a highly aerial migrant, the common swift Apus apus, revealed by light-level geolocators. *PLoS ONE* **7**: 1–9. doi: 10.1371/journal.pone.0041195.

Alerstam T. 1979. Optimal use of wind by migrating birds: combined drift and over-compensation. *Journal of Theoretical Biology* **79**: 341–353. doi: 10.1016/0022-5193(79)90351-5.

Alerstam T. 2011. Optimal bird migration revisited. *Journal of Ornithology* **152**: 5–23. doi: 10.1007/s10336-011-0694-1.

Alerstam T, Hedenström A. 1998. The development of bird migration theory. *Journal of Avian Biology* **29**: 343–369. doi: 10.2307/3677155.

Allen PE, Goodrich LJ, Bildstein KL. 1996. Within- and among-year effects of cold fronts on migrating raptors at Hawk Mountain, Pennsylvania, 1934-1991. *The Auk* **113**: 329–338.

Auger-Méthé M, Albertsen CM, Jonsen ID, Derocher AE, Lidgard DC, Studholme KR, Bowen WD, Crossin GT, Mills Flemming J. 2017. Spatiotemporal modelling of marine movement data using Template Model Builder (TMB). *Marine Ecology Progress Series* **565**: 237–249. doi: 10.3354/meps12019.

Avgar T, Street G, Fryxell JM. 2014. On the adaptive benefits of mammal migration. *Canadian Journal of Zoology* **92**: 481–490. doi: 10.1139/cjz-2013-0076.

Bedrosian BE, Domenech R, Shreading A, Hayes MM, Booms TL, Barger CR. 2018. Migration corridors of adult Golden Eagles originating in northwestern North America. *PLoS ONE* **13**: e0205204. doi: 10.1371/ journal.pone.0205204.

Bivand R, Lewin-Koh N. 2016. maptools: Tools for Reading and Handling Spatial Objects.
URL `https://cran.r-project.org/package=maptools`

Blackwell PG. 1997. Random diffusion models for animal movement. *Ecological Modelling* **100**: 87–102. doi: 10.1016/S0304-3800(97)00153-1.

Blackwell PG. 2003. Bayesian inference for Markov processes with diffusion and discrete components. *Biometrika* **90**: 613–627.

Blackwell PG, Niu M, Lambert MS, Lapoint SD. 2015. Exact Bayesian inference for animal movement in continuous time. *Methods in Ecology and Evolution* **7**: 184–195. doi: 10.1111/2041-210X.12460.

Bohrer G, Brandes D, Mandel JT, Bildstein KL, Miller TA, Lanzone M, Katzner T, Maisonneuve C, Tremblay JA. 2012. Estimating updraft velocity components over large spatial scales: contrasting migration strategies of golden eagles and turkey vultures. *Ecology Letters* **15**: 96–103. doi: 10.1111/j.1461-0248.2011.01713.x.

Both C, Visser ME. 2001. Adjustment to climate change is constrained by arrival date in a long-distance migrant bird. *Nature* **411**: 296–298. doi: 10.1038/35077063.

Brandes D, Ombalski DW. 2004. Modeling raptor migration pathways using a fluid-flow analogy. *Journal of Raptor Research* **38**: 195–207.

Breed GA, Costa DP, Goebel ME, Robinson PW. 2011. Electronic tracking tag programming is critical to data collection for behavioral time-series analysis. *Ecosphere* **2**: 10. doi: 10.1890/ES10-00021.1.

Breed GA, Costa DP, Jonsen ID, Robinson PW, Mills-Flemming J. 2012. State-space methods for more completely capturing behavioral dynamics from animal tracks. *Ecological Modelling* **235-236**: 49–58. doi: 10.1016/j.ecolmodel.2012.03.021.

Breed GA, Golson EA, Tinker MT. 2017. Predicting animal home-range structure and transitions using a multistate Ornstein-Uhlenbeck biased random walk. *Ecology* **98**: 32–47. doi: 10.1002/ecy.1615.

Bridge ES, Thorup K, Bowlin MS, Chilson PB, Diehl RH, Fléron RW, Hartl P, Kays R, Kelly JF, Robinson WD, Wikelski M. 2011. Technology on the Move: Recent and Forthcoming Innovations for Tracking Migratory Birds. *BioScience* **61**: 689–698. doi: 10.1525/bio.2011.61.9.7.

Burnham KP, Anderson R. 2004. Multimodel inference: understanding AIC and BIC in model selection. *Sociological Methods & Research* **33**: 261–304. doi: 10.1177/0049124104268644.

Cassone VM. 1990. Effects of melatonin on vertebrate circadian systems. *Trends in Neurosciences* **13**: 457–464.

Chevallier D, Le Maho Y, Brossault P, Baillon F, Massemin S. 2011. The use of stopover sites by Black Storks (Ciconia nigra) migrating between West Europe and West Africa as revealed by satellite telemetry. *Journal of Ornithology* **152**: 1–13. doi: 10.1007/s10336-010-0536-6.

Clark CW, Butler RW. 1999. Fitness components of avian migration: A dynamic model of Western Sandpiper migration. *Evolutionary Ecology Research* **1**: 443–453.

Dekker D. 1985. Hunting behavior of golden eagles, Aquila chrysaetos, migrating in southwestern Alberta. *The Canadian Field-Naturalist* **99**: 383–385.

Dodge S, Bohrer G, Weinzierl R, Davidson SC, Kays R, Douglas D, Cruz S, Han J, Brandes D, Wikelski M. 2013. The environmental-data automated track annotation (Env-DATA) system: linking animal tracks with environmental data. *Movement Ecology* **1**: 3. doi: 10.1186/2051-3933-1-3.

Duerr AE, Miller Ta, Lanzone M, Brandes D, Cooper J, O'Malley K, Maisonneuve C, Tremblay J, Katzner T. 2012. Testing an emerging paradigm in migration ecology shows surprising differences in efficiency between flight modes. *PLoS ONE* **7**: e35548. doi: 10.1371/journal.pone.0035548.

Duerr AE, Miller TA, Lanzone M, Brandes D, Cooper J, O'Malley K, Maisonneuve C, Tremblay JA, Katzner T. 2015. Flight response of slope-soaring birds to seasonal variation in thermal generation. *Functional Ecology* **29**: 779–790. doi: 10.1111/1365-2435.12381.

Dunn JE, Gipson PS. 1977. Analysis of radio telemetry data in studies of home range. *Biometrics* **33**: 85–101.

Fox J, Weisberg S. 2019. *An R Companion to Applied Regression*. Thousand Oaks, California: SAGE Publications, Inc, 3rd edition.

Gelman A, Jakulin A, Pittau MG, Su YS. 2008. A weakly informative default prior distribution for logistic and other regression models. *Annals of Applied Statistics* **2**: 1360–1383. doi: 10.1214/08-AOAS191.

Ghosh J, Li Y, Mitra R. 2015. On the use of Cauchy prior distributions for Bayesian logistic regression. *ArXiv* : 1507.07170.

Gill FB. 2007. *Ornithology*. New York: W. H. Freeman and Company, third edition.

Gurarie E, Fleming CH, Fagan WF, Laidre KL, Hernández-Pliego J, Ovaskainen O. 2017. Correlated velocity models as a fundamental unit of animal movement: Synthesis and applications. *Movement Ecology* **5**: 1–18. doi: 10.1186/s40462-017-0103-3.

Hedenström A. 1993. Migration by soaring or flapping flight in birds: The relative importance of energy cost and speed. *Philosophical Transactions of the Royal Society B: Biological Sciences* **342**: 353–361. doi: 10.1098/rstb.1993.0164.

Hedenström A. 2008. Adaptations to migration in birds: behavioural strategies, morphology and scaling effects. *Philosophical Transactions of the Royal Society B* **363**: 287–299. doi: 10.1098/rstb.2007.2140.

Hooten MB, Johnson DS, McClintock BT, Morales JM. 2017. *Animal movement: statistical models for telemetry data.* New York: CRC Press.

Johnson DS, London JM, Lea MA, Durban JW. 2008. Continuous-time correlated random walk model for animal telemetry data. *Ecology* **89**: 1208–1215. doi: 10.1890/10-1922.1.

Jonsen ID, Basson M, Bestley S, Bravington MV, Patterson TA, Pedersen MW, Thomson R, Thygesen UH, Wotherspoon SJ. 2013. State-space models for bio-loggers: a methodological road map. *Deep-Sea Research Part II: Topical Studies in Oceanography* **88-89**: 34–46. doi: 10.1016/j.dsr2.2012.07.008.

Jonsen ID, McMahon CR, Patterson TA, Auger-Méthé M, Harcourt R, Hindell MA, Bestley S. 2019. Movement responses to environment: fast inference of variation among southern elephant seals with a mixed effects model. *Ecology* **100**: 1–8. doi: 10.1002/ecy.2566.

Jonsen ID, Myers RA, James MC. 2006. Robust hierarchical state-space models reveal diel variation in travel rates of migrating leatherback turtles. *Journal of Animal Ecology* **75**: 1046–1057. doi: 10.1111/j.1365-2656.2006.01129.x.

Kareiva PM, Shigesada N. 1983. Analyzing insect movement as a correlated random walk. *Oecologia* **56**: 234–238.

Katzner TE, Brandes D, Miller T, Lanzone M, Maisonneuve C, Tremblay JA, Mulvihill R, Merovich GT. 2012. Topography drives migratory flight altitude of golden eagles: implications for on-shore wind energy development. *Journal of Applied Ecology* **49**: 1178–1186. doi: 10.1111/j.1365-2664.2012.02185.x.

Katzner TE, Turk PJ, Duerr AE, Miller TA, Lanzone MJ, Cooper JL, Brandes D, Tremblay JA, Lemaître J. 2015. Use of multiple modes of flight subsidy by a soaring terrestrial bird, the golden eagle Aquila chrysaetos, when on migration. *Journal of Royal Society Interface* **12**: 20150530. doi: 10.1098/rsif.2015.0530.

Kerlinger P, Bingman V, Able KP. 1985. Comparative flight behavior of migrating hawks studied with tracking radar during autumn in Central New York. *Canadian Journal of Zoology* **63**: 755–761. doi: 10.1139/z85-110.

Klaassen RH, Schlaich AE, Bouten W, Koks BJ. 2017. Migrating Montagu's harriers frequently interrupt daily flights in both Europe and Africa. *Journal of Avian Biology* **48**: 180–190. doi: 10.1111/jav.01362.

Kochert MN, Steenhof K, McIntyre CL, Craig EH. 2002. Golden Eagle (Aquila chrysaetos). In Poole A (ed.) *The Birds of North America*. Ithaca: Cornell Lab of Ornithology.

Lanzone MJ, Miller Ta, Turk P, Brandes D, Halverson C, Maisonneuve C, Tremblay J, Cooper J, O'Malley K, Brooks RP, Katzner T. 2012. Flight responses by a migratory soaring raptor to changing meteorological conditions. *Biology Letters* **8**: 710–713. doi: 10.1098/rsbl.2012.0359.

Leshem Y, Yom-Tov Y. 1989. The use of thermals by soaring migrants. *Ibis* **183**: 667–674.

Luschi P, Hays GC, Del Seppia C, Marsh R, Papi F. 1998. The navigational feats of green sea turtles migrating from Ascension Island investigated by satellite telemetry. *Proceedings of the Royal Society of London. Series B: Biological Sciences* **265**: 2279–2284. doi: 10.1098/rspb.1998.0571.

Mallon JM, Bildstein KL, Katzner TE. 2016. In-flight turbulence benefits soaring birds. *The Auk* **133**: 79–85. doi: 10.1642/AUK-15-114.1.

Mateos-Rodríguez M, Liechti F. 2012. How do diurnal long-distance migrants select flight altitude in relation to wind? *Behavioral Ecology* **23**: 403–409. doi: 10.1093/beheco/arr204.

McClintock BT, King R, Thomas L, Matthiopoulos J, McConnell BJ, Morales JM. 2012. A general discrete-time modeling framework for animal movement using multistate random walks. *Ecological Monographs* **82**: 335–349. doi: 10.1890/11-0326.1.

McIntyre CL, Douglas DC, Collopy MW. 2008. Movements of Golden Eagles (Aquila chrysaetos) from Interior Alaska during their first year of independence. *The Auk* **125**: 214–224. doi: 10.1525/auk.2008.125.1.214.

Michelot T, Blackwell PG. 2019. State-switching continious-time correlated random walks. *Methods in Ecology and Evolution* **In press**. doi: 10.1111/2041-210X.13154.

Michelot T, Langrock R, Patterson TA. 2016. moveHMM: an R package for the statistical modelling of animal movement data using hidden Markov models. *Methods in Ecology and Evolution* **7**: 1308–1315. doi: 10.1111/2041-210X.12578.

Miller TA, Brooks RP, Lanzone MJ, Brandes D, Cooper J, Tremblay JA, Wilhelm JAY, Duerr A, Katzner TE. 2016. Limitations and mechanisms influencing the migratory performance of soaring birds. *Ibis* **158**: 116–134. doi: 10.1111/ibi.12331.

Morales JM, Haydon DT, Frair J, Holsinger KE, Fryxell JM. 2004. Extracting more out of relocation data: building movement models as mixtures of random walks. *Ecology* **85**: 2436–2445. doi: 10.1890/03-0269.

Murgatroyd M, Photopoulou T, Underhill LG, Bouten W, Amar A. 2018. Where eagles soar: Fine-resolution tracking reveals the spatiotemporal use of differential soaring modes in a large raptor. *Ecology and Evolution* **8**: 6788–6799. doi: 10.1002/ece3.4189.

Nathan R, Getz WM, Revilla E, Holyoak M, Kadmon R, Saltz D, Smouse PE. 2008. A movement ecology paradigm for unifying organismal movement research. *Proceedings of the National Academy of Sciences* **105**: 19052–9. doi: 10.1073/pnas.0800375105.

Newton I. 2008. *The migration ecology of birds*. London: Academic Press.

Patterson TA, Parton A, Langrock R, Blackwell PG, Thomas L, King R. 2017. Statistical modelling of individual animal movement: an overview of key methods and a discussion of practical challenges. *AStA Advances in Statistical Analysis* **101**: 399–438. doi: 10.1007/s10182-017-0302-7.

Pennycuick C. 1998. Field observations of thermals and thermal streets, and the theory of cross-country soaring flight. *Journal of Avian Biology* **29**: 33–43. doi: 10.2307/3677338.

Pennycuick CJ. 1971. Soaring behavior and performance of some East African birds, observed from a motor-glider. *Ibis* **114**: 178–218.

Piersma T. 2007. Using the power of comparison to explain habitat use and migration strategies of shorebirds worldwide. *Journal of Ornithology* **148**: S45–S59. doi: 10.1007/s10336-007-0240-3.

Pirotta E, Katzner T, Miller TA, Duerr AE, Braham MA, New L. 2018. State-space modelling of the flight behaviour of a soaring bird provides new insights to migratory strategies. *Functional Ecology* **32**: 2205–2215. doi: 10.1111/1365-2435.13180.

Pohle J, Langrock R, van Beest FM, Schmidt NM. 2017. Selecting the number of states in hidden Markov models: pragmatic solutions illustrated using animal movement. *Journal of Agricultural, Biological, and Environmental Statistics* **22**: 270–293. doi: 10.1007/s13253-017-0283-8.

R Core Team. 2016. R: A language and environment for statistical computing. URL `https://cran.r-project.org/`

Ralph FM, Neiman PJ, Levinson D. 1997. Lidar observations of a breaking mountain wave associated with extreme turbulence. *Geophysical Research Letters* **24**: 663–666. doi: 10.1029/97GL00349.

Rus AI, Duerr AE, Miller TA, Belthoff JR, Katzner TE. 2017. Counterintuitive roles of experience and weather on migratory performance. *The Auk* **134**: 485–497. doi: 10.1642/AUK-16-147.1.

Safi K, Kranstauber B, Weinzierl R, Griffin L, Rees EC, Cabot D, Cruz S, Proaño C, Takekawa JY, Newman SH, Waldenström J, Bengtsson D, Kays R, Wikelski M, Bohrer G. 2013. Flying with the wind: scale dependency of speed and direction measurements in modelling wind support in avian flight. *Movement Ecology* **1**: 4. doi: 10.1186/2051-3933-1-4.

Sawyer H, Lindzey F, McWhirter D. 2005. Mule deer and pronghorn migration in western Wyoming. *Wildlife Society Bulletin* **33**: 1266–1273. doi: 10.2193/0091-7648(2005)33[1266:mdapmi]2.0.co;2.

Shamoun-Baranes J, Bouten W, Loon EEV, Meijer C, Camphuysen CJ, Shamoun-baranes J. 2016. Flap or soar? How a flight generalist responds to its aerial environment. *Philosophical Transactions of the Royal Society B* **371**: 20150395. doi: 10.1098/rstb.2015.0395.

Shamoun-Baranes J, Bouten W, Van Loon EE. 2010. Integrating meteorology into research on migration. *Integrative and Comparative Biology* **50**: 280–292. doi: 10.1093/icb/icq011.

Shamoun-Baranes J, Liechti F, Vansteelant WM. 2017. Atmospheric conditions create freeways, detours and tailbacks for migrating birds. *Journal of Comparative Physiology A: Neuroethology, Sensory, Neural, and Behavioral Physiology* **203**: 509–529. doi: 10.1007/s00359-017-1181-9.

Shepard ELC, Wilson RP, Rees WG, Grundy E, Lambertucci SA, Vosper SB. 2013. Energy landscapes shape animal movement ecology. *The American Naturalist* **182**: 298–312. doi: 10.1086/671257.

Spaar R, Bruderer B. 1996. Soaring migration of Steppe Eagles Aquila nipalensis in Southern Israel: flight behaviour under various wind and thermal conditions. *Journal of Avian Biology* **27**: 289–301. doi: 10.2307/3677260.

Spaar R, Bruderer B. 1997. Optimal flight behavior of soaring migrants: a case study of migrating steppe buzzards, Buteo buteo vulpinus. *Behavioral Ecology* **8**: 288–297. doi: 10.1093/beheco/8.3.288.

Stan Development Team. 2016. RStan: the R interface to Stan, Version 2.10.1. URL `http://mc-stan.org`

Strandberg R, Alerstam T. 2007. The strategy of fly-and-forage migration, illustrated for the osprey (Pandion haliaetus). *Behavioral Ecology and Sociobiology* **61**: 1865–1875. doi: 10.1007/s00265-007-0426-y.

Turchin P. 1998. *Quantitative analysis of movement: measuring and modeling population redistribution in animals and plants.* Sunderland, Massachusetts, USA: Sinauer Associates.

Vansteelant WMG, Bouten W, Klaassen RHG, Koks BJ, Schlaich AE, Diermen JV, Loon EEV. 2015. Regional and seasonal flight speeds of soaring migrants and the role of weather conditions at hourly and daily scales. *Journal of Avian Biology* **46**: 25–39. doi: 10.1111/jav.00457.

Vansteelant WMG, Shamoun-Baranes J, Mclaren J, van Diermen J, Bouten W. 2017. Soaring across continents: decision-making of a soaring migrant under changing atmospheric conditions along an entire flyway. *Journal of Avian Biology* **48**: 887–896. doi: 10.1111/jav.01298.

Vehtari A, Gelman A, Gabry J. 2016. loo: efficient leave-one-out cross-validation and WAIC for Bayesian models. R package version 1.0.0.

Vehtari A, Gelman A, Gabry J. 2017. Practical Bayesian model evaluation using leave-one-out cross-validation and WAIC. *Statistics and Computing* **27**: 1413–1432. doi: 10.1007/s11222-016-9696-4.

Watson J. 2010. *The Golden Eagle*. New Haven: Yale University Press, second edition.

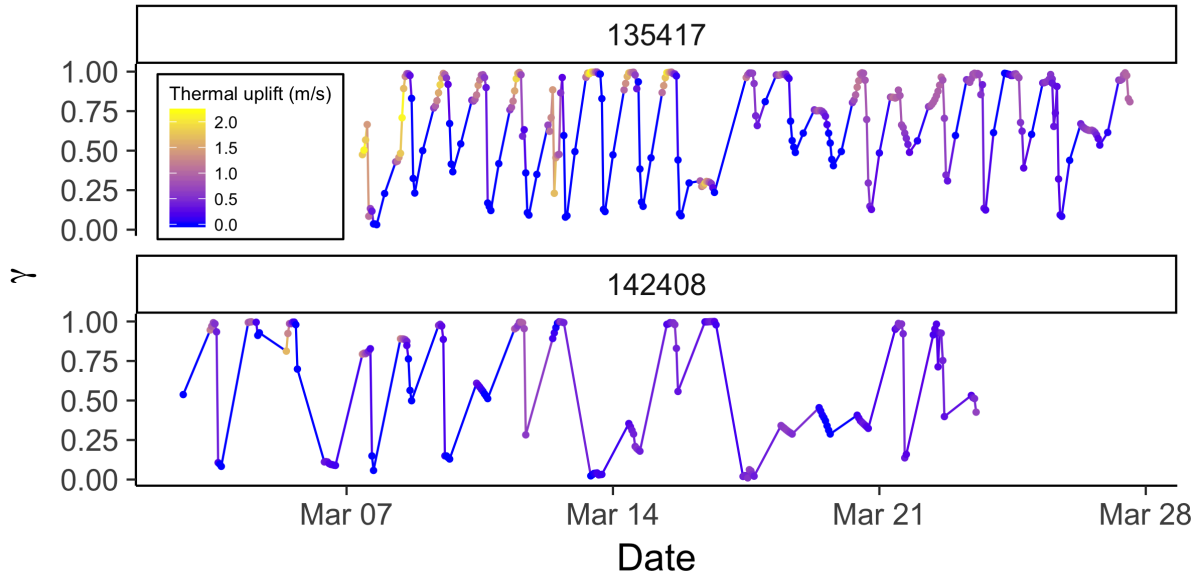

Figure 3.1: Time series of behavior parameter γ from correlated random walk model with full behavioral process (orographic uplift, thermal uplift, and wind support as predictors) for two golden eagles during spring migration with PTTs reporting on different duty cycles. Upper panel is 13 hourly centered on solar noon plus one at midnight, and the lower panel is 8 hourly centered on solar noon. γ close to one reflect movements associated with migratory behavior, and γ close to zero stopover behavior. Points are times of observations, and lines are linear interpolations between points. Hue indicates intensity of thermal uplift, with yellow indicating greater and blue lower. Note the daily rhythm in behavior associated with intense thermal uplift, stopover periods of one or more days, and the intermediate periods suggesting fly-and-forage.

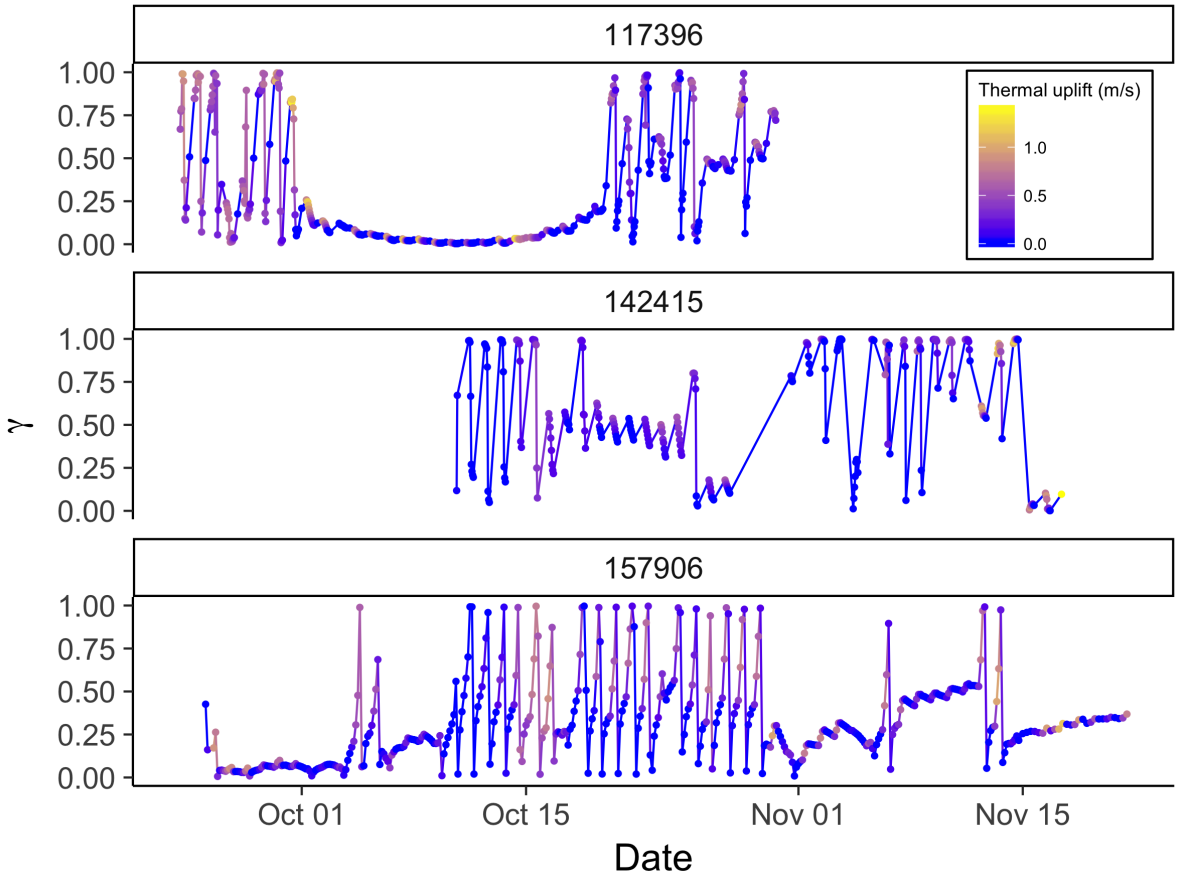

Figure 3.2: Time series of behavior parameter γ from correlated random walk model with full behavioral process (orographic uplift, thermal uplift, and wind support as predictors) for three golden eagles during fall migration with PTTs reporting on different duty cycles. Upper panel is 13 hourly centered on solar noon plus one at midnight, middle panel is 8 hourly centered on solar noon, and lower panel is fixed 3-hr interval. γ close to one reflect movements associated with migratory behavior, and γ close to zero stopover behavior. Points are times of observations, and lines are linear interpolations between points. Hue indicates intensity of thermal uplift, with yellow indicating greater thermal uplift and blue lower. Note the daily rhythm in behavior and extended stopovers as well as periods intermediate values suggesting fly-and-forage.

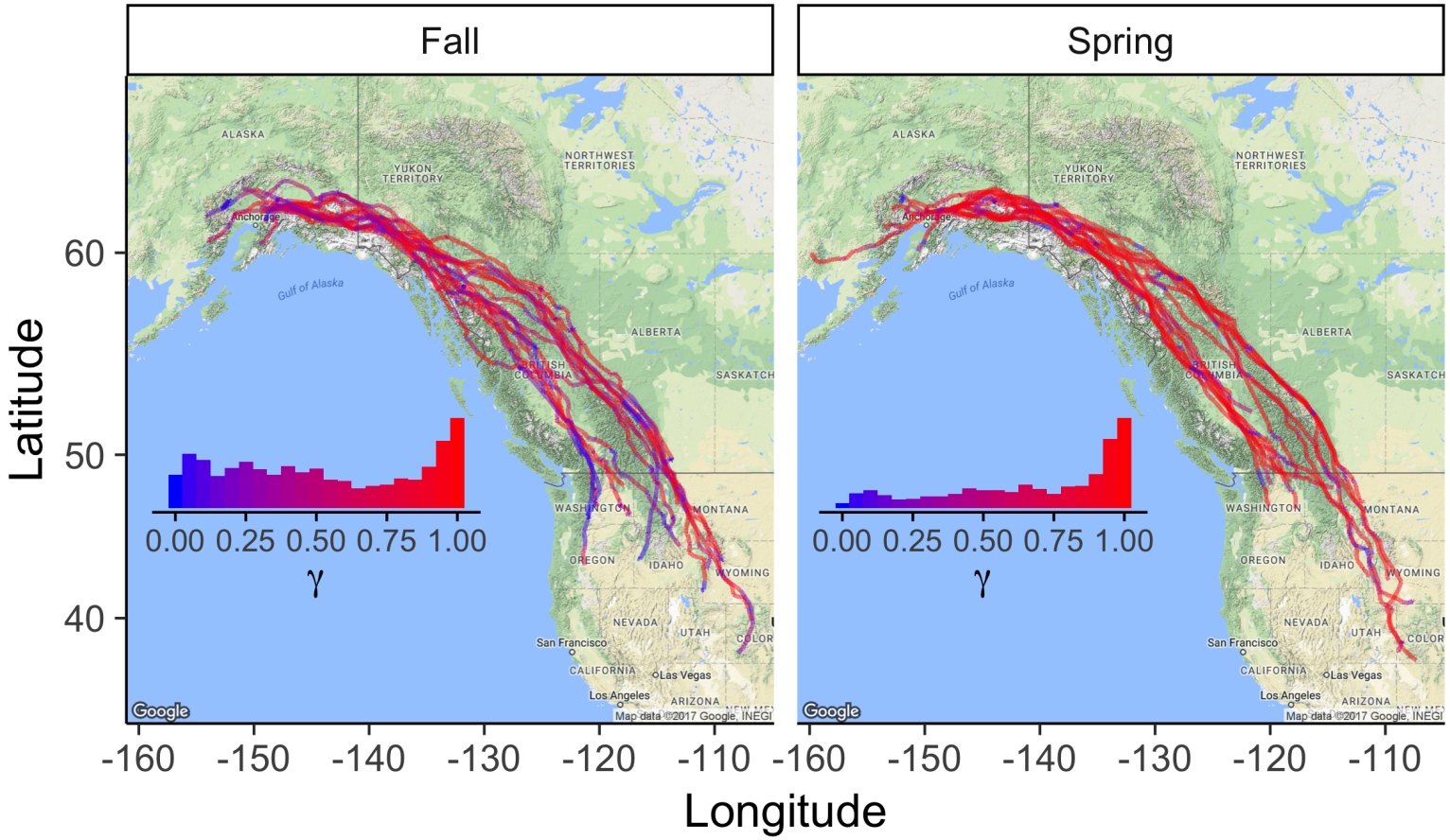

Figure 3.3: Golden eagle migration trajectories ($N = 15$ spring and $N = 16$ fall). Hue indicates value of behavioral parameter γ estimated with the correlated random walk model with full behavioral process, including orographic uplift, thermal uplift, and wind support as predictors. Insets show the relative frequencies of estimates of γ assigned to the displacements between observed daytime GPS locations. γ close to one reflect movements associated with migratory behavior, and γ close to zero stopover behavior. Daily rhythms, revealed in figures 3.1 and 3.2, are not apparent here because the birds moved so little at night.

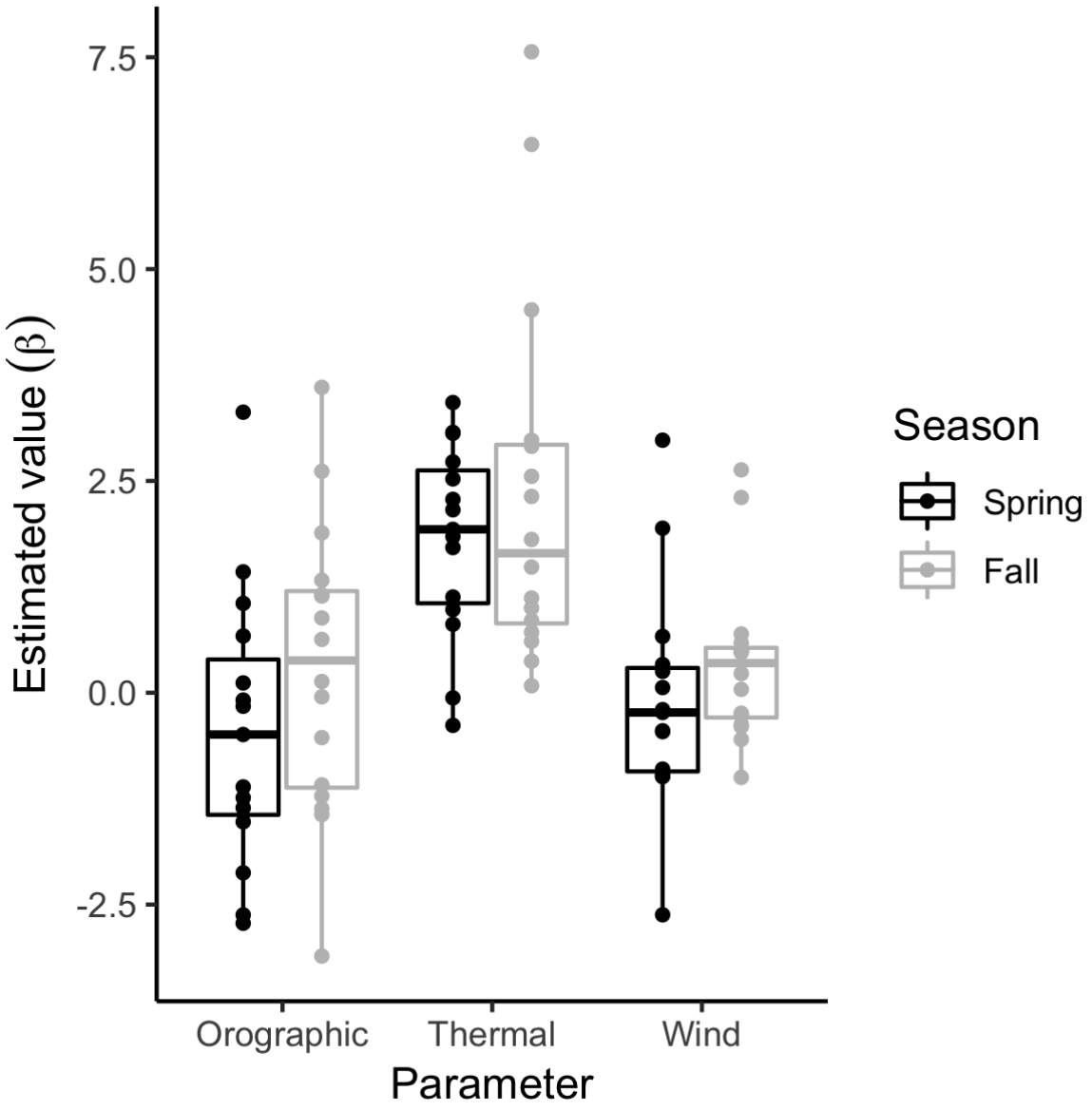

Figure 3.4: Point estimates of environmental covariate effect parameters (β_{ou}, β_{tu}, β_{tw}) on golden eagle behavior and movements during migration ($N = 15$ spring and $N = 16$ fall). Estimates are from the correlated random walk model with full behavioral process, including orographic uplift, thermal uplift, and wind support as predictors.

3.13 Tables

Table 3.1: Summary statistics of flight subsidies encountered by migrating golden eagles that summer in Alaska. Variables were interpolated in space and time from weather reanalyses to eagle locations recorded by GPS telemetry. Units for all variables are m/s.

Season	**Orographic Uplift**	**Thermal Uplift**	**Wind Support**
	mean[a] (*s.d.*)	*mean* (*s.d.*)	*mean* (*s.d.*)
Spring	0.41 (0.71)	0.61 (0.48)	2.09 (3.06)
Fall	0.43 (0.71)	0.39 (0.34)	1.37 (3.45)

[a]grand mean across discrete GPS locations with individual migration tracks pooled

Table 3.2: Number of golden eagle migration tracks recorded by GPS transmitters that each candidate formulation of the behavioral process in the correlated random walk model fit the best, according to approximate leave-one-out cross-validation (Table S7.1). 'therm' corresponds to thermal uplift, 'oro' to orographic uplift, and 'twind' to wind suppport.

Model	**looic Tally**[a]		
	spring	fall	total
full[b]	4	3	7
therm + twind	2	4	6
oro + therm	3	3	6
oro	3	3	6
therm	2	3	5
oro + twind	2	2	4
twind	0	3	3
null	1	1	2

[a]tally given to model with lowest information criterion (looic; Vehtari et al., 2016); if one or more models were within two looic of the top model, each was given a tally

[b]oro + therm + twind

Chapter 4: Novel step selection analyses on energy landscapes reveal how linear features alter migrations of soaring birds

4.1 Abstract

Human modification of landscapes includes extensive addition of linear features, such as roads and transmission lines. These can alter animal movement and space use and affect the intensity of interactions among species, including predation and competition. Effects of linear features on animal movement have seen relatively little research in avian systems, despite ample evidence of their effects in mammalian systems and that some types of linear features, including both roads and transmission lines, are substantial sources of mortality. Here, we used satellite telemetry combined with step-selection functions designed to explicitly incorporate the energy landscape (el-SSFs) to investigate the effects of linear features and habitat on movements and space use of a large soaring bird, the golden eagle *Aquila chrysaetos*, during migration. Our sample consisted of 32 adult eagles tracked for 45 spring and 39 fall migrations from 2014-2017. Fitted el-SSFs indicated eagles had a strong general preference for south-facing slopes, where thermal uplift develops predictably, and that these areas are likely important aspects of migratory pathways. el-SSFs also revealed that roads and railroads affected movement during both spring and fall migrations, but eagles selected areas near roads to a greater degree in spring compared to fall and at higher latitudes compared to lower latitudes. During spring, time spent near linear features often occurred during slower-paced or stopover movements, perhaps in part to access carrion produced by vehicle collisions. Regardless of the behavioral mechanism of selection, use of these features could expose eagles and other soaring species to elevated risk via collision with vehicles and/or transmission lines. Linear features have been previously documented to affect the ecology of terrestrial species (e.g., large mammals) by modifying individuals' movement patterns; our

Eisaguirre, JM, TL Booms, CP Barger, SB Lewis, GA Breed. 2020. Novel step selection analyses on energy landscapes reveal how linear features alter migrations of soaring birds. Journal of Animal Ecology: Under review. bioRxiv preprint: 805374

work shows these effects on movement extend to avian taxa.

4.2 Introduction

Linear features, such as roads, railroads, and transmission line corridors, are major anthropogenic modifications to landscapes worldwide and disrupt the natural spatial heterogeneity of habitats. Linear features have changed how animals move (James and Stuart-Smith, 2000; Dyer et al., 2002; Whittington et al., 2004, 2005, 2011; Dickson et al., 2005; Latham et al., 2011; Dickie et al., 2017; Scrafford et al., 2018), which in turn has altered predator functional responses (McKenzie et al., 2012), increased stress levels in free-living animals (Wasser et al., 2011), and changed other ecosystem interactions (Haddad et al., 2003).

These effects arise via a myriad of mechanisms. Linear features change the permeability of the landscape (Dyer et al., 2002; Whittington et al., 2004; Dickson et al., 2005; McKenzie et al., 2012; Tremblay and Clair, 2009), the distribution of food (Latham et al., 2011; Whittington et al., 2011; McKenzie et al., 2012; Dickie et al., 2017), and the spatial distribution of mortality risk (James and Stuart-Smith, 2000; Latham et al., 2011; Whittington et al., 2011; DeGregorio et al., 2014; Popp et al., 2018). Some linear features have negative effects that are unidirectional in predator-prey interactions. Seismic lines, for example, increase a predator's (wolf) access to prey (caribou), negatively affecting prey but imposing no additional risk or harm to the predator (McKenzie et al., 2012; DeMars et al., 2016; Dickie et al., 2019).

Many linear features, such as roads and railroads, broadly impact whole ecosystems. Roads and railroads can have marked effects on ecological communities. Vehicle collisions are responsible for substantial mortality in animals (Trombulak and Frissell, 2000; Fahrig and Rytwinski, 2009; Becker and Grauvogel, 1991; Gundersen and Andreassen, 1998; Popp et al., 2018), and vehicle traffic elicits avoidance responses in a wide variety of taxa (Prokopenko et al., 2016; Scrafford et al., 2018). Roads can also serve as barriers to movement and disrupt population connectivity (Strasburg, 2006; Shepard et al., 2008). The repeated clearing of roadway margins also creates edge habitat and maintains large

areas of habitat in earlier successional stages than surrounding habitats, which can attract species with matching habitat requirements (e.g., for open grass- or shrubland; Forman and Alexander, 1998; Meunier et al., 2000). Such roadside habitat changes, as well as road noise and general disturbance by moving vehicles, has altered the distribution, abundance, and behavior of many species (Meunier et al., 2000; Fahrig and Rytwinski, 2009; McClure et al., 2013). Carrion is also often disproportionately abundant along roads and railways due to vehicle collisions (Becker and Grauvogel, 1991; Gundersen and Andreassen, 1998; Trombulak and Frissell, 2000; Fahrig and Rytwinski, 2009; Popp et al., 2018), which can subsequently attract scavengers and opportunistic predators (Prosser et al., 2008; Lambertucci et al., 2009; Santos and Carvalho, 2011). These conditions generally create a unique species assemblage and an associated set of resources and risks; that risk is often imposed on both predator and prey.

Despite roadway mortality and mortality associated with transmission lines (i.e. collision and electrocution) being substantial sources of anthropogenic mortality in birds (Loss et al., 2015), work to understand the effects of linear features on individual animal movement has been almost entirely restricted to movement of large mammals. Consequently, the effects of linear features on on individual- and population-level avian movement are largely unknown. Their effects on some large birds (e.g., eagles and vultures) are of particular interest for conservation, considering these species are long-lived with slow reproductive rates, and even small amounts of additional anthropogenic mortality may not be sustainable. Many of these species also use carrion as a source of food, a potential attractant to linear features that comes with an increased risk of vehicle collision.

The migration period is already physiologically taxing and associated with elevated mortality in many birds (Newton, 2008; Harrison et al., 2011; Klaassen et al., 2014). While birds differ from landbound taxa in that they should be able to avoid vehicle collisions by flying over roadways and railways, it is unclear whether these features affect the movement or behavior of migrant birds in other ways, such as through habitat modification, changes in prey or carrion distribution and abundance, and/or use of linear features as migration corridors. Given that habitat and potential food resources are important to how a bird

uses space during migration (Gill, 2007), there are several biological reasons to expect linear features to alter movement of avian taxa across the landscape.

While effects of habitat and food are important drivers in individual- and population-level movement of migrant birds (Bildstein, 2006; Gill, 2007), the process is more complicated for soaring migrants due to their ability to use air currents to subsidize the energetic costs of flight (i.e. with wind and uplift). The effects of meteorology, especially air currents that develop due to pressure gradients in the atmospheric boundary layer, on movement metrics in many soaring birds are well established (Pennycuick, 1971; Alerstam, 1979; Spaar and Bruderer, 1997; Pennycuick, 1998; Duerr et al., 2012; Lanzone et al., 2012; Duerr et al., 2015; Katzner et al., 2015; Vansteelant et al., 2015; Miller et al., 2016; Shamoun-Baranes et al., 2016; Rus et al., 2017), with mechanistic links between meteorology and movement decisions also demonstrated (Eisaguirre et al., 2018). These atmospheric flight subsides are major components of a soaring bird's energy landscape (Shepard et al., 2013); however, such subsidies only offset energetic expenses with kinetic energy. Consequently, the distribution of available food energy, which is likely affected by linear features, remains an important component of a soaring bird's energy landscape, in terms of energy acquisition. Thus, we should expect movement of soaring birds to be dynamically affected by both food resource distributions and available atmospheric flight subsidies (Shepard et al., 2011).

As tools for understanding animal movement, step selection functions (SSFs) have emerged as powerful and robust analytical methods (Fortin et al., 2005; Forester et al., 2009; Potts et al., 2014a,b; Thurfjell et al., 2014; Avgar et al., 2016; Hooten et al., 2017), and when appropriately implemented are able to parse the importance of these different effects on movement decisions. Recent advances allow practical population-level inference while considering individual-level variability in selection and movement (Craiu et al., 2011; Muff et al., 2018). Still, SSFs typically assume that attraction toward or away from different habitats is statistically stationary—that selection does not change through time depending upon an animal's behavioral or physiological state. Animal behavior and physiology, however, changes across temporal and spatial scales, and attraction or avoid-

ance of different habitats is unquestionably dynamic. Although this is widely recognized (Thurfjell et al., 2014; Hooten et al., 2014; Avgar et al., 2016; Gurarie et al., 2017), behavioral changes are rarely accounted for in any habitat selection analyses, including SSFs, due to the additional complexity models require to capture the non-stationary condition (but see Avgar et al., 2016).

As an animal's behavioral state changes over time and space, the availability and utility of different habitats across the landscape will also change (Hooten et al., 2014). For example, a migrating animal has an evolved life-history constraint such that it must make migration progress towards a seasonal home range, and, consequently, movements that do not afford progress should be relatively infrequent for that animal. In contrast, while stopped over during migration for foraging or resting, an animal's movements and habitat selection should change substantially due to differences in energy and habitat requirements during stopover; such a behavioral change would result not only in different use of habitat, but also change in habitat preferences as well. How soaring birds budget behavior and movements, ranging from stopover to migratory, each day across a migration has been shown to be driven by the spatiotemporally-explicit state of the atmosphere (Eisaguirre et al., 2019; Miller et al., 2016), so it is reasonable to suspect that the state of the atmosphere, in part, also influences a soaring migrant's time-dependent use of the landscape, step selections, and movement decisions. Within such behaviorally-specific use of the landscape, use of linear features could also emerge as being behavioral state- and weather-dependent.

Here, we used a migratory population of golden eagles *Aquila chrysaetos*, a large soaring raptor, as a model system and implemented a novel, biologically justified SSF to investigate how the movement of a long distance migratory soaring bird is affected by both natural and anthropogenic linear features along migration routes. Our SSF incorporated key biologically relevant processes affecting both the energy and resource landscapes, including how soaring migration is driven strongly by wind and uplift conditions. This allowed careful testing of competing hypotheses regarding how terrain and vegetation likely influence movement on individual and population levels. Importantly, this SSF

framework allowed us to explicitly show the additional effects linear features can have on space use after accounting for both foraging habitats and dynamic energy landscapes, even despite possible coincidental alignment of migration routes with linear features.

4.3 Methods

4.3.1 Model system

Golden eagles are a large, long-lived, soaring raptor distributed across the Holarctic (Watson, 2010). Most individuals that summer and breed at high latitudes are long-distance migrants (Watson, 2010; Kochert et al., 2002). Golden eagles are opportunistic predators, capable of using many taxa for food resources, ranging from small mammals and birds to ungulates, and often scavenging carrion (Kochert et al., 2002; Watson, 2010). The population we studied summers primarily in the western Alaska Range and Talkeetna and Chugach Mountains of Alaska, USA and overwinters in the Rocky Mountain West, including Colorado, Utah, Wyoming, Montana, Idaho, Oregon, and Washington, in the US and mid to southern Alberta and British Columbia in Canada (Fig. 4.1; Eisaguirre et al., 2019; Bedrosian et al., 2018).

4.3.2 Telemetry data collection

We captured golden eagles with a remote-fired net launcher placed over carrion bait near Gunsight Mountain, Alaska (61.67°N 147.35°W). Captures occurred during spring migration, mid-March to mid-April 2014-2016. Adult and sub-adult eagles were equipped with 45-g back pack solar-powered Argos/GPS platform transmitter terminals (PTTs; Microwave Telemetry, Inc., Columbia, MD, USA). Eagles were sexed molecularly and aged by plumage.

PTTs were programmed to record GPS locations on duty cycles, ranging from 8-14 fixes per day during migration, depending on year of deployment. In 2014, PTTs were set to record 13 locations at one-hour intervals centered around solar noon plus a location at midnight local time. 2015 PTTs were programmed to record 8 locations with one-hour intervals centered around solar noon, and in 2016 we revised our programming approach

so that PTTs took eight fixes daily with a fixed 3-hr time interval. Poor battery voltage in fall, winter, and spring (September to March) occasionally resulted in PTTs failing to take all programmed fixes, so the resulting GPS tracks had missing observations. Note that such irregular sampling schedules preclude the use of many discrete-time analytical techniques (e.g., conventional and integrated step-selection analyses; Avgar et al., 2016; Hooten et al., 2017).

4.3.3 Energy landscape step selection function

Step selection functions (SSFs) typically take the form of a separable model, the product of a selection-independent movement kernel and a time invariant selection function:

$$f(\mathbf{x}_i|\mathbf{x}_{i-1},\mathbf{x}_{i-2};Z) = \frac{\phi(\mathbf{x}_i|\mathbf{x}_{i-1},\mathbf{x}_{i-2};\boldsymbol{\theta}_i)\omega(\mathbf{Z}(\mathbf{x}_i);\boldsymbol{\beta})}{\int_{\mathbf{x}'\in\Omega_i}\phi(\mathbf{x}'|\mathbf{x}_{i-1},\mathbf{x}_{i-2};\boldsymbol{\theta}_i)\omega(\mathbf{Z}(\mathbf{x}');\boldsymbol{\beta})d\mathbf{x}'}. \tag{4.1}$$

$f(\cdot)$ is the marginal probability density of $\mathbf{x}_i$, the location of the animal at time t_i, given that the animal arrived there after moving from $\mathbf{x}_{i-2}$ to $\mathbf{x}_{i-1}$ over resource field Z. $\phi(\cdot)$ is the selection-independent movement kernel, characterized by movement parameters $\boldsymbol{\theta}_i$ and describing how the animal would move over a homogeneous landscape Z (Forester et al., 2009). $\omega(\cdot)$ describes how the animal preferentially selects resources in Z based on weights $\boldsymbol{\beta}$ and typically takes a log-linear form (Forester et al., 2009):

$$\omega(\mathbf{Z}(\mathbf{x}_i);\boldsymbol{\beta}) = \exp(\mathbf{Z}(\mathbf{x}_i)^T\boldsymbol{\beta}). \tag{4.2}$$

$\mathbf{Z}(\mathbf{x}_i)^T$ is the transpose of a vector-valued function that returns the resource values of interest at $\mathbf{x}_i$, and $\mathbf{x}'$ is any point in Ω_i, the domain of space available to the animal at t_i.

$\phi(\cdot)$, along with many modern models for animal movement, is typically a discrete-time correlated random walk (CRW) parameterized in terms of polar coordinates (or step lengths and turn angles; Patterson et al., 2017; Hooten et al., 2017). Such models present challenges, though, in dealing with unequal time intervals between animal locations; step lengths can be normalized by time, but there is not an analogous operation

for turn angles. Irregular observations are often handled in the observation equation of discrete-time state-space models; however, with GPS data, we can typically assume negligible observation error and save considerable model complexity by modeling the observations directly with the movement equation (Patterson et al., 2008, 2017; Hooten et al., 2017). Notably, parameterizing a CRW in terms of displacement vectors in a continuous-time framework allows for straightforward relationships with time without an observation equation (Auger-Méthé et al., 2017; Gurarie et al., 2017; Eisaguirre et al., 2019; Jonsen et al., 2019).

To account for behavioral heterogeneity, its predictors, and irregular observations, we implemented our SSF with the following movement model representing $\phi(\cdot)$ (Auger-Méthé et al., 2017; Eisaguirre et al., 2019; Jonsen et al., 2019):

$$\mathbf{x}_i|\mathbf{x}_{i-1}, \mathbf{x}_{i-2} \sim \mathcal{N}_2\left(\mathbf{x}_{i-1} + \gamma_i \frac{\Delta t_i}{\Delta t_{i-1}}(\mathbf{x}_{i-1} - \mathbf{x}_{i-2}),\ \mathbf{\Sigma}_i\right), \tag{4.3}$$

where

$$\mathbf{\Sigma}_i = \begin{bmatrix} \Delta t_i^2 \sigma_x^2 & 0 \\ 0 & \Delta t_i^2 \sigma_y^2 \end{bmatrix}, \quad \sigma_x, \sigma_y > 0. \tag{4.4}$$

Here, $\Delta t_i = t_i - t_{i-1}$ represents the time interval between Cartesian coordinate vectors $\mathbf{x}_i$ and $\mathbf{x}_{i-1}$ for the observed locations of the animal at times t_i and t_{i-1}, and $i = 1, 2, \ldots, N$ for a track with N observations. Note that the movement parameters in equation 4.1 are $\boldsymbol{\theta}_i = (\gamma_i, \mathbf{\Sigma}_i)$. The latent variable γ_i correlates displacements (or 'steps') and can be interpreted to understand the type of movement, and thus behavior, of migrating individuals: estimates of γ_i closer to one indicate directionally-persistent, larger-scale migratory movement, while estimates of γ_i closer to zero indicate more-tortuous, smaller-scale stopover movement (Breed et al., 2012; Auger-Méthé et al., 2017; Eisaguirre et al., 2019; Jonsen et al., 2019). The behavioral process can be written

$$\gamma_i' = \gamma_{i-1}' + \mathbf{S}_i^T \boldsymbol{\alpha} + \epsilon_i, \tag{4.5}$$

where

$$\gamma_i' = \log\left(\frac{\gamma_i}{1-\gamma_i}\right), \tag{4.6}$$

$$\epsilon_i \sim \mathcal{N}\left(0,\ \Delta t_i^2 \sigma_\nu^2\right), \tag{4.7}$$

and $\mathbf{S}_i$ is the vector of environmental covariates at location $\mathbf{x}_i$ and time t_i. Each element of $\boldsymbol{\alpha}$ is an estimated parameter representing the magnitude and direction of the effect of its respective covariate on γ_i in addition to the effect of γ_{i-1}. Including γ_{i-1} here specifies explicit serial correlation in the behavioral process so that any environmental effect is not overestimated.

4.3.4 Inference

Practical inference with SSFs often requires estimating the movement process $\phi(\cdot)$ and selection function $\omega(\cdot)$ separately (Fortin et al., 2005; Forester et al., 2009; Potts et al., 2014b,a; Thurfjell et al., 2014; Hooten et al., 2017). Here, doing such corresponds to first making inference about the animal's movement and behavioral processes in addition to effects of environmental covariates on those processes (equations 4.3-4.7). We then proceed to estimate effects of habitat features that could additionally affect space use through the animal's preferential selection (equation 4.2). Although, estimating $\phi(\cdot)$ and $\omega(\cdot)$ independently could affect inference of respective parameters, it has been shown to have little to no effect on $\phi(\cdot)$ (Potts et al., 2014b), and there are ways to minimize bias in $\omega(\cdot)$ (*sensu* Forester et al., 2009).

We fit our movement model (equations 4.3-4.7), representing $\phi(\cdot)$ in equation 1, in a Bayesian framework with Stan in R (Stan Development Team, 2018; R Core Team, 2018), following Eisaguirre et al. (2019), with five chains of 200,000 Hamiltonian Monte Carlo (HMC) iterations, including 100,000 for warm-up, and retaining 10,000 samples for inference (see Eisaguirre et al. (2019) and/or the code provided as supporting information for prior choice). Fitting $\phi(\cdot)$ was done independently of $\omega(\cdot)$ for each individual migration.

The integral in the denominator of equation 4.1 is essentially always computationally prohibitive. However, a number of approximate methods have been proposed (see Hooten

et al. 2017). To estimate an SSF with an use-availability design, k available steps with endpoints $\mathbf{x}_i^j$ for $j = 1, 2, \ldots, k$ matched to the move from $\mathbf{x}_{i-1}$ to $\mathbf{x}_i$ are generated from $\phi(\mathbf{x}|\mathbf{x}_{i-1}, \mathbf{x}_{i-2}; \boldsymbol{\theta}_i)$. Then, the resource vectors $\mathbf{Z}(\mathbf{x}_i)$ and $\mathbf{Z}(\mathbf{x}_i^j)$ are populated from the appropriate data sources. We chose $k = 5$ for our analysis (Thurfjell et al., 2014), and under the Bayesian paradigm, simulating from our fitted $\phi(\mathbf{x}|\mathbf{x}_{i-1}, \mathbf{x}_{i-2}; \boldsymbol{\theta}_i)$ is analogous to sampling from the conditional posterior predictive distribution (Hooten et al., 2014, 2017)—the probability of a new ith observation given the observed data—which, for a 'new observation' $\mathbf{x}_i^j$, we denote $p(\mathbf{x}_i^j|\mathbf{X} = \mathbf{x}_{i-1}, \mathbf{x}_{i-2})$, where $\mathbf{X}$ is the $N \times 2$ matrix containing each $\mathbf{x}_i$ (Fig. 4.2). Sampling from each $p(\mathbf{x}_i^j|\mathbf{X} = \mathbf{x}_{i-1}, \mathbf{x}_{i-2})$ has the advantage of accounting for all parameter uncertainty and is fairly simple in the most commonly used Bayesian modeling languages (e.g., Stan and BUGS). Note that $p(\mathbf{x}_i^j|\mathbf{X} = \mathbf{x}_{i-1}, \mathbf{x}_{i-2})$ is (analytically) the result of integrating over the model parameters, including the time-varying latent behavioral variable γ_i, so each $p(\mathbf{x}_i^j|\mathbf{X} = \mathbf{x}_{i-1}, \mathbf{x}_{i-2})$ is conditioned on the animal's behavior at time t_i. Finally, to estimate $\boldsymbol{\beta}$, the comparison of used and available steps for each animal is carried out with conditional logistic regression. Hooten et al. (2014) present a similar approach that leverages the posterior predictive of a continuous time CRW fit with a Kalman filter (Johnson et al., 2008) to estimate $\boldsymbol{\beta}$ based on the smoother (use) and predictor (available) distributions. An advantage to their method is handling observation error; however, since observation error is negligible in our case, we decided to characterize use with the observed data, rather than a predicted distribution.

In presenting our energy landscape SSF (el-SSF), above, we did not account for multiple individuals, but this was just for notational simplicity. We estimated habitat selection parameters hierarchically across individuals. Hierarchical conditional logistic regression to estimate individual- and population-level effects presents estimation challenges (Duchesne et al., 2010), so we chose to implement a Poisson approximation of the hierarchical case, which allows Bayesian inference with integrated nested Laplace approximations (INLA; Muff et al., 2018). We followed Muff et al. (2018) and used R and the package `r-INLA` to estimate the resource weights $\boldsymbol{\beta}$ in $\omega(\cdot)$ (Rue et al., 2009; R Core Team, 2018). See Muff et al. (2018) for prior choice. A 3-knot linear spline with knot locations at

the quartiles of the step lengths was included in each candidate selection model to minimize bias in estimating $\boldsymbol{\beta}$, as $p(\mathbf{x}_i^j|\mathbf{X} = \mathbf{x}_{i-1}, \mathbf{x}_{i-2})$ is not actually selection-independent (Forester et al., 2009). Parameterizing a movement kernel with real data that is truly selection-independent is essentially impossible, given that we cannot observe animals moving over a homogeneous Z landscape (but see Avgar et al., 2016).

As golden eagles are diurnal, we chose to only include daytime movements, which we defined as those between sunrise and sunset, in estimating the el-SSF. Sunrise and sunset times local to each GPS point were calculated with the R package `maptools` (Bivand and Lewin-Koh, 2016).

4.3.5 Candidate models of movement & selection

We proposed a set of candidate models of movement and habitat selection and compared them using the widely applicable information criterion (WAIC; Watanabe, 2010), which is calculated by `r-INLA`, asymptotically equivalent to Bayesian cross validation, and an improvement over the deviance information criterion (Gelman et al., 2014). Each model represented a hypothesis for how golden eagles move and select for space during migration. Both the environment and the internal state of eagles varies substantially between spring and fall, so we fit the el-SSF and ranked candidate models independently for each season. A number of the variables included in our models were temporally dynamic, so much of any inter-annual variation was captured implicitly.

Given that golden eagle flight and behavior is driven by atmospheric flight subsidies (Duerr et al., 2012, 2015; Katzner et al., 2015; Miller et al., 2016; Rus et al., 2017; Eisaguirre et al., 2019), thermal uplift, orographic uplift, and wind support were included in all candidate models (in $\phi(\cdot)$; see below) to account for the dynamic energy landscape. Before comparing models including effects of anthropogenic linear features, we first wanted to determine which natural variables are most important to habitat selection, so we constructed a set of six candidate models, in addition to a 'no selection' null model, that generally corresponded to effects of the following: terrain, landcover, terrain + landcover, terrain + waterways, landcover + waterways, and terrain + landcover +

waterways. Comparing these models first allowed us to pare down the set of biologically plausible models that might otherwise be quite large if all habitat and linear feature variables were considered together.

We characterized terrain with elevation and slope aspect. We suspected that eagles would select for higher elevations, and given that conditions at higher elevations vary strongly along a latitudinal gradient, elevation was included in models as an interaction with latitude. South-facing slopes are exposed to more intense solar radiation, and thus produce more thermal uplift. Although thermal uplift is a favored energetic subsidy (Duerr et al., 2012), changes in urgency, especially as individuals approach the breeding grounds, might lead them to forego use of south-facing slopes in favor of a more direct route (Miller et al., 2016). Additionally, ambient conditions (e.g., prevailing air temperature/pressure) generally change substantially with latitude, which could affect the degree to which eagles favor south-facing slopes as a source of uplift. We thus also included aspect as an interaction with latitude. We considered including terrain ruggedness; however, it was highly colinear with elevation, so it was not included.

Landcover was characterized by vegetation and snow cover. Prey availability likely varies with vegetation and snow, but densely vegetated areas could generate thermal uplift (Howard and Stull, 2013). In the field while capturing eagles during spring migration, we observed eagles seemingly thermal soaring over areas predominantly flat and densely covered with dark vegetation (i.e. *Picea* spp.) comprising an otherwise snow covered landscape, which would typically not offer thermal uplift.

Waterways were treated as natural linear features. Waterways would be a source of prey (i.e. waterfowl), but could also be used for navigation. Golden eagles that migrate to Alaska have been shown to use the long 'trenches' (very straight, long valleys) in the Canadian Rocky Mountains (Kochert et al., 2002; McIntyre et al., 2008; Eisaguirre et al., 2019). Large bodies of water could also be barriers to movement (Kochert et al., 2002).

After selecting the best approximating model given our set of models that included natural covariates, we generated another set of three candidate models that included anthropogenic linear features; the two types considered were roads and railroads. Given

that collisions with vehicles and transmission lines along roads are a leading cause of anthropogenic avian mortality (Loss et al., 2015), we suspected eagles might avoid them due to mortality risk. Alternatively, roads likely provide carrion, which could attract eagles, perhaps even to follow them during migration. Railways have not been documented as a major source of mortality risk to raptors and other birds—although a juvenile eagle banded in Alaska was killed by a train (T. Booms, *unpubl. data*). Railways are, however, responsible for substantial mortality in large mammals (e.g., ungulates; Becker and Grauvogel, 1991; Gundersen and Andreassen, 1998; Popp et al., 2018), potentially concentrating carrion resources for migrating eagles. As both railway and road densities decline with increasing latitude in North America, they were included in models as an interaction with latitude in addition to their main effects.

We were interested in investigating effects of transmission lines on eagle movement as they are a leading cause of raptor mortality (Loss et al., 2015). However, power line corridor data are largely proprietary and confidential and thus were not available to include in models. We were also interested in the effects of wind energy developments (Pagel et al., 2013; Loss et al., 2015); however, we did not include them in candidate models due to their apparent minimal availability to the eagle migrations we sampled. We present summary statistics regarding interactions between eagles and wind energy developments in Appendix S1.

4.3.6 Covariate data

Flight subsidies We gathered meteorological flight subsidy data for eagle tracks with the Track Annotation Service in Movebank (Dodge et al., 2013). These variables were introduced as covariates $\mathbf{S}_i$ into the behavioral process in the the movement kernel $\phi(\cdot)$ (Eisaguirre et al., 2019). In our SSF, flight subsidies $\mathbf{S}_i$ coupled with $\boldsymbol{\alpha}$ modify what is available to an eagle at each t_i by driving the behavioral dynamics (equations 4.5-4.7).

Thermal uplift was bilinearly interpolated from European Centre for Medium-Range Weather Forecasts (ECMWF) reanalyses, and orographic uplift from the nearest neighbor (grid cell) by pairing National Center for Environmental Predictions (NCEP) North

American Regional Reanalysis (NARR) data with the Advanced Spaceborne Thermal Emission Reflection Radiometer (ASTER) Global Digital Elevation Model (GDEM; Brandes and Ombalski, 2004; Bohrer et al., 2012). Wind data were interpolated bilinearly from the NCEP NARR u (westerly/zonal) and v (southerly/meridional) components of wind, from which we calculated the wind support (Safi et al., 2013).

Terrain & habitat Elevation, slope, vegetation, and snow cover data were gathered for all locations $\mathbf{x}_i$ and $\mathbf{x}_i^j$ with the Env-DATA system (Dodge et al., 2013). The source of the elevation and slope data was the ASTER. Env-DATA provides the u and v components of slope. We used the v (south to north) component as it represents the degree to which the slopes in the grid cell for each $\mathbf{x}_i$ and $\mathbf{x}_i^j$ are south-facing (hereafter slope southing). Percent vegetation and snow cover of grid cells were predicted with the NCEP NARR.

Linear features Waterway data were gathered from the Commission for Environmental Cooperation 2009 Lakes and Rivers dataset. Road and railroad data were gathered from the United States Geological Survey National Transportation dataset and Canadian National Road/Railway Network. The road types included in models were those considered arterials, (state or county) highways, and freeways.

These data were included in candidate models of selection as distance to nearest (waterway, road, or railroad) measured at step endpoints. All distances were measured in R with the package `sp` (Pebesma and Bivand, 2005; Bivand et al., 2013).

We chose to include only endpoint effects in candidate models of selection for two main reasons. First, irregular observations lead to inconsistent uncertainty between observed locations. Interpolations between observed points are less accurate with larger Δt_i, so normalizing by Δt_i, although simple, would not be entirely appropriate; other assumptions would be required (Thurfjell et al., 2014). Second, migrants are essentially required (by their life history) to cross linear features that are not precisely parallel to movement during migration, so movements that do not cross roads, for example, would be minimally available, making quantifying any effect of crossings on selection difficult.

Lastly, we conducted a brief simulation study, which we present in Appendix S3, to validate that the SSFs detected real effects of linear features. This was to ensure that

apparent selection for linear features as estimated within the SSF framework was not simply an artifact of the distribution of linear features on the landscape, even if they coincidentally aligned with migration routes.

4.4 Results

Of the tags deployed, 32 provided at least one migration with sufficient data to estimate the movement kernel $\phi(\cdot)$. Nine were deployed on females and 23 on males, and all were adults (at least five years old). From those individuals, 17,386 realized (used) daytime steps were included in the step selection analysis spanning 45 spring and 39 fall individual migrations 2014-2017. Median (interquartile range) spring and fall departure dates across years were 10 March (6 days) and 2 October (11.5 days), respectively, and arrival dates were 30 March (6 days) and 13 November (20 days). Only 25 of the 17,386 steps analyzed intersected 1 km buffers surrounding wind turbines; twenty endpoints of the steps were within 5 km of a wind turbine; and only two were within 2 km (Appendix S1).

4.4.1 Atmospheric flight subsidies

We found thermal uplift to be the main driver of migratory behavior during both spring and fall migrations across years, though there was a high degree of variability in how flight subsidies (wind and uplift) drove behavior among individuals (Fig. 4.3). Our sample contained more than twice as many males as females, but we found little evidence for an effect of sex on the behavioral process (Fig. 4.3). While an eagle's response to flight subsidies did not change markedly between seasons (Fig. 4.3), eagles tended to adjust their pace to move more quickly in the spring by budgeting more time to faster, directed movement. During fall migrations, eagles moved more slowly, and budgeted comparatively more time to slower, less directed movement resembling searching and stopover (Fig. 4.1).

4.4.2 Model selection

All habitat variables included in the SSF improved fit, though we note that terrain was especially informative, strong evidence that habitat is an important component of the movement process (Table 4.1). Although the CRW and flight subsidies $\phi(\cdot)$ can predict a relatively large area of high probability for step selection (Fig. 4.2a), when habitat is considered, the high probability region becomes quite concentrated (Fig. 4.2c). A model including elevation, slope southing, snow and vegetation cover, and waterways was top ranking in both spring and fall (Table 4.1). The addition of linear features further improved fit (Table 4.1), with substantial support for both roads and railroads driving movement in spring and fall in addition to terrain, landcover, and waterways.

4.4.3 Natural landscape features

Eagles generally used and preferred lower elevations in the spring and higher in the fall (Fig. 4.4 & 4.5), though there was considerable variation among individuals (Fig. 4.5). In spring, selection for higher elevation decayed with latitude, while in fall, change in elevation preference with latitude was variable across individuals (Fig. 4.5). All eagles favored south-facing slopes in both seasons, showing a stronger preference with increasing latitude in spring (Fig. 4.5). Although snow-covered and vegetated areas were used to a greater degree in spring (Fig. 4.4), all individuals showed a preference for snow-covered and less vegetated areas in spring (Fig. 4.5).

In both seasons, eagles showed a preference for areas close to waterways given the habitat available (Fig 4.5–4.7). However, there was less selection for areas near waterways in the fall compared to spring.

4.4.4 Anthropogenic linear features

Eagles were often near linear features but more frequently closer to roads and railroads during spring migration than fall (Fig. 4.8). SSF predictions indicated that probability of using a given area increased if that area was closer to a road, especially in spring (Fig 4.7). Eagles' preference for areas near roads decayed slightly with increasing latitude

(Fig. 4.5 & 4.9), and there was considerably individual variability in preference for areas near roads during fall migration (Fig. 4.5 & 4.9). Eagles exhibited a slight preference for railroads in fall (Fig. 4.5 & 4.9); however, there was, again, substantial variability among individuals in both seasons (Fig. 4.5 & 4.9). See Appendix S3 for results of simulations showing SSFs parse actual selection from incidental use of linear features when linear features and movement routes are coincidentally parallel.

4.4.5 Effects of behavior on habitat use

The use of anthropogenic linear features and habitat changed substantially depending upon expressed behavior, as captured by estimates of γ_i (Fig. 4.4 & 4.6). When eagles engaged in less directed, more tortuous movements, typically associated with stopover, these behaviors were performed in areas closer to roads and railroads in spring and farther from roads and railroads in fall (Fig. 4.6). Areas with higher percent vegetation cover were used when eagles were moving with intermediate directional persistence and movement rate, while very low persistence and very high persistence states were associated with less vegetated areas (Fig. 4.4). Use of space near waterways also varied with behavioral state, such that eagles were closer to waterways while moving with intermediate directional persistence and rate (Fig. 4.6). During fall migration, eagles generally used higher elevation terrain while making faster-paced, directionally-persistent movements, and during both spring and fall migration, eagles used more south facing slopes while making faster-paced, directionally-persistent movements (Fig. 4.4).

4.5 Discussion

The effects of linear features on the movement of large terrestrial mammals are relatively well understood (Dyer et al., 2002; Whittington et al., 2004; Dickson et al., 2005; Latham et al., 2011; Whittington et al., 2011; McKenzie et al., 2012; Tremblay and Clair, 2009; DeMars et al., 2016; Dickie et al., 2017; Popp et al., 2018; Dickie et al., 2019), but, here, we showed that anthropogenic linear features can also affect movement and space use of avian species during migration. Our approach was analytically nuanced,

incorporating the affects of energy subsidies key to soaring movement into the the movement process. This helped disentangle the effects of such subsidies from habitat selection, which would not have otherwise been possible with more phenomenological models, such as conventional resource or step selection functions. Specifically, the el-SSF accounted for favorable uplift and wind conditions (i.e. a soaring bird's energy landscape), which probabilistically restricted the habitats available for selection; the effects of linear features could then be additionally estimated to further explain movement and space use (Fig. 4.2). Such an approach is superior, as it mechanistically restricts where a soaring bird is likely to move based on the energy landscape and weather conditions. A migrant can be less likely to make moves that accrue several hundred kilometers of migration progress during a day when there is limited uplift, for example, so dynamically restricting the el-SSF movement process based on these conditions is a natural extension of the current static, discrete-time CRWs employed in conventional SSFs (e.g., Fortin et al., 2005; Forester et al., 2009; Thurfjell et al., 2014; Potts et al., 2014b,a).

Building movement kernels with more biological relevance—beyond basic random walks—into SSFs has been suggested (Thurfjell et al., 2014; Jonsen et al., 2019), but to our knowledge, this is the first time it has been executed while maintaining the practicality of (hierarchical) conditional logistic regression for estimation of resource selection parameters. The el-SSF also allowed us to account for and detect variation among individuals, which has been shown to be key to correct inference of resource selection patterns (Lesmerises and St-Laurent, 2017), while still making population-level inference of habitat and resource selection. Lastly, we were able to show that use of habitat varied with the expressed behavior (tracked with the dynamic value of γ_i, the movement correlation parameter), ranging from slower-paced, stopover movements to faster-paced, migration movements.

These behavioral changes were built into the CRW movement kernel in the el-SSF, allowing us to leverage aspects of related mathematical and movement ecology theory. In spring, eagles used areas closer to roads and railroads while performing slower-paced movements suggestive of migratory stopover (Fig. 4.6). As movements that tend to

keep an animal in the same area (i.e. slower-paced/searching movements) coincide with greater residence time (Turchin, 1991, 1998), we can infer that eagles' residence time nearer roads and railroads during spring migration is higher compared to other areas on the landscape. While this also implies eagles would be relatively more abundant there at any given time (Odendaal et al., 1989), eagle residence time would be conditional on atmospheric conditions, as stopover movements are more likely when weather conditions do not support thermal uplift (Fig. 4.3; Eisaguirre et al., 2019; Miller et al., 2016). So, eagles' use of areas nearer roads and railroads might ultimately vary with uplift conditions. However, as uplift conditions are driven by the daily development of the atmospheric boundary layer—uplift is least available in morning and evening due to limited insolation during those times of day—eagle residence time near linear features may generally be greatest in morning and evening.

4.5.1 Extending SSFs

The el-SSF approach offers novel analytical utility, but using movement data to investigate some important questions regarding details of animals' use of linear features requires a statistical method that can assess state-specific selection for different landscape features. An important question, here, is how an eagle might balance scavenging road-killed carrion with the risk of vehicle collision across different behavioral or physiological states. State-specific selection in SSFs is an active area of analytical development (Hooten et al., 2014; Avgar et al., 2016; Hooten et al., 2017; Karelus et al., 2019; Scharf et al., 2019), and while the el-SSF did not explicitly incorporate behaviorally-specific selection into its framework, we were still able to infer behavior-specific use of linear features and habitat plus seasonal variation in those patterns (Figs. 4.4-4.6). While progress is being made (e.g., Avgar et al., 2016), these findings further support the need to consider behavioral heterogeneity in resource selection analyses and work towards overcoming related analytical obstacles.

Estimating behaviorally-specific selection coefficients requires introducing movement parameters into both the movement and selection processes, and thus imparts dependence

between $\phi(\cdot)$ and $\omega(\cdot)$ (equation 4.1). This structure often precludes the use of conditional logistic regression for obtaining unbiased estimates of $\boldsymbol{\beta}$ without special consideration of that dependence (Forester et al., 2009; Avgar et al., 2016).

4.5.2 Eagle migration & anthropogenic linear features

Behaviorally-dependent use of linear features There are a number of possible reasons for why migrating eagles might select and use areas close to anthropogenic linear features. They may use linear features for (1) navigation, (2) increased movement rate—these features may produce favorable flight conditions—and/or (3) access to food resources. Although other taxa have been shown to use linear features to increase movement rate (Latham et al., 2011; McKenzie et al., 2012; Dickie et al., 2017), possibilities (1) and (2) seem unlikely for some soaring birds, such as eagles. During spring migration, eagles were on average nearly twice as close to roads and railroads while engaged in slower-paced, stopover-like movements as compared to faster-paced, migratory movements (Fig. 4.6). We would expect the reverse pattern (i.e. closer association with linear features during more rapid movement phases) if linear features accelerated eagle movement or if eagles were following them during migration.

Slower-paced, tortuous movements are less autocorrelated, and more frequently associated with area restricted search and/or foraging behavior (*sensu*, e.g., Breed et al., 2009; Patterson et al., 2017; Jonsen et al., 2019), so linear features may be targeted as a source of food energy for migrating eagles or serve as open pathways for foraging searches during migratory stopover. Carrion, which is often available along linear features due to vehicle collisions, can be an important food resource for eagles and other raptors (Watson, 2010; Newton, 1979; Bildstein, 2006), and even detection rates of carrion by raptors can be higher near linear features (Lambertucci et al., 2009). Moreover, using linear features to access food aligns with findings in terrestrial mammals; wolves are thought to use seismic lines to access caribou (Dickie et al., 2017), and bears use railroads to access key supplemental food (Murray et al., 2017).

Latitudinal patterns in linear feature use Eagles' selection for areas close to roads

tended to increase with latitude (Fig. 4.5 & 4.9), such that selection for roads became stronger as roads became less dense on the landscape, perhaps also coinciding with reduced prey availability. The lower elevation areas eagles used and selected for during spring migration (Fig. 4.4 & 4.5) are predominantly boreal forest at high latitudes. Roads and railroads, therefore, contrast markedly with the thick forested landscape, potentially providing open habitat and offering visibility advantages for capturing prey and/or detecting carrion. Other features associated with roads and railroads, such as power poles, likely also offer convenient, high-visibility perches (Meunier et al., 2000).

Seasonal patterns in linear feature use Carrion is usually an ephemeral resource on the landscape; however, it can be more predictable along linear features due to vehicle collisions with wildlife, offering scavenging migrants an efficient and reliable source of food (Lambertucci et al., 2009). While we found eagles exhibit a general preference for areas near roads during both spring and fall migration (Fig. 4.5), we also found less variable (Fig. 4.5 & 4.9) and heavier (Fig. 4.6–4.9) use of roadways during spring. With the likely association between roads and foraging, such narrow individual-level variability in selection for roads (Fig. 4.5 & 4.9) might be expected from theory, as time- and energy-minimization strategies for migration are tied strongly to fuel deposition rate, leading to selective pressure on en-route foraging strategy (Hedenstrom and Alerstam, 1997). Furthermore, shorter overall migration times in spring than fall—an apparent >50% difference in our sample of eagles—have been found to be owed to differences in foraging-related factors across a number of studies (Nilsson et al., 2013).

Carrion along linear features could be important for an eagle's timely arrival on the breeding grounds in spring, such that the reward of carrion or benefit of using linear features to detect prey or access carrion could outweigh the real or perceived risk of being struck by a vehicle. By contrast, in fall, there is less urgency for timely arrival on the overwintering grounds, so the elevated mortality risk associated with food resources along linear features would not outweigh the risk. Migrants should, then, spend more time searching for food away from linear features in the fall, which is consistent with our results (Fig. 4.1 & 4.6). A key aspect to this reasoning, however, is that individuals

assess the mortality risk at linear features correctly. In cases where using a linear feature is more dangerous than an individual's assessment, use of that linear feature may be maladaptive. For example, high-traffic roads may be easy to assess correctly; however, rural highways with infrequent but fast-moving vehicles may be difficult to assess but quite dangerous.

During fall migration, eagles tended to associate less with linear features as compared to spring (Fig. 4.6 & 4.8). This could be a result of more intense pressure to reach summer breeding grounds, but these patterns may simply emerge from eagles responding to relative seasonal abundances of food available across the landscape. In spring, golden eagles migrate earlier than other avian migrants and prior to the emergence of hibernating mammals. In contrast, eagles migrate in fall when migratory birds and mammals not yet hibernating, including many young of the year, are available as prey. Thus, prey may be available across the landscape away from linear features and more easily captured during fall migration compared to spring. Additionally, fall migration coincides with many hunting seasons in western North America, so eagles might also be feeding on unsalvaged large mammal remains (e.g., gut piles) left in the field by hunters away from major roads. Annual moose harvest in British Columbia, Canada averages $\sim 10,000$ animals between 15 August and 10 December (Kuzyk, 2016), leaving potentially abundant scavenging opportunities on the landscape. Even if roads provide the same access to carrion during both seasons, in fall the higher relative abundance of prey elsewhere on the landscape would decrease the relative value of roads, which might explain eagles' less frequent use of linear features in fall. Scavenging opportunities along roads are likely more frequent in late winter and spring, though, due to, for example, accumulated carcasses melting out of snow (Jennelle et al., 2009; Santos and Carvalho, 2011).

4.5.3 Effects of habitat on eagle space use

Although investigating the effects of anthropogenic linear features was the primary goal of this paper, incorporating other biologically important variables revealed some noteworthy patterns. Unsurprisingly, eagles showed a very strong preference for south-

facing slopes (Fig. 4.5). Given that eagles' use of south-facing slopes aligned with migratory movements each day (Fig. 4.4), actively seeking out south-facing slopes is a likely mechanism for how thermal uplift emerges as an important driver of golden eagle movement and behavior during migration (Fig. 4.3; Eisaguirre et al., 2019; Miller et al., 2016; Duerr et al., 2012). Although biologically expected, this finding provides additional confidence that other estimated parameters are also biologically meaningful.

Although we expected eagles would forego use of south-facing slopes to make more direct routes when under the greater time pressure of spring migration, preference for south-facing slopes actually increased with latitude during spring (Fig. 4.5 & 4.9), suggesting eagles balance time- and energy-minimization migratory strategies (Miller et al., 2016); this is also consistent with findings supporting the efficiency of thermal soaring (Duerr et al., 2012). As eagles approach the breeding grounds in spring, thermal uplift and the energetic subsidy it provides are likely more limited due to snow cover increasing with latitude (Eisaguirre et al., 2019), eliciting the greater selective response for south-facing slopes.

Similar to use of linear features, we also found that use of certain habitats was behavior-specific. Use of vegetated areas appeared associated with fly-and-forage movements, identified by lower and intermediate estimates of γ_i, and less associated with migratory movement (Fig. 4.4). In fly-and-forage movement strategies, migrants opportunistically forage while making progress, albeit somewhat more slowly than in directed movement, along the migration route (Strandberg and Alerstam, 2007; Klaassen et al., 2008; Alerstam, 2011). Making wider searches over less than ideal hunting habitat (i.e. a fly-and-forage strategy) might offer occasional food payoffs that, combined with the migration progress, outweigh targeting better hunting areas with more intensive search, which yields no migration progress (Nilsson et al., 2013).

The latter episodic intensive search strategy aligns with the traditional notion of stopover (Gill, 2007); however, migratory "pacing" was recently suggested as a better conceptual framework for stopover behavior in soaring species, such as eagles, that naturally encompasses the fly-and-forage strategy (Eisaguirre et al., 2019). During fall migration

when making fly-and-forage movements, eagles used south facing slopes (Fig. 4.4), perhaps to use thermal uplift to minimize energy expenditure. These periods also coincided with using slightly more vegetated and lower elevation areas (Fig. 4.4). Use of areas close to waterways also correlated with fly-and-forage movements (Fig. 4.6), and as many of the waterways encountered along migration routes would be frozen and snow covered during spring migration, these areas could offer open and edge habitat for foraging.

4.5.4 Individual heterogeneity in movement and space use

There was marked individual-level variability in both behavioral responses to flight subsidies and preference for habitat features (Figs. 4.3, 4.5, & 4.9), which did not seem to be explained by sex (Figs. 4.3 & 7.4). In particular, although generally individuals selected areas closer to linear features, some individuals tended to avoid them (Figs. 4.5 & 4.9). Similar variation in use of anthropogenic linear features has been reported in grizzly bears *Ursus arctos* (Murray et al., 2017).

Additionally, individual animals can exhibit different habitat preferences depending upon the predominant habitats available to them (Gilbert et al., 2017); however, we did not find such correlations between availability and preference prevalent for individual eagles (Figs. 7.5 & 7.6). An exception was for elevation, which could be owed to longitudinal trends in available elevations along the migration routes (Figs. 7.5 & 7.7).

Lastly, the effects of learning and variation in personality traits should not be discounted as possible causes for the differences among individuals we found (Fagan et al., 2013; Wolf et al., 2007; Dingemanse et al., 2010). Variation in use of risky sources of food near roads has been shown to exist among an assemblage of raptor species that exhibit a range of risk aversion behavior (Lambertucci et al., 2009). This variation should also exist among individuals within species; each individual would have a unique risk-aversion personality (Wolf et al., 2007; Dingemanse et al., 2010). Thus, it is reasonable to expect that some of the variance among eagles in our sample, in terms of their attraction/repulsion to linear features (Figs. 4.5 & 4.9), could be due to variance in personality along the shy-bold spectrum and/or behavioral conditioning.

4.5.5 Conclusions & Implications

One inference drawn from our results reflects how time of day and thermal uplift relates to eagles' use of linear features. This raises the question of how uplift drives migrant abundance along linear features and whether or not poor uplift conditions might elevate vehicle collision risk for migrants. While we have shown that eagle behavior correlates with use of areas close to roads and railroads and that they can prefer such areas, we could not infer mortality risk. Limited thermal uplift and how it effects raptor behavior has been suggested to elevate risk of raptor collisions with wind turbines though (Barrios and Rodríguez, 2004). Higher frequency telemetry and observational studies along roads during migration could help reveal and perhaps quantify vehicle collision risk; a network of carrion baited camera traps might also be useful and cost effective (*sensu* Jachowski et al., 2015). The parameterized el-SSF, however, could be used to predict eagle space use patterns to identify potential hot spots of elevated mortality risk, as well as how those spots might change with weather. Such application could at least increase the efficiency and effectiveness of targeted studies of mortality risk within this migration corridor, which spans half the continent (Fig. 4.1), as well as other expansive movement corridors. Moreover, the el-SSF could also be used to help inform eagle-vehicle collision risk models (e.g., Lonsdorf et al., 2018), and it could more generally be used to predict and test hypotheses regarding changes in eagle space use patterns following continued development of linear futures, other habitat changes, and/or changes in weather patterns.

As continued human development has the potential for introducing additional mortality risk onto the landscape, it is important to keep in mind that anthropogenic mortality is considered the greatest threat to many populations of long-lived raptors (Newton, 2008). Further, elevated mortality during migration—an already risky time for birds—can carry over to impact population reproductive rates (Newton, 2008; Harrison et al., 2011). Such carry-over effects were suggested as a possible cause for the long term decline in reproductive success of long-distance migratory golden eagles in a study area in interior Alaska (McIntyre and Schmidt, 2012). While there are apparently few wind

energy developments along the migration corridors of our sample of eagles (Fig. 7.3), there will certainly be continued development, potentially creating more opportunities for migratory golden eagles to interact with wind turbines. Here, we have clearly shown the importance of considering the effects of linear features on avian movement and space use during migration. We thus should not discount the potential movement-related effects and mortality risk that anthropogenic linear features can impose on avian migrants, despite a bird's ability to fly over such human infrastructure during migration.

4.6 Acknowledgements

T. & D. Hawkins, M. Kohan, B. Robinson, and many others provided support in the field, and J. Liguori and N. Paprocki helped age eagles. M. Auger-Mèthè offered motivating and invaluable discussion regarding the movement model. C. McIntyre, K. Kielland, and P. Doak provided excellent feedback that helped improve this research and manuscript. To all of these friends, we are most grateful. Funding was provided by the Alaska Department of Fish & Game (ADF&G) through the federal State Wildlife Grant Program, and the U.S. Fish & Wildlife Service (USFWS) provided additional PTTs and data. JME was supported by the Calvin J. Lensink Fund during part of the project. The findings and conclusions of this paper are those of the authors and do not necessarily represent the views of the USFWS.

4.7 Data accessibility

All movement data used for this manuscript are managed in the online repository Movebank (https://www.movebank.org/; IDs 17680093 and 19389828). The data contain information considered confidential and sensitive by the State of Alaska (State Statute 16.05.815(d)), but they could be made available for research at the discretion of the Alaska Department of Fish & Game and U.S. Fish & Wildlife Service. Code to fit the movement model to data and sample from the posterior predictive distribution is provided as supporting information.

4.8 References

Alerstam T. 1979. Optimal use of wind by migrating birds: combined drift and overcompensation. *Journal of Theoretical Biology* **79**: 341–353. doi: 10.1016/0022-5193(79)90351-5.

Alerstam T. 2011. Optimal bird migration revisited. *Journal of Ornithology* **152**: 5–23. doi: 10.1007/s10336-011-0694-1.

Auger-Méthé M, Albertsen CM, Jonsen ID, Derocher AE, Lidgard DC, Studholme KR, Bowen WD, Crossin GT, Mills Flemming J. 2017. Spatiotemporal modelling of marine movement data using Template Model Builder (TMB). *Marine Ecology Progress Series* **565**: 237–249. doi: 10.3354/meps12019.

Avgar T, Lele SR, Keim JL, Boyce MS. 2017. Relative selection strength: quantifying effect size in habitat- and step-selection inference. *Ecology and Evolution* **7**: 5322–5330. doi: 10.1002/ece3.3122.

Avgar T, Potts JR, Lewis MA, Boyce MS. 2016. Integrated step selection analysis: Bridging the gap between resource selection and animal movement. *Methods in Ecology and Evolution* **7**: 619–630. doi: 10.1111/2041-210X.12528.

Barrios L, Rodríguez A. 2004. Behavioural and environmental correlates of soaring-bird mortality at on-shore wind turbines. *Journal of Applied Ecology* **41**: 72–81. doi: 10.1111/j.1365-2664.2004.00876.x.

Becker E, Grauvogel C. 1991. Relationship of reduced train speed on moose-train collisions in Alaska.

Bedrosian BE, Domenech R, Shreading A, Hayes MM, Booms TL, Barger CR. 2018. Migration corridors of adult Golden Eagles originating in northwestern North America. *PLoS ONE* **13**: e0205204. doi: 10.1371/ journal.pone.0205204.

Bildstein KL. 2006. *Migrating raptors of the world: their ecology and conservation*. Ithaca: Cornell University Press.

Bivand R, Lewin-Koh N. 2016. maptools: Tools for Reading and Handling Spatial Objects.

URL `https://cran.r-project.org/package=maptools`

Bivand R, Pebesma E, Gomez-Rubio V. 2013. *Applied spatial data analysis with R*. Springer, NY, second edition.

Bohrer G, Brandes D, Mandel JT, Bildstein KL, Miller TA, Lanzone M, Katzner T, Maisonneuve C, Tremblay JA. 2012. Estimating updraft velocity components over large spatial scales: contrasting migration strategies of golden eagles and turkey vultures. *Ecology Letters* **15**: 96–103. doi: 10.1111/j.1461-0248.2011.01713.x.

Brandes D, Ombalski DW. 2004. Modeling raptor migration pathways using a fluid-flow analogy. *Journal of Raptor Research* **38**: 195–207.

Breed GA, Costa DP, Jonsen ID, Robinson PW, Mills-Flemming J. 2012. State-space methods for more completely capturing behavioral dynamics from animal tracks. *Ecological Modelling* **235-236**: 49–58. doi: 10.1016/j.ecolmodel.2012.03.021.

Breed GA, Jonson ID, Myers RA, Bowen WD, Leonard ML. 2009. Sex-specific, seasonal foraging tactics in adult gray seals (Halichoerus grypus) are revealed by behaviour discriminating state-space models. *Ecology* **90**: 3209–3221.

Craiu RV, Duchesne T, Fortin D, Baillargeon S. 2011. Conditional logistic regression with longitudinal follow-up and individual-level random coefficients: a stable and efficient two-step estimation method. *Journal of Computational and Graphical Statistics* **20**: 767–784. doi: 10.1198/jcgs.2011.09189.

DeGregorio BA, Weatherhead PJ, Sperry JH. 2014. Power lines, roads, and avian nest survival: Effects on predator identity and predation intensity. *Ecology and Evolution* **4**: 1589–1600. doi: 10.1002/ece3.1049.

DeMars CA, Breed GA, Potts JR, Boutin S. 2016. Spatial patterning of prey at reproduction to reduce predation risk: what drives dispersion from groups? *The American Naturalist* **187**: 678–687. doi: 10.1086/685856.

Dickie M, McNay RS, Sutherland GD, Cody M, Avgar T. 2019. Corridors or risk? Movement along, and use of, linear features vary predictably among large mammal predator and prey species. *Journal of Animal Ecology* **00**: 1–12. doi: 10.1111/1365-2656.13130.

Dickie M, Serrouya R, McNay RS, Boutin S. 2017. Faster and farther: wolf movement on linear features and implications for hunting behaviour. *Journal of Applied Ecology* **54**: 253–263. doi: 10.1111/1365-2664.12732.

Dickson BG, Jenness JS, Beier P. 2005. Influence of Vegetation, Topography, and Roads on Cougar Movement in Southern California. *Journal of Wildlife Management* **69**: 264–276. doi: 10.2193/0022-541X(2005)069<0264:IOVTAR>2.0.CO;2.

Dingemanse NJ, Kazem AJN, Réale D, Wright J. 2010. Behavioural reaction norms: animal personality meets individual plasticity. *Trends in Ecology & Evolution* **25**: 81–89. doi: 10.1016/j.tree.2009.07.013.

Dodge S, Bohrer G, Weinzierl R, Davidson SC, Kays R, Douglas D, Cruz S, Han J, Brandes D, Wikelski M. 2013. The environmental-data automated track annotation (Env-DATA) system: linking animal tracks with environmental data. *Movement Ecology* **1**: 3. doi: 10.1186/2051-3933-1-3.

Duchesne T, Fortin D, Courbin N. 2010. Mixed conditional logistic regression for habitat selection studies. *Journal of Animal Ecology* **79**: 548–555. doi: 10.1111/j.1365-2656.2010.01670.x.

Duerr AE, Miller TA, Lanzone M, Brandes D, Cooper J, O'Malley K, Maisonneuve C, Tremblay J, Katzner T. 2012. Testing an emerging paradigm in migration ecology shows surprising differences in efficiency between flight modes. *PLoS ONE* **7**: e35548. doi: 10.1371/journal.pone.0035548.

Duerr AE, Miller TA, Lanzone M, Brandes D, Cooper J, O'Malley K, Maisonneuve C, Tremblay JA, Katzner T. 2015. Flight response of slope-soaring birds to seasonal variation in thermal generation. *Functional Ecology* **29**: 779–790. doi: 10.1111/1365-2435.12381.

Dyer SJ, O'Neill JP, Wasel SM, Boutin S. 2002. Quantifying barrier effects of roads and seismic lines on movements of female woodland caribou in northeastern Alberta. *Canadian Journal of Zoology* **80**: 839–845. doi: 10.1139/z02-060.

Eisaguirre JM, Auger-Méthé M, Barger CP, Lewis SB, Booms TL, Breed GA. 2019. Dynamic-parameter movement models reveal drivers of migratory pace in a soaring bird. *Frontiers in Ecology and Evolution* **7**: 317. doi: 10.3389/fevo.2019.00317.

Eisaguirre JM, Booms TL, Barger C, McIntyre CL, Lewis SB, Breed G. 2018. Local meteorological conditions reroute a migration. *Proceedings of the Royal Society B* **285**: 20181779.

Fagan WF, Lewis MA, Auger-Méthé M, Avgar T, Benhamou S, Breed G, LaDage L, Schlägel UE, Tang Ww, Papastamatiou YP, Forester J, Mueller T. 2013. Spatial memory and animal movement. *Ecology Letters* **16**: 1316–1329. doi: 10.1111/ele.12165.

Fahrig L, Rytwinski T. 2009. Effects of roads on animal abundance: An empirical review and synthesis. *Ecology and Society* **14**. doi: 10.5751/ES-02815-140121.

Forester JD, Im HK, Rathouz PJ. 2009. Accounting for animal movement in estimation of resource selection functions: sampling and data analysis. *Ecology* **90**: 3554–3565.

Forman RTT, Alexander LE. 1998. Roads and their major ecological effects. *Annual Review of Ecology and Systematics* **29**: 207–231. doi: 10.1146/annurev.ecolsys.29.1.207.

Fortin D, Beyer HL, Boyce MS, Smith DW, Duchesne T, Mao JS. 2005. Wolves influence elk movements: behavior shapes a trophic cascade in Yellowstone National Park. *Ecology* **86**: 1320–1330. doi: 10.1890/04-0953.

Gelman A, Hwang J, Vehtari A. 2014. Understanding predictive information criteria for Bayesian models. *Statistics and Computing* **24**: 997–1016. doi: 10.1007/s11222-013-9416-2.

Gilbert SL, Hundertmark KJ, Person DK, Lindberg MS, Boyce MS. 2017. Behavioral plasticity in a variable environment: snow depth and habitat interactions drive deer movement in winter. *Journal of Mammalogy* **98**: 246–259. doi: 10.1093/jmammal/-gyw167.

Gill FB. 2007. *Ornithology.* New York: W. H. Freeman and Company, third edition.

Gundersen H, Andreassen HP. 1998. The risk of moose Alces alces collision: A predictive logistic model for moose-train accidents. *Wildlife Biology* **4**: 103–110. doi: 10.2981/wlb.1998.007.

Gurarie E, Fleming CH, Fagan WF, Laidre KL, Hernández-Pliego J, Ovaskainen O. 2017. Correlated velocity models as a fundamental unit of animal movement: Synthesis and applications. *Movement Ecology* **5**: 1–18. doi: 10.1186/s40462-017-0103-3.

Haddad NM, Bowne DR, Cunningham A, Danielson BJ, Levey DJ, Sargent S, Spira T. 2003. Corridor use by diverse taxa. *Ecology* **84**: 609–615.

Harrison XA, Blount JD, Inger R, Norris DR, Bearhop S. 2011. Carry-over effects as drivers of fitness differences in animals. *Journal of Animal Ecology* **80**: 4–18. doi: 10.1111/j.1365-2656.2010.01740.x.

Hedenstrom A, Alerstam T. 1997. Optimum fuel loads in migratory birds: distinguishing between time and energy minimization. *Journal of Theoretical Biology* **189**: 227–234.

Hooten MB, Hanks EM, Johnson DS, Alldredge MW. 2014. Temporal variation and scale in movement-based resource selection functions. *Statistical Methodology* **17**: 82–98. doi: 10.1016/j.stamet.2012.12.001.

Hooten MB, Johnson DS, McClintock BT, Morales JM. 2017. *Animal movement: statistical models for telemetry data.* New York: CRC Press.

Howard R, Stull R. 2013. IR radiation from trees to a ski run: A case study. *Journal of Applied Meteorology and Climatology* **52**: 1525–1539. doi: 10.1175/JAMC-D-12-0222.1.

Jachowski DS, Conservation E, Hall L. 2015. Monitoring landscape-level distribution and migration phenology of raptors using a volunteer camera-trap network. *Wildlife Society Bulletin* **39**: 553–563. doi: 10.1002/wsb.571.

James A, Stuart-Smith A. 2000. Distribution of caribou and wolves in relation to linear corridors. *The Journal of Wildlife Management* **64**: 154–159.

Jennelle CS, Samuel MD, Nolden CA, Berkley EA. 2009. Deer carcass decomposition and potential scavenger exposure to chronic wasting disease. *Journal of Wildlife Management* **73**: 655–662. doi: 10.2193/2008-282.

Johnson DS, London JM, Lea MA, Durban JW. 2008. Continuous-time correlated random walk model for animal telemetry data. *Ecology* **89**: 1208–1215. doi: 10.1890/10-1922.1.

Jonsen ID, McMahon CR, Patterson TA, Auger-Méthé M, Harcourt R, Hindell MA, Bestley S. 2019. Movement responses to environment: fast inference of variation among southern elephant seals with a mixed effects model. *Ecology* **100**: 1–8. doi: 10.1002/ecy.2566.

Karelus DL, McCown JW, Scheick BK, van de Kerk M, Bolker BM, Oli MK. 2019. Incorporating movement patterns to discern habitat selection: black bears as a case study. *Wildlife Research* **46**: 76. doi: 10.1071/wr17151.

Katzner TE, Turk PJ, Duerr AE, Miller TA, Lanzone MJ, Cooper JL, Brandes D, Tremblay JA, Lemaître J. 2015. Use of multiple modes of flight subsidy by a soaring terrestrial bird, the golden eagle Aquila chrysaetos, when on migration. *Journal of Royal Society Interface* **12**: 20150530. doi: 10.1098/rsif.2015.0530.

Klaassen RHG, Hake M, Strandberg R, Koks BJ, Trierweiler C, Exo KM, Bairlein F, Alerstam T. 2014. When and where does mortality occur in migratory birds? Direct evidence from long-term satellite tracking of raptors. *Journal of Animal Ecology* **83**: 176–184. doi: 10.5061/dryad.ds388.

Klaassen RHG, Strandberg R, Hake M, Alerstam T. 2008. Flexibility in daily travel routines causes regional variation in bird migration speed. *Behavioral Ecology and Sociobiology* **62**: 1427–1432. doi: 10.1007/s00265-008-0572-x.

Kochert MN, Steenhof K, McIntyre CL, Craig EH. 2002. Golden Eagle (Aquila chrysaetos). In Poole A (ed.) *The Birds of North America*. Ithaca: Cornell Lab of Ornithology.

Kuzyk GW. 2016. Provincial population and harvest estimates of moose in British Columbia. *Alces* **52**: 1–11.

Lambertucci SA, Speziale KL, Rogers TE, Morales JM. 2009. How do roads affect the habitat use of an assemblage of scavenging raptors? *Biodiversity and Conservation* **18**: 2063–2074. doi: 10.1007/s10531-008-9573-3.

Lanzone MJ, Miller Ta, Turk P, Brandes D, Halverson C, Maisonneuve C, Tremblay J, Cooper J, O'Malley K, Brooks RP, Katzner T. 2012. Flight responses by a migratory soaring raptor to changing meteorological conditions. *Biology Letters* **8**: 710–713. doi: 10.1098/rsbl.2012.0359.

Latham ADM, Latham MC, Boyce MS, Boutin S. 2011. Movement responses by wolves to industrial linear features and their effect on woodland caribou in northeastern alberta. *Ecological Applications* **21**: 2854–2865. doi: 10.1890/11-0666.1.

Lesmerises R, St-Laurent MH. 2017. Not accounting for interindividual variability can mask habitat selection patterns: a case study on black bears. *Oecologia* **185**: 415–425. doi: 10.1007/s00442-017-3939-8.

Lonsdorf E, Sanders-Reed CA, Boal C, Allison TD. 2018. Modeling golden eagle-vehicle collisions to design mitigation strategies. *Journal of Wildlife Management* **82**: 1633–1644. doi: 10.1002/jwmg.21527.

Loss SR, Will T, Marra PP. 2015. Direct mortality of birds from anthropogenic causes. *Annual Review of Ecology, Evolution, and Systematics* **46**: annurev–ecolsys–112414–054133. doi: 10.1146/annurev-ecolsys-112414-054133.

McClure CJW, Ware HE, Carlisle J, Kaltenecker G, Barber JR, Barber JR. 2013. An experimental investigation into the effects of traffic noise on distributions of birds: avoiding the phantom road. *Proceedings of the Royal Society B* **280**: 20132290. doi: 10.1098/rspb.2013.2290.

McIntyre CL, Douglas DC, Collopy MW. 2008. Movements of Golden Eagles (Aquila chrysaetos) from Interior Alaska during their first year of independence. *The Auk* **125**: 214–224. doi: 10.1525/auk.2008.125.1.214.

McIntyre CL, Schmidt JH. 2012. Ecological and environmental correlates of territory occupancy and breeding performance of migratory Golden Eagles Aquila chrysaetos in interior Alaska. *Ibis* **154**: 124–135. doi: 10.1111/j.1474-919X.2011.01181.x.

McKenzie HW, Merrill EH, Spiteri RJ, Lewis MA. 2012. How linear features alter predator movement and the functional response. *Interface Focus* **2**: 205–216. doi: 10.1098/rsfs.2011.0086.

Meunier FD, Verheyden C, Jouventin P. 2000. Use of roadsides by diurnal raptors in agricultural landscapes. *Biological Conservation* **92**: 291–298. doi: 10.1016/S0006-3207(99)00094-4.

Miller TA, Brooks RP, Lanzone MJ, Brandes D, Cooper J, Tremblay JA, Wilhelm JAY, Duerr A, Katzner TE. 2016. Limitations and mechanisms influencing the migratory performance of soaring birds. *Ibis* **158**: 116–134. doi: 10.1111/ibi.12331.

Muff S, Signer J, Fieberg J. 2018. Accounting for individual-specific variation in habitat-selection studies: Efficient estimation of mixed-effects models using Bayesian or frequentist computation. *bioRxiv* : 1–45doi: 10.1101/411801.

Murray MH, Fassina S, Hopkins JB, Whittington J, Clair CC. 2017. Seasonal and individual variation in the use of rail-associated food attractants by grizzly bears (Ursus arctos) in a national park. *PLoS ONE* **12**: 1–16. doi: 10.1371/journal.pone.0175658.

Newton I. 1979. *Population ecology of raptors*. London: T & AD Poyser Ltd.

Newton I. 2008. *The migration ecology of birds.* London: Academic Press.

Nilsson C, Klaassen RH, Alerstam T. 2013. Differences in speed and duration of bird migration between spring and autumn. *American Naturalist* **181**: 837–845. doi: 10.1086/670335.

Odendaal FJ, Turchin P, Stermitz FR, Odendaal FJ, Turchin P, Stermitz FR. 1989. Influence of Host-Plant Density and Male Harassment on the Distribution of Female Euphydryas anicia (Nymphalidae). *Oecologia* **78**: 283–288.

Pagel JE, Kritz KJ, Millsap BA, Murphy RK, Kershner EL, Covington S. 2013. Bald Eagle and Golden Eagle mortalities at wind energy facilities in the contiguous United States. *Journal of Raptor Research* **47**: 311–315. doi: 10.3356/JRR-12-00019.1.

Patterson TA, Parton A, Langrock R, Blackwell PG, Thomas L, King R. 2017. Statistical modelling of individual animal movement: an overview of key methods and a discussion of practical challenges. *AStA Advances in Statistical Analysis* **101**: 399–438. doi: 10.1007/s10182-017-0302-7.

Patterson Ta, Thomas L, Wilcox C, Ovaskainen O, Matthiopoulos J. 2008. State-space models of individual animal movement. *Trends in Ecology and Evolution* **23**: 87–94. doi: 10.1016/j.tree.2007.10.009.

Pebesma E, Bivand R. 2005. Classes and methods for spatial data in R. *R News* **5**.

Pennycuick C. 1998. Field observations of thermals and thermal streets, and the theory of cross-country soaring flight. *Journal of Avian Biology* **29**: 33–43. doi: 10.2307/3677338.

Pennycuick CJ. 1971. Soaring behavior and performance of some East African birds, observed from a motor-glider. *Ibis* **114**: 178–218.

Popp J, Hamr J, Chan C, Mallory F. 2018. Elk (Cervus elaphus) railway mortality in Ontario. *Canadian Journal of Zoology* **96**: 1066–1070. doi: 10.1139/cjz-2017-0255.

Potts JR, Bastille-Rousseau G, Murray DL, Schaefer JA, Lewis MA. 2014a. Predicting local and non-local effects of resources on animal space use using a mechanistic step selection model. *Methods in Ecology and Evolution* **5**: 253–262. doi: 10.1111/2041-210X.12150.

Potts JR, Mokross K, Stouffer PC, Lewis MA. 2014b. Step selection techniques uncover the environmental predictors of space use patterns in flocks of Amazonian birds. *Ecology and Evolution* **4**: 4578–4588. doi: 10.1002/ece3.1306.

Prokopenko CM, Boyce MS, Avgar T. 2016. Characterizing wildlife behavioural responses to roads using integrated step selection analysis. *Journal of Applied Ecology* doi: 10.1111/1365-2664.12768.

Prosser P, Nattrass C, Prosser C. 2008. Rate of removal of bird carcasses in arable farmland by predators and scavengers. *Ecotoxicology and Environmental Safety* **71**: 601–608. doi: 10.1016/j.ecoenv.2007.10.013.

R Core Team. 2018. R: a language and environment for statistical computing. URL `https://www.r-project.org/`

Rue H, Martino S, Chopin N. 2009. Approximate Bayesian inference for latent Gaussian models by using integrated nested Laplace approximations. *Journal of the Royal Statistical Society Series B: Statistical Methodology* **71**: 319–392.

Rus AI, Duerr AE, Miller TA, Belthoff JR, Katzner TE. 2017. Counterintuitive roles of experience and weather on migratory performance. *The Auk* **134**: 485–497. doi: 10.1642/AUK-16-147.1.

Safi K, Kranstauber B, Weinzierl R, Griffin L, Rees EC, Cabot D, Cruz S, Proaño C, Takekawa JY, Newman SH, Waldenström J, Bengtsson D, Kays R, Wikelski M, Bohrer G. 2013. Flying with the wind: scale dependency of speed and direction measurements in modelling wind support in avian flight. *Movement Ecology* **1**: 4. doi: 10.1186/2051-3933-1-4.

Santos SM, Carvalho F. 2011. How long do the dead survive on the road? Carcass persistence probability and implications for road-kill monitoring surveys. *PLoS ONE* **6**: e25383. doi: 10.1371/journal.pone.0025383.

Scharf HR, Hooten MB, Wilson RR, Durner GM, Atwood TC. 2019. Accounting for phenology in the analysis of animal movement. *Biometrics* : 810–820doi: 10.1111/biom.13052.

Scrafford M, Avgar T, Heeres R, Boyce MS. 2018. Roads elicit negative movement and habitat-selection responses by wolverines (Gulo gulo luscus). *Behavioral Ecology* **29**: 534–542. doi: 10.1093/beheco/arx182.

Shamoun-Baranes J, Bouten W, Loon EEV, Meijer C, Camphuysen CJ, Shamoun-baranes J. 2016. Flap or soar? How a flight generalist responds to its aerial environment. *Philosophical Transactions of the Royal Society B* **371**: 20150395. doi: 10.1098/rstb.2015.0395.

Shepard DB, Kuhns AR, Dreslik MJ, Phillips CA, Shepard DB, Oklahoma SN. 2008. Roads as barriers to animal movement in fragmented landscapes. *Animal Conservation* **11**: 288–296. doi: 10.1111/j.1469-1795.2008.00183.x.

Shepard EL, Lambertucci SA, Vallmitjana D, Wilson RP. 2011. Energy beyond food: Foraging theory informs time spent in thermals by a large soaring bird. *PLoS ONE* **6**: 1–6. doi: 10.1371/journal.pone.0027375.

Shepard ELC, Wilson RP, Rees WG, Grundy E, Lambertucci SA, Vosper SB. 2013. Energy landscapes shape animal movement ecology. *The American Naturalist* **182**: 298–312. doi: 10.1086/671257.

Spaar R, Bruderer B. 1997. Optimal flight behavior of soaring migrants: a case study of migrating steppe buzzards, Buteo buteo vulpinus. *Behavioral Ecology* **8**: 288–297. doi: 10.1093/beheco/8.3.288.

Stan Development Team. 2018. RStan: the R interface to Stan, Version 2.17.3. URL `http://mc-stan.org`

Strandberg R, Alerstam T. 2007. The strategy of fly-and-forage migration, illustrated for the osprey (Pandion haliaetus). *Behavioral Ecology and Sociobiology* **61**: 1865–1875. doi: 10.1007/s00265-007-0426-y.

Strasburg JL. 2006. Roads and genetic connectivity. *Nature* **440**: 875–876. doi: 10.1021/ja057057b.

Thurfjell H, Ciuti S, Boyce MS. 2014. Applications of step-selection functions in ecology and conservation. *Movement Ecology* **2**: 26. doi: 10.1186/2051-3933-2-4.

Tremblay MA, Clair CCS. 2009. Factors affecting the permeability of transportation and riparian corridors to the movements of songbirds in an urban landscape. *Journal of Applied Ecology* **46**: 1314–1322. doi: 10.1111/j.1365-2664.2009.01717.x.

Trombulak SC, Frissell CA. 2000. Review of ecological effects of roads on terrestrial and aquatic communities. *Conservation Biology* **14**: 18–30. doi: 10.1046/j.1523-1739.2000.99084.x.

Turchin P. 1991. Translating foraging movements in heterogeneous environments into the spatial distribution of foragers. *Ecology* **72**: 1253–1266.

Turchin P. 1998. *Quantitative analysis of movement: measuring and modeling population redistribution in animals and plants*. Sunderland, Massachusetts, USA: Sinauer Associates.

Vansteelant WMG, Bouten W, Klaassen RHG, Koks BJ, Schlaich AE, Diermen JV, Loon EEV. 2015. Regional and seasonal flight speeds of soaring migrants and the role of weather conditions at hourly and daily scales. *Journal of Avian Biology* **46**: 25–39. doi: 10.1111/jav.00457.

Wasser SK, Keim JL, Taper ML, Lele SR. 2011. The influences of wolf predation, habitat loss, and human activity on caribou and moose in the Alberta oil sands. *Frontiers in Ecology and the Environment* **9**: 546–551. doi: 10.1890/100071.

Watanabe S. 2010. Asymptotic equivalence of Bayes cross validation and widely applicable information criterion in singular learning theory. *Journal of Machine Learning Research* **11**: 3571–3594. doi: 10.1101/gad.12.12.1871.

Watson J. 2010. *The Golden Eagle*. New Haven: Yale University Press, second edition.

Whittington J, Hebblewhite M, Decesare NJ, Neufeld L, Bradley M, Wilmshurst J, Musiani M. 2011. Caribou encounters with wolves increase near roads and trails: A time-to-event approach. *Journal of Applied Ecology* **48**: 1535–1542. doi: 10.1111/j.1365-2664.2011.02043.x.

Whittington J, St Clair CC, Mercer G. 2004. Path tortuosity and the permeability of roads and trails to wolf movement. *Ecology and Society* **9**. doi: 10.5751/ES-00617-090104.

Whittington J, St Clair CC, Mercer G. 2005. Spatial responses of wolves to roads and trails in mountain valleys. *Ecological Applications* **15**: 543–553. doi: 10.1890/03-5317.

Wolf M, van Doorn GS, Leimar O, Weissing FJ. 2007. Life-history trade-offs favour the evolution of animal personalities. *Nature* **447**: 581–4. doi: 10.1038/nature05835.

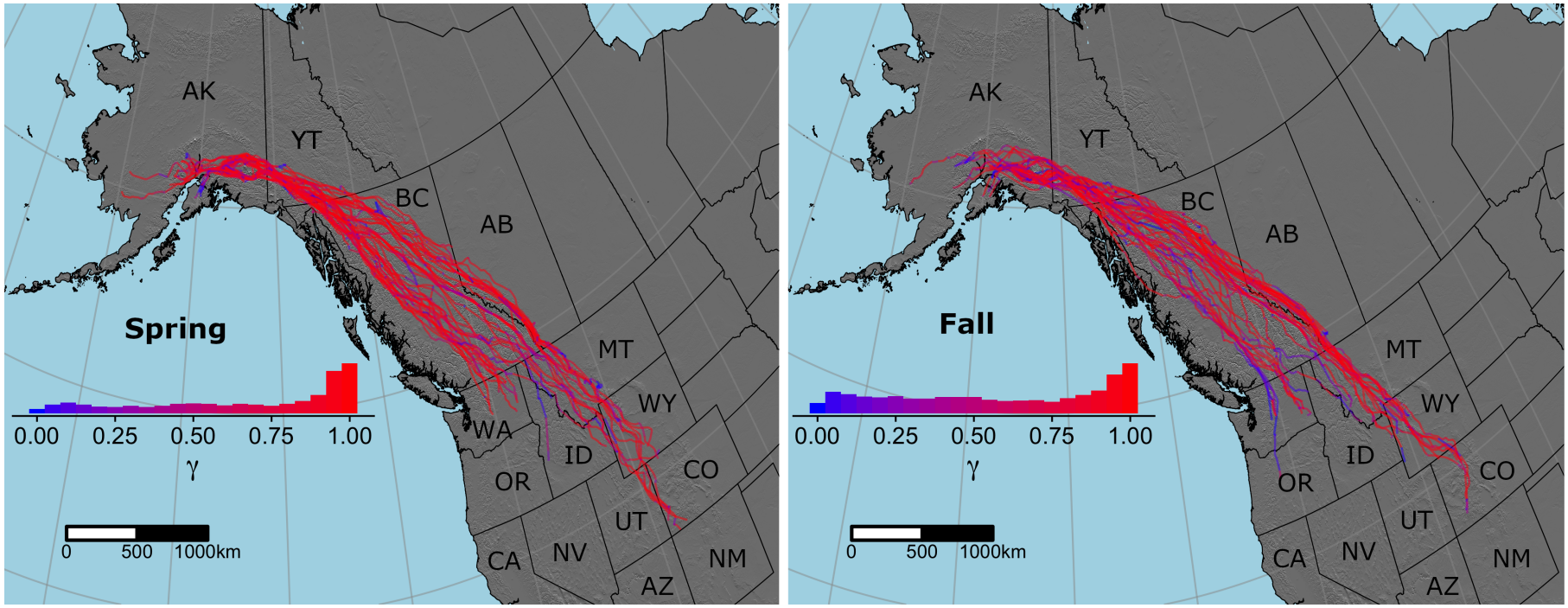

Figure 4.1: Map of 45 spring and 39 fall individual golden eagle migrations recorded with GPS transmitters in western North America 2014-2017. Insets show frequency distributions of γ_i, a time-varying latent variable driven by flight subsidies in a CRW movement model. γ_i close to one (red) indicates more directed, larger-scale migratory movements, and γ_i close to zero (blue) more tortuous, smaller-scale stopover movements

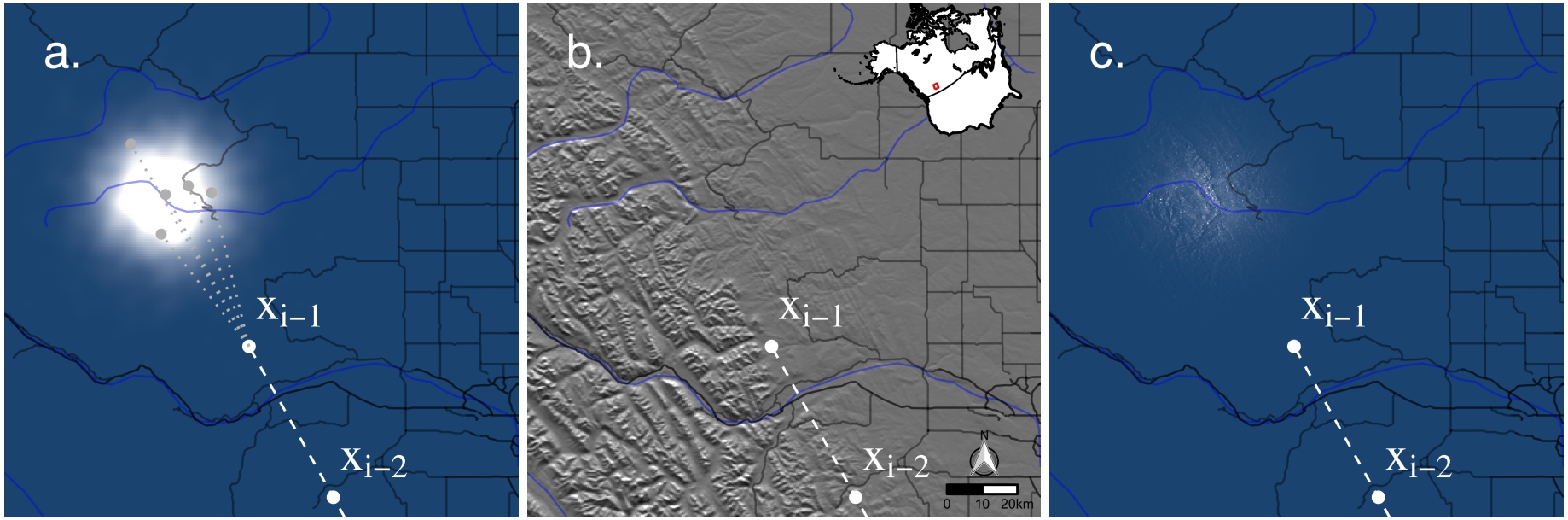

Figure 4.2: Example movement kernels from an SSF fitted to golden eagle migrations 2014-2017 conditioned on the displacement vector from $\mathbf{x}_{i-2}$ to $\mathbf{x}_{i-1}$. (a) $p(\mathbf{x}_i^j|\mathbf{X} = \mathbf{x}_{i-1}, \mathbf{x}_{i-2})$ is the conditional posterior predictive distribution of the fitted selection independent kernel $\phi(\mathbf{x}_i|\mathbf{x}_{i-1}, \mathbf{x}_{i-2})$, (b) is an elevation map showing roads and waterways, representing aspects of the landscape Z, and (c) $\hat{f}(\mathbf{x}_i|\mathbf{x}_{i-1}, \mathbf{x}_{i-2}; Z)$ is the product of the fitted selection independent kernel and fitted habitat weighting function. Grey points show example available points $\mathbf{x}_i^j$ drawn from $p(\mathbf{x}_i^j|\mathbf{X} = \mathbf{x}_{i-1}, \mathbf{x}_{i-2})$ for use in estimation of $\omega(\cdot)$ with the use-availability design. Note that both (a) and (c) show spatiotemporally explicit probability densities for $\mathbf{x}_i$, a golden eagle's location during migration at time t_i given that the eagle traveled from $\mathbf{x}_{i-2}$ to $\mathbf{x}_{i-1}$ with (estimated) correlation $\gamma_i \approx 1$ driven by uplift.

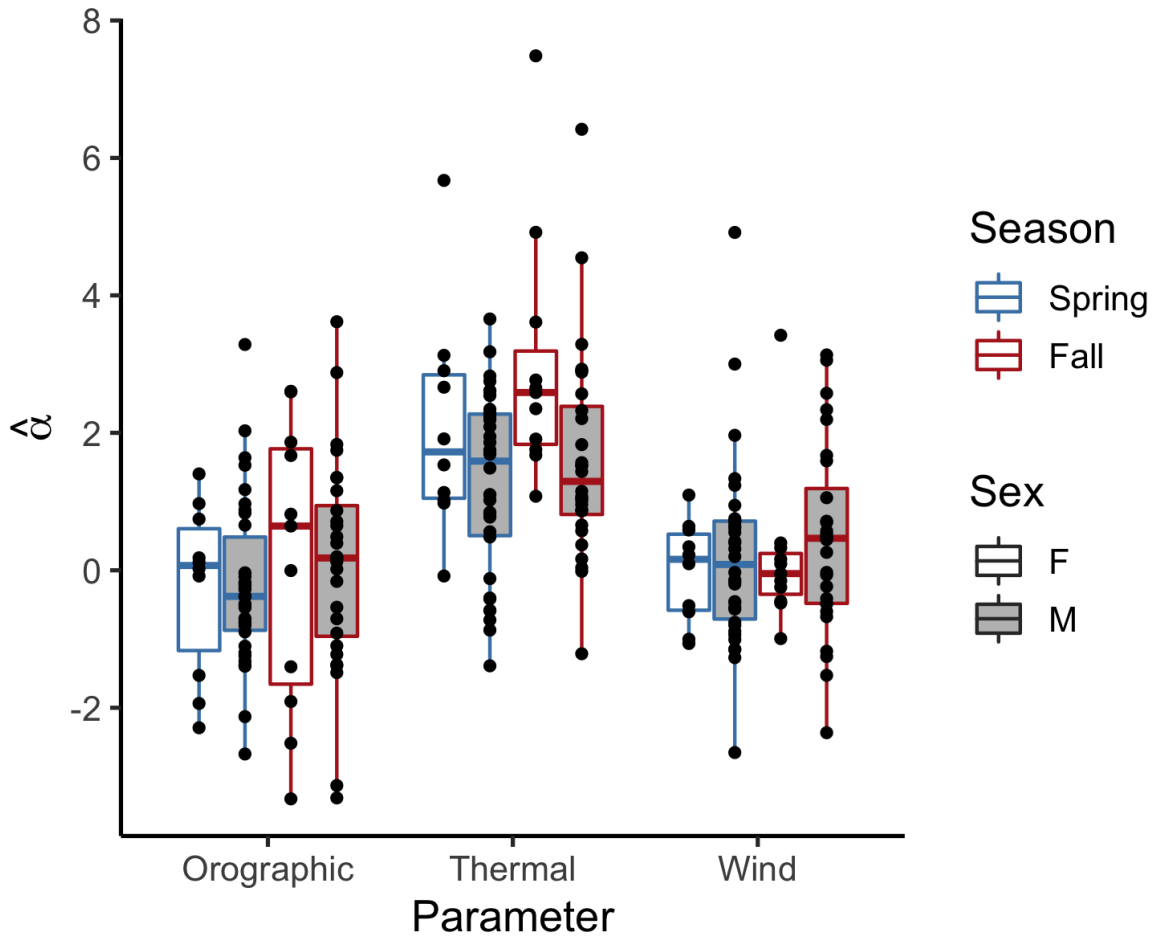

Figure 4.3: Effects of flight subsidies (orographic uplift, thermal uplift, and wind support) on golden eagle movement during migration 2014-2017 estimated with a CRW movement model. $\hat{\alpha} > 0$ indicates the flight subsidy is associated with more directed, larger-scale migratory movements, and $\hat{\alpha} < 0$ more tortuous, smaller-scale stopover movements.

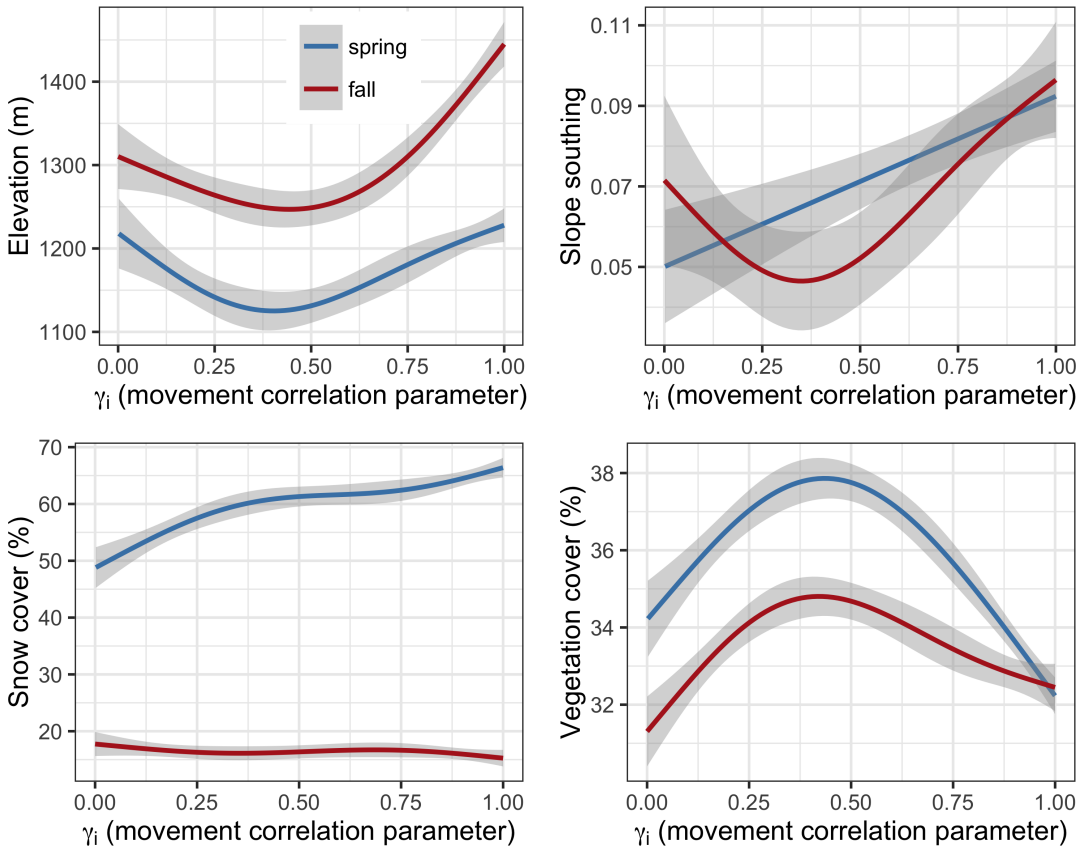

Figure 4.4: Empirical use distributions smoothed with a generalized additive model ($df = 4$; shaded areas are 95% confidence intervals) over all golden eagle spring and fall migrations 2014-2017 as a function of the movement parameter γ_i. γ_i is a time-varying latent variable driven by flight subsidies in a CRW movement model. γ_i close to one indicates more directed, larger-scale migratory movements, and γ_i close to zero more tortuous, smaller-scale stopover movements.

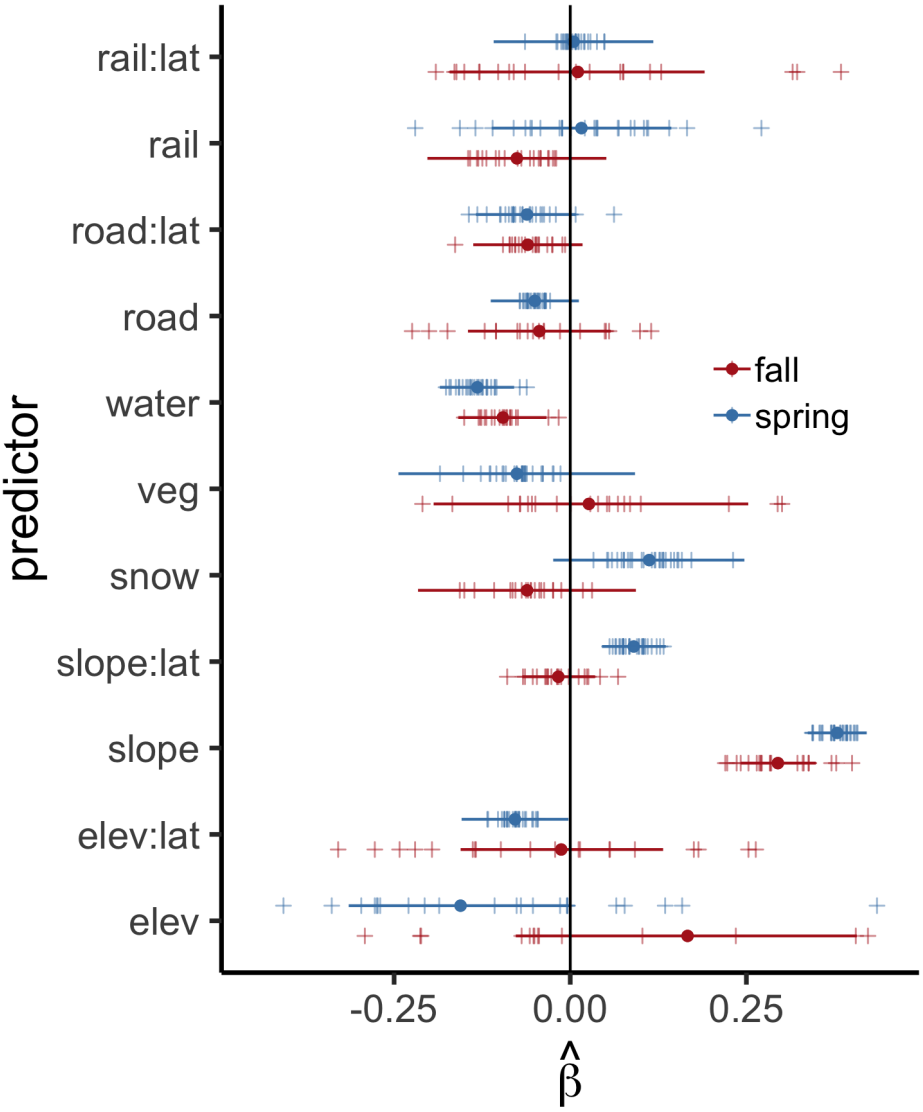

Figure 4.5: Effects of habitat variables on golden eagle habitat selection during spring and fall migration 2014-2017 estimated with SSFs. Points are posterior means and horizontal lines 95% highest posterior density (HPD) intervals for the population-level effects. Crosses correspond to the individual-level posterior means. Predictors included were elevation ('elev'), slope southing ('slope'), percent snow cover ('snow'), percent vegetation cover ('veg'), and distance to nearest railroad ('rail'), road ('road'), waterway ('water'), some as an interaction with latitude ('lat'). Negative estimates on distance to nearest linear feature correspond to selection for areas close to the linear feature. Estimates are on a standardized scale. Note that we have shortened the x axis here for clarity, but the full version is provided in the Appendix.

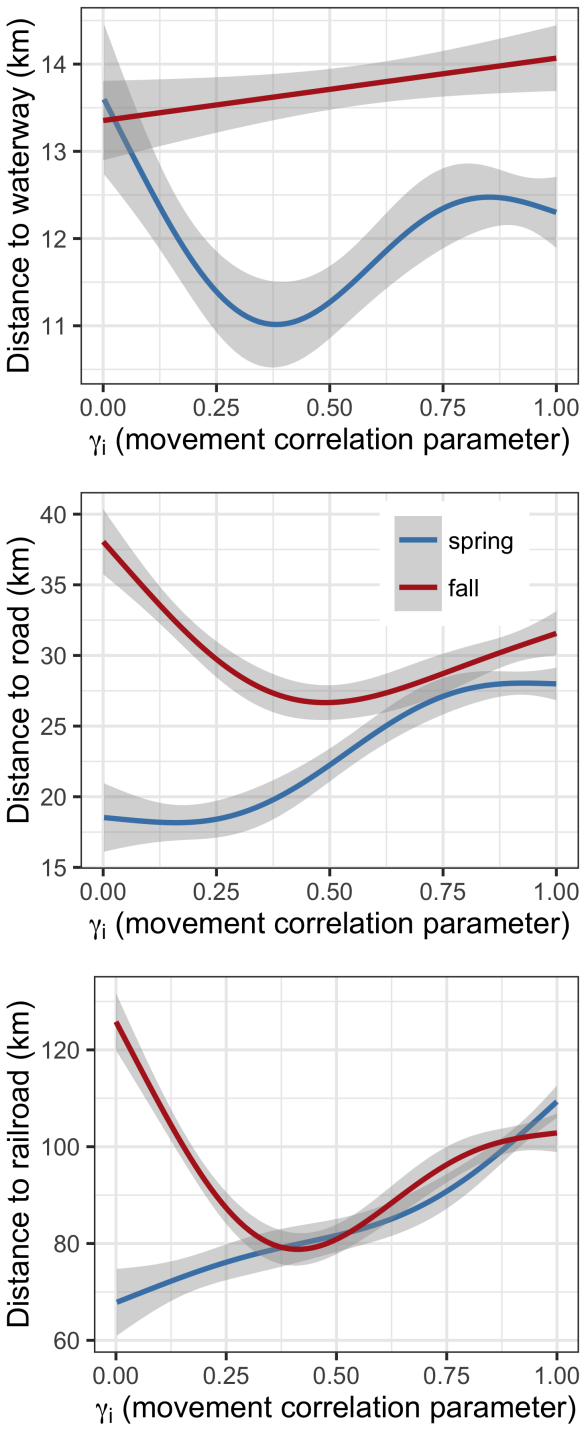

Figure 4.6: Empirical use distributions for linear features smoothed with a generalized additive model ($df = 4$; shaded areas are 95% confidence intervals) over all golden eagle spring and fall migrations 2014-2017 as a function of the estimated movement parameter γ_i. γ_i is a time-varying latent variable driven by flight subsidies in a CRW movement model. γ_i close to one indicates more directed, larger-scale migratory movements, and γ_i close to zero more tortuous, smaller-scale stopover movements.

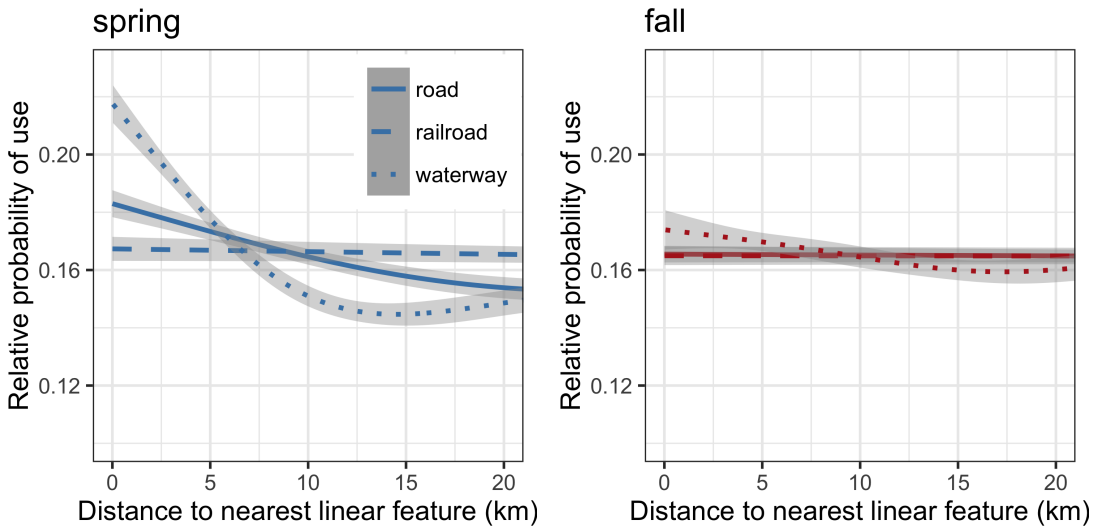

Figure 4.7: Average effect of distance to nearest linear feature on space use of golden eagles during spring and fall migrations 2014-2017 estimated with SSFs. This is conditioned on how habitat was distributed within the availability distribution for the population sampled (Avgar et al., 2017). Curves depict the smoothed (generalized additive model, $df = 6$) nonparametric function between the distance to linear feature and relative probability of use, and shaded areas correspond to 95% confidence intervals.

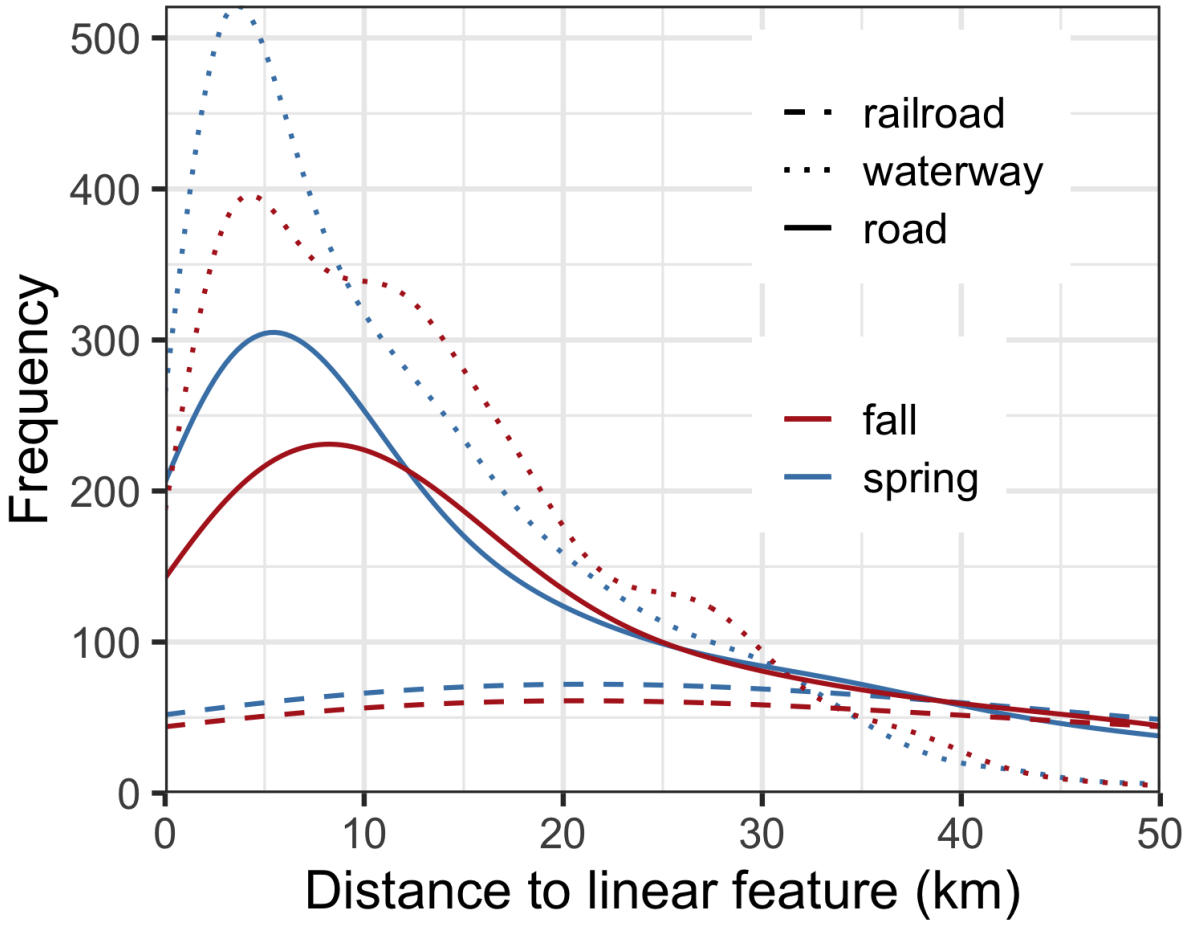

Figure 4.8: Smoothed empirical distributions of distance from 17,386 daytime golden eagle GPS transmitter locations to the nearest road, railroad, and waterway during spring and fall migrations 2014-2017 in western North America.

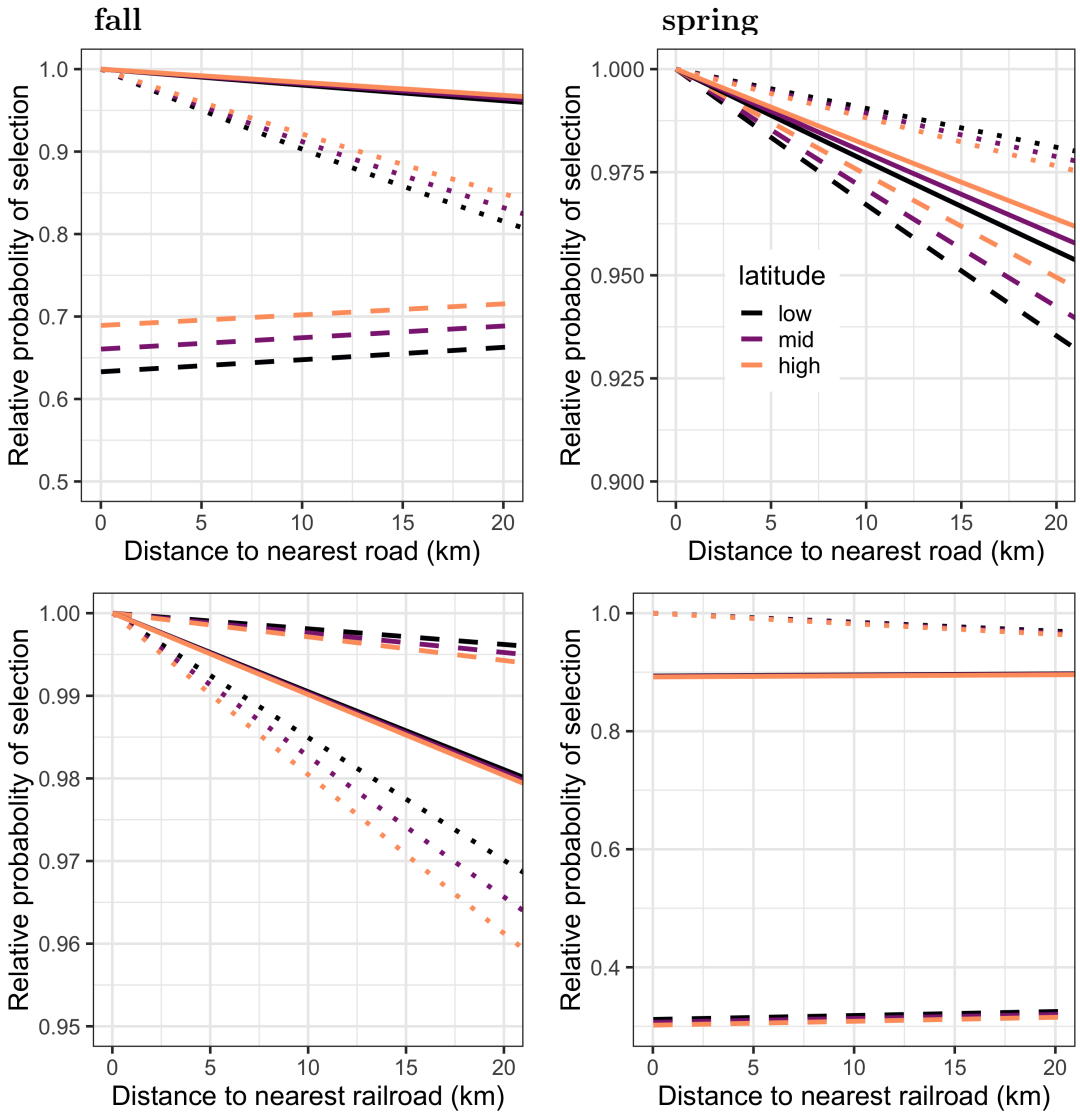

Figure 4.9: Population-level (solid) and two individual-level (dashed and dotted) preference curves for anthropogenic linear features predicted by an SSF fitted to golden eagle migrations 2014-2017. These describe the relative probability of selection by golden eagles during spring and fall migration, assuming road distances are uniformly distributed and equally available to eagles (Avgar et al., 2017). Individual-level curves shown to highlight the variation among individuals. 'low', 'mid', and 'high' latitude correspond to approximately 41°, 51°, and 61°N latitude, respectively.

Table 4.1: Ranking of candidate models of habitat selection by golden eagles during migration 2014-2017 by the widely-applicable information criterion (WAIC). 'terrain' includes elevation and slope southing; 'cover' includes percent vegetation and snow cover; and linear features (roads, railroads, and waterways) were included as distance to nearest. * corresponds to the model with only natural variables chosen to include with anthropogenic linear features.

Model	**Spring**		**Fall**	
	WAIC	ΔWAIC	WAIC	ΔWAIC
* + roads + railroads	53921	0	52119	0
* + railroads	53935	14	52139	20
* + roads	53936	15	52133	14
terrain + cover + waterways	53951*	30	52160*	41
terrain + waterways	53955	34	52162	43
terrain + cover	53986	65	52174	55
terrain	53991	70	52178	59
cover + waterways	54665	744	52860	741
cover	54750	829	52894	775
no selection	54752	831	52902	783

Chapter 5: Differential resource selection between territorial and floater golden eagles revealed with an Ornstein-Ulhenbeck space use model

5.1 Abstract

Populations of many taxa consist in part of individuals that do not breed but are attempting to enter the breeding population. Such individuals, often referred to as "floaters", are key components of these populations, playing critical roles in determining population dynamics and stability. Floaters are difficult to study, however, so we lack data on the roles they play in population ecology and conservation status of many species. Here, we paired satellite telemetry and a mechanistic space use model to study the differential habitat selection and space use of floater and territorial golden eagles *Aquila chrysaetos*. Our sample consisted of 49 individuals tracked over complete breeding seasons across four years, totalling 104 eagle breeding seasons. Floaters generally had more expansive space use patterns and larger home ranges, partitioning space with territorial individuals seemingly on fine scales through differential habitat and resource selection. Floater and territorial eagle home ranges overlapped markedly, suggesting floaters use the interstices between territories. Further, floater and territorial eagles differed in how they selected for uplift variables, key components of soaring birds' energy landscape, with territorial eagles apparently more adept at finding and using thermal uplift. We also found relatively low individual heterogeneity in resource selection, especially among territorial individuals, suggesting a narrow realized niche. This work furthers our understanding of floaters' potential roles in population ecology of territorial species, as well as suggests that conserving landscapes occupied by territorial eagles also protects floaters.

Eisaguirre, JM, TL Booms, CP Barger, SB Lewis, CL McIntyre, GA Breed. 2020. Differential resource selection between territorial and floater golden eagles revealed with an Ornstein-Ulhenbeck space use model. Prepared for submission: Journal of Animal Ecology.

5.2 Introduction

Many long-lived species have extended pre-breeding stages with considerable variation in the age at first reproduction (Zack and Stutchbury, 1992; Gill, 2007). These characteristics often promote a demographic class that is reproductively capable, but members of which do not attempt to breed. In birds, individuals in this demographic group are often referred to as "floaters." The social dynamics of this class can be highly complex and ordered but receive little attention from biologists who tend to focus on breeding individuals (Penteriani et al., 2011). The idea of a structured but unseen "underworld" within the floater demographic class was introduced as a concise metaphor for their behavioral dynamics and interactions (Brown, 1969; Smith, 1978).

Members of the underworld are individuals that do not breed because of saturated breeding territories and/or fitness trade-offs between occupying low versus high quality territories (Brown, 1969; Newton, 1992; Zack and Stutchbury, 1992; Ens et al., 1995; Kokko and Sutherland, 1998; Newton, 1998; Hunt, 1998; Penteriani et al., 2003; Ferrer et al., 2015). Floaters were initially hypothesized as nomadic individuals that passively await an available territory or poor competitors excluded from territories (i.e. a "doomed surplus"; Krebs, 1971; Stutchbury and Robertson, 1985; Eckert and Weatherhead, 1987; Newton, 1992). However, floaters have been shown to be capable competitors simply employing a different strategy (Smith, 1978; Smith and Arcese, 1989), and their presence and behavior are often important to population dynamics and evolutionary processes (Kokko and Sutherland, 1998; Hunt, 1998; Penteriani et al., 2005, 2011; Lee et al., 2017). The stability of some populations may even be more sensitive to changes in population vital rates of floaters than breeders (Hunt, 1998; Penteriani et al., 2011), and discounting floaters in demographic studies can mask low population growth rates (Penteriani et al., 2011; Lee et al., 2017; Hunt et al., 2017).

Populations of slow-maturing species that lack floaters, or that simply lack floaters adjacent to territories, may be more susceptible to variation in mortality of reproductive adults. Younger and less mature individuals could replace losses of breeding-age individuals, but these less mature, inexperienced individuals would be of lower quality

and many would be incapable of actually breeding successfully (Carrete et al., 2006b). This situation would decrease overall reproductive performance at the population level, magnifying impacts of breeder mortality. Floaters in a population can buffer against such elevated breeder mortality, as more experienced floaters can rapidly fill territory vacancies and maintain reproductive success of the population (Hunt, 1998; Penteriani et al., 2011). Although many floaters have not yet bred for the first time, all have spent at least one, but in some cases many, years as floaters before recruiting to the breeding class, which affords experience in foraging and survival as well as more time to physically mature. Depending on how floaters use space, they may of have persisted within or near breeding territories for some time and accrued experience with its resources and risks that will increases the odds of success once an opening becomes available (Stamps, 1995; Fagan et al., 2013). Such information can improve realized fitness (Forrester et al., 2015), leaving them primed to immediately perform as capable breeders and act as a demographic buffer. Further, within the underworld social structure, experience also likely helps floaters compete amongst themselves, with better competitors taking over territories when they become available.

There are essentially three basic space use strategies employed by floaters (Newton, 1976, 1979; Penteriani et al., 2011). They may (1) geographically segregate from breeders, (2) establish along the fringes of breeding habitat, or (3) persist in the interstices among and occasionally within breeding territories. A floater utilizing strategy (3) would have access to information and experience with candidate territories, but would also have to cope with conflict with defending territorial individuals. Individuals employing strategy 1, by contrast, would establish a presence near to, but segregated from, viable territories while awaiting a territorial opening, thereby minimizing agonistic interactions with territorial individuals (Hunt, 1998; Caro et al., 2011; Penteriani et al., 2011). However, floaters may still prefer habitat and/or have requirements otherwise similar to breeders, but lacking a central place to defend. Alternatively, they could also have different habitat preferences. In either case, floaters and breeders would be spatially segregated, reducing the territorial defense requirements of breeders but leaving floaters with less information

and experience about the resources available in territories. Further, if left undiscovered, spatial segregation between floaters and breeders could lead to ineffective conservation or management actions, as any action would likely be focused on habitats used by breeding individuals (Penteriani et al., 2005, 2011).

When floaters persist along the fringes of breeding habitat or in the interstices of breeding territories—strategies 2 and 3—they gain knowledge of habitat and territories but may affect territorial individuals and put themselves at risk. More frequent territory defense against floaters could potentially reduce reproductive success (López-Sepulcre and Kokko, 2005; Carrete et al., 2006a; Bretagnolle et al., 2008). Floaters may also affect the survival of territorial individuals through fatal conflict; some have hypothesized that survival of territory-holders may be lower than floaters' due to repeated territorial conflict elicited by floaters (Hunt, 1998). We would expect these effects on breeding behavior, success, and survival to be greatest when floaters persist in the interstices of territories, likely making temporary intrusions into territories as well (strategy 3). However, this strategy would simultaneously allow floaters to gain the most knowledge of candidate territories. In contrast, floaters persisting on the fringes of breeding habitat (strategy 2), possibly excluded by breeders, would relax defense requirements of breeders, but would only allow limited opportunity for floaters to learn about territories.

Spatial learning in home ranges and territories could benefit certain taxa more than others (Fagan et al., 2013). For example, soaring birds rely on dynamic energy landscapes (Shepard et al., 2013) in the form of local upward air currents (i.e. uplift) to offset the energetic expense of flight, and these flight subsidies can drive soaring bird movement and behavioral processes (Shepard et al., 2011, 2013; Katzner et al., 2015; Miller et al., 2016; Eisaguirre et al., 2018, 2019a). Given that topography and atmospheric process vary spatially, the energy landscape, in addition to other key resources such as habitat and food availability, likely varies among territories. Thus, learning territory-specific energy landscapes could allow individuals to move around a territory more efficiently and quickly (Stamps, 1995), improving resource acquisition and risk avoidance, as well as increasing the probability of reproductive success and thus realized fitness. We might therefore

expect that floater space use patterns and overall floater strategy in soaring birds and other taxa could differ from breeders with respect to use of dynamic energy landscapes.

How floaters use space and their social dynamic within a population likely plays a key role in how they impact population dynamics and their ability to act as buffer against breeder mortality (Hunt, 1998; Penteriani et al., 2011; López-Sepulcre and Kokko, 2005; Carrete et al., 2006a; Bretagnolle et al., 2008). Moreover, although often overlooked, understanding these individuals may be considerably more important in assessing conservation status and developing conservation strategies than is often assumed (Penteriani et al., 2011). However, few detailed investigations into the spatial ecology of floaters have been undertaken (Rohner, 1997; Campioni et al., 2012; Tanferna et al., 2013; Penteriani et al., 2015). This is due in part due to the difficultly of studying this segment of the population, as floaters are often secretive as to avoid conflicts with breeders and, unlike breeders, lack spatial fidelity to specific locations on the landscape (e.g., nests; Sergio et al., 2009; Penteriani et al., 2011).

Technological advances in animal telemetry now permit collection of detailed data throughout substantial periods of animals' lives. Paired with appropriate statistical tools recently developed for inferring behavior from telemetry data (reviewed by Hooten et al., 2017), we are now better positioned to understand the secretive underworld of floaters, how they interact with their territory-holding conspecifics, and infer the potential importance of this demographic class to population stability and dynamics.

Ornstein-Uhlenbeck (OU) processes have long been used to model the movement and space use of animals (Dunn and Gipson, 1977; Blackwell, 1997; Johnson et al., 2008; Breed et al., 2017). The process naturally captures movement around a central place and, when coupled with a resource weighting function, can account for and allow inference about an animal's preferences for features on heterogeneous landscapes, such as habitats and dynamic uplift (Johnson et al., 2008; Eisaguirre, 2019). Modelling approaches based on the OU process have been developed to allow for multiple home range or territory core areas, which might be expected for an animal with one or multiple established foraging areas, in addition to a nest or den (Johnson et al., 2008; Breed et al., 2017; Eisaguirre,

2019). Such models are thus appropriate for revealing how floater and breeder movement and space use strategies vary based on central places as well as static and dynamic landscape features.

Here, we used a large data set on the movements of individual breeding-age golden eagles *Aquila chrysaetos* collected with GPS telemetry in southcentral Alaska, coupled with a mechanistic OU space use model, to determine how floaters use space, resources, and dynamic energy landscapes as compared to breeding individuals. Specifically, we investigated whether floaters (1) are geographically segregated from territorial breeders, (2) establish along the fringes of breeding habitat, or (3) persist in the interstices of established and occupied breeding territories. Golden eagles are a long-lived, territorial species, populations of which can consist of large segments of floaters about which little is known (Watson, 2010), making them an excellent study system for understanding the behavior and potential importance of this poorly understood demographic class to population dynamics across large spatial scales. Further, as golden eagles are soaring birds, we additionally accounted for and investigated how energy landscapes influenced floater and breeder space use dynamics, and looked for differences among these groups in accessing features of those energy landscapes.

5.3 Methods

5.3.1 Study area & system

Golden eagles are widely distributed, exhibit high territory fidelity, and most commonly nest on cliffs in many parts of their Holarctic range (Kochert et al., 2002; Watson, 2010). Golden eagles are also generally central place foragers (Kochert et al., 2002; Watson, 2010), so suitable nesting habitat must lie within or adjacent to suitable foraging habitat. The number of viable territories is, therefore, limited in many areas, which has given rise to sometimes large floater sectors of populations, about which we know very little (Watson, 2010).

Like many northern populations, the eagles we studied are long distance migratory (Watson, 2010). Eagles in our sample summered primarily in the western Alaska Range

and Talkeetna and Chugach Mountains of Alaska, USA and overwintered in the Rocky Mountain West, including Colorado, Utah, Wyoming, Montana, Idaho, Oregon, and Washington, in the US and mid to southern Alberta and British Columbia in Canada (Eisaguirre et al., 2019a). The summering area is a diverse matrix of habitats, including boreal forest, open tundra, high alpine, and glaciers. Aerial surveys of the nest sites of the tagged eagles indicated that all nested on cliffs, except for one that nested in a tree.

5.3.2 Telemetry data

We captured golden eagles with a remote-fired net launcher placed over carrion bait near Gunsight Mountain, Alaska (61.67°N 147.35°W). Captures occurred during spring migration, 15 March to 15 April 2014-2016. Our capture period overlapped the time when territory holders would be returning to their territories. Adult and sub-adult eagles were equipped with 45-g back pack solar-powered Argos/GPS platform transmitter terminals (PTTs; Microwave Telemetry, Inc., Columbia, MD, USA). Eagles were sexed molecularly and aged by plumage.

PTTs were programmed to record GPS locations on duty cycles, ranging from 8-14 fixes per day during the breeding season, depending on year of deployment. In 2014, PTTs were set to record 13 locations at one-hour intervals centered around solar noon plus a location at midnight local time. 2015 PTTs were programmed to record eight locations with one-hour intervals centered around solar noon very early and late in the season and 10 locations for most of the season. In 2016, we revised our programming approach so that PTTs took eight fixes daily early and late and 12 fixes most of the season with a fixed 3-/2-hr time interval. Fifteen PTTs were deployed in 2014, 23 in 2015, and 15 in 2016.

5.3.3 Mechanistic space use model

Given that golden eagles are generally central place foragers and rely on dynamic energy landscapes (Watson, 2010), we used a recently introduced approach designed for making practical, mechanistic inference about animal space use while considering such

patterns (Eisaguirre et al., 2020). This approach is based on the Ornstein-Uhlenbeck (OU) process (Dunn and Gipson, 1977; Blackwell, 1997). Although a continuous-time process, the inherently discrete nature of data collected with GPS telemetry makes the position likelihood of the OU process, which takes the form of an OU biased random walk (BRW), most useful:

$$\mathbf{x}_t|\mathbf{x}_{t-1} \sim \mathcal{N}\left(\boldsymbol{\mu} + e^{-\boldsymbol{\omega}\Delta t}(\mathbf{x}_{t-1} - \boldsymbol{\mu}),\ \boldsymbol{\Sigma} - e^{-\boldsymbol{\omega}\Delta t}\boldsymbol{\Sigma}e^{-\boldsymbol{\omega}^T\Delta t}\right). \tag{5.1}$$

Here, $\mathbf{x}_t$ is a coordinate vector of the location of the animal at time t, $\boldsymbol{\omega} = \omega\mathbf{I}_2$ with ω describing the strength of the animal's tendency toward the animal's central point $\boldsymbol{\mu}$, $\boldsymbol{\Sigma} = \sigma^2\mathbf{I}_2$, and $\sigma > 0$. The particular isotropic form presented here, with a single centralizing parameter ω and diffusion parameter σ, gives rise to the steady-state space use distribution $\mathcal{N}(\boldsymbol{\mu}, \boldsymbol{\Sigma})$, contours of which are circular about $\boldsymbol{\mu}$. The OU parameters naturally lend themselves to direct biological interpretation. As σ is the diffusion parameter of the OU process and ω is the intensity of the attraction to the home range center, larger values of σ and smaller values of ω equate to larger, more diffuse home ranges. In contrast, smaller values of σ and large values of ω equate to smaller, more concentrated home range cores.

The distribution $\mathcal{N}(\boldsymbol{\mu}, \boldsymbol{\Sigma})$ is what a bird's space use distribution would look like while tending a nest surrounded by uniformly distributed average habitat. Nonuniform and possibly dynamic resources plus a bird's preferences for those resources would give rise to a time-varying modified form of that distribution though. This can be accounted for in the framework of a resource selection function, such that we can write the conditional probability density of the animal's location at time t (Johnson et al., 2008):

$$f_u(z|\mathbf{x}_{t-\Delta t}) = K^{-1}\exp[z(\mathbf{x}_t)^T\boldsymbol{\beta} - (\mathbf{x}_t - \boldsymbol{\mu}_t)^T\boldsymbol{\Sigma}_t^{-1}(\mathbf{x}_t - \boldsymbol{\mu}_t)/2], \tag{5.2}$$

where z is the landscape over which the animal is moving, $z(\mathbf{x}_t)$ corresponds to a vector of environmental (e.g., weather and habitat) variables at $\mathbf{x}_t$ and time t, $\boldsymbol{\beta}$ weights the elements of $z(\mathbf{x}_t)$ based on the animal's preferences, $\boldsymbol{\mu}_t = \boldsymbol{\mu} + e^{-\boldsymbol{\omega}\Delta t}(\mathbf{x}_{t-\Delta t} - \boldsymbol{\mu})$, and

$\boldsymbol{\Sigma}_t = \boldsymbol{\Sigma} - e^{-\boldsymbol{\omega}\Delta t}\boldsymbol{\Sigma}e^{-\boldsymbol{\omega}^T\Delta t}$. The steady state form of equation 5.2 is simply the product of an exponential weighting function and $\mathcal{N}(\boldsymbol{\mu}, \boldsymbol{\Sigma})$ (Eisaguirre et al., 2020).

As an eagle's space use could be centered around multiple locations, rather than just a single nest, such as roosts or hunting locations (Watson, 2010), we accounted for the presence of multiple central points in estimating eagle space use, following Eisaguirre et al. (2020). Given we did not have fixed time intervals for all tags deployed on eagles, we forewent modeling transitions as a Markov process (*sensu* Eisaguirre et al. 2020), and simply used an indexing approach that did not estimate transition probabilities among K many cores (*sensu* Johnson et al., 2008). Note that utilizing the OU model weights the use of central points, such as nest sites and perches, independent of the habitat selection, reducing any overestimation of the importance of habitat or terrain features possibly correlated with the locations of central points.

5.3.4 Weather and habitat variables

Static landscape variables We used the Alaska Center for Conservation Science Alaska Vegetation and Wetland Composite (AKVWC; 30 m resolution) data for characterizing habitat type. We collapsed the numerous habitat types in the data set to eight for this analysis. These were shrub, open (but vegetated; e.g., meadows and open tundra), bare, forest, wet (e.g., marsh), water, ice (i.e. perennial snow and ice), and human. See the Appendix for details.

Elevation data were gathered using the Mapzen Terrain Service with the `elevatr` package (Hollister and Shah, 2018). We specified the 'zoom' variable such that the resolution closely matched that of the habitat data. We included elevation and slope ($slope \in [0, \pi/2]$ radians) as predictors in the model.

Dynamic variables We used a state-wide data set of snow-off date (date of which an area became snow free) to derive a dynamic binary indicator variable of whether or not grid cells were free of snow (Macander et al., 2015). While one might expect some confounding between the (perennial) snow and ice habitat variable and this snow indicator, it would be limited due to few glaciated and perennial snow-covered areas

frequented by eagles sampled.

The remaining variables included in the model were related to orographic and thermal uplift and were derived from the elevation data and Center for Environmental Predictions (NCEP) North American Regional Reanalysis (NARR) data. Angle of incidence was included for the effect of orographic uplift on eagle space use. It is the deviation of the relative wind from the aspect of a slope and was computed such that $aoi \in [0, \pi]$ (Murgatroyd et al., 2018); $\pi/2$ corresponds to a wind orthogonal to a slope, and π a wind perfectly parallel blowing up slope. Wind direction was computed trigonometrically from the meridional and zonal wind components estimated by the NCEP NARR 10 m above the surface.

The effect of thermal uplift was included with a hill shade variable. Hill shade was computed following Murgatroyd et al. (2018), such that $hs \in [0, 1]$, and we gathered the required location-, date-, and time-specific azimuth and zenith of the sun using the package `maptools` (Bivand and Lewin-Koh, 2016). Higher hill shade corresponds to more direct sun and thus more potential for thermal uplift.

5.3.5 Inference

We fit the mechanistic space use model to four breeding seasons of data, 2014-2017, with Stan and R following Eisaguirre et al. (2020) (Stan Development Team, 2016, 2018; R Core Team, 2018). We estimated the selection parameters $\boldsymbol{\beta}$ hierarchically across individuals, but for computational reasons we fit the model separately for certain cases.

When the nestling(s) of a breeding pair of golden eagles can thermoregulate at about three weeks after hatching, the female, who does the majority of incubating and parental care, is no longer required to care for them as regularly, so she is free to move about the territory and help with provisioning (Watson, 2010). We suspected that when this occurs, space use may change substantially due to members of a pair possibly partitioning space. We assumed this may impact floater movement as well due to the female being more free to defend the territory against floating intruders. So, within each year, we fit the model separately for the four combinations of floater or territorial and early or late

breeding season. Aerial observations of the nests of the tagged golden eagles indicated that 20 June was, on average, the approximate date nestlings were about three weeks old, so we used this date to partition the data into early and late periods of the breeding season.

Distinguishing floater from territorial eagles was done a priori by visual inspection of each individual's movement data. As we suspected eagles might use resources and habitat differently in different home range cores, we also estimated core-specific effects for each predictor. All continuous predictors were centered and standardized to mean zero and unit variance for estimation. Additionally, given that eagles had different numbers of home range cores and core-specific movement parameters, we chose to summarize and interpret the OU movement parameter estimates for the most used home range core (i.e. that in which an eagle spent the most time) for each eagle breeding season to help understand movement and home range behavior (Dunn and Gipson, 1977).

Lastly, given the properties of the OU model, we were able to compute analytical estimates of eagle space use distributions (Eisaguirre et al., 2020). We used a Bayesian hierarchical Gamma regression (2000 iterations, default priors; Stan Development Team, 2016) to assess the differences in home range size between floaters and territorial eagles and early and late breeding season. To be comparable with other home range estimation methods, we defined our home range estimator as the 95% contour of the utilization distribution (Hooten et al., 2017). Year and individual were included as random effects to account for repeated measures. Differences were assessed by constructing each respective posterior predictive distribution.

5.4 Results

We were able to determine both arrival and departure dates in at least one year for 49 individual eagles between 2014-2017 (Table 5.1), and thus our total data set consisted of 104 eagle breeding seasons. Of those, 78 were territorial (44 male and 34 female) and 26 were floaters (24 male and 2 female).

Sixteen of the floater breeding seasons were from eagles aged as entering their fifth

year at capture, six from eagles entering some year after their fourth year, two after their fifth year, and two as 'adult' (likely after fifth year). Nearly all territorial eagle breeding seasons were from individuals aged as after their fifth year at capture, but six were fifth year, one after fourth year, and two as 'adult' (likely after fifth year).

5.4.1 Movement parameters

Floaters and territorial eagles established similar numbers of home range cores, but it seemed territorial eagles established slightly more cores later in the breeding season (Fig. 5.1). OU movement parameters varied markedly between floaters and territory holders (Figs. 5.1). Compared to floaters, territorial eagles had smaller home range cores, indicated by smaller movement variance $\hat{\sigma}$ (Fig. 5.1), and stronger attraction toward the center of their home range core, indicated by larger $\hat{\omega}$ (Fig. 5.1). Additionally, there was some evidence that an eagle's most used core was smaller during late breeding season (Fig. 5.1).

5.4.2 Habitat selection

Effects of static landscape variables Both floater and territorial eagles selected for higher elevations and steeper slopes (Fig. 5.2). Four of the habitat types (bare, open, forest, and shrub) comprised over 99% of the habitats used by both territorial and floater eagles, so we report and interpret the results for those here. The habitat types territorial and floater eagles selected were generally similar (Fig. 5.2 & 5.3), but there were a few important differences. Floaters used forested areas more than territorial eagles and much less during late breeding season than early (Fig. 5.3). Additionally, floaters more strongly selected for shrub and open areas than territorial eagles, and territorial eagles used bare areas more frequently than floaters (Fig. 5.2 & 5.3).

Effects of dynamic landscape variables Both territorial and floater eagle space use was affected by thermal and orographic uplift nearly identically (Fig. 5.4). However, the effective responses to thermal uplift actually came from territorial eagles preferentially selecting areas with more thermal uplift stronger than floaters (Fig. 5.4). Both territorial

and floater eagles selected strongly against snow cover during late breeding season with generally weaker selection against it during early breeding season (Fig. 5.2).

Individual and home range core variance Unlike OU movement parameters, there was relatively low among-individual variance in habitat selection parameters, especially for territorial individuals (Fig. 5.5). Though, there was more individual heterogeneity in selection parameters for floaters than territory-holders (Fig. 5.5). In contrast, among-core variability in selection parameters was markedly high (Fig. 5.5), suggesting eagles exhibited different habitat selection patterns in different home range cores. This difference between individual and core variance was further supported by permutation tests on paired medians of the variance point estimates ($p << 0.001$).

Further, both the estimated among-individual and among-core variances for thermal and orographic uplift were very low (Fig. 5.5). This suggests strong similarity in how different eagles respond to these variables as well as similarity in how those eagles respond within different home range cores.

5.4.3 Realized home range size

Recall, due to the properties of the OU model, estimating home ranges with the model can be done by simply taking the product of two steady state distributions (Eisaguirre et al., 2020). Applying this, here, we found that floaters had larger home ranges than territorial eagles during both early and late breeding season (Fig. 5.6). Additionally, both territorial and floater eagles exhibited larger home ranges early in the breeding season compared to late (Fig. 5.6), consistent with the pattern in home range core size mentioned above (Fig. 5.1). Median (IQR) home range sizes for territorial eagles were 31 km^2 (18, 143) and 24 km^2 (13, 53) for early and late breeding season, respectively, and 581 km^2 (326, 704) and 346 km^2 (143, 496) for floaters.

5.5 Discussion

We found that floater and territorial eagles exhibited slight differential selection for habitat and resources, yet floater space use patterns were much more expansive, which is

consistent with other taxa (e.g., great horned owl *Bubo virginianus* and black kite *Milvus migrans*; Rohner, 1997; Tanferna et al., 2013). Although we only sampled a relatively small proportion of golden eagles that summer in southcentral Alaska, an expanded view of some neighboring tagged individuals (Fig. 5.7) suggests that many floaters use much of the same or closely adjacent space to territorial eagles. This further suggests that there is an underworld of floater eagles in this area likely employing strategy 3, persisting in the interstitial spaces among and within breeding territories.

For very long lived species, this strategy should be particularly adaptive. Gaining knowledge of habitat and resource distributions within territories prior to occupation and attempted breeding would improve individuals' initial reproductive success (Stamps, 1995). This advantage should then outweigh the risks associated with constant contention with breeders and physical interactions likely required for displacing territory-holders. Further, our results suggest this period of learning is likely not limited to static habitats and terrain but extends to dynamic features of the energy landscape as well (Fig. 5.4). Floaters exhibiting weaker selection for thermal uplift than territorial eagles is possibly due to floaters still learning where and when this dynamic resource is available within and around candidate territories. In contrast, territorial eagles have often maintained their territory for several breeding seasons, having ample time to learn the intricacies of the space and dynamic resources available to them.

5.5.1 Energy home range

There is abundant work in the literature on the effects of uplift and wind on the behavior of and movement of soaring birds (e.g., Shepard et al., 2011; Katzner et al., 2015; Péron et al., 2017; Eisaguirre et al., 2018, 2019a), but less work has focused on how these variables affect emergent individual- and population-level space use patterns (Shepard et al., 2013; Watson et al., 2014; Eisaguirre et al., 2019b). Our finding that golden eagles use space within their home ranges in accordance with thermal uplift contrasts with studies that have used static variables to proxy thermal uplift (Watson et al., 2014). So, accounting for the inherently dynamic nature—both across seasons and within days—of

thermal uplift, as we did by computing spatio-temporally explicit hill shade, is important to drawing correct inferences about soaring bird space use.

Using orographic uplift is key for golden eagles and other soaring taxa to find food and patrol territories (McLeod et al., 2002; Harmata, 1982; Collopy and Edwards, 1989). The benefits and utility of using orographic uplift is likely not restricted just to territorial individuals, however, as floaters too need to find food and patrol territory boundaries looking for a vacancy or usurping opportunity. Indeed, we found that orographic uplift drove space use similarly for floaters and territorial eagles (Fig. 5.4).

5.5.2 Terrain & habitat use

Topography affects the movement and space use of a range of taxa (Boyce et al., 2003; Shepard et al., 2013), but for eagles, it has been hypothesized that its effect is primarily through interaction with wind (i.e. orographic uplift; McLeod et al., 2002). However, in addition to the dynamic effects of orographic uplift that we found, we also found selection for higher elevations and steeper slopes (Fig. 5.2), which is consistent with findings for golden eagles elsewhere in North America (Watson et al., 2014). These patterns were also generally similar between territorial and floater eagles, supporting our conclusion that there is not large scale spatial segregation (e.g., along an elevation gradient) between the two groups.

Floaters are more free to select space based on prey abundance, however, due to the lack of nesting and territorial defense requirements (Penteriani et al., 2011). During early breeding season, we found floaters tended to select and use forested areas in addition to shrubbier and open habitats (Fig. 5.3 & 5.2). Much of early breeding season, as we've defined it here, is prior to the emergence of hibernating Arctic ground squirrels *Urocitellus parryii*, which are a primary prey of golden eagles in Alaska (McIntyre and Adams, 1999; McIntyre and Schmidt, 2012; Herzog et al., 2019). During that time floaters could be favoring forested, shrub, and/or edge habitats slightly, such to optimize their access to snowshoe hare and ptarmigan, while still maintaining their proximity to candidate territories.

5.5.3 Home range structure

Finding that floaters used more space and were less tied to central points than territorial individuals (Fig. 5.1 & 5.6) was not surprising, and it is consistent with floaters' ability to move more freely about the landscape without tending a nest or young. Furthermore, territorial individuals likely do not tolerate floaters within or near territory boundaries for long (Watson, 2010), causing more expansive movements and perhaps 'pinballing' among territories. Our results also suggest that the more expansive movements of floaters were influenced by differential habitat use and resource selection (Fig. 5.2). The higher elevation, barer terrain with suitable nest cliffs is primarily occupied by territorial individuals. Resident pairs' agonistic behavior toward floaters excludes them from these primary areas, leaving floaters to occupy the interstices between territories or, temporarily, areas within territories (i.e. before being expelled by a resident pair; Fig. 5.7).

Several species of eagles establish multiple home range cores (Watson, 2010), as do other taxa (e.g., sea otters *Enhydra lutris*; Breed et al., 2017). Here, cores and home range size varied with breeding phenology. The shift to smaller home ranges during late breeding season (Fig. 5.1 & 5.6) was consistent with our expectation of shifts in space use for floaters and breeders. During late breeding season, nestlings require less immediate attention (e.g., brooding or shading), so females are able to more actively defend the territory, possibly suppressing the more expansive movements of floaters, as well as aid in provisioning during a time when nestlings require more food to support growth and development (Watson, 2010). The increase in number of core areas in late breeding season for territorial eagles is consistent with added home range structure likely resulting from these additional activities. Further, with more prey available later in the breeding season, due to the emergence of hibernators and offspring production, breeding pairs can likely use less space to sufficiently provision themselves and young.

Within these different home range cores, however, we found that individuals selected habitats and resources differently (Fig. 5.2), which aligns with our predictions about individuals partitioning space for different activities, such as roosting and forging. What

we did not predict was the generally low among-individual variance in habitat and resource selection. While among-floater variance was slightly greater, which could be due to their greater flexibility in movement strategy compared to territorial individuals, there was overall low individual heterogeneity (Fig. 5.5). This is somewhat in contrast to other work that highlights the importance of accounting for individual variation in resource selection studies (Lesmerises and St-Laurent, 2017) and recent findings of high heterogeneity in golden eagle selection for certain landscape features during migration (Eisaguirre et al., 2019b). Our findings, here, suggest that it is perhaps just has important to condition inference of habitat and resource selection patterns on the structure of individuals' home ranges, as it is on the individuals. Further, the extremely low individual heterogeneity among territorial individuals suggests that the realized niche of territorial eagles during the breeding season in this area is relatively narrow.

Our analytical estimates of home range size were of similar size to those estimated using descriptive approaches for golden eagles elsewhere (Watson, 2010; Watson et al., 2014; Moss et al., 2014; Braham et al., 2015). However, some of the overlap between neighboring territorial individuals that we found (Fig. 5.7) could be due to home ranges being larger than defended territories and/or over estimating space use density in the tails of the utilization distributions. If one had all of the individuals within an area tagged, it would be simple to incorporate a variable for the distance to neighboring individual (or territory center) in the habitat weighting function $\exp(z(\mathbf{x}_t)^T\boldsymbol{\beta})$, which might remove the tails of the utilization distributions and increase the density at the boundaries. Such a space use pattern is consistent with other mechanistic home range models that incorporate territory marking in mammals (Moorcroft and Lewis, 2006).

5.5.4 Implications & conclusions

Given the importance of floaters to the population ecology of many long-lived taxa, such as golden eagles, we shed some new light on the differential space use patterns between floaters and territorial individuals. The comparatively expansive movements of floaters and their proximity to territorial individuals—both in spatial and habitat

distances—suggests the potential for some of the complex density-dependent effects an underworld of floaters can have on breeders, such as competition for food, alteration of breeder behavior through territory intrusions, and reduced survival through fatal conflicts (Hunt, 1998; Ferrer et al., 2004; López-Sepulcre and Kokko, 2005; Carrete et al., 2006a; Bretagnolle et al., 2008; Watson, 2010; Ferrer et al., 2015). We may also conclude that habitat and landscape conservation plans that prioritize areas known to encompass golden eagle territories in this, and perhaps other, study areas likely benefit floater eagles as well, which helps ensure population stability.

While the importance of floaters to the populations of long-lived, territorial species is understood (Penteriani et al., 2011), pre-breeding age individuals, although not included in our sample, here, should also not be ignored, as they must survive to become floaters. Pre-breeding age individuals (i.e. typically those in their first to third summers for golden eagles) can have markedly different movement and space use patterns, as they are not yet attempting to enter the breeding population (Delgado and Penteriani, 2008; Delgado et al., 2009; Caro et al., 2011; McIntyre and Lewis, 2018). Once they enter the floater segment of the population, they, as we have shown, utilize similar areas on the landscape as territorial individuals, exhibiting only slight differential resource selection patterns. This transition, therefore, likely marks the onset of one to several breeding seasons of balancing time and effort between awaiting a territory vacancy, usurping a territorial resident, maintaining access to food, and learning about incredibly dynamic resources that could improve future reproductive success.

5.6 Acknowledgements

T. & D. Hawkins, M. Kohan, B. Robinson, and many others provided support in the field, and J. Liguori and N. Paprocki helped age eagles. K. Kielland and P. Doak provided excellent feedback that helped improve this research and manuscript. To all of these friends, we are most grateful. Funding was provided by the Alaska Department of Fish & Game (ADF&G) through the federal State Wildlife Grant Program, and the U.S. Fish & Wildlife Service (USFWS) provided additional PTTs and data. JME was

supported by the Calvin J. Lensink Fund during part of the project. The findings and conclusions of this paper are those of the authors and do not necessarily represent the views of the USFWS.

5.7 References

Bivand R, Lewin-Koh N. 2016. maptools: Tools for Reading and Handling Spatial Objects.
URL `https://cran.r-project.org/package=maptools`

Blackwell PG. 1997. Random diffusion models for animal movement. *Ecological Modelling* **100**: 87–102. doi: 10.1016/S0304-3800(97)00153-1.

Boyce MS, Mao JS, Merrill EH, Fortin D, Turner MG. 2003. Scale and heterogeneity in habitat selection by elk in Yellowstone National Park. *Ecoscience* **10**: 421–431.

Braham M, Miller T, Duerr AE, Lanzone M, Fesnock A, LaPre L, Driscoll D, Katzner T. 2015. Home in the heat: Dramatic seasonal variation in home range of desert golden eagles informs management for renewable energy development. *Biological Conservation* **186**: 225–232. doi: 10.1016/j.biocon.2015.03.020.

Breed GA, Golson EA, Tinker MT. 2017. Predicting animal home-range structure and transitions using a multistate Ornstein-Uhlenbeck biased random walk. *Ecology* **98**: 32–47. doi: 10.1002/ecy.1615.

Bretagnolle V, Mougeot F, Thibault JC. 2008. Density dependence in a recovering osprey population: Demographic and behavioural processes. *Journal of Animal Ecology* **77**: 998–1007. doi: 10.1111/j.1365-2656.2008.01418.x.

Brown JL. 1969. Territorial behavior and population regulation in birds: A review and re-evaluation. *The Wilson Bulletin* **81**: 293–329.

Campioni L, Lourenço R, Delgado MdM, Penteriani V. 2012. Breeders and floaters use different habitat cover: Should habitat use be a social status-dependent strategy? *Journal of Ornithology* **153**: 1215–1223. doi: 10.1007/s10336-012-0852-0.

Caro J, Ontiveros D, Pizarro M, Pleguezuelos JM. 2011. Habitat features of settlement areas used by floaters of Bonellis and Golden Eagles. *Bird Conservation International* **21**: 59–71. doi: 10.1017/S0959270910000213.

Carrete M, Donázar JA, Margalida A. 2006a. Density-dependent productivity depression in Pyrenean Bearded Vultures: Implications for conservation. *Ecological Applications* **16**: 1674–1682. doi: 10.1890/1051-0761(2006)016[1674:DPDIPB]2.0.CO;2.

Carrete M, Sánchez-Zapata JA, Tella JL, Gil-Sánchez JM, Moleón M. 2006b. Components of breeding performance in two competing species: Habitat heterogeneity, individual quality and density-dependence. *Oikos* **112**: 680–690. doi: 10.1111/j.0030-1299.2006.14528.x.

Collopy M, Edwards T. 1989. Territory Size, Activity Budget, and Role of Undulating Flight in Nesting Golden Eagles. *Journal of Field Ornithology* **60**: 43–51.

Delgado MM, Penteriani V. 2008. Behavioral states help translate dispersal movements into spatial distribution patterns of floaters. *American Naturalist* **172**: 475–485. doi: 10.1086/590964.

Delgado MM, Penteriani V, Nams VO, Campioni L. 2009. Changes of movement patterns from early dispersal to settlement. *Behavioral Ecology and Sociobiology* **64**: 35–43. doi: 10.1007/s00265-009-0815-5.

Dunn JE, Gipson PS. 1977. Analysis of radio telemetry data in studies of home range. *Biometrics* **33**: 85–101.

Eckert CG, Weatherhead PJ. 1987. Owners, floaters and competitive asymmetries among territorial red-winged blackbirds. *Animal Behaviour* **35**: 1317–1323. doi: 10.1016/S0003-3472(87)80003-9.

Eisaguirre J. 2019. *Multistate Ornstein-Uhlenbeck space use models reveal sex-specific partitioning of the energy landscape in a soaring bird.* M.s. project, University of Alaska Fairbanks.

Eisaguirre J, Breed G, Booms T, Barger C, Goddard S. 2020. Multistate Ornstein-Uhlenbeck space use models reveal sex-specific partitioning of the energy landscape in a soaring bird. *In prep.* .

Eisaguirre JM, Auger-Méthé M, Barger CP, Lewis SB, Booms TL, Breed GA. 2019a. Dynamic-parameter movement models reveal drivers of migratory pace in a soaring bird. *Frontiers in Ecology and Evolution* **7**: 317. doi: 10.3389/fevo.2019.00317.

Eisaguirre JM, Booms TL, Barger C, McIntyre CL, Lewis SB, Breed G. 2018. Local meteorological conditions reroute a migration. *Proceedings of the Royal Society B* **285**: 20181779.

Eisaguirre JM, Booms TL, Barger CP, Lewis SB, Breed GA. 2019b. Step selection functions on energy landscapes reveal how linear features alter migration movement in a large soaring bird. *bioRxiv* doi: 10.1101/805374.

Ens BJ, Weissing FJ, Drent RH. 1995. The despotic distribution and deferred maturity: two sides of the same coin. *The American Naturalist* **146**: 625–650.

Fagan WF, Lewis MA, Auger-Méthé M, Avgar T, Benhamou S, Breed G, LaDage L, Schlägel UE, Tang Ww, Papastamatiou YP, Forester J, Mueller T. 2013. Spatial memory and animal movement. *Ecology Letters* **16**: 1316–1329. doi: 10.1111/ele.12165.

Ferrer M, Morandini V, Newton I. 2015. Floater interference reflects territory quality in the Spanish Imperial Eagle Aquila adalberti: A test of a density-dependent mechanism. *Ibis* **157**: 849–859. doi: 10.1111/ibi.12289.

Ferrer M, Otalora F, García-Ruiz JM. 2004. Density-Dependent Age of First Reproduction as a Buffer Affecting Persistence of Small Populations. *Ecological Applications* **14**: 616–624.

Forrester TD, Casady DS, Wittmer HU. 2015. Home sweet home: fitness consequences of site familiarity in female black-tailed deer. *Behavioral Ecology and Sociobiology* **69**: 603–612. doi: 10.1007/s00265-014-1871-z.

Gill FB. 2007. *Ornithology*. New York: W. H. Freeman and Company, third edition.

Harmata AR. 1982. What is the function of undulating flight display in Golden Eagles? *Raptor Research* **16**: 103–109.

Herzog J, Eisaguirre JM, Linkhart B, Booms TL. 2019. Golden eagle diet in western Alaska. *Journal of Raptor Research* **53**: 393–401. doi: 10.3356/0892-1016-53.4.393.

Hollister J, Shah T. 2018. elevatr: access elevation data from various APIs. URL `https://cran.r-project.org/package=elevatr`

Hooten MB, Johnson DS, McClintock BT, Morales JM. 2017. *Animal movement: statistical models for telemetry data*. New York: CRC Press.

Hunt W. 1998. Raptor floaters at Moffat's equilibrium. *Oikos* **82**: 191–197.

Hunt WG, Wiens JD, Law PR, Fuller MR, Hunt TL, Driscoll DE, Jackman RE. 2017. Quantifying the demographic cost of humanrelated mortality to a raptor population. *PLoS ONE* **12**: 1–22. doi: 10.1371/journal.pone.0172232.

Johnson DS, Thomas DL, Ver Hoef JM, Christ A, Service F. 2008. A general framework for the analysis of animal resource selection from telemetry data. *Biometrics* **64**: 968–976. doi: 10.1111/j.1541-0420.2007.00943.x.

Katzner TE, Turk PJ, Duerr AE, Miller TA, Lanzone MJ, Cooper JL, Brandes D, Tremblay JA, Lemaître J. 2015. Use of multiple modes of flight subsidy by a soaring terrestrial bird, the golden eagle Aquila chrysaetos, when on migration. *Journal of Royal Society Interface* **12**: 20150530. doi: 10.1098/rsif.2015.0530.

Kochert MN, Steenhof K, McIntyre CL, Craig EH. 2002. Golden Eagle (Aquila chrysaetos). In Poole A (ed.) *The Birds of North America*. Ithaca: Cornell Lab of Ornithology.

Kokko H, Sutherland WJ. 1998. Optimal floating and queuing strategies: consequences for density dependence and habitat loss. *The American Naturalist* **152**: 354–366. doi: 10.1086/286174.

Krebs JR. 1971. Territory and breeding density in the great tit, Parsus major L. *Krebs, JR* **52**: 2–22.

Lee AM, Reid JM, Beissinger SR. 2017. Modelling effects of nonbreeders on population growth estimates. *Journal of Animal Ecology* **86**: 75–87. doi: 10.1111/1365-2656.12592.

Lesmerises R, St-Laurent MH. 2017. Not accounting for interindividual variability can mask habitat selection patterns: a case study on black bears. *Oecologia* **185**: 415–425. doi: 10.1007/s00442-017-3939-8.

López-Sepulcre A, Kokko H. 2005. Territorial Defense, Territory Size, and Population Regulation. *The American Naturalist* **166**: 317–325. doi: 10.1086/432560.

Macander MJ, Swingley CS, Joly K, Raynolds MK. 2015. Landsat-based snow persistence map for northwest Alaska. *Remote Sensing of Environment* **163**: 23–31. doi: 10.1016/j.rse.2015.02.028.

McIntyre CL, Adams LG. 1999. Reproductive Characteristics of Migratory Golden Eagles in Denali National Park, Alaska. *The Condor* **101**: 115–123.

McIntyre CL, Lewis SB. 2018. Statewide movements of non-territorial Golden Eagles in Alaska during the breeding season: Information for developing effective conservation plans. *Alaska Park Science* **17**: 65–73.

McIntyre CL, Schmidt JH. 2012. Ecological and environmental correlates of territory occupancy and breeding performance of migratory Golden Eagles Aquila chrysaetos in interior Alaska. *Ibis* **154**: 124–135. doi: 10.1111/j.1474-919X.2011.01181.x.

McLeod DRA, Whitfield DP, Fielding AH, Haworth PF, Mcgrady MJ. 2002. Predicting home range use by Golden Eagles Aquila chrysaetos in western Scotland. *Avian Science* **2**: 1–17.

Miller TA, Brooks RP, Lanzone MJ, Brandes D, Cooper J, Tremblay JA, Wilhelm JAY, Duerr A, Katzner TE. 2016. Limitations and mechanisms influencing the migratory performance of soaring birds. *Ibis* **158**: 116–134. doi: 10.1111/ibi.12331.

Moorcroft P, Lewis M. 2006. *Mechanistic home range analysis.* Princeton, NJ: Princeton University Press.

Moss EH, Hipkiss T, Ecke F, Dettki H, Sandström P, Bloom PH, Kidd JW, Thomas SE, Hörnfeldt B. 2014. Home-range size and examples of post-nesting movements for adult Golden Eagles (Aquila chrysaetos) in boreal Sweden. *Journal of Raptor Research* **48**: 93–105. doi: 10.3356/jrr-13-00044.1.

Murgatroyd M, Photopoulou T, Underhill LG, Bouten W, Amar A. 2018. Where eagles soar: Fine-resolution tracking reveals the spatiotemporal use of differential soaring modes in a large raptor. *Ecology and Evolution* **8**: 6788–6799. doi: 10.1002/ece3.4189.

Newton I. 1976. Population limitation in diurnal raptors. *Canadian Field-Naturalist* **90**: 274–300.

Newton I. 1979. *Population ecology of raptors.* London: T & AD Poyser Ltd.

Newton I. 1992. Experiments on the limitation of bird numbers by territorial behaviour. *Biological Review* **67**: 129–173.

Newton I. 1998. *Population limitation in birds.* San Diego: Academic Press.

Penteriani V, Balbontin J, Ferrer M. 2003. Simultaneous effects of age and territory quality on fecundity in Bonelli's Eagle Hieraaetus fasciatus. *Ibis* **145**: E77–E82. doi: 10.1046/j.1474-919x.2003.00159.x.

Penteriani V, Del Mar Delgado M, Campioni L. 2015. Quantifying space use of breeders and floaters of a long-lived species using individual movement data. *Science of Nature* **102**. doi: 10.1007/s00114-015-1271-x.

Penteriani V, Ferrer M, Delgado MM. 2011. Floater strategies and dynamics in birds, and their importance in conservation biology: Towards an understanding of nonbreeders in avian populations. *Animal Conservation* **14**: 233–241. doi: 10.1111/j.1469-1795.2010.00433.x.

Penteriani V, Otalora F, Ferrer M. 2005. Floater survival affects population persistence. The role of prey availability and environmental stochasticity. *Oikos* **108**: 523–534. doi: 10.1111/j.0030-1299.2005.13514.x.

Péron G, Fleming CH, Duriez O, Fluhr J, Itty C, Lambertucci S, Safi K, Shepard EL, Calabrese JM. 2017. The energy landscape predicts flight height and wind turbine collision hazard in three species of large soaring raptor. *Journal of Applied Ecology* doi: 10.1111/1365-2664.12909.

R Core Team. 2018. R: a language and environment for statistical computing. URL `https://www.r-project.org/`

Rohner C. 1997. Non-territorial 'floaters' in great horned owls: space use during a cyclic peak. *Animal Behaviour* **53**: 901–912.

Sergio F, Blas J, Hiraldo F. 2009. Predictors of floater status in a long-lived bird: a cross-sectional and longitudinal test of hypotheses. *Journal of Animal Ecology* **78**: 109–118. doi: 10.1111/j.1365-2656.2008.01484.x.

Shepard EL, Lambertucci SA, Vallmitjana D, Wilson RP. 2011. Energy beyond food: Foraging theory informs time spent in thermals by a large soaring bird. *PLoS ONE* **6**: 1–6. doi: 10.1371/journal.pone.0027375.

Shepard ELC, Wilson RP, Rees WG, Grundy E, Lambertucci SA, Vosper SB. 2013. Energy landscapes shape animal movement ecology. *The American Naturalist* **182**: 298–312. doi: 10.1086/671257.

Smith JNM, Arcese P. 1989. How fit are floaters? Consequences of alternative territorial behaviors in a nonmigratory sparrow. *The American Naturalist* **133**: 830–845.

Smith SM. 1978. The "underworld" in a territorial sparrow: adaptive strategy for floaters. *The American Naturalist* **112**: 571–582.

Stamps J. 1995. Motor learning and the value of familiar space. *The American Naturalist* **146**: 41–58. doi: 10.1086/285786.

Stan Development Team. 2016. rstanarm: Bayesian applied regression modeling via Stan. R package version 2.13.1.

Stan Development Team. 2018. RStan: the R interface to Stan, Version 2.17.3. URL `http://mc-stan.org`

Stutchbury BJ, Robertson R. 1985. Floating populations of female tree swallows. *The Auk* **102**: 651–654. doi: 10.2307/4086820.

Tanferna A, López-Jiménez L, Blas J, Hiraldo F, Sergio F. 2013. Habitat selection by Black kite breeders and floaters: Implications for conservation management of raptor floaters. *Biological Conservation* **160**: 1–9. doi: 10.1016/j.biocon.2012.12.031.

Watson J. 2010. *The Golden Eagle*. New Haven: Yale University Press, second edition.

Watson JW, Duff AA, Davies RW. 2014. Home range and resource selection by GPS-monitored adult Golden Eagles in the Columbia Plateau Ecoregion: Implications for wind power development. *Journal of Wildlife Management* **78**: 1012–1021. doi: 10.1002/jwmg.745.

Zack S, Stutchbury BJ. 1992. Delayed breeding in avian social systems: The role of territory quality and "floater" tactics. *Behaviour* **123**: 194–219.

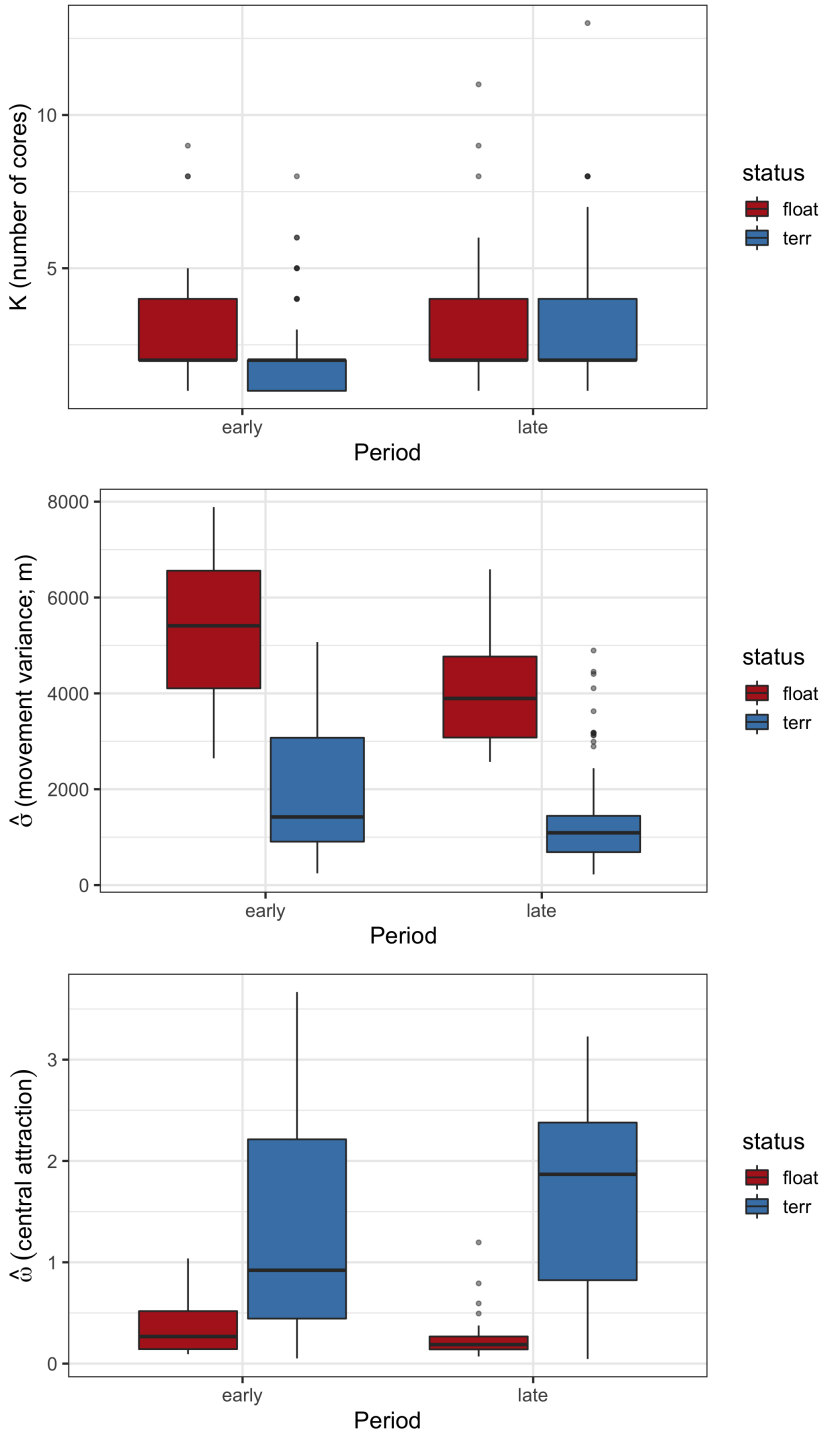

Figure 5.1: Summaries of the number of home range cores K, posterior means of the movement variance parameter σ, and posterior means of the centralizing tendency parameter ω in an Ornstein-Uhlenbeck space use model for golden eagles summering in southcentral Alaska.. Summaries of the OU parameters are for the most used home range core, and the model was fit separately for early and late breeding. K was estimated with a k-means clustering algorithm.

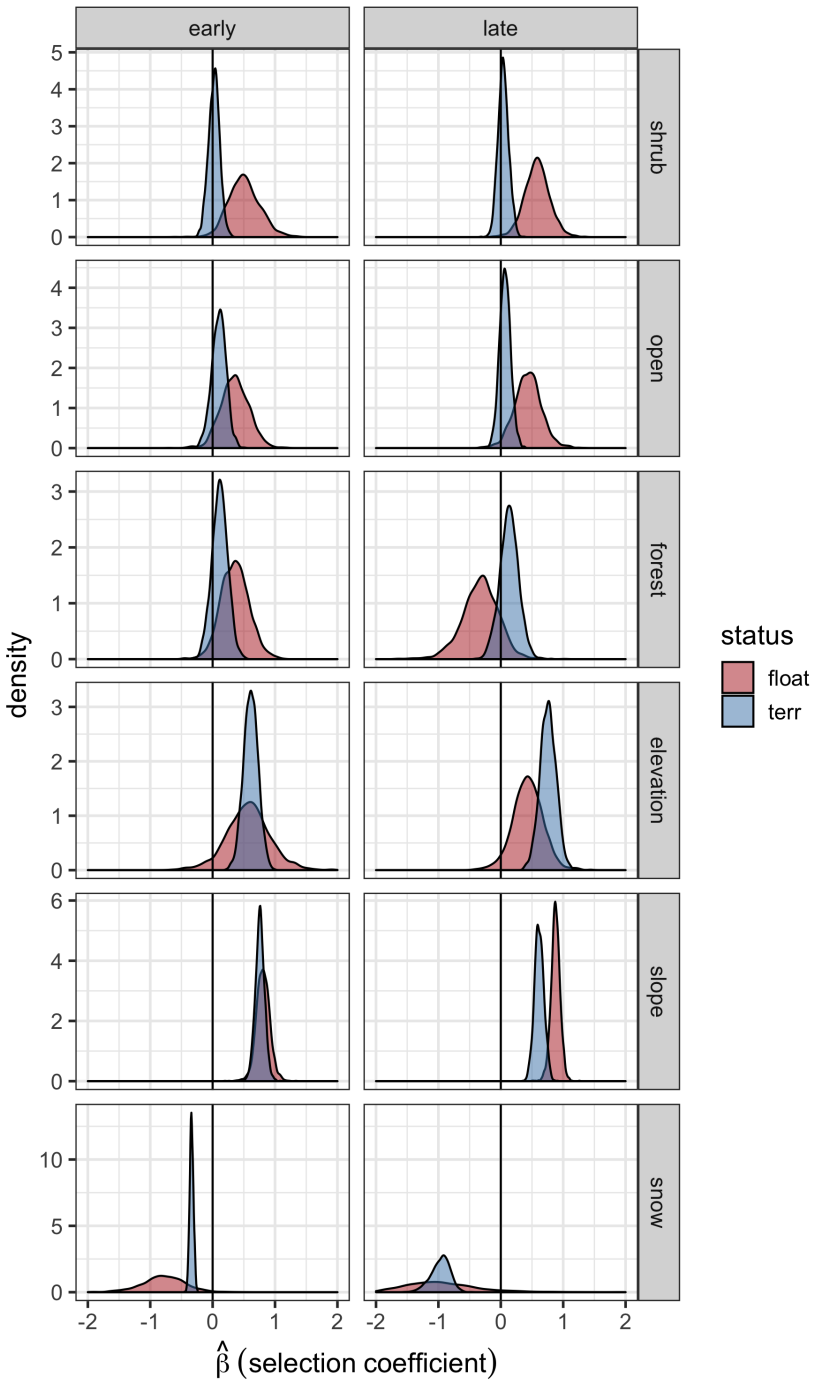

Figure 5.2: Estimated marginal posteriors for the population-level selection coefficients from an Ornstein-Uhlenbeck space use model fit to summer golden eagle GPS data in southcentral Alaska. The model was fit separately for early and late breeding season and floater and territorial eagles. 'bare' (bare ground) is the reference category.

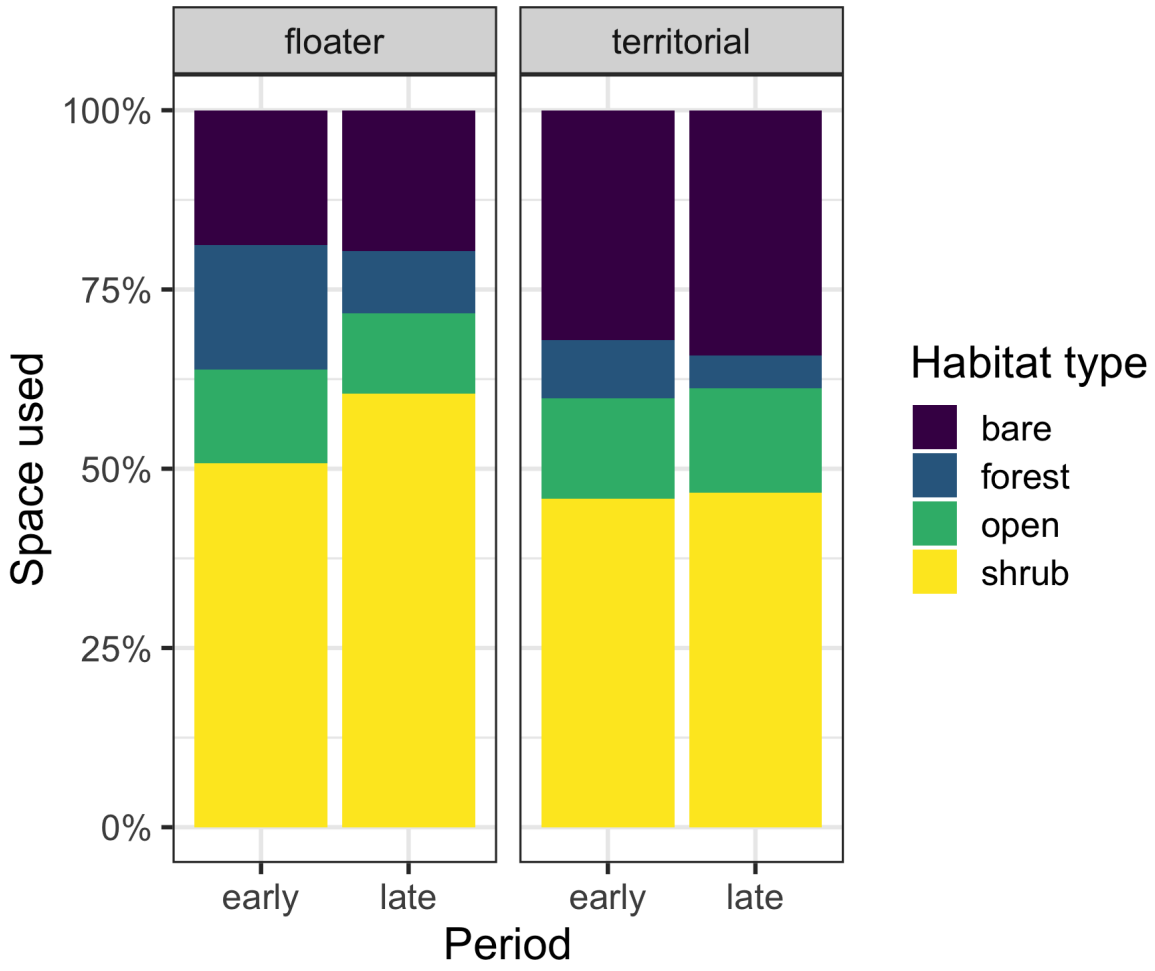

Figure 5.3: Proportion of habitat types used by golden eagles summering in southcentral Alaska.

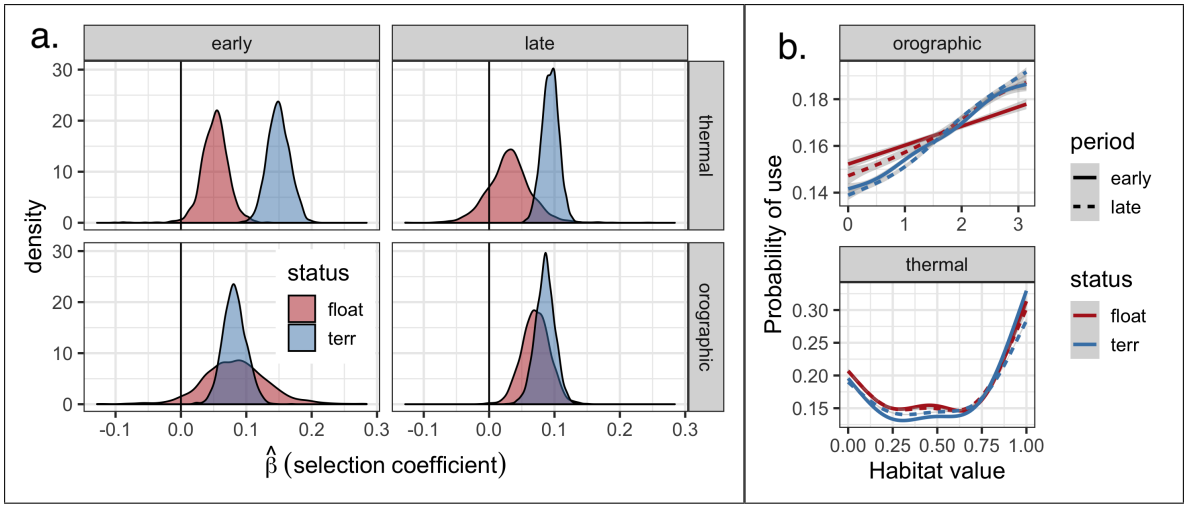

Figure 5.4: (a.) Estimated marginal posteriors for the population-level selection coefficients for golden eagles in southcentral Alaska estimated with an Ornstein-Uhlenbeck (OU) space use model, and (b.) probability of a golden eagle using a spatial location within its breeding season home range in southcentral Alaska as a function of habitat variables. The model was fit separately for early and late breeding season and floater and territorial eagles. In b. predictions were smoothed over the availability points with a generalized additive model ($df = 6$) and ribbons are 95% confidence intervals. Units are radians for orographic uplift (angle of incidence). Higher hill shade corresponds to more direct sun and greater thermal uplift potential. Years were pooled for presentation, but the year-specific figures are provided in the Appendix.

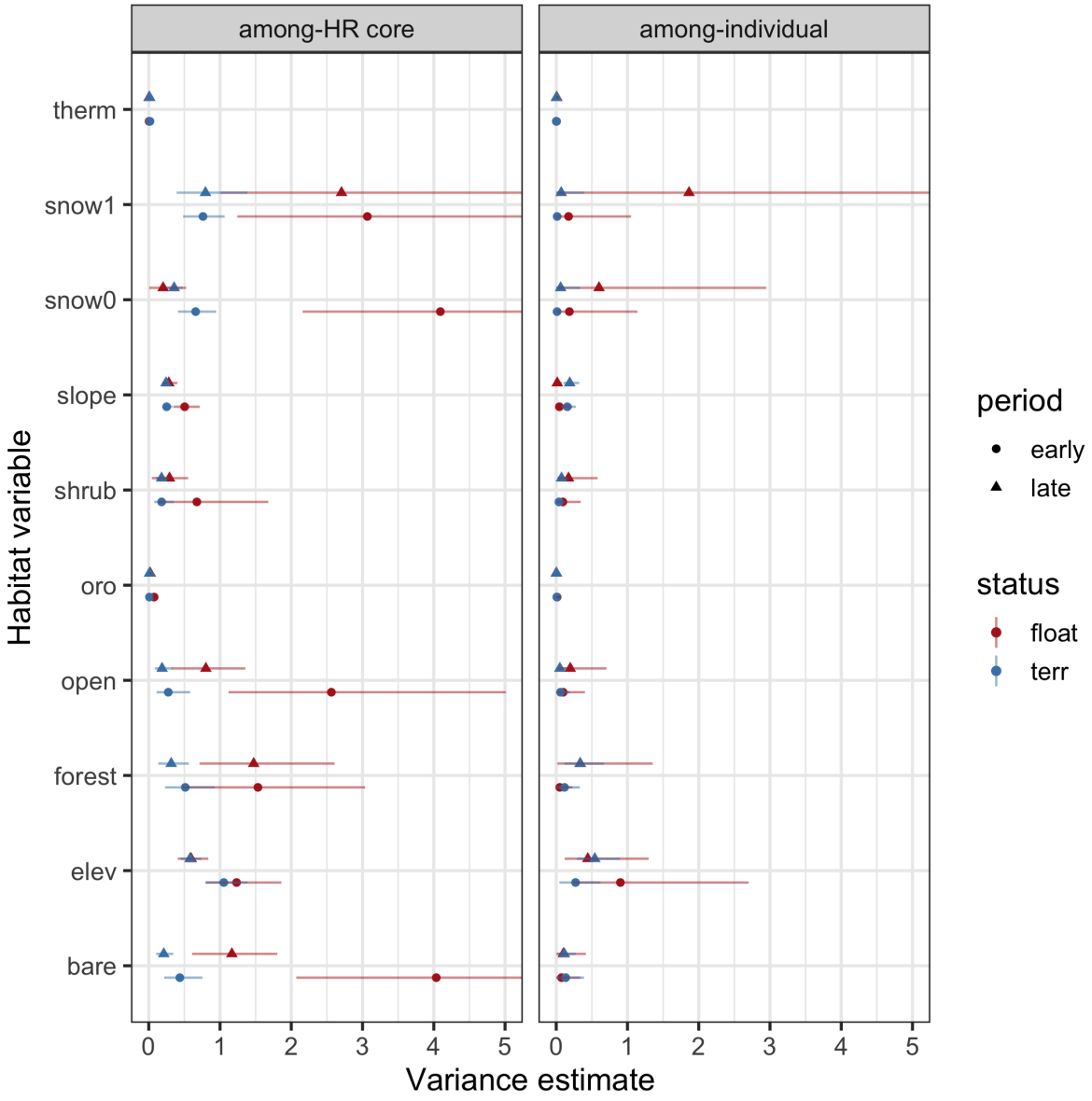

Figure 5.5: Estimated among-home range core variance and among-individual variance for the selection coefficients from an Ornstein-Uhlenbeck space use model fit to summer golden eagle GPS data in southcentral Alaska. The model was fit separately for early and late breeding season and floater and territorial eagles. Points are posterior means, and horizontal lines are 95% credible intervals. Note the horizontal axis has been truncated for presentation.

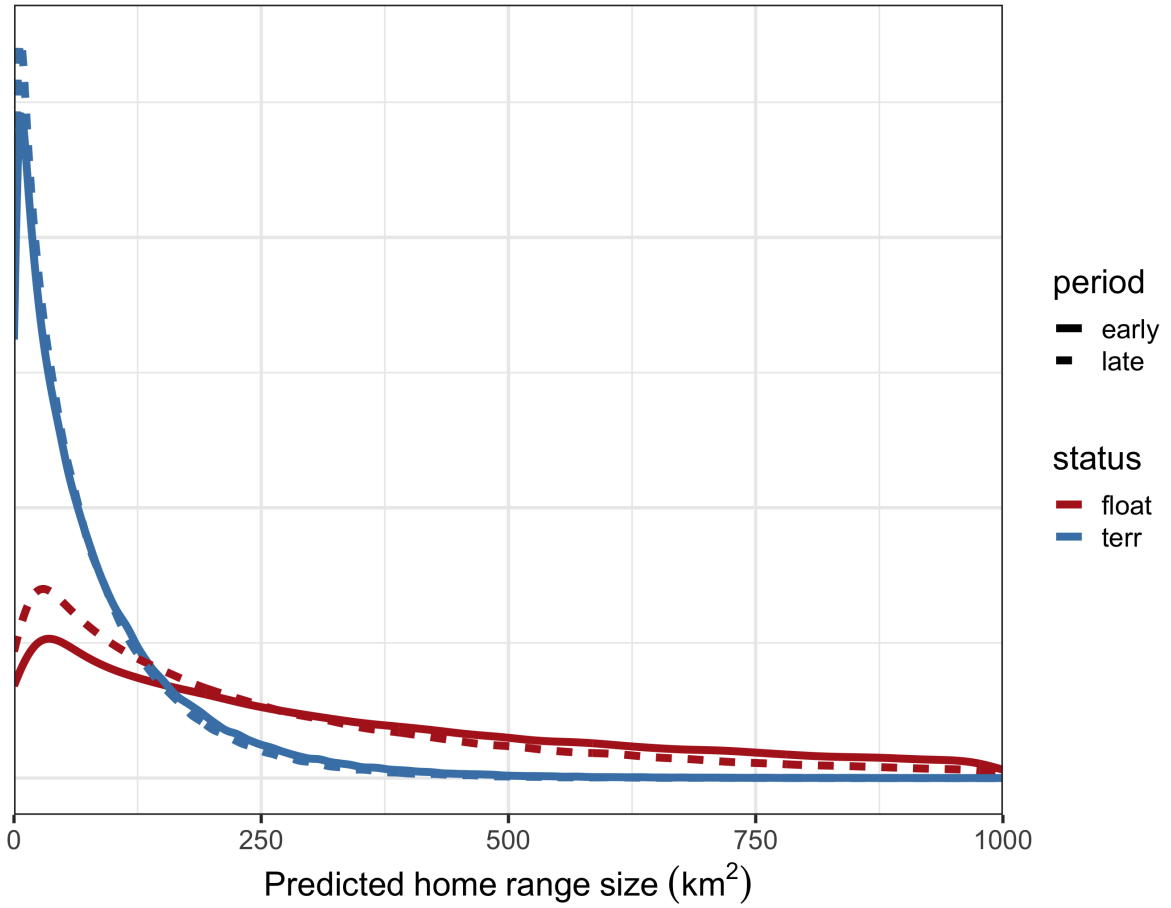

Figure 5.6: Posterior predictive densities of a hierarchical Gamma regression on golden eagle home range size predicted with an Ornstein-Uhlenbeck home range model for golden eagles summering in southcentral Alaska 2014-2017. Period of breeding season (early or late) and status (floater or territorial) were included as fixed effects, and individual and year were included as random effects.

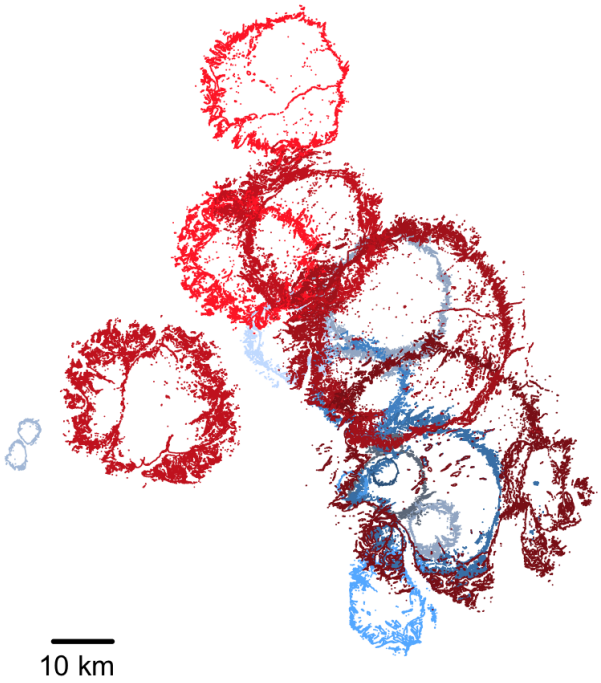

Figure 5.7: Estimated home range boundaries for nine territorial (blue hues) and four floater (red hues) golden eagles in southcentral Alaska during late breeding season in 2016. Home range estimates are the 95% contour of the utilization distribution constructed from the posterior predictive distribution of an Ornstein-Uhlenbeck space use model.

Table 5.1: Median (interquartile range) dates of arrival on and departure from the summer range of golden eagles tagged with GPS telemetry in southcentral Alaska.

	2014	2015	2016	2017
Territorial				
Arrival	29 March (5)	27 Mar (4)	26 Mar (8)	1 Apr (6)
Departure	28 Sep (28)	7 Oct (17)	5 Oct (13)	4 Oct (18)
Floater				
Arrival	5 Apr (3)	30 Mar (6)	24 Mar (10)	1 Apr (2)
Departure	24 Sep (12)	24 Sep (4)	29 Sept (4)	6 Oct (13)

Chapter 6: Conclusion

A major area of work in the growing field of movement ecology involves investigating how fine-scale movement decisions interact with intrinsic and extrinsic factors to emerge as an animal's observed movement pattern (Nathan et al., 2008). In this dissertation, I investigated questions regarding some of the external and internal factors that give rise to individual- and population-level movement and behavioral patterns in animals, using migratory golden eagles as a model system. Specifically, these questions were: (1) How can discrete decisions give rise to large changes in animal movement corridors? (2) How do the behavioral budgets and the energetic subsidies that drive those budgets vary between spring and fall migration? (3) How do linear features affect the movement and space use of soaring birds? and (4) How do space use and resource selection patterns vary between floater and territorial individuals?

Changes in climate and weather along migration corridors will affect the efficiency and risk associated with certain migration routes and timing (Vansteelant et al., 2017). These effects will also interact with climate-driven landcover change to influence both en route weather conditions and food resources. Identifying how weather, such as wind and cloud prevalence, drives individual decisions is, therefore, key to predicting potential shifts in migration routes. However, despite being an undoubted source of changes in migration routes, discrete navigation decisions are infrequently addressed in the migration literature (Shamoun-Baranes et al., 2017). I was able to use the golden eagle as a model to show how weather can influence a single, binary, discrete decision to give rise to a major change in migration route.

A consistent theme across the chapters within this dissertation was the importance of weather, notably wind and uplift, to the movement and space use of golden eagles. While long understood to influence soaring bird movement (Pennycuick, 1971), I showed how wind and uplift are linked to the emergent movement patterns of a soaring bird during migration, and their influence on where and when migrants stopover to rest and refuel. I accomplished this by developing and implementing novel continuous-time movement

models. Similar models are proving to be quite flexible and applicable across taxa (Jonsen et al., 2019).

I was able to build on those models to design a model that even more completely captures animal movement and space use processes, in addition to their various internal and external drivers. This model took the form of a step selection function (SSF; Fortin et al., 2005). SSFs typically do not capture or account for changes in animal movement and behavioral state and have underlying discrete-time random walks that are not robust to irregularly sampled data (Thurfjell et al., 2014). This presented a challenge for implementing it on migratory golden eagles, as a migrating eagle has an evolved life-history constraint such that they must make migration progress toward a seasonal home range, and, consequently, movements that do not afford progress should be relatively infrequent. In contrast, while stopped over during migration for foraging or resting, an eagle's movements and habitat selection should change substantially due to differences in energy, habitat requirements, and the need to deposit energy reserves during stopover. Thus, I designed a new form of SSF that accounted for these widely recognized patterns and important effects (Thurfjell et al., 2014; Hooten et al., 2014; Avgar et al., 2016; Gurarie et al., 2017). Furthermore, the SSF allowed wind and uplift to drive those behavioral changes and thus constituted a more biologically justified model for animal movement and space use.

The development of the SSF was motivated to investigate how linear features affected golden eagle movement during migration. It allowed me to account for various factors impacting soaring subsidies and movement, to tease apart some of the effects of linear features from other habitat and dynamic environmental effects, as well as some correlations with certain behaviors. Finding that eagles tended to use space near roads when making localized, stopover movements suggests they may be capitalizing on road-killed carrion and/or roadside habitat modifications that could increase prey availability or foraging success. This pattern contrasts with other taxa that use linear features to increase movement rate (Latham et al., 2011; McKenzie et al., 2012; Dickie et al., 2017), but is similar to wolves' use of seismic lines to access caribou (Dickie et al., 2017) and bears'

use of railroads to access key supplemental food (Murray et al., 2017). In addition to these findings, the parameterized SSF could be used to predict eagle space use patterns to identify potential hot spots of elevated mortality risk by vehicle collisions, as well as the conditional effects of weather (as flight subsidies) on the use of those more risky areas. Further, it could more generally be used to predict and test hypotheses regarding changes in eagle space use patterns following continued development of linear futures, other habitat changes, and/or changes in weather patterns.

Much of this dissertation focused on movements during migration, but the same factors affect animal movement during breeding and wintering seasons. For long-lived, territorial species, floating is an often prevalent but important strategy for a subset of the breeding-age population. Given the importance of floaters to the population ecology of many long-lived territorial species, including golden eagles, in my last chapter I developed and implemented a mechanistic space use model based on an Ornstein-Uhlenbeck process (Dunn and Gipson, 1977; Blackwell, 1997), to shed some much needed light on the differential space use patterns between floaters and territorial individuals. I reveal that floaters have comparatively expansive space use patterns but are proximal to territorial individuals. This suggests the potential for some of the complex density-dependent effects floaters can have on breeders, such as behavioral modification and suppressed prey availability (Ferrer et al., 2004; Penteriani et al., 2011). While I could not draw precise inferences about these effects with the data on hand, my findings strongly indicate their importance. Furthermore, having shown that golden eagle floaters fit into similar areas on the landscape as territorial individuals, exhibiting only slight differential space use patterns, it is likely that habitat and landscape conservation plans that prioritize areas known to encompass golden eagle territories, would benefit floater eagles as well and ensure population stability.

The field of movement ecology is advancing rapidly with technological developments in transmitter technology, as well as mathematical and statistical advances (Hooten et al., 2017). The latter is particularly often under appreciated, and technologies have tended to advance quickly with little plan for analyzing the vast amounts of data they collect. As I

demonstrated in this dissertation, new statistical tools can be developed and specifically tailored to drawing novel inference with existing data on the movement ecology of species, and this new insight comes with minimal additional expense compared to investing in new technologies and data collection efforts. As understanding an organism's movement, including where, when, and why it occurs on a landscape, is fundamental to understanding its ecology, such statistical and technological development should yield many new insights into the ecology of a wide breadth of taxa, similar to what I hope my work presented in this dissertation has done for migratory golden eagles.

6.1 References

Avgar T, Potts JR, Lewis MA, Boyce MS. 2016. Integrated step selection analysis: Bridging the gap between resource selection and animal movement. *Methods in Ecology and Evolution* **7**: 619–630. doi: 10.1111/2041-210X.12528.

Blackwell PG. 1997. Random diffusion models for animal movement. *Ecological Modelling* **100**: 87–102. doi: 10.1016/S0304-3800(97)00153-1.

Dickie M, Serrouya R, McNay RS, Boutin S. 2017. Faster and farther: wolf movement on linear features and implications for hunting behaviour. *Journal of Applied Ecology* **54**: 253–263. doi: 10.1111/1365-2664.12732.

Dunn JE, Gipson PS. 1977. Analysis of radio telemetry data in studies of home range. *Biometrics* **33**: 85–101.

Ferrer M, Otalora F, García-Ruiz JM. 2004. Density-Dependent Age of First Reproduction as a Buffer Affecting Persistence of Small Populations. *Ecological Applications* **14**: 616–624.

Fortin D, Beyer HL, Boyce MS, Smith DW, Duchesne T, Mao JS. 2005. Wolves influence elk movements: behavior shapes a trophic cascade in Yellowstone National Park. *Ecology* **86**: 1320–1330. doi: 10.1890/04-0953.

Gurarie E, Fleming CH, Fagan WF, Laidre KL, Hernández-Pliego J, Ovaskainen O. 2017. Correlated velocity models as a fundamental unit of animal movement: Synthesis and applications. *Movement Ecology* **5**: 1–18. doi: 10.1186/s40462-017-0103-3.

Hooten MB, Hanks EM, Johnson DS, Alldredge MW. 2014. Temporal variation and scale in movement-based resource selection functions. *Statistical Methodology* **17**: 82–98. doi: 10.1016/j.stamet.2012.12.001.

Hooten MB, Johnson DS, McClintock BT, Morales JM. 2017. *Animal movement: statistical models for telemetry data.* New York: CRC Press.

Jonsen ID, McMahon CR, Patterson TA, Auger-Méthé M, Harcourt R, Hindell MA, Bestley S. 2019. Movement responses to environment: fast inference of variation among southern elephant seals with a mixed effects model. *Ecology* **100**: 1–8. doi: 10.1002/ecy.2566.

Latham ADM, Latham MC, Boyce MS, Boutin S. 2011. Movement responses by wolves to industrial linear features and their effect on woodland caribou in northeastern alberta. *Ecological Applications* **21**: 2854–2865. doi: 10.1890/11-0666.1.

McKenzie HW, Merrill EH, Spiteri RJ, Lewis MA. 2012. How linear features alter predator movement and the functional response. *Interface Focus* **2**: 205–216. doi: 10.1098/rsfs.2011.0086.

Murray MH, Fassina S, Hopkins JB, Whittington J, Clair CC. 2017. Seasonal and individual variation in the use of rail-associated food attractants by grizzly bears (Ursus arctos) in a national park. *PLoS ONE* **12**: 1–16. doi: 10.1371/journal.pone.0175658.

Nathan R, Getz WM, Revilla E, Holyoak M, Kadmon R, Saltz D, Smouse PE. 2008. A movement ecology paradigm for unifying organismal movement research. *Proceedings of the National Academy of Sciences* **105**: 19052–9. doi: 10.1073/pnas.0800375105.

Pennycuick CJ. 1971. Soaring behavior and performance of some East African birds, observed from a motor-glider. *Ibis* **114**: 178–218.

Penteriani V, Ferrer M, Delgado MM. 2011. Floater strategies and dynamics in birds, and their importance in conservation biology: Towards an understanding of nonbreeders in avian populations. *Animal Conservation* **14**: 233–241. doi: 10.1111/j.1469-1795.2010.00433.x.

Shamoun-Baranes J, Liechti F, Vansteelant WM. 2017. Atmospheric conditions create freeways, detours and tailbacks for migrating birds. *Journal of Comparative Physiology A: Neuroethology, Sensory, Neural, and Behavioral Physiology* **203**: 509–529. doi: 10.1007/s00359-017-1181-9.

Thurfjell H, Ciuti S, Boyce MS. 2014. Applications of step-selection functions in ecology and conservation. *Movement Ecology* **2**: 26. doi: 10.1186/2051-3933-2-4.

Vansteelant WMG, Shamoun-Baranes J, Mclaren J, van Diermen J, Bouten W. 2017. Soaring across continents: decision-making of a soaring migrant under changing atmospheric conditions along an entire flyway. *Journal of Avian Biology* **48**: 887–896. doi: 10.1111/jav.01298.

Appendix

Chapter 2

Chapter 2: Supplementary Tables & Figures

Table S1. Candidate models of route choice around the Wrangell Mountains ranked by leave-one-out cross-validation approximated by Pareto-smoothed importance sampling. Lower information criterion (looic) indicates better model fit. All models include random intercept for individual. Interaction models include all main effects. Meteorological predictors were interpolated to the approximate location and time each eagle chose a route. 'Wind' is the velocity of south to north wind. Negative thermal uplift (surface sensible heat flux) is flux towards the surface.

Model	looic	Δlooic
wind × season	146.5	0
wind × season + pressure × season	148.1	1.6
wind × season + thermal	148.8	2.3
wind × season + pressure × season + thermal	149.2	2.7
wind × season + pressure	149.4	2.9
pressure × season	149.5	3.0
wind × season + pressure × season + humidity	149.8	3.3
wind × season + humidity	149.9	3.4
wind × season + thermal × season	151.0	4.5
pressure × season + thermal	151.3	4.8
season	151.4	4.9
wind × season + pressure × season + thermal + humidity	151.6	5.1
wind × season + pressure × season + thermal × season	151.8	5.3
wind × season + pressure + thermal	152.0	5.5
pressure × season + humidity	152.3	5.8
wind × season + humidity × season	152.4	5.9
wind × season + pressure + humidity	152.8	6.3
wind × season + pressure + humidity + thermal	154.3	7.8
wind × season + pressure × season + thermal × season + humidity	154.5	8.0
pressure × season + humidity × season	154.8	8.3
humidity × season	154.9	8.4
thermal × season	154.9	8.4
wind × season + pressure × season + humidity × season + thermal	155.1	8.6
thermal	156.1	9.6
humidity × season + pressure	156.9	10.4
thermal × season + pressure	157.4	10.9
wind × season + pressure × season + humidity × season + thermal × season	157.7	11.2
thermal × season + humidity	157.9	11.4
null	159.7	13.2
humidity	159.8	13.3
pressure	161.0	14.5

Table S2. Candidate models of route choice around the Wrangell Mountains, including day of year as a covariate, ranked by leave-one-out cross-validation approximated by Pareto-smoothed importance sampling. Lower information criterion (looic) indicates better model fit. All models include random intercept for individual. Interaction models include all main effects. Meteorological predictors were interpolated to the approximate location and time each eagle chose a route. 'Wind' is the velocity of south to north wind. Negative thermal uplift (surface sensible heat flux) is flux towards the surface. Day was included as deviation from the median for each season to avoid collinearity with season. Top 30 models shown.

Model	looic	Δlooic
wind × season	146.5	0
wind × season + pressure × season	148.1	1.6
wind × season + day	148.3	1.8
wind × season + thermal	148.8	2.3
wind × season + pressure × season + thermal	149.2	2.7
wind × season + pressure	149.4	2.9
pressure × season	149.5	3.0
wind × season + pressure × season + humidity	149.8	3.3
wind × season + humidity	149.9	3.4
wind × season + pressure × season + day	150.3	3.8
wind × season + day × season	150.8	4.3
wind × season + thermal × season	151.0	4.5
wind × season + pressure + day	151.2	4.7
pressure × season + thermal	151.3	4.8
season	151.4	4.9
wind × season + pressure × season + thermal + humidity	151.6	5.1
pressure × season + day	151.6	5.1
wind × season + pressure × season + thermal × season	151.8	5.3
wind × season + thermal + day	151.8	5.3
wind × season + pressure + thermal	152.0	5.5
pressure × season + humidity	152.3	5.8
wind × season + humidity × season	152.4	5.9
wind × season + pressure × season + day × season	152.6	6.1
wind × season + pressure + humidity	152.8	6.3
wind × season + thermal × season + day	152.9	6.4
wind × season + thermal + day × season	153.2	6.7
wind × season + humidity × season + day	153.6	7.1
wind × season + pressure + day × season	153.8	7.3
wind × season + pressure + thermal + day	154.2	7.7

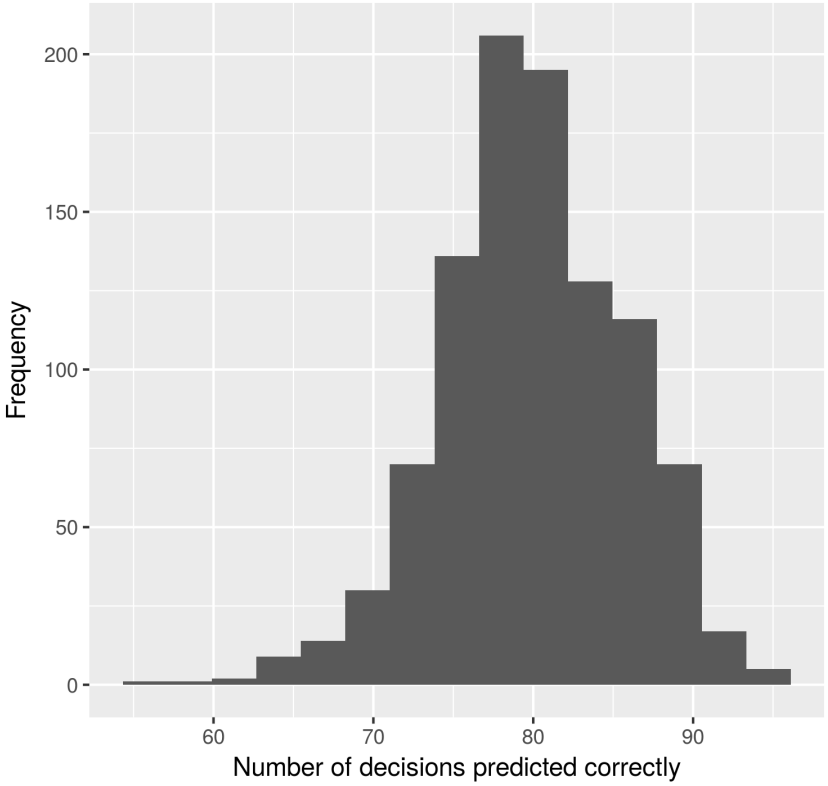

Figure S1. Number of decisions correctly predicted by the top model of eagle route choice around the Wrangell Mountains, Alaska based on 1000 posterior predictive draws. Each draw consisted of a set of 135 decisions, which were compared to the observed set of 135 decisions.

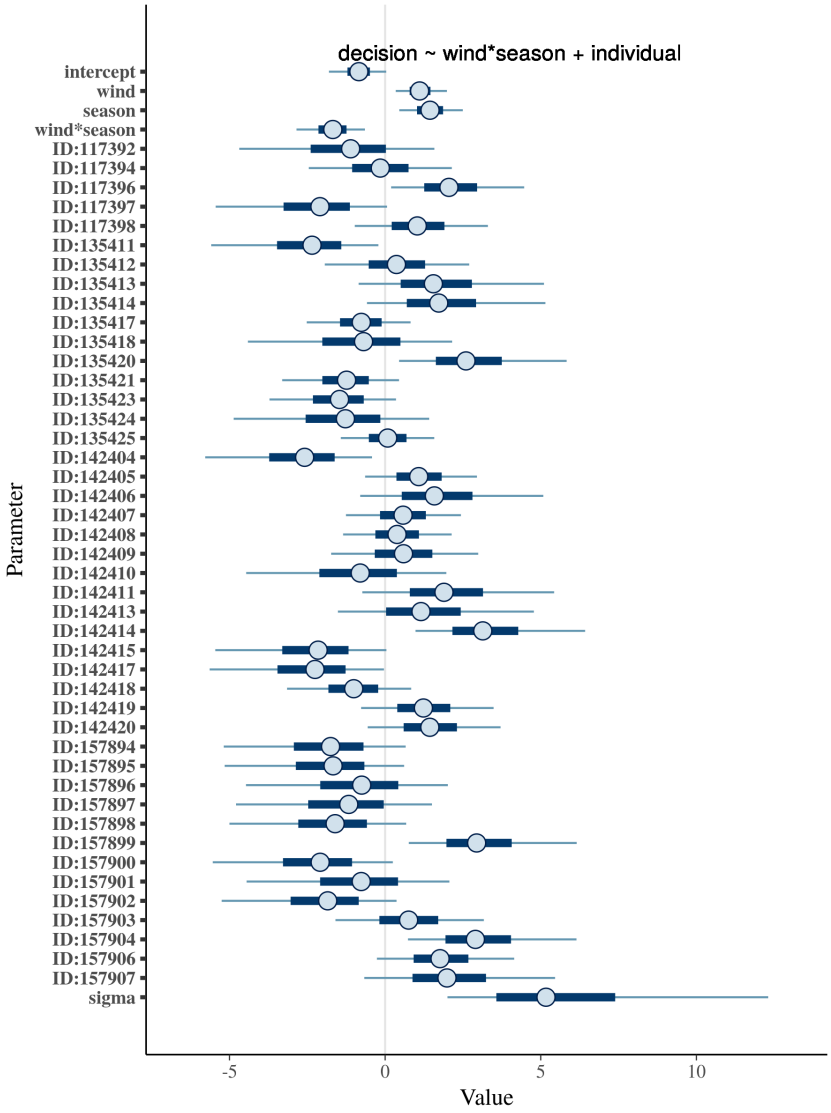

Figure S2. Estimates of intercepts and coefficients on explanatory variables for top fitting Bayesian hierarchical logistic regression model of choice of route north around the Wrangell Mountains, Alaska. Points are posterior medians and intervals are 50% and 90% Bayesian credible intervals. '*' indicates an interaction term. Meteorological predictors were interpolated to the approximate location and time each eagle chose a route. 'Wind' is the velocity of south to north wind. IDs are individual random intercept estimates. Estimated intercepts greater or less than zero indicate greater and lower probability of choosing the north route, respectively, independent of covariates.

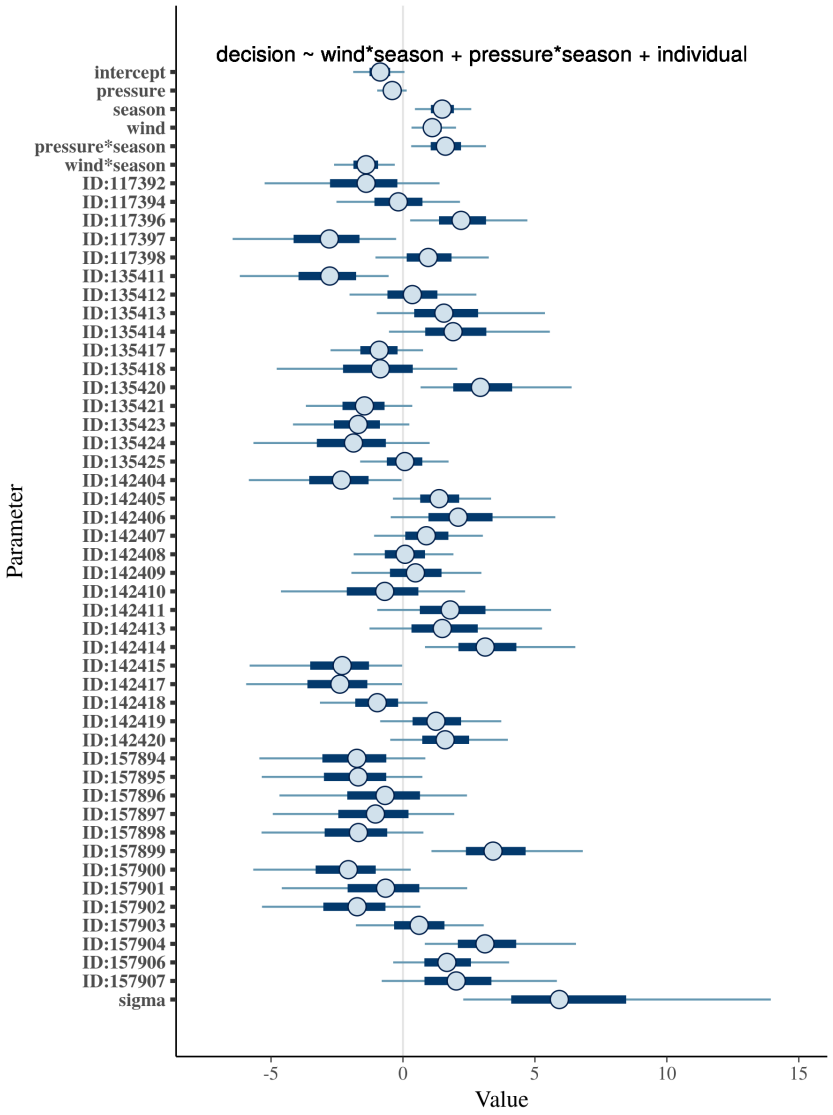

Figure S3. Estimates of intercepts and coefficients on explanatory variables for second best fitting Bayesian hierarchical logistic regression model of choice of route north around the Wrangell Mountains, Alaska. Points are posterior medians and intervals are 50% and 90% Bayesian credible intervals. '*' indicates an interaction term. Meteorological predictors were interpolated to the approximate location and time each eagle chose a route. 'Wind' is the velocity of south to north wind. IDs are individual random intercept estimates. Estimated intercepts greater or less than zero indicate greater and lower probability of choosing the north route, respectively, independent of covariates.

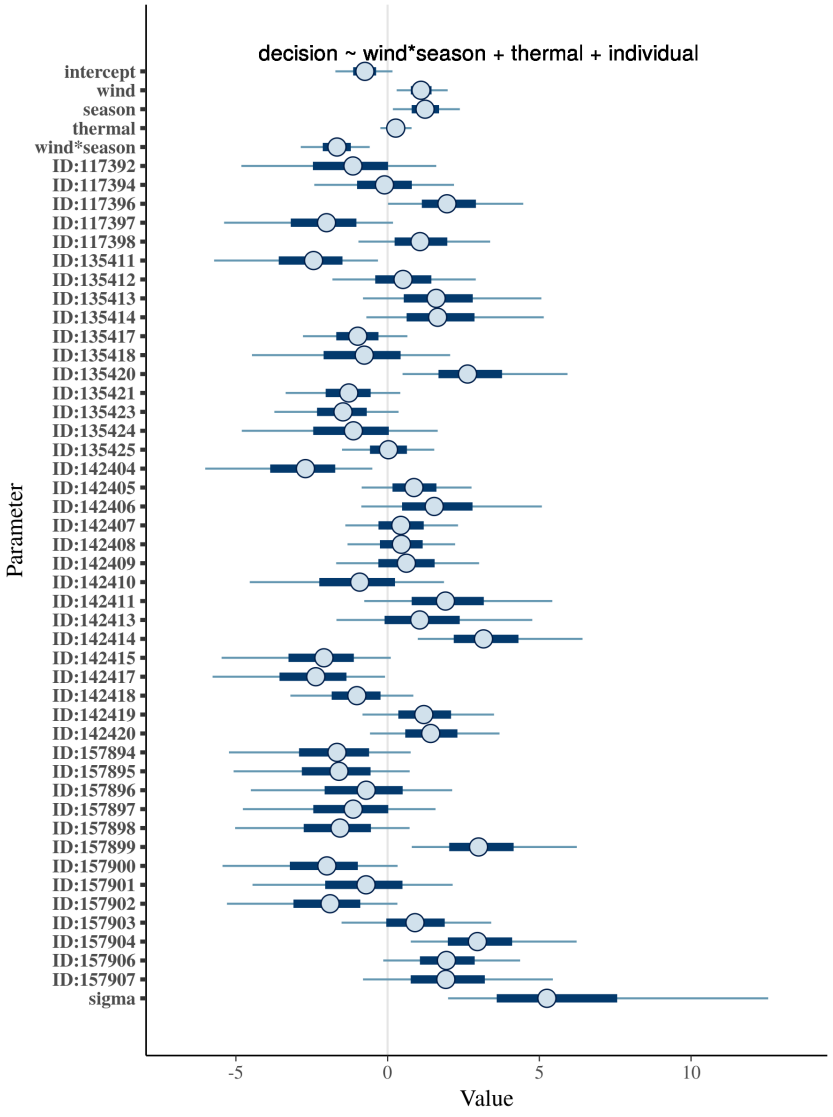

Figure S4. Estimates of intercepts and coefficients on explanatory variables for third best fitting Bayesian hierarchical logistic regression model of choice of route north around the Wrangell Mountains, Alaska. Points are posterior medians and intervals are 50% and 90% Bayesian credible intervals. '*' indicates an interaction term. Meteorological predictors were interpolated to the approximate location and time each eagle chose a route. 'Wind' is the velocity of south to north wind. Negative thermal uplift (surface sensible heat flux) is flux towards the surface. IDs are individual random intercept estimates. Estimated intercepts greater or less than zero indicate greater and lower probability of choosing the north route, respectively, independent of covariates.

Chapter 2: R code

```
##########################################
Code for analyses in:
# Eisaguirre, JM, TL Booms, CP Barger, CL McIntyre, SB Lewis, GA Breed. 2018. Local
# meteorological conditions reroute a migration. J. Royal Soc. Proceedings B.
# doi 10.1098/rspb.2018.1779
##########################################


### read in the decision data
# mth = month of year
# dec = 1,0 (north,south)
# mig = 1,0 (spring,fall)
# t = timestamp just prior to decision
dec = read.csv('dec_dat.csv')


### fit some candidate models
library(rstanarm)

# intercept only
fitno = stan_glmer(dec ~ (1|id), family = binomial(link = "logit"),
                   data = dec, iter=2000)
# season only
fitn1 = stan_glmer(dec ~ mig + (1|id), family = binomial(link = "logit"),
                   data = dec, iter=2000)
# north wind by season interaction
fit1 = stan_glmer(dec ~ vwind*mig + (1|id), family = binomial(link = "logit"),
                  data = dec, iter=2000)


### rank candidate models
library(loo)

loono = loo(fitno)
loon1 = loo(fitn1)
loo1 = loo(fit1)

compare_models(loono,loon1,loo1)
```

```
### draw from the posterior predictive

# draws with empirical data
y_pred = posterior_predict(fit1, draws = 1000)

# create vector of standardized wind shifted one st. dev.
vwind.shiftup = dec$vwind + 1
# draws with wind shifted one st. dev.
y_pred_plus = posterior_predict(fit1,
                                newdata = data.frame(rhum=dec$rhum, vwind=vwind.shiftup,
                                                     mig=dec$mig, yr=dec$yr, id=dec$id),
                                                   draws = 1000)



### calculate proportion north route from pp draws
## fall
# empirical
propf_ppc = rep(0,1000)
for(i in 1:1000){
  propf_ppc[i] = mean(y_pred[i,dec$mig==0])
}
# shifted
propf_plus = rep(0,1000)
for(i in 1:1000){
  propf_plus[i] = mean(y_pred_plus[i,dec$mig==0])
}

## spring
# empirical
props_ppc = rep(0,1000)
for(i in 1:1000){
  props_ppc[i] = mean(y_pred[i,dec$mig==1])
}
# shifted
props_plus = rep(0,1000)
for(i in 1:1000){
  props_plus[i] = mean(y_pred_plus[i,dec$mig==1])
}
```

Chapter 3: supplementary tables & figures

Table S7.1: Estimates of environmental covariate effects on golden eagle behavior and movements during migrations. Parameter estimates are from the correlated random walk model with full behavioral process, including and intercept (β_0) orographic uplift (β_{ou}), thermal uplift (β_{tu}), and wind support (β_{tw}) as predictors. Top model is the best fitting candidate of the behavioral process resulting from an approximate leave-one-out cross-validation model selection procedure. $\overline{\text{elpd}}$ is the mean across pointwise estimates of the expected log pointwise predictive density estimated with approximate leave-one-out cross-validation model for the full model; larger $\overline{\text{elpd}}$ indicates better fit.

ID[a]	**Season**	**Parameter**[b]				**Top Model**[c]	$\overline{\textbf{elpd}}$[e] (SE)
		β_0	β_{ou}	β_{tu}	β_{tw}		
117394	spring	-2.68	-1.52	0.98	0.67	oro	0.68 (0.21)
117396	spring	-2.70	-0.49	3.07	-0.46	-	0.62 (0.12)
	fall	-0.53	-3.11	0.08	0.49	full[d] / oro + twind	3.26 (0.62)
117397	spring	-4.80	1.43	3.06	0.25	therm + twind / therm	0.64 (0.13)
117398	spring	-2.21	-0.09	0.81	-0.45	oro / therm	0.39 (0.22)
135411	spring	-2.55	-2.62	1.84	-0.98	oro + therm / full / oro + twind	0.54 (0.19)
135413	spring	-2.98	0.12	1.13	0.06	oro	0.96 (0.22)
135414	spring	-0.74	-1.11	-0.38	1.94	oro + twind	1.69 (0.81)
135417	spring	-2.53	-1.36	2.28	-0.20	oro + therm	0.51 (0.13)
	fall	-2.90	-0.53	0.85	2.30	therm	1.75 (0.36)
135421	fall	-2.78	-1.09	2.91	0.69	twind	1.12 (0.16)
135423	spring	-2.80	-1.24	2.52	-0.99	null	0.86 (0.19)
	fall	-2.12	0.13	1.00	-0.24	therm + twind	2.04 (0.44)
135425	fall	-2.29	-1.37	1.81	0.51	twind	1.78 (0.36)
142404	spring	-2.90	3.31	1.71	-2.62	full	1.01 (0.12)
142405	spring	2.34	1.06	1.93	-0.96	full / oro + therm	0.90 (0.22)
142407	spring	-2.11	-0.16	2.72	2.98	therm + twind / full	0.67 (0.12)
	fall	-0.57	-1.22	0.37	0.23	full / oro + therm	1.32 (0.24)
142408	spring	-2.66	-2.13	-0.06	-0.90	-	0.69 (0.19)
	fall	-4.82	2.61	2.32	-1.00	oro + therm	1.05 (0.16)
142409	spring	-1.29	0.67	2.16	0.33	-	0.54 (0.11)
142415	fall	-4.26	1.16	0.61	2.63	oro + twind	1.10 (0.24)
142417	spring	-0.83	-2.72	3.43	-0.23	-	0.69 (0.16)
157895	fall	-0.65	0.88	1.12	0.04	therm / oro	0.74 (0.38)
157896	fall	-0.73	0.63	1.48	-0.40	-	1.44 (0.48)
157899	fall	-2.10	1.89	6.47	0.47	oro / therm + twind / therm	1.00 (0.50)
157900	fall	-0.42	-0.05	2.98	-0.27	null / therm + twind	1.41 (0.47)
157902	fall	-1.98	-1.44	7.56	-0.38	oro + therm	2.30 (0.94)
157903	fall	-0.74	1.14	0.71	0.59	full	3.10 (2.16)
157904	fall	-1.31	3.60	2.55	0.51	oro / oro + therm	0.34 (0.22)
157906	fall	-1.16	1.33	4.52	-0.55	twind	1.25 (0.35)
mean	spring	-2.10	-0.46	1.81	-0.10		0.76
	fall	-1.83	0.29	2.33	0.35		1.56
sd	spring	1.57	1.64	1.13	1.31		0.31
	fall	1.34	1.72	2.18	0.96		0.79

[a]individual eagles; blank indicates second season for previous ID

[b]posterior means of parameter estimates

[c]model with lowest looic (**?**); all models within two looic of the top model listed in order of fit (separated by /); - indicates null did not converge

[d]oro + therm + twind

[e]the mean across pointwise estimates of the expected log pointwise predictive density estimated with PSIS-LOO (**??**)

Table S7.2: Pearson's correlations among estimated effects of thermal uplift, orographic uplift, and wind support on eagle movements during fall migration.

	Orographic	Thermal	Wind
Orographic	-	0.15	-0.11
Thermal	-	-	-0.35
Wind	-	-	-

Table S7.3: Pearson's correlations among estimated effects of thermal uplift, orographic uplift, and wind support on eagle movements during spring migration.

	Orographic	Thermal	Wind
Orographic	-	0.11	-0.22
Thermal	-	-	-0.06
Wind	-	-	-

Table S7.4: Estimates of environmental covariate effects on golden eagle behavior and movements during migrations. Parameter estimates are from the correlated random walk model with full behavioral process modified to assume equal variance in the x and y dimensions, which assures invariance under linear transformation of the coordinate system. Note that these estimates are similar to those in table S1, despite the modification.

ID[a]	**Season**	**Parameter**[b]			
		β_0	β_{ou}	β_{tu}	β_{tw}
135411	spring	-2.79	-2.77	1.75	-0.44
135414	spring	-1.09	-1.36	-0.48	1.01
135417	spring	-2.52	-1.41	2.30	0.07
	fall	-3.13	-0.76	1.29	2.39
135423	spring	-2.59	-1.51	2.41	-0.05
	fall	-1.81	0.07	0.67	0.16
135425	fall	-2.70	-1.47	2.20	0.88
142404	spring	-2.40	2.99	1.11	-2.71
157902	fall	-2.23	-1.36	7.43	-0.55
157904	fall	-1.28	3.48	2.42	0.04

[a]individual eagles; blank indicates second season for previous ID
[b]posterior means of parameter estimates

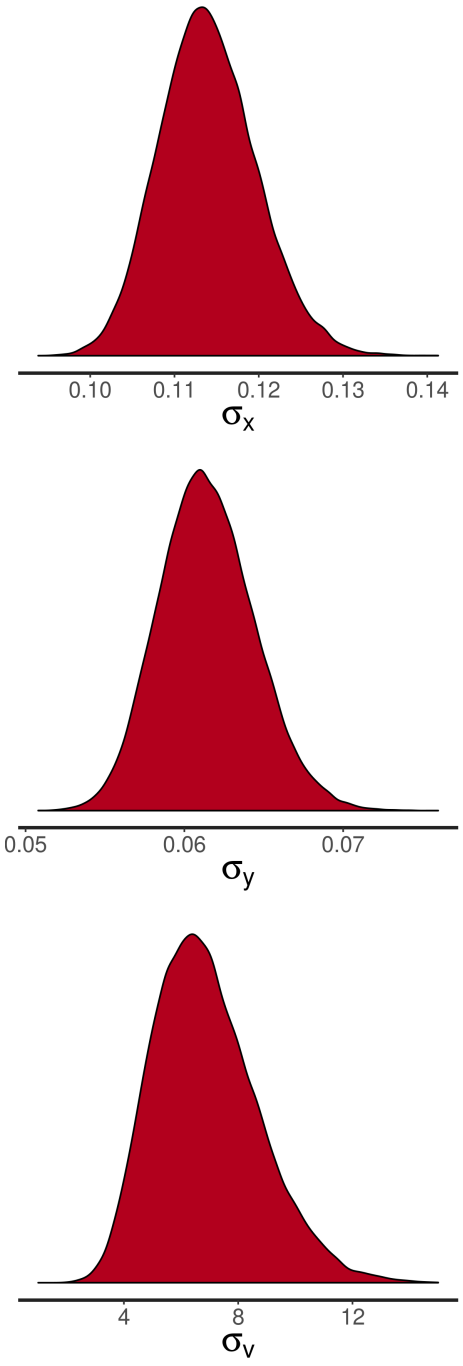

Figure S7.1: Posterior plots of variance components of the correlated random walk model with orographic uplift, thermal uplift, and wind support as behavioral predictors for the spring track of golden eagle 135423. Curves are approximately Gaussian, indicating the model was well behaved and likely converged to the posterior.

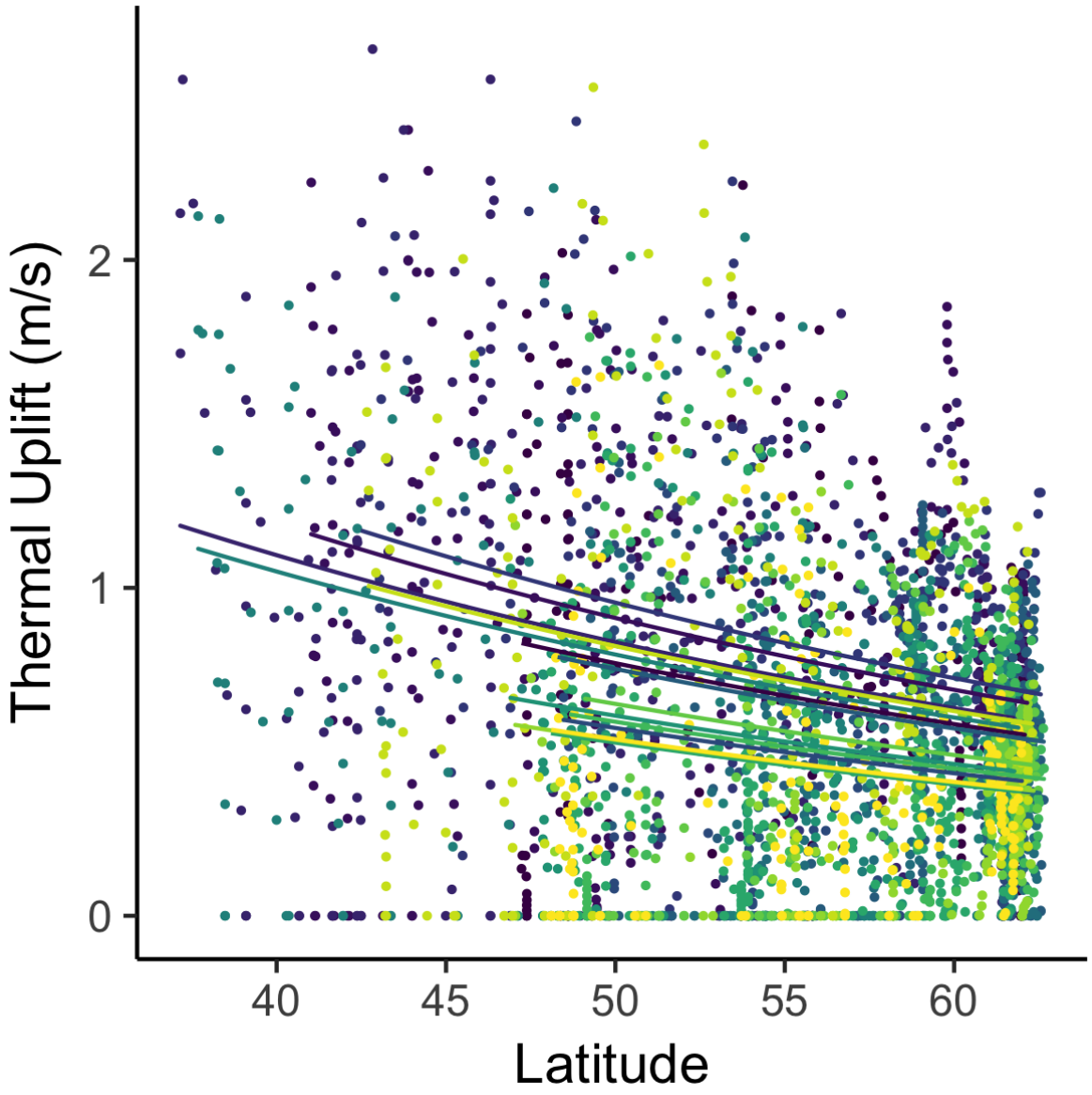

Figure S7.2: Interpolated thermal uplift as a function of latitude during spring migration. Hue corresponds to individual. Curves are from the individual level of a Bayesian hierarchical Gamma regression. The 95% Bayesian credible interval for the latitude coefficient was $-0.040 < \beta_{lat} < -0.015$, strong evidence for a decreasing trend in thermal uplift with increasing latitude.

Stan model

```
data {

  int N;                // # of fixes in track
  vector[N] x;          // x coordinates
  vector[N] y;          // y coordinates
  vector[N] dt;         // time intervals

  vector[N] oro;        // covariates
  vector[N] therm;
  vector[N] twind;
  vector[N] tod;

}

transformed data {

  vector[N] c_oro;
  vector[N] c_therm;
  vector[N] c_twind;
  vector[N] oro_inter;
  vector[N] therm_inter;
  vector[N] twind_inter;

  // shifted log transform and standardize
  c_oro = ( log( oro + 1 ) * ( 0.5 / sd( log( oro + 1 ) ) ) );

  c_therm = ( log( therm + 1 ) * ( 0.5 / sd( log( therm + 1 ) ) ) );
```

```
  // center and standardize twind
  c_twind = ( ( twind  ) * ( 0.5 / sd( twind ) ) )
  - mean( twind * ( 0.5 / sd( twind ) ) );

  // interactions
  oro_inter = c_oro .* tod;
  therm_inter = c_therm .* tod;
  twind_inter = c_twind .* tod;

}

parameters {

  vector[N] gamma_raw;                // logit behavior parameter
                                      //-- time-varying, correlates steps
  real<lower=0> sigmax;               // variance in x
  real<lower=0> sigmay;               // variance in y
  real<lower=0> sigmav;               // behavior variance
  vector[4] beta;                     // covariate coefficients

}

transformed parameters{

  // introduce logit link
  vector<lower=0,upper=1>[N] gamma;

  for(j in 1:N){
```

```
    gamma[j] = inv_logit( gamma_raw[j] );
  }

}

model {

  // NOTE: Stan uses st. dev. for normals, whereas JAGS uses precision
  // Stan also truncates appropriately based on specified constraints

  // prior on behavior process noise
  // prior density away from zero--assume there is variability in behavior
  sigmav ~ normal( 3 , 3 );

  // priors on movement process noise--close to zero
  sigmax ~ normal( 0 , 1 );
  sigmay ~ normal( 0 , 1 );

  // priors on coefficients
  // prior density on zero--assume no effect of covariates on behavior
  beta ~ student_t( 5, 0 , 2.5 );

  for (i in 3:N) {

    // behavior linear combination of covariates plus previous behavior
    // this can be modified to make candidate formulations
    gamma_raw[i] ~ normal( gamma_raw[i-1] + beta[1]
    + beta[2] * oro_inter[i] + beta[3] * therm_inter[i]
    + beta[4] * twind_inter[i] , dt[i] * sigmav );
```

```
    // movement process is independent in x and y
    x[i] ~ normal( x[i-1] + gamma[i] * ( dt[i] / dt[i-1] )
    * ( x[i-1] - x[i-2] ) , dt[i] * sigmax );

    y[i] ~ normal( y[i-1] + gamma[i] * ( dt[i] / dt[i-1] )
    * ( y[i-1] - y[i-2] ) , dt[i] * sigmay );

  }

}

generated quantities {

  // generate log likelihoods for PSIS-LOO
  // test prediction of next step from previous with estimated gamma
  vector[N] log_lik;
  log_lik[1] = 0.1;  // need something here; simplest to fix across tracks
  log_lik[2] = 0.1;

  for (n in 3:N){

    log_lik[n] = normal_lpdf( x[n] | x[n-1] + gamma[n]
    * ( dt[n] / dt[n-1] ) * ( x[n-1] - x[n-2] ) , dt[n] * sigmax )
    *normal_lpdf( y[n] | y[n-1] + gamma[n] * ( dt[n] / dt[n-1] )
    * ( y[n-1] - y[n-2] ) , dt[n] * sigmay );

  }
```

```
}
```

R code

```
library(rstan)
library(loo)

#################################
## model variables
# x -- vector of x coordinates
# y -- vector of y coordinates
# dt -- vector of time intervals
# N -- number of fixes in track
# oro -- vector of raw orographic uplift data
# therm -- vector of raw thermal uplift data
# twind -- vector of raw tailwind data
# tod -- vector of times of day (1=day, 0=night)
#################################

dat = read.csv('examp_dat.csv')

x = dat$x
y = dat$y
dt = dat$dt
N = nrow(dat)
oro = dat$oro
therm = dat$therm
twind = dat$twind
tod = dat$tod

# fit Stan model with HMC, using default no-u-turn sampler
# model code should be saved as a .stan file
```

```
# arguments should be modified as required
stan.fit = stan("model.stan",
                data = list(x, y, dt, N, oro, therm, twind, tod),
                chains = 2,
                iter = 1000,
                thin=1,
                cores = 1,
                control = list(adapt_delta = 0.9))
# last argument helps with divergent transitions

# PSIS-LOO
log_lik = extract_log_lik(stan.fit)
loo = loo(log_lik_00)
print(loo)
# use compare(loo1, loo2, ...) to rank candidate models
```

Chapter 3: additional mathematical details

From combing components of equations 1 and 5 from the main text, we see that Δt_i is accounted for when introducing the linear combination of environmental covariates, despite that Δt_i is not explicitly included in equation 5:

$$\gamma_i \frac{\Delta t_i}{\Delta t_{i-1}} = \frac{\exp(\gamma'_{i-1} + \mathbf{Z}_i^{\mathrm{T}}\boldsymbol{\beta} + \epsilon_i)}{\exp(\gamma'_{i-1} + \mathbf{Z}_i^{\mathrm{T}}\boldsymbol{\beta} + \epsilon_i) + 1} \frac{\Delta t_i}{\Delta t_{i-1}} = \frac{\exp(\gamma'_{i-1} + \mathbf{Z}_i^{\mathrm{T}}\boldsymbol{\beta} + \epsilon_i)\Delta t_i}{\exp(\gamma'_{i-1} + \mathbf{Z}_i^{\mathrm{T}}\boldsymbol{\beta} + \epsilon_i)\Delta t_{i-1} + \Delta t_{i-1}}.$$

Equation 1, then, can be rewritten in its entirety as

$$\mathbf{x}_i | \mathbf{x}_{i-1}, \mathbf{x}_{i-2} \sim \mathcal{N}_2 \left(\mathbf{x}_{i-1} + \frac{\exp(\gamma'_{i-1} + \mathbf{Z}_i^{\mathrm{T}}\boldsymbol{\beta} + \epsilon_i)\Delta t_i}{\exp(\gamma'_{i-1} + \mathbf{Z}_i^{\mathrm{T}}\boldsymbol{\beta} + \epsilon_i)\Delta t_{i-1} + \Delta t_{i-1}} (\mathbf{x}_{i-1} - \mathbf{x}_{i-2}),\ \boldsymbol{\Sigma}_i \right),$$

or equivalently as

$$\mathbf{x}_i | \mathbf{x}_{i-1}, \mathbf{x}_{i-2} \sim \mathcal{N}_2 \left(\mathbf{x}_{i-1} + \frac{\exp(\gamma'_{i-1} + \mathbf{Z}_i^{\mathrm{T}}\boldsymbol{\beta} + \log\Delta t_i + \epsilon_i)}{\exp(\gamma'_{i-1} + \mathbf{Z}_i^{\mathrm{T}}\boldsymbol{\beta} + \log\Delta t_{i-1} + \epsilon_i) + \Delta t_{i-1}} (\mathbf{x}_{i-1} - \mathbf{x}_{i-2}),\ \boldsymbol{\Sigma}_i \right).$$

Chapter 4: wind energy developments

Locations of commercial grade wind turbines were gathered from the United States Geological Survey US Wind Turbine Database, EnergyBC, and Alberta Human Footprint Monitoring Program. Coordinates for the two wind turbines in the Yukon Territory were approximated using Google Earth. Only those turbines indicated as operational or were projected to be operational during each year of the eagle migrations were included when distances to turbines and buffer intersections were computed.

Only 25 of the 17,386 steps analyzed intersected 1 km buffers surrounding wind turbines. Twenty endpoints of the steps were within 5 km of a wind turbine, and only two were within 2 km. Of those 45 cases (of either step intersection or endpoint within 5 km), only four occurred in the USA, with the remainder in Canada, and four individuals were responsible for 33 of them. These findings indicate that areas containing wind energy developments are likely not available at high frequency to the population of eagles we have sampled—golden eagles that summer in southcentral Alaska—during migration, but perhaps isolated to a few locations used repeatedly by certain individuals. We thus chose not to include effects of wind energy developments in candidate models of selection, as the ability to detect a true effect on the scale of inference possible with the data on hand would be extremely low. It is important to keep in mind that there are currently relatively few wind energy developments along the routes of these golden eagles, so further developments could increase the availability of them to Alaska's migratory golden eagles.

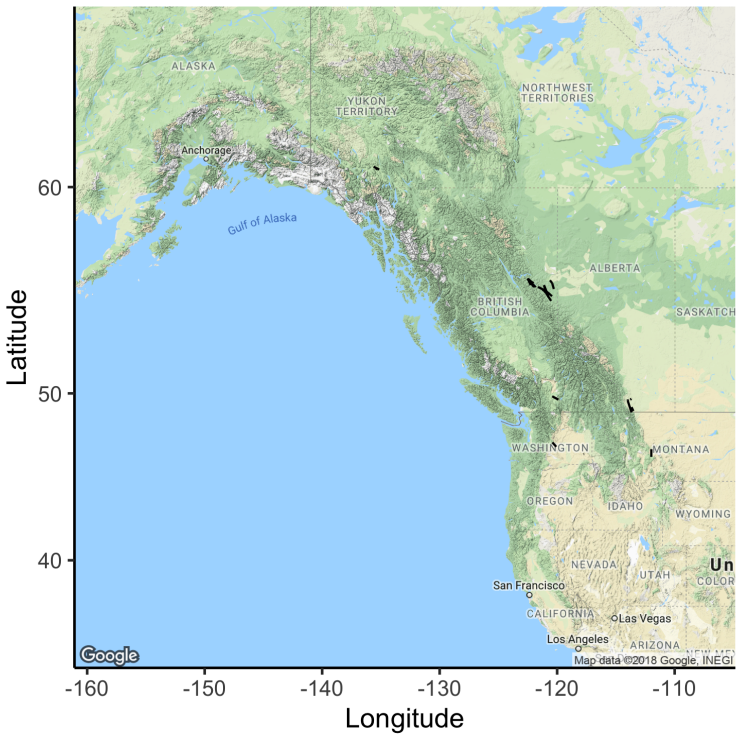

Figure S 7.3: Golden eagle migration track segments that intersect a 1-km buffer around a wind turbine or with a point that is within a 5 km of a wind turbine.

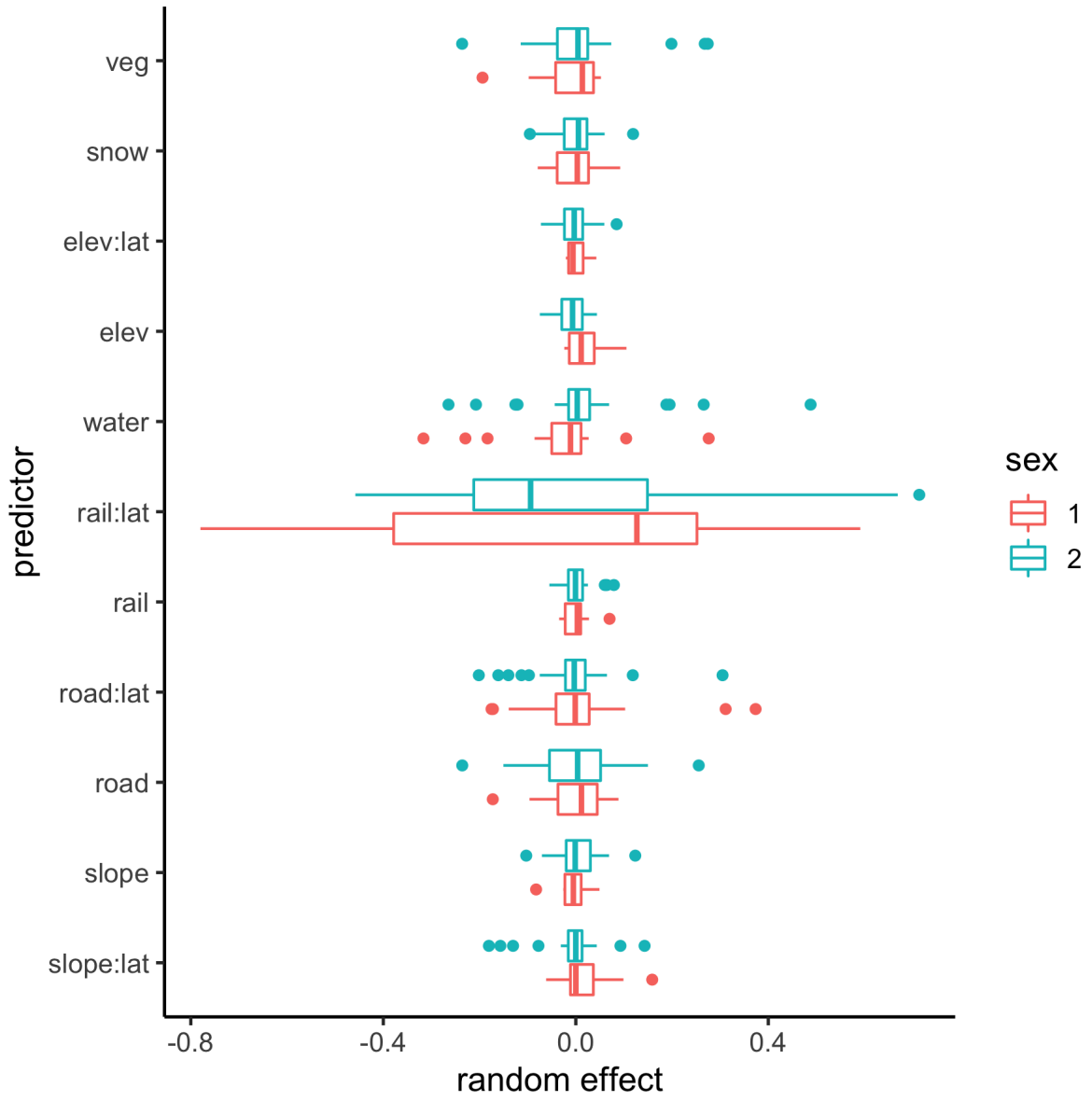

Figure S 7.4: Individual-level golden eagle migration habitat selection effects estimated with a step selection function shown grouped by sex.

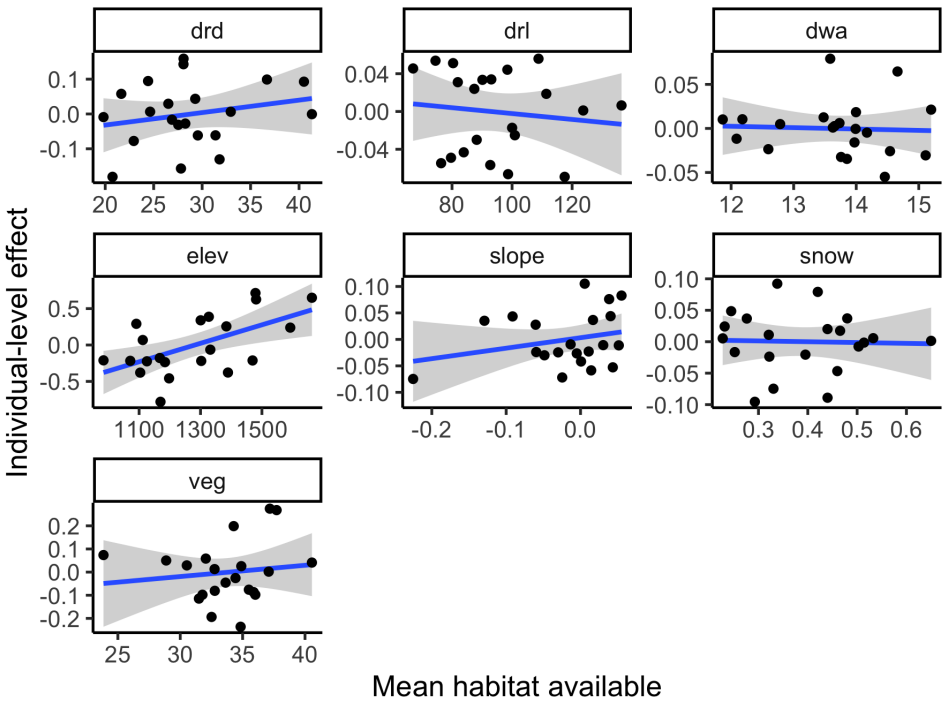

Figure S 7.5: Effects of habitat available during fall migration on individual-level habitat selection effects. 'drd', 'drl', 'dwa', 'elev', 'slope', 'snow', and 'veg', correspond to distance to nearest road, distance to nearest railway, distance to nearest waterway, elevation, slope southing, percent snow cover, and percent vegetation cover, respectively. Spearman's rank correlation tests indicated only available elevation correlated significantly with selection for elevation ($p < 0.05$). Shaded areas represent 95% confidence intervals of the simple linear regressions.

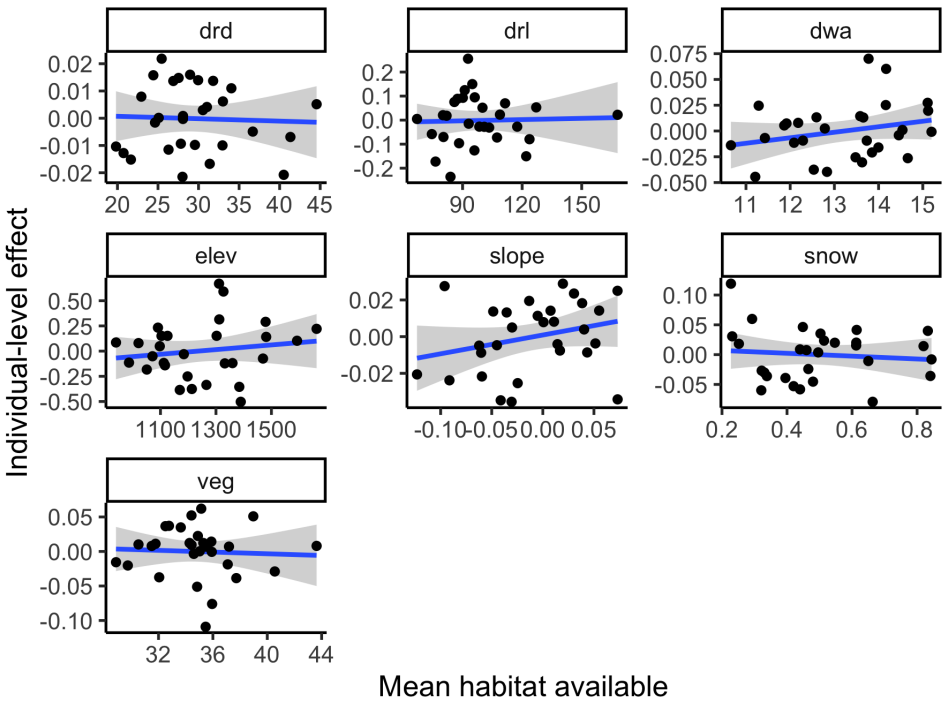

Figure S 7.6: Effects of habitat available during spring migration on individual-level habitat selection effects. 'drd', 'drl', 'dwa', 'elev', 'slope', 'snow', and 'veg', correspond to distance to nearest road, distance to nearest railway, distance to nearest waterway, elevation, slope southing, percent snow cover, and percent vegetation cover, respectively. None of the correlations were statistically significant. Shaded areas represent 95% confidence intervals of the simple linear regressions.

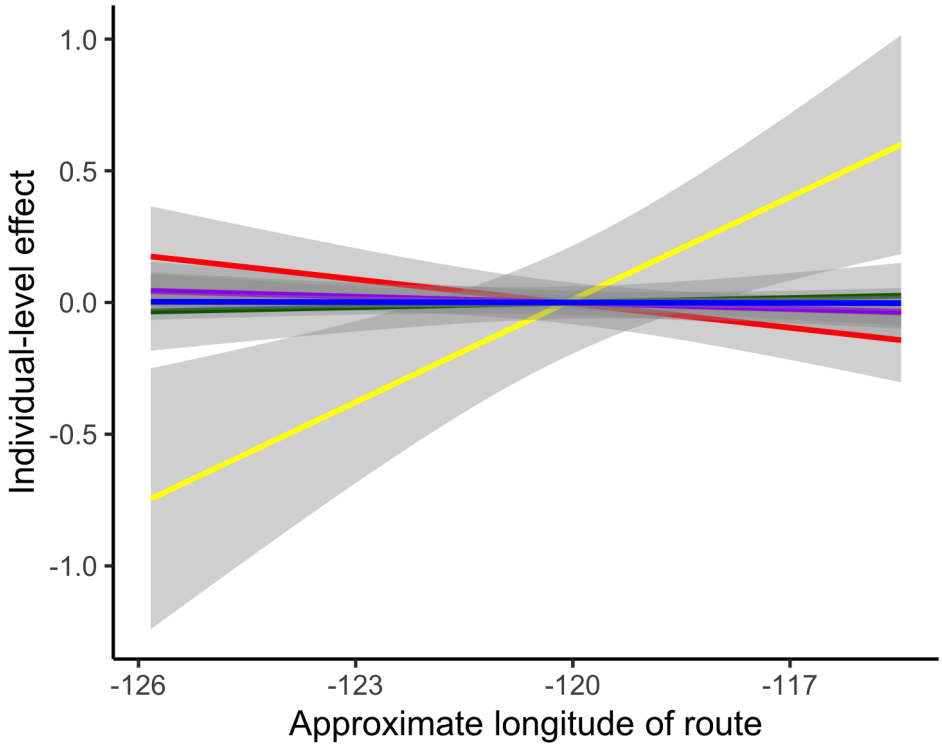

Figure S 7.7: Effects of longitudinal location of individual eagles' routes (when crossing 53°N latitude) on individual-level habitat selection effects during fall migration. Yellow curve corresponds to elevation. Shaded areas represent 95% confidence intervals of the simple linear regressions.

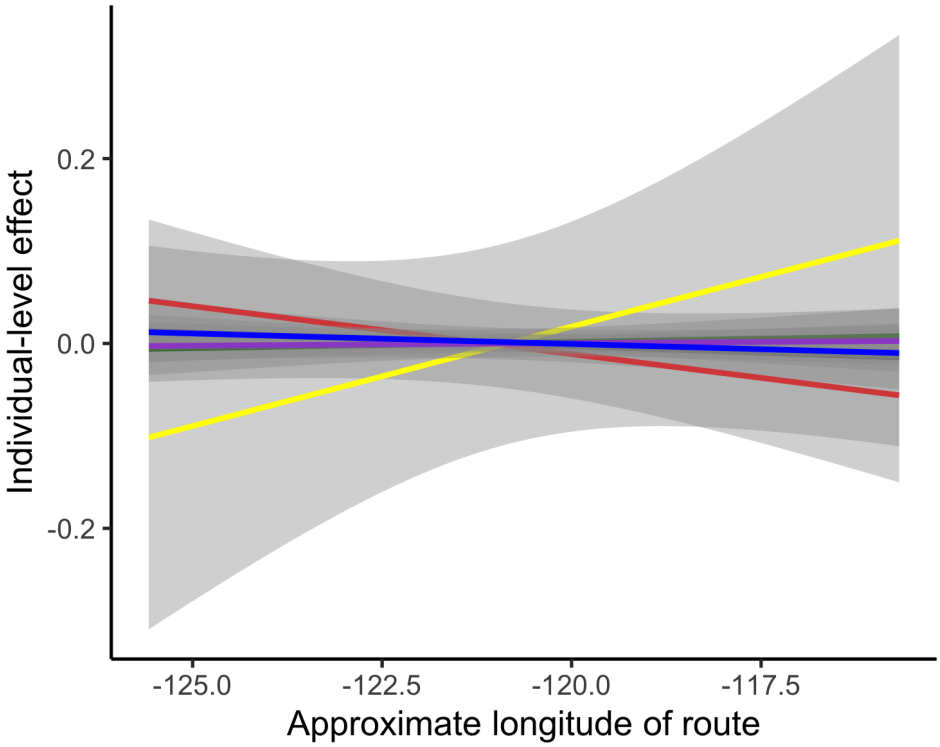

Figure S 7.8: Effects of longitudinal location of individual eagles' routes (when crossing 53°N latitude) on individual-level habitat selection effects during spring migration. Yellow curve corresponds to elevation. Shaded areas represent 95% confidence intervals of the simple linear regressions.

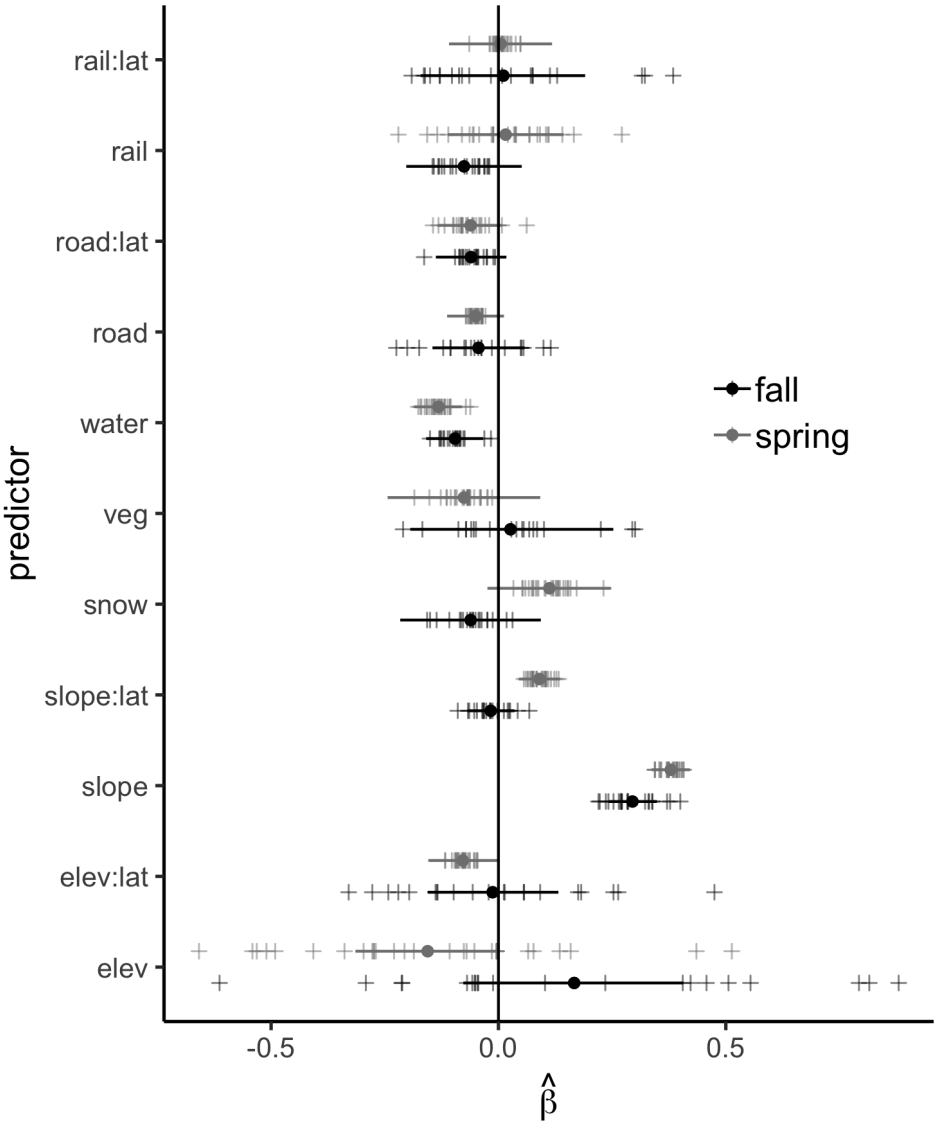

Figure S 7.9: Full version of figure 4.5 in the main text.

Chapter 4: simulation study

The goal of this brief simulation study was to ensure that a step selection function (SSF) similar to the one used for the study presented in the main text can recover a known effect a linear feature on animal space use, as well as discern occasions when a linear feature does not affect space use. Over real landscapes, some linear features often occur parallel to each other (e.g., roads and railroads, roads and transmission lines, etc.), and many animals might move in parallel to linear features if, for example, their migration corridors are aligned with those features. We were, thus, primarily interested in assuring the SSF yields robust inferences under these scenarios, both when a linear feature does and does not affect space use.

To test these points, we simulated 10,000 tracks of 100 steps in length over a hypothetical landscape void of features except for two straight, parallel linear features (Fig. 7.10). The tracks were simulated from the movement model presented in the main text (equations 4.3-4.4) modified slightly with a directional bias paralleling the linear feature plus γ_i modeled as a sine wave. We approximated the fitted movement kernel with a bivariate Gaussian kernel and imparted additional random noise on γ_i to reflect imperfect fit of the movement kernel. The conditional logistic regression was then carried out for each simulated track with five available points drawn from the the 'fitted' movement kernel using `clogit()` from the `survival` package in R.

In the simulations, selection for space nearer the linear feature of interest was imparted by shifting each point in each track 10% closer to that linear feature, while leaving the availability (i.e. the 'fitted' movement kernel) unchanged. For each simulated track and respective fit, we retained the estimated coefficients $\hat{\beta}_j$ for distance to each linear feature, where $j = 1$ for the linear feature selected for and $j = 2$ for the parallel, and the resulting p-values from the tests of H_0: $\hat{\beta}_j = 0$.

We found that the SSF performed well in recovering selection for the linear feature, and additionally it successfully showed when a parallel linear feature was not selected for (Fig. 7.11). As expected, the SSF did not find (at $\alpha = 0.05$) $\hat{\beta}_j \neq 0$, $j = 1, 2$ for 94% percent of the simulated tracks prior to selection for the linear feature being

imparted. After selection was imparted on each track, the SSF found $\hat{\beta}_1 \neq 0$ for 91% of the tracks and $\hat{\beta}_2 = 0$ for 72%. More explicitly, the SSF correctly identified when both linear features were not selected for in 94% of the simulations; it correctly identified the selection in 91% of the simulations; and it correctly identified no selection for the parallel linear feature in 72% of the simulations when selection for the other linear feature was imparted. While it was not correct (based on p-values) in 29% of the simulations when there was no selection for the parallel feature, this simulation study represents a sort of worst case scenario, where two linear features are perfectly parallel over a large portion of a study area. We would thus expect even better performance of the SSF over a real landscape, where such perfect correlation would occur much less frequently.

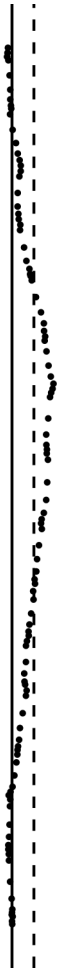

Figure S 7.10: One simulated track over the hypothetical landscape with two parallel linear features. In the simulation study, selection was imparted for the solid line, and the dashed line was the parallel linear feature.

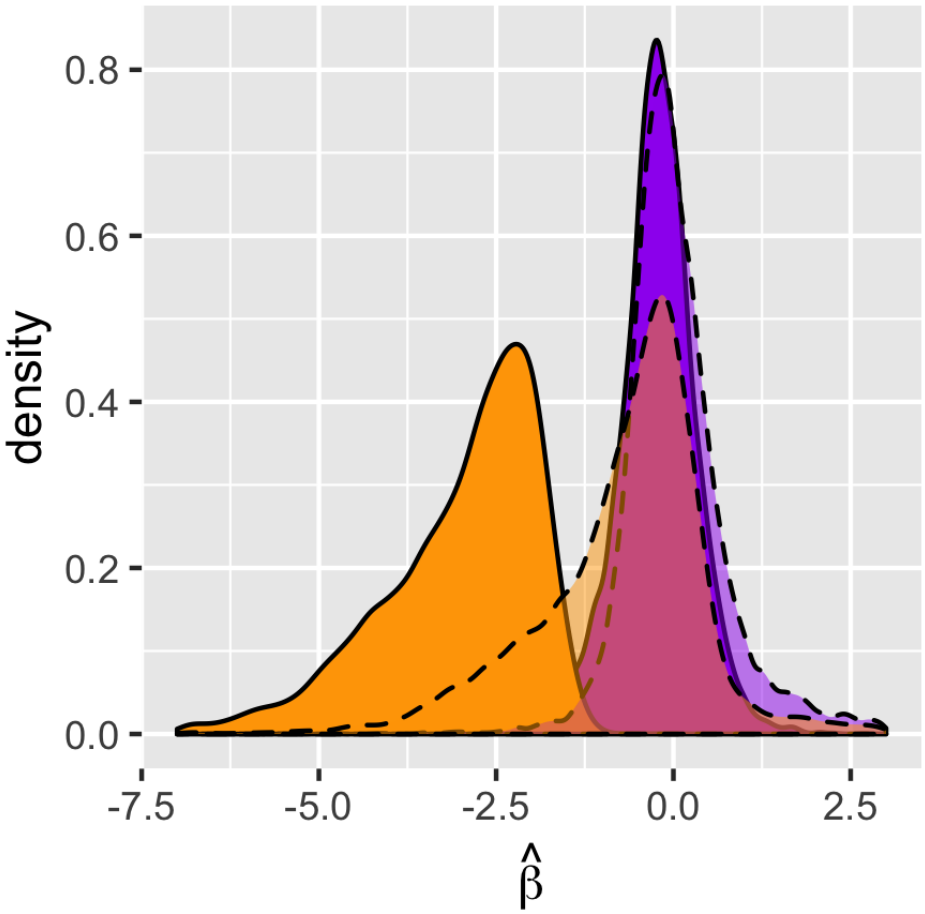

Figure S 7.11: Density plots of estimated selection coefficients from the simulation study. Dashed curves are the densities of the estimated selection coefficients for the parallel linear feature. Orange densities correspond to estimated selection for the linear features after selection was artificially imparted. Purple densities are of the estimates with no selection imparted.

Chapter 5: Supplementary material

Habitat types

Table S 7.5: Habitat types used in analysis.

AKVWC class	habitat type
'Bareground'	'bare'
'Freshwater or Saltwater'	'water'
'Bareground (Beach or Tide Flat) (Southern Alaska)', 'Herbaceous (Marsh) (Interior Alaska, Cook Inlet Basin)', 'Herbaceous (Marsh) (Northern and Western Alaska)', 'Herbaceous (Tidal) (Southern Alaska)', 'Herbaceous (Wet-Marsh) (Southern Alaska)', 'Herbaceous (Aquatic)', 'Low Shrub (Tidal) (Southern Alaska)', 'Herbaceous (Wet-Marsh) (Tidal)'	'wet'
'Herbaceous (Mesic) (Interior Alaska, Cook Inlet Basin)', 'Herbaceous (Mesic) (Northern and Western Alaska)', 'Herbaceous (Mesic) (Southern Alaska)', 'Herbaceous (Peatland) (Southern Alaska)', 'Herbaceous (Wet) (Interior Alaska, Cook Inlet Basin)', 'Herbaceous (Wet) (Northern and Western Alaska)', 'Lichen', 'Moss', 'Moss (Southern Alaska)', 'Sparse Vegetation (Interior Alaska, Cook Inlet Basin)', 'Sparse Vegetation (Northern and Western Alaska)', 'Tussock Tundra (Low shrub or Herbaceous)', 'Fire Scar'	'open'
'Low Shrub', 'Low Shrub (Peatland) (Southern Alaska)', 'Dwarf Shrub', 'Dwarf Shrub (Southern Alaska)', 'Dwarf Shrub-Lichen', 'Dwarf Shrub, or Herbaceous (Mesic) (Southern Alaska)', 'Low Shrub or Tall Shrub (Open-Closed)', 'Low Shrub/Lichen', 'Low-Tall Shrub (Southern Alaska)', 'Tall Shrub (Open-Closed)'	'shrub'
'Deciduous Forest (Open-Closed)', 'Deciduous Forest (Open-Closed) (Seasonally Flooded) (Southern Alaska)', 'Deciduous Forest (Woodland-Closed) (Southern Alaska)', 'Hemlock (Woodland-Closed)', 'Hemlock-Sitka Spruce (Woodland-Closed)', 'Needleleaf Forest (Open-Closed) (Seasonally Flooded) (Southern Alaska)', 'Needleleaf Forest (Woodland-Open) (Peatland) (Southern Alaska)', 'Sitka Spruce (Woodland-Closed)', 'White Spruce or Black Spruce (Open-Closed)', 'White Spruce or Black Spruce (Woodland)', 'White Spruce or Black Spruce-Deciduous (Open-Closed)', 'White Spruce or Black Spruce/Lichen (Woodland-Open)'	'forest'
'Urban, Agriculture, Road'	'human'
'Ice-Snow'	'ice'

Area of 95% contour of kernel density estimates

Median (IQR) for territorial eagles: 55 (37, 126) km^2

Median (IQR) for floater eagles: 5483 (3110, 13974) km^2